UNIVERSITÀ DEGLI STUDI DI PADOVA
DIPARTIMENTO DI SCIENZE CHIMICHE

SCUOLA DI DOTTORATO IN SCIENZE MOLECOLARI
INDIRIZZO SCIENZE CHIMICHE
CICLO XXVI

Tesi di dottorato:

PORPHYRIN DERIVATIVES FOR FUNCTIONAL NANOMATERIALS

Direttore della Scuola: Prof. Antonino Polimeno

Coordinatore Indirizzio: Prof. Antonino Polimeno

Supervisore: Prof. Tommaso Carofiglio

Dottorando: Prashant Chauhan

2011-2013

Dedicated to

My PARENTS

Acknowledgements

First of all, I take this opportunity to express my gratitude to **Prof. Tommaso Carofiglio**, my research supervisor, for his guidance, fruitful discussions, support and advices throughout the course. It has been an honour to be his first international Ph.D. student. The joy and enthusiasm for his research was contagious and motivational for me, even during tough time in the Ph.D. pursuit.

I would also thank **Prof. Michele Maggini** for allowing me to carry out research activities in his laboratory, for his constant support and advices. I am grateful to all my co-workers with whom I have spent wonderful time during the research in Lab 205. Special thanks to lab members: **Dr. Miriam Mba**, Prasenjit Maity, Tommaso Lanza, Emiliano Rossi, Patrizio Salice, Simone Silvestrini and Edmondo Benetti for scientific and technical support in the laboratory. It was also great experience to work with and guiding the undergraduate students Gabrio Rossi, Andrea Sartorelli and Marco Zarattini. A heartiest thank to Alessandro Gambarin, Alessandro Cazzolaro and Marta Diez Castellanou from graduate school for spending the quality time in the office. Special thanks to Elisa Zambon and Daniela Longo for their administrative support during the course.

I am grateful to all the friends for making my stay in Padua so memorable. Finally, thanks to my parents and family members for their undying support and all my strength from their unconditional love. I derived inspiration from their sacrifice, encouragement from their faith and found happiness in their pride.

I would also like to acknowledge the financial support from Willpower: Erasmus Mundus scholarship from India and European Union.

ABSTRACT

The thesis consists of two major research topic i.e. Porphyrin and Nano crystalline cellulose.

The porphyrin project started with the production of porphyrin chromophores for dye sensitized solar cells. These derivatives were required as references for an ongoing project of the research group that hosted me. In addition, some porphyrin-porphyrin tweezers were prepared using a one pot synthetic methodology developed in our lab, based on the use of trichloro triazine as a linker. These derivatives were necessary for collaboration with Professor Nina Berova at Columbia University that studies their use for the determination of the absolute configuration of chiral molecules by circular dichroism. After this training period, the thesis project continued with an original research based on the use of click-chemistry for porphyrin functionalization.

The nanocellulose project started with the production of nanocrystalline cellulose from microcrystalline cellulose by acid hydrolysis. The nanocellulose has chemically modifiable OH groups on the surface. This allows the use of a wide range of chemical reactions for its functionalization. The linking of a pH sensitive dye on the surface of NCC was studied. In addition, several strategies were being employed for the functionalization of NCC with other groups such as cationic substituents (using (2,3-epoxypropyl)trimethylammonium chloride), amino (using epichlorohydrin and 3-aminopropyltrimethoxysilane), carboxy (using ammonium persulfate and TEMPO). Out of various chemical modifications carried out on NCC, the TEMPO mediated carboxylation for introduction of carboxyl group on NCC was proved to be easy, convenient and even resulted in high degree of functionalization. Using these material and typical carbodiimide chemistry, functional groups such as porphyrins (that acts as a sensitizer for singlet oxygen production) and a nitro-derivative (capable of producing NO upon irradiation) were prepared. These features are under study to verify their potential in various therapeutic applications.

RIASSUNTO

La Tesi si compone di due principali temi di ricerca che riguardano le porfirine e la nano-cellulosa.

Il progetto sulle profirine è iniziato con la produzione cromofori per celle solari a sensibilizzatore organico. Questi derivati sono stati usati come riferimento per un progetto sulla conversione della luce solare in energia che coinvolge il gruppo di ricerca che mi ha ospitato. Inoltre, sono stati preparati dei dimeri porfirina-porfirina, basati sull'uso di una procedura "one-pot" che impiega la triclorotriazina come linker. Questi derivati sono stati preparati nell'ambito di una collaborazione con la Professoressa Nina Berova (Columbia University) che studia il loro uso per la determinazione della configurazione assoluta di molecole chirali mediante dicroismo circolare. Dopo questo periodo di formazione, il progetto di tesi è proseguito con una ricerca originale, basato sull'uso di click -chemistry per la funzionalizzazione del macrociclo profirinico.

Il progetto che riguarda la nanocellulosa, è iniziato con la produzione di cellulosa nanocristallina da cellulosa microcristallina mediante idrolisi acida. La nanocellulosa possiede dei gruppi OH modificabili chimicamente sulla superficie che consentono l'utilizzo di una vasta gamma di reazioni chimiche per la sua funzionalizzazione. Si è quindi studiata la funzionalizzazione della nanocellulosa con un colorante sensibile al pH sulla superficie dei nanocristalli. Inoltre, sono state valutate diverse strategie per la funzionalizzazione superficiale con gruppi cationici (utilizzando 2,3-epossipropil cloruro di trimetil ammonio), ammino (con epicloridrina e 3-amminopropiltrimetossisilano), carbossi (utilizzando persolfato di ammonio e TEMPO). Tra le varie strategie di funzionalizzazione esaminate, la carbossilazione mediata dal TEMPO si è dimostrata efficace e robusta. L'utilizzo di questi materiali e la chimica tipica delle carbodiimidi, ha permesso di legare covalentemente alla nanocellulosa gruppi funzionali come porfirine (che agisce come un sensibilizzatore per la produzione ossigeno singoletto) e un nitro- derivato (in grado di produrre NO sotto illuminazione). Questi materiali sono in fase di studio per verificare il loro potenziale in varie applicazioni terapeutiche.

Glossary

PDT- Photo dynamic therapy

DSSC- Dye sensitized solar cell

DDQ- 2,3-Dichloro-5,6-dicyano-1,4-benzoquinone

DBU- 1,8-Diazabicyclo[5.4.0]undec-7-ene

CD- Circular dichroism

TCT- Trichloro triazine / Cyanuric chloride

D-A- Donor acceptor

DFT- Density functional theory

BODIPY- Boron-dipyrromethene

NMR- Nuclear magnetic resonance

AGU- β-D-anhydroglucopyranose

DP- Degree of crystallinity

TC- Terminal complexes

NCC- Nano crystalline cellulose / Crystalline nanocellulose

TEM- Transmission electron microscopy

AFM- Atomic force microscopy

DS- Degree of substitution

ESI- Electrospray ionization

TLC- Thin layer chromatography

AC-Absolute configuration

TFA- Trifluoroacetic acid

R_f- Retardation factor

DIPEA- N,N-Diisopropylethylamine

NBS- N-Bromosuccinimide

TBAF- Tetrabutylammonium fluoride

COSY- Correlation spectroscopy

HMQC- Heteronuclear multiple quantum coherence spectroscopy

DLS- Dynamic light scattering

TGA- Thermal gravimetric analysis

XPS- X-ray photoelectron spectroscopy

TEMPO- 2,2,6,6-Tetramethylpiperidine 1-oxyl

TMβCD- 2,3,6-trimethyl-β-cyclodextrin

MES- 2-(N-morpholino)-ethanesulfonic acid

EDC.HCl- N-(3-dimethylaminopropyl)-N'-ethylcarbodiimide hydrochloride

NHS- N-hydroxy succinimide

List of Figures

List of Tables

Contents

Chapter-1

INTRODUCTION

I Porphyrin

1.1 Background

The ubiquitous tetrapyrrolic macrocycles play diverse roles in biological system.[1] The natural roles of these pigments of life have stimulated the search of new synthetic porphyrins to understand the molecular mechanism of natural reactions and development of porphyrins for photodynamic therapy (PDT) and material chemistry (Figure 1.1).

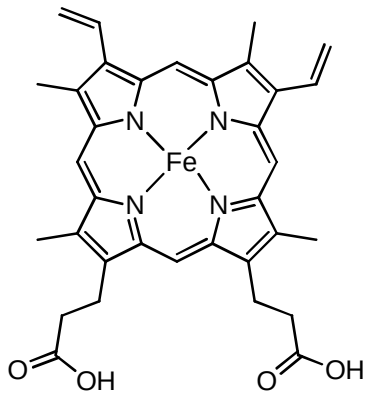

Protoporphyrin IX (1)

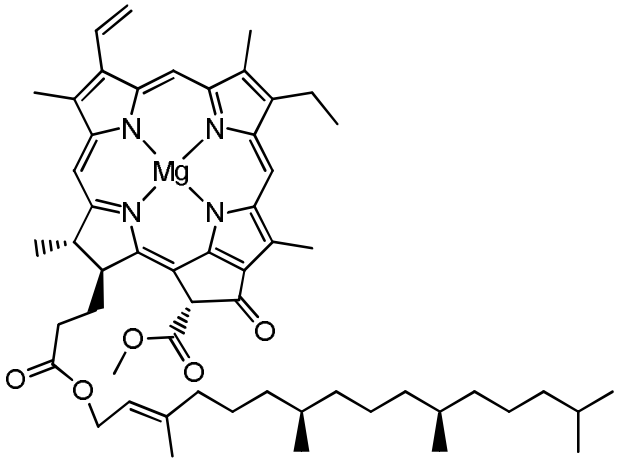

Chlorophyll a (2)

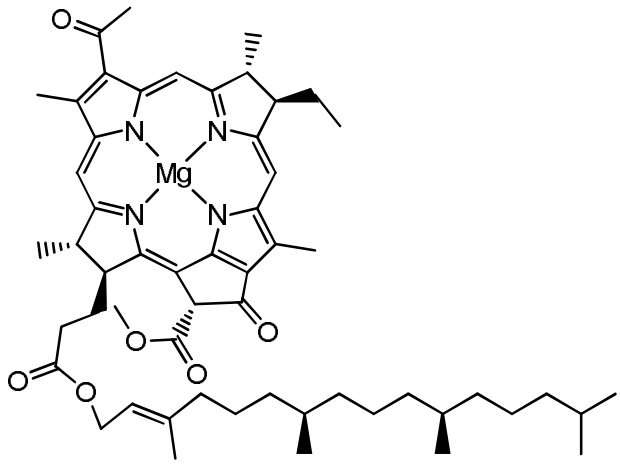

Bacteriochlorophyll (3)

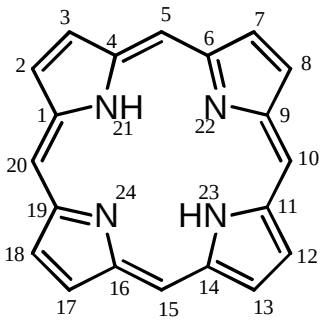

Porphine (4)

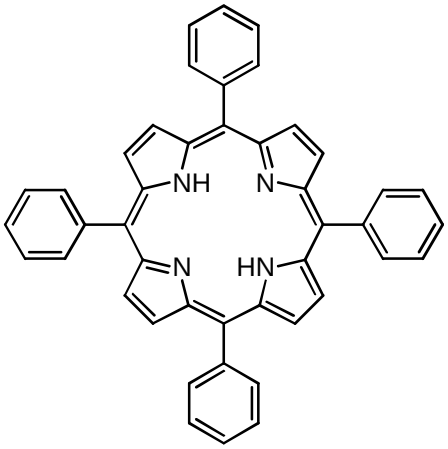

Tetra phenyl porphyrin (5)

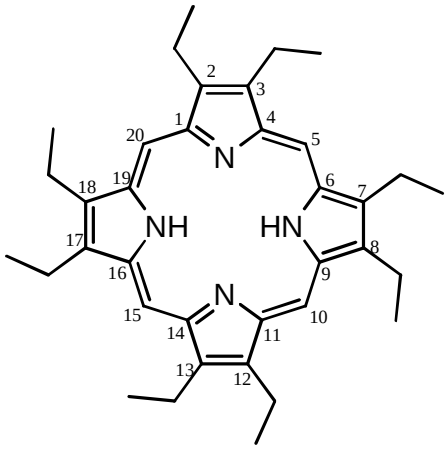

Octaethyl porphyrin (6)

Figure 1.1: Natural and synthetic porphyrins

The heme (1) is involved in the prosthetic group of cytochrome P450, horse-radish peroxidase and other iron enzymes.[2-4] The Mg complex of modified heme are called chlorophylls (2), which are green colouring matters of plants[5] (Figure 1.1) and involved in plant photosynthesis. Further, the Mg complexes of (3) are called bacteriochlorophyll and they are involved in photosynthesis in bacteria.

The spectral properties, macrocyclic aromaticities and properties of natural porphyrins (1 and 2) are comparable to synthetic porphyrins (3 and 4). Hence in the recent years the synthesis of various 5,10,15,20-tetraaryl porphyrins (5) and 2,3,7,8,12,13,17,18-octaethyl porphyrins (6) and their modifications at porphyrin core have been considered to understand the molecular mechanism of photosynthesis, mechanism of heme enzymes[6], development of porphyrinoid dyes[7] and solar photovoltaic cells[8].

1.2 Synthetic Methodologies of Porphyrins

The most of natural and synthetic porphyrins have been synthesized either by use of total synthesis and functionalization of a preformed porphyrin ring.

1.2.1 Total Synthesis

The retro analysis of porphine or porphyrin molecules predicts that porphyrins may be synthesized from monopyrroles i.e. reaction of pyrrole with aldehydes, substituted dipyyromethanes and their modifications, tripyrromethanes and their cyclization, and cyclization of open chain structures.

1.2.1.1 Monopyrrole and its modifications

The condensation of aryl aldehydes with pyrrole followed by oxidation with molecular oxygen in refluxing pyridine or propionic acid in open air has been developed by Rothermund[9] and Alder[10] respectively. The reaction of aryl aldehydes with pyrrole in acetic acid or propionic acid in presence of nitrobenzene followed by direct crystallization give the corresponding 5,10,15,20-tetraaryl porphyrins (7).[11] The effect of nitrobenzene as oxidant and aromatic agent has been reported in the oxidation of porphyrinogen to porphyrin and chlorin (Scheme 1.1).[12]

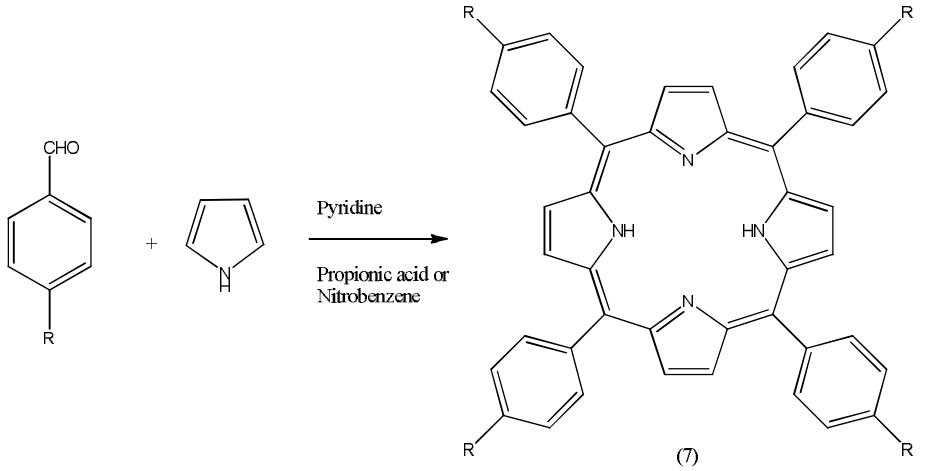

Scheme 1.1

Mixed cyclo-condensation of two aromatic aldehydes and pyrroles is an important method for the synthesis of the mixture of six porphyrins, which can be separated by extensive chromatography but with low yields (Scheme 1.2). These porphyrins are involved in various supramolecular models and material chemistry.

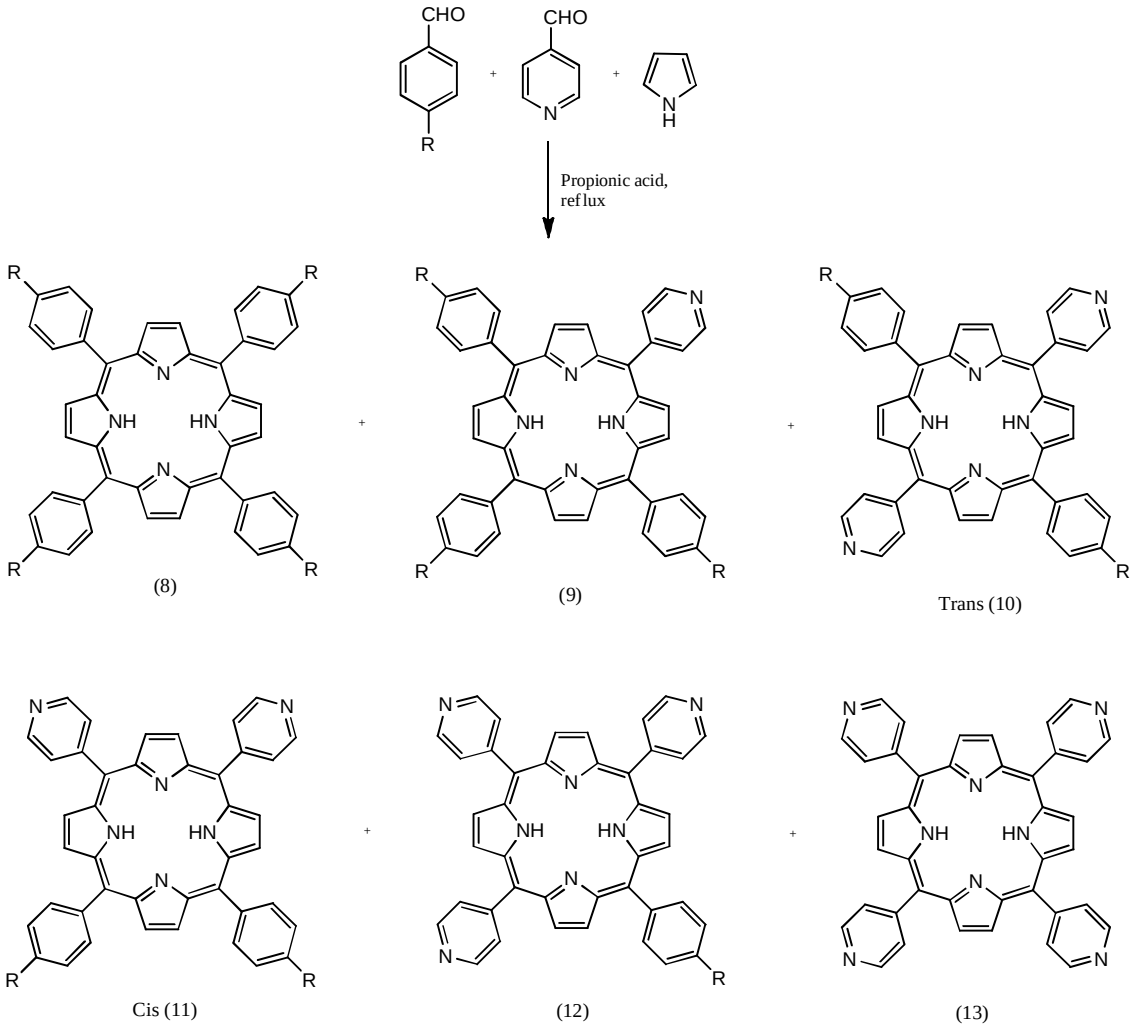

Scheme 1.2

The two step porphyrin synthesis has been developed by reactions of ortho substituted aryl aldehydes with pyrrole in presence of BF_3 etherate in dichloromethane that form the porphyrinogens (14), which are oxidized by DDQ or other oxidizing agents in dichloromethane yield to corresponding porphyrins (15) (Scheme 1.3).[13-15] Mixed aryl benzaldehyde and pyrrole cyclo-condensation methods have been used in the preparation of unsymmetrical porphyrins by modification of Lindsey method. The modification in the ratio of two aryl aldehydes gives a mixture of various isomers which can be separated by extensive column chromatography.

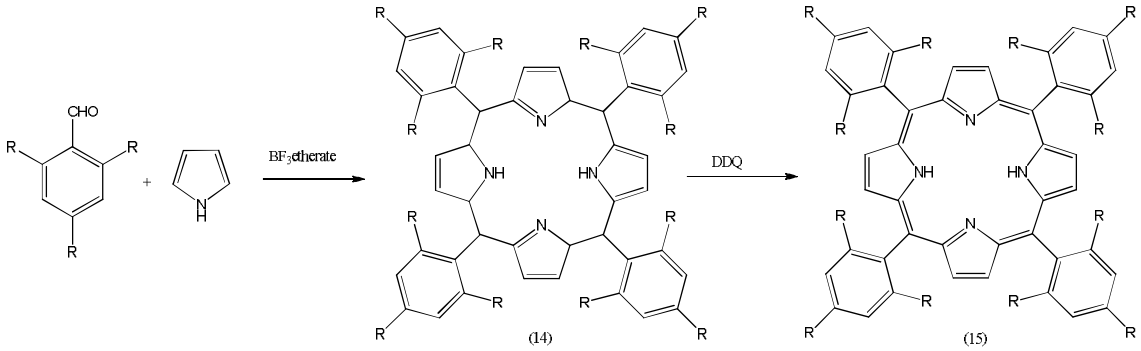

Scheme 1.3

1.2.1.2 Dipyrromethane and its modifications

The reaction of formaldehyde or aryl aldehydes with pyrrole in presence of acid originates a dipyrromethane.[16] The reaction of formaldehyde and aryl aldehyde with dipyrromethane in presence of acids forms porphine and 5,15-diaryl porphyrins (Scheme 1.4).[17]

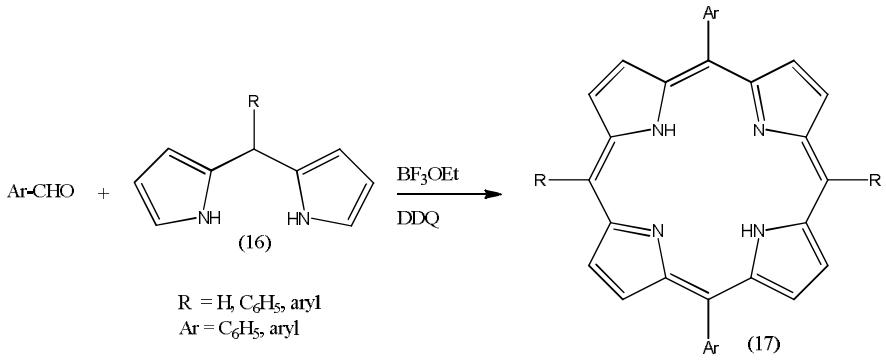

Scheme 1.4

The 2+2 approach has been used in the condensation reaction of dipyrromethane 2-carbinol and 1,9-dicarbinol dipyyromethane (18) in the synthesis of unsymmetrical 5,10,15,20- tetraryl porphyrins (19) (Scheme 1.5).[18,19]

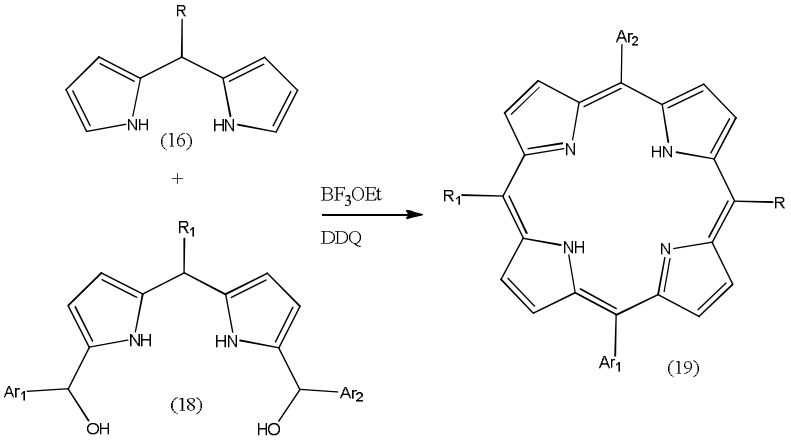

Scheme 1.5

1.2.1.3 Tripyrromethane

The reaction of 2,5-bis(hydroxymethyl)pyrrole (20) with excess pyrrole forms the tripyromethane (21)[19], which on subsequent reaction with 2,5-bis(hydroxymethyl)pyrrole (20) forms the porphine (Scheme 1.6).[20] The reaction of meso aryl tripyrromethane with 2,5-bis(α-hydroxy-α-phenyl) (22) methane in the presence of acids forms the porphyrins (23).[21] This method has also been used in the synthesis of cis-porphyrins and core modified porphyrins.

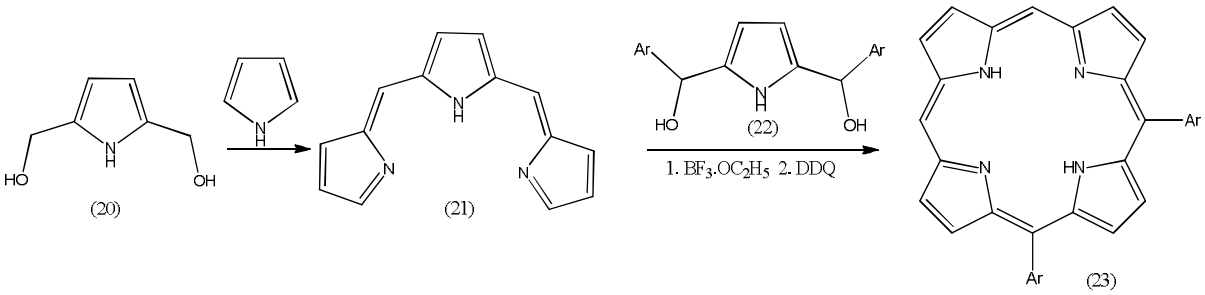

Scheme 1.6

1.2.1.4 Open chain cyclization

The reaction of open chain tetrapyrrole (24) forms the ABCD porphyrin in non-scrambling method. The $MgBr_2$/DBU mediated bilane (24) cyclization methods have been used in the synthesis of unsymmetrical porphyrins (25) (Scheme 1.7).[22,23] This method may also be used for the preparation of intrinsic chiral porphyrins.

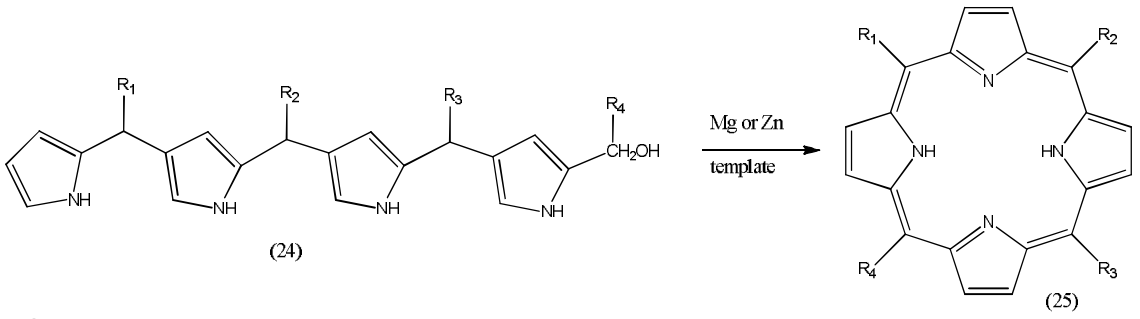

Scheme 1.7

1.2.2 Functionalization of the porphyrin periphery

Functionalization of porphyrin involves the modulation of various properties of porphyrin macrocycles and constructions of new valuable porphyrins. A brief survey of functionalization of periphery of porphyrins is given as follows.

1.2.2.1 Electrophilic substitution on porphyrin

Porphyrins are aromatic macrocyles[24] and they undergo various types of electrophilic substitution reactions in different reaction conditions.

1.2.2.1.1 Halogenation

Halogenation of porphyrins is important step in the peripheral modification of porphyrins in recent years. [25,26] The bromination of meso as well as β,β-substituted bromoporphyrins have been achieved by selection of brominating agents and types of porphyrins.[25,26]

The bromination of 5,10-diarylporphyrins (26) have been achieved with N-bromo succinimide in organic solvents gives 5-monobromo (27) and 5,10-dibromo (28) porphyrins (Scheme 1.8). The bromination of metallo-5,10,15,20-tetraphenyl porphyrin at β,β-position have been achieved by using Br_2 in organic solvents.

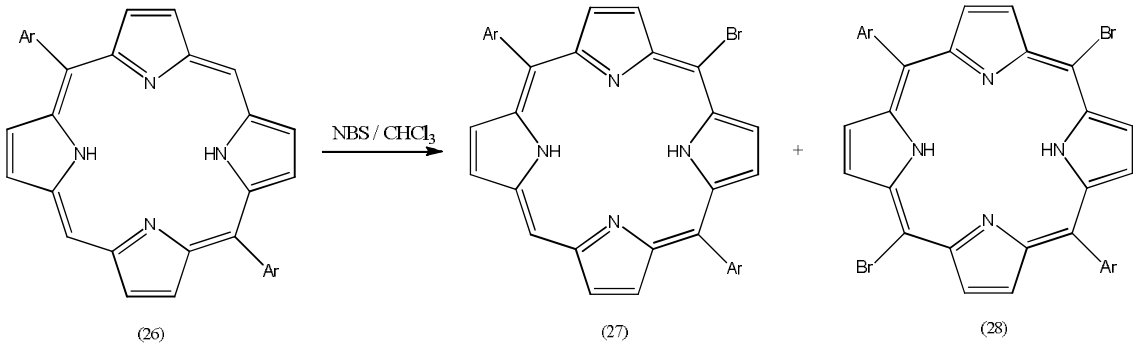

(26) (27) (28)

Scheme 1.8

1.2.2.1.2 Nitration

Nitration of porphyrins (29) can be achieved by various nitrating agents. The regioselective nitration of tetraphenyl porphyrins have been carried out with a mixture of nitric acid and acetic acid (Scheme 1.9).[27] The nitronium salts have been used in the nitration of selected porphyrins in milder conditions.[28]

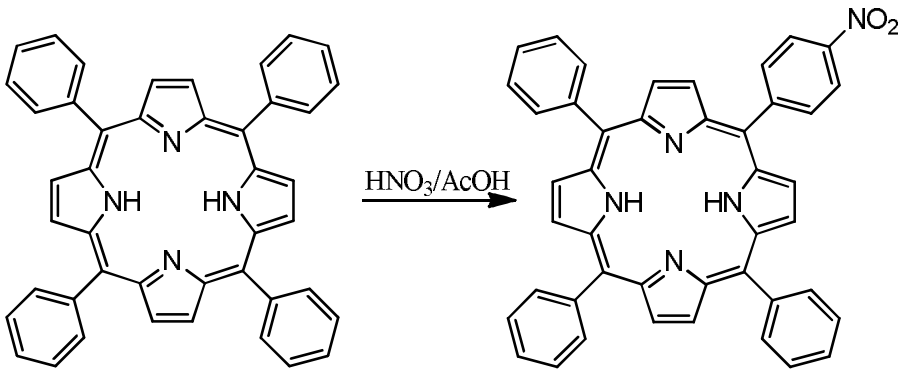

(29) (30)

Scheme 1.9

1.2.2.1.3 Sulphonation

The sulphonation of electron rich porphyrins have been realized by conc. H_2SO_4,[29] whereas sulphonation of electron deficient porphyrins (31) with fuming sulphuric acid, followed by reaction with sodium bicarbonate may be used the preparation of anionic water soluble porphyrin (32) (Scheme 1.10).[30] The sulphonation with conc. sulphuric acid gives better yields and cleaner products.

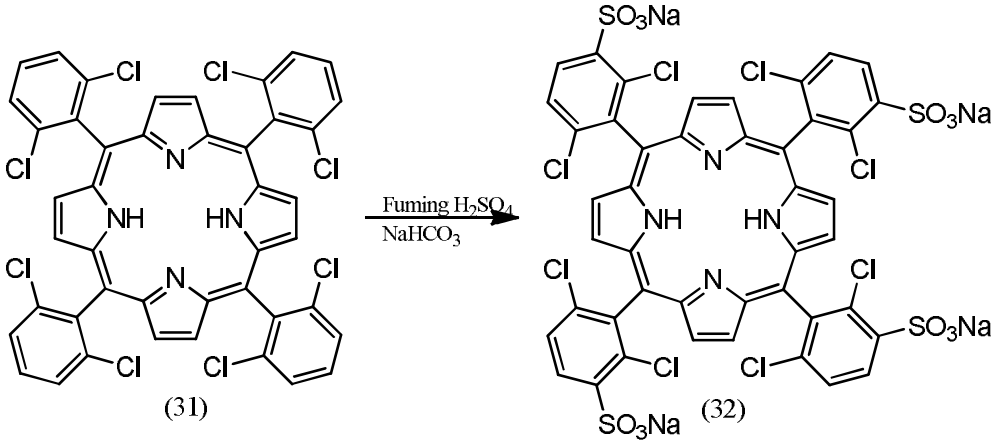

(31) (32)

Scheme 1.10

1.2.2.1.4 Formylation

Formylation of porphyrins at meso as well as β positions have been realized by selection of proper porphyrins and formylation reagents (Scheme 1.11).[31-33]

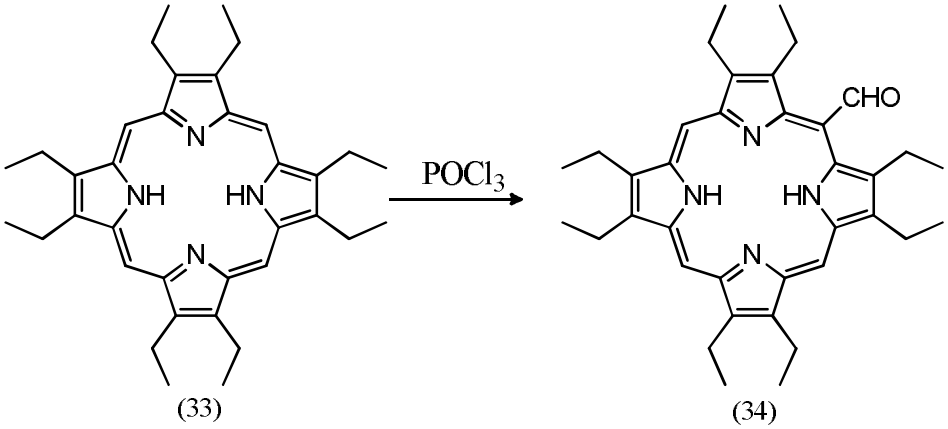

Scheme 1.11

1.2.2.2 Transition metal catalyzed reactions

Transition metal catalyzed coupling reactions of meso-halo porphyrins have been used in the carbon-carbon bond and carbon-hetero atom formation in porphyrin chemistry.[34-38]

The bromoporphyrins undergo the palladium(0) oxidative addition and reductive elimination by nucleophile releases the functionalized porphyrins.

Brominated porphyrins have been used in the cross coupling reactions including Heck[39,40], Suzuki[41-43], Sonogashira[44-47], Stille[48-50], Takahashi[51] and Negishi[52] reactions in the formation of carbon-carbon and carbon-hetero atom bond formation (Scheme 1.12).

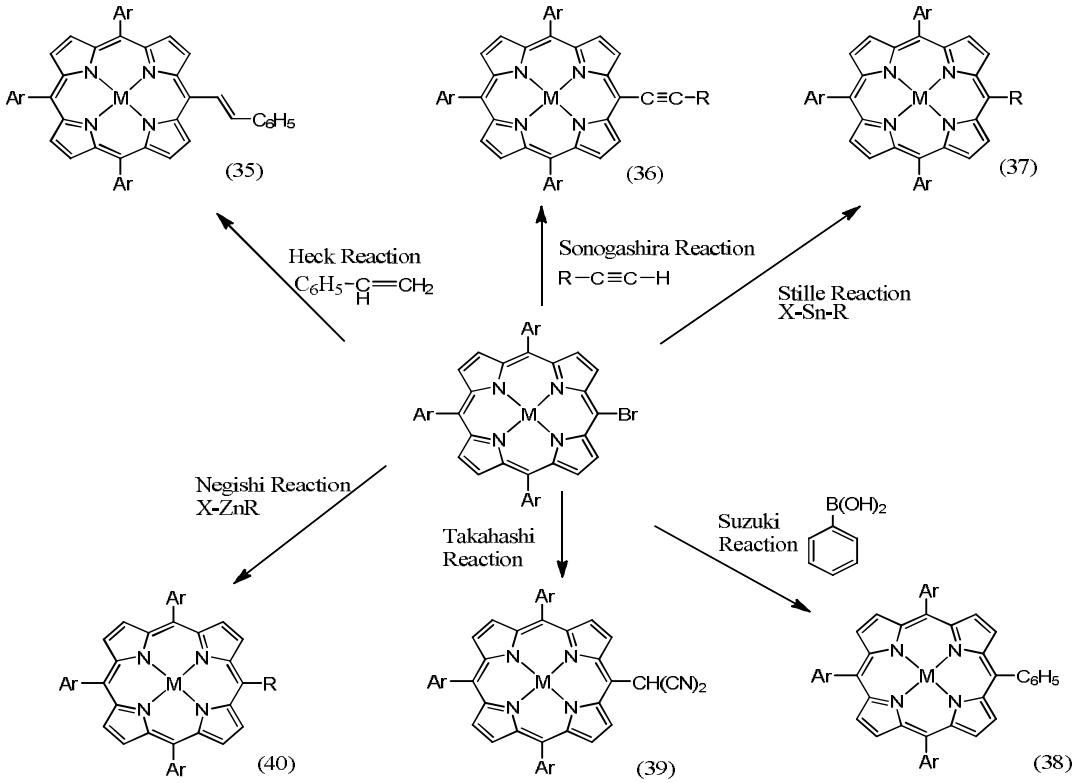

Scheme 1.12

1.2.2.3 Nucleophilic reactions

Organolithium and organomagnesium halides have been used for meso substitution in porphine to give unique and unknown symmetrical and unsymmetrical alkyl and aryl porphyrins.[53-54] The reaction of organic nucleophiles with porphine (4) at meso position yields an anionic species which is hydrolyzed to porphodimethene followed by oxidation with DDQ to yield the desired 5-substituted porphyrin (41) (Scheme 1.13). The synthetic applications have been observed by trapping the intermediate anion with electrophiles and transformation into meso-meso linked bis porphyrins.

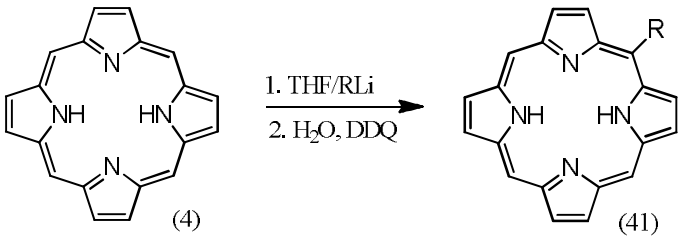

Scheme 1.13

Nucleophilic reactions with organometallic reagents followed by oxidations have been developed in the porphyrin chemistry.[55-56]

1.2.2.4 Iodium (III) reaction

The coupling reactions of a metalloporphyrins (42) have been easily and efficiently promoted by hyper valent iodine (III) and it has been used in the synthesis of diporphyrins and fused diporphyrins (43) (Scheme 1.14).[57-58] The porphyrin radical cation produced by single electron transfer oxidation coupled itself to form bis-porphyrins.

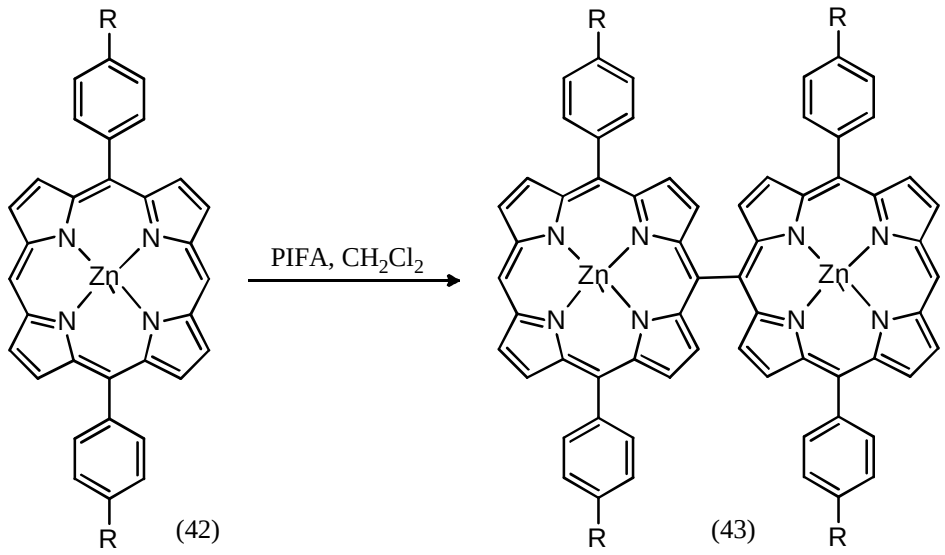

Scheme 1.14

Nucleophilic reactions involving porphyrin Π-cation radicals have been developed by use of iodinium salts in the preparation of valuable bis-porphyrins.[57-58] This oxidative coupling has been used in zinc chlorin monomers with phenyliodine bis(trifluoroacetate) to realize a regioselective oxidative coupling. Catalyst free nucleophilic substitution of meso-bromo porphyrin (44) with azide anion has been developed for the synthesis of useful meso-azido porphyrins (45) (Scheme 1.15).[59]

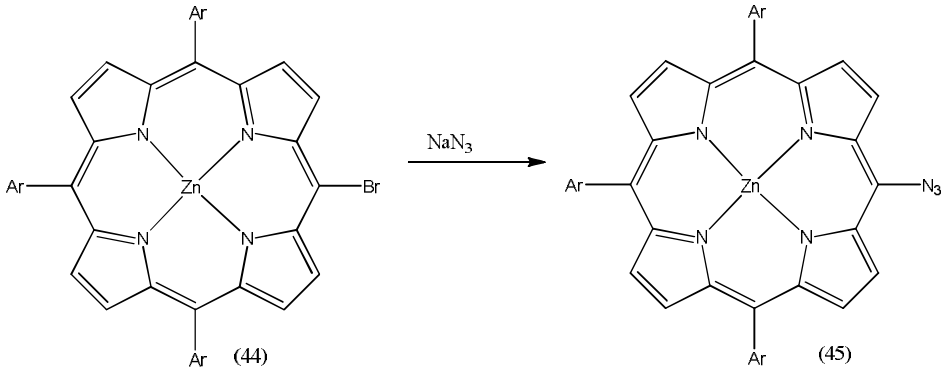

Scheme 1.15

Thus, functionalizations of the porphyrin periphery have been used in the construction of novel porphyrins with unique chemical, biological and optical properties derived from the extended Π electron system.

Further, the above methods have been used in the preparation of models for photosynthesis[60] and photonics.[61] These porphyrins derivatives also have been used in the development nanomaterials[62], supramolecular chemistry[63], and other newer fields in chemistry, biology and material chemistry.[64]

1.3 Porphyrin as Chiral Sensors

Chirality relates to molecules and supramolecular systems, atoms and other components that are asymmetrically arranged in three dimensions around a centre, axis or a plane. The chirality of a porphyrin arises from chiral substituents (intrinsic chirality) or by arrangement of achiral substituent along a chiral axis or on a chiral plane to tetrapyrrole ring of porphyrin. Chiral porphyrins are of special interest in molecular recognition, asymmetric catalysis and as optical probes.

Supramolecular chirogenesis is based on a smart combination of supramolecular chemistry and chirality science and deals with the various aspects of asymmetric induction, chirality transfer, amplification and modulation. These chiral processes are governed by non-covalent supramolecular forces such as hydrogen bonding, hydrophobic interaction and metal ligand binding. Porphyrins are ideal chromophores to study the processes of supramolecular chirogenesis due to their specific and highly appropriate spectral, physio-chemical and chemical properties, facial handling and superior propensity to form various supramolecular assemblies.[65-73]

In the formation of a chiral host-guest supramolecular complex between an achiral bis-zinc porphyrin and a chiral non-racemic guest, a CD response occurs in porphyrin spectral region which is diagnostic of the absolute configuration of guest. In the formation of 1:1 host-guest complex through bidentate metal coordination, chirality is transferred from the guest to host introducing a preferential chiral twist in the porphyrin-porphyrin arrangement and generates an exciton coupled CD response. The sign of soret CD couplet is related to the absolute configuration of the substrate and the intensity depends on structure of bis-porphyrin and reaction medium.

The exciton chirality rule has been exploited by strong theoretical basic which is applied to bis-porphyin supramolecular complexes to the relate the observed sign of the CD couplet to the relative spatial orientation exhibited by the chromophore in the supramolecular structure.[74] Theoretical calculations have been used to predict CD spectra from given supramolecular structures and their interactions with chiral molecules and their comparison with the experimental values are used in the rationalization of the supramolecular chirogenesis processes.[84,87]

The bis-porphyrin derivative (47) was easily synthesized in few steps starting from monoporphyrin (46) residue[83] and this Zn-tweezer (47a) is commercially available.[81] The achiral zinc bis(tetraphenyl) porphyrin tweezer is capable of binding to several chiral diamines. This results in formation of a supramolecular host-guest complex with preferred interporphyrin helicity which in fact reports and amplifies the chirality of the guest substrate.

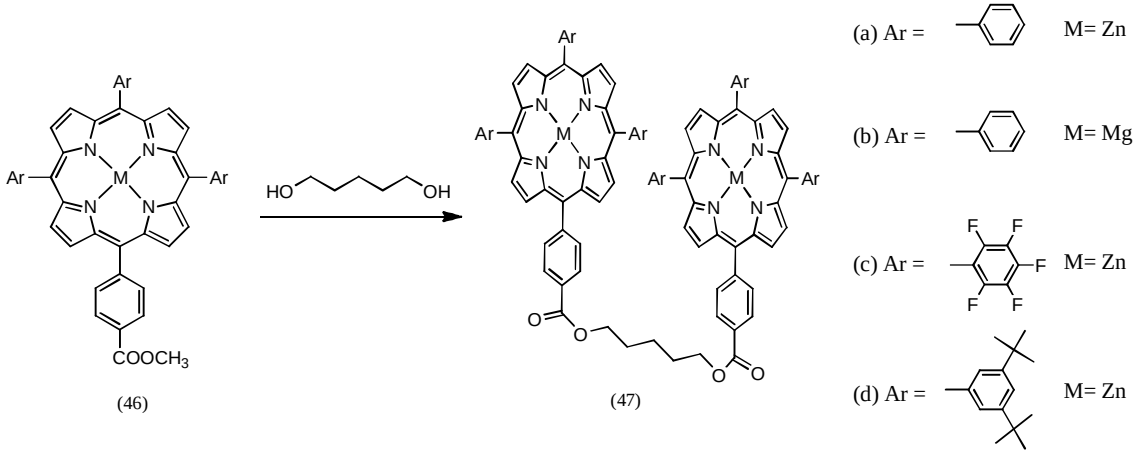

Scheme 1.16

The Mg-TPP tweezer (47b) was synthesized[76] and chirality of diamines was determined. The pentafluorinated (47c) is very useful host in case of very weak guest binding affinity.[80] The tert-butyl tweezer enhance the degree of interporphyrin stereo-differentiation and amplification of CD response.[82] Achiral bis-porphyrin (47d) tweezer receptors are powerful tools for the determination of absolute configurational analysis of organic compounds using CD than other bis porphyrins (47a-c).[81,83,88]

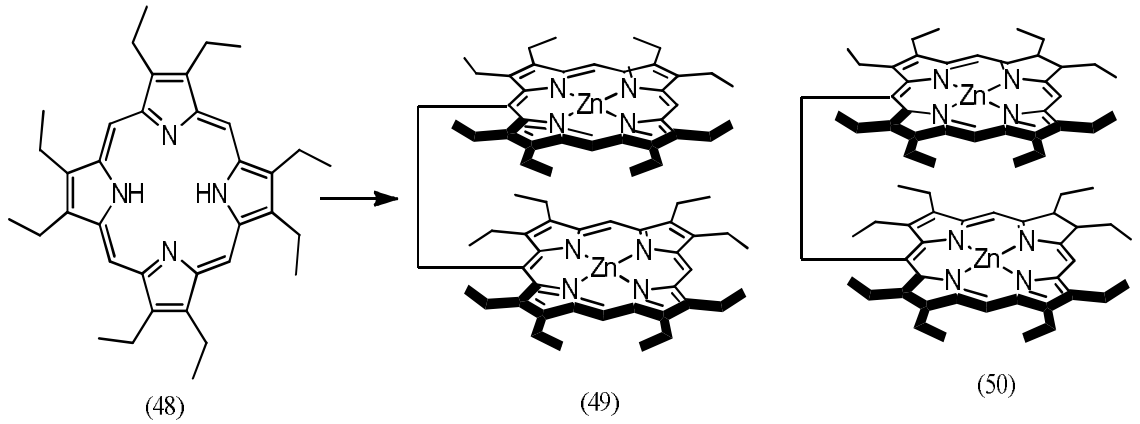

Scheme 1.17

The bis porphyrin (49) and bis chlorin (50) (Scheme 1.17) are in a syn "face to face" spatial conformational in nonpolar, noncoordinating solvents owing to the strong interaction between porphyrin subunits.[78,89] Interaction with an external guest induces a conformational rearrangement to yield the extended anti-form in the case monodentate guests or gives the tweezer type structure in the case of bidentate guests. The binding events are highly cooperative regardless of the chirality of guest. The zinc-1,2- bis (meso-octaethylporphyrinyl) ethane are used in the determination of syn-anti conformational switching and configuration of organic compounds.[78] The optical activity modulation of bis-chlorin versus bis porphyrin in the chiral hosts by interaction with chiral amines have been investigated by UV-visible, CD and ^{1}H NMR spectroscopy.[89]

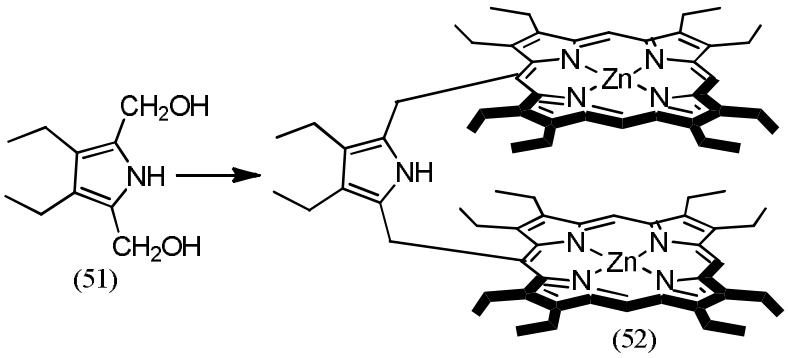

Scheme 1.18

The pyrrole derivatives of bis-porphyrin derivatives (52) have been synthesized and tweezer conformation induced by axial ligands (Scheme 1.18).[90,77] The modified di-zinc bis-porphyrins (54) have been synthesized starting from dialdehyde (53) and induction of supramolecular chirality in (54) via tweezer formation has been rationalized (Scheme 1.19).[75]

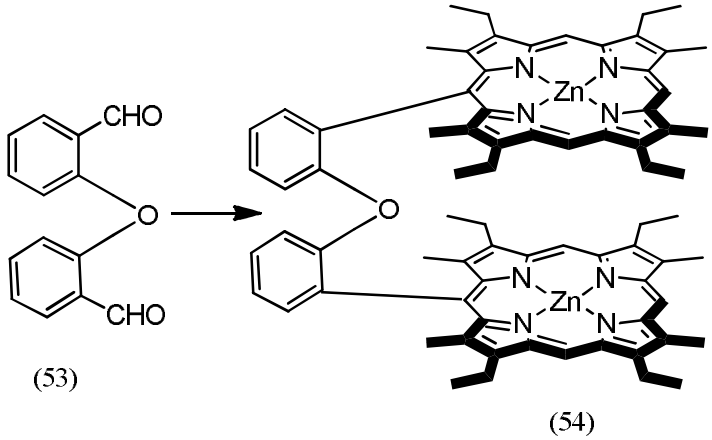

Scheme 1.19

The Zn and Rh porphyrins (57) have been synthesized by reaction of pyridine derivative (55) and amino porphyrin (56) (Scheme 1.20). The influence of the solvents and metal centre on supramolecular chirality induction with bis-porphyrins (57) have been examined.[79]

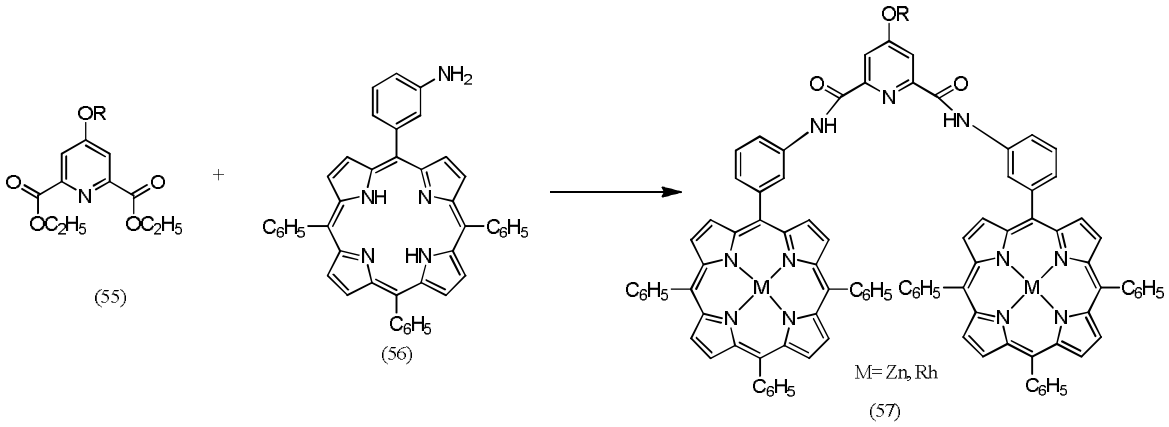

Scheme 1.20

The unique temperature dependent reactivity of cyanuric chloride (58) toward nucleophiles (Scheme 1.21) and subsequent metallation with metal salts in methanol have been used in synthesis of 2-piperidino-4,6-bis(5-aminophenyl,10,15,20-phenyl) porphinato zinc (60a).[91] This has been used as CD probes for molecular chirality.[95,96] The reaction of 5-(4-aminophenyl)-10,15,20-trimesityl porphyrin (59b)[93] with cyanuric chloride and subsequent metallation reaction with zinc acetate give corresponding bis-porphyrin (60b).[98] Further, "one flask" synthetic protocol has been used for the reaction of 5-(4-aminophenyl)-10,15,20-tri(3',5'-tertbutyl)phenyl porphyrin (59c) with cyanuric chloride and subsequent reaction with zinc acetate give the bis porphyrin (60c) (Scheme 1.21).[99]

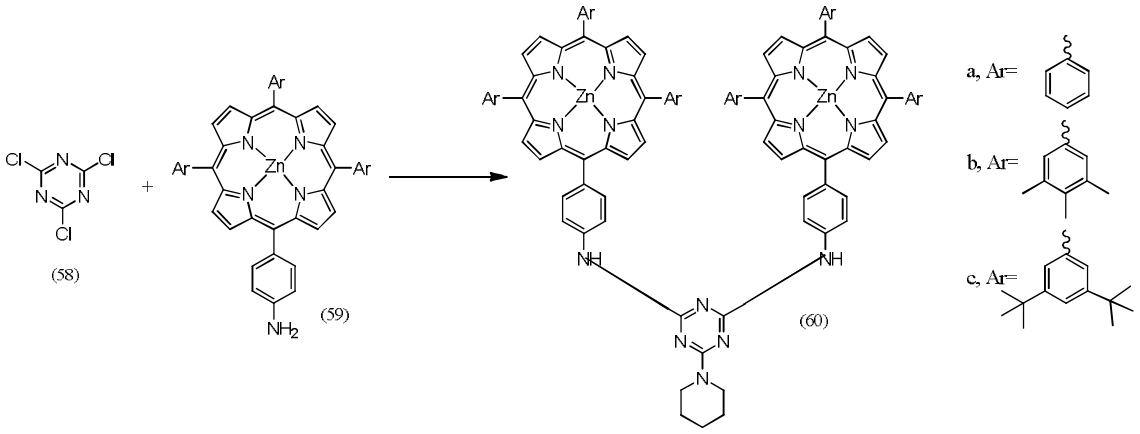

Scheme 1.21

A combined approach based on an experimental CD analysis and a theoretical prediction of the prevailing inter-porphyrin helicity demonstrate that above tweezers display favourable properties for chiral recognition of diverse set of chiral guests such as 1,2-diamines, α-amino acid esters and amides, secondary alcohols and 1,2-amino alcohols. The bulky periphery and presence of a rigid porphyrin linkage leads to a more enhanced CD sensitivity than that reported for other tweezers.[99]

1.4 Porphyrin in Dye sensitized solar cells

The dye sensitized solar cells represent one of the most promising area of research for the development of affordable, high performance and clean energy reserve.[100] In photosensitized solar cells, a thin layer of a dye sensitizer, chemically bound to nanoporous TiO_2 is photoexcited and ultimately provide a photo current. Metal free organic dyes have been used as sensitizer, but the most efficient ones results in cell efficiency in the range of 9-10%.[101]

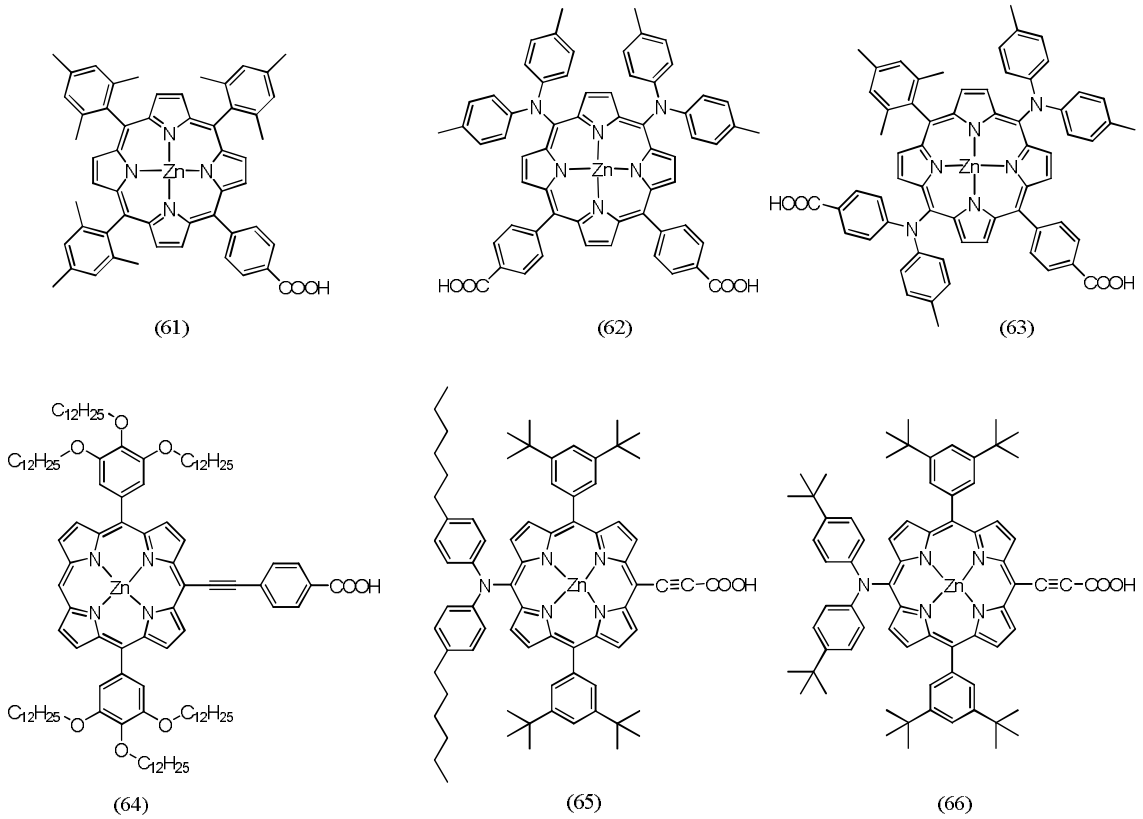

Figure 1.2: Porphyrin derivatives for DSSC

Porphyrin derivatives exhibit intense absorption band in 420-450 nm and moderate Q bands in the 550-650 nm regions. Further, the orbital energy levels allow for efficient electron injection into the TiO_2 band and regeneration of the oxidized dye by the electrolyte in solar cells. The suitable functionalization of porphyrin ring, either in the meso or β-positions, allows for their spectral and redox properties tuning, thus allowing the control of solar cell efficiency.

The zinc complex of porphyrin (61) was synthesized to increase the solubility and reduce the aggregation. The Cis-porphyrin (62) and Trans-porphyrin (63) possess two aryl amino groups at the 5,10-meso position and 5,15-meso position have been synthesized and power efficiency conversion of Cis (5.5%) and Trans (3.8%) has been observed.[102] The diarylamino group attached to the porphyrin ring as electron donor and ethynylbenzoic acid as acceptor with Soret band at 460 nm with efficiency of 11.9 % is reported.[103] The porphyrins with ortho-substituted alkoxy groups and electron donating and withdrawing groups porphyrin having efficiency conversion 10.17% have also been reported (Figure 1.2).[104]

The different carboxy group at β-position have been synthesized by Knoevenagel condensation and Sonogashira coupling having efficiency upto 5.08% have been reported.[105] Recently, two novel porphyrin dyads with 1,3,5-triazine bridged have been synthesized which shows an efficiency upto 5%.[106]

However, mass production and long term thermal stability of porphyrins are the major concern owing to an expensive palladium catalyzed step in the preparation and presence of an unstable ethynyl bridged unit.[107-111] Therefore in search of simple, efficient and cost effective sensitizers, an attempt of the synthesis of various zinc porphyrins by mixed condensation methods, metallation and base hydrolysis forms the corresponding carboxy derivatives. A series of attempts have been made for the synthesis of selected porphyrins by use of click chemistry.

1.5 Click reaction in Porphyrin chemistry

A greener and high efficient method in organic synthesis have been developed in recent years due to threat of global warming climate change.[112-114] "Click chemistry", in particular Huisgen reaction, has emerged as a convenient and effective approach for the preparation of a large amount of novel compounds with desired functionalities.[115-119] This reaction

describes the formation of triazoles from copper (I)-catalysed 1,3-dipolar cycloaddition of azides with alkynes (Scheme 1.22). It can be conducted in mild conditions, in various solvents, with generally high yields and independently of the steric hindrance and of the electronic properties of the reagents, with both electron-rich or electron–deficient substrates.

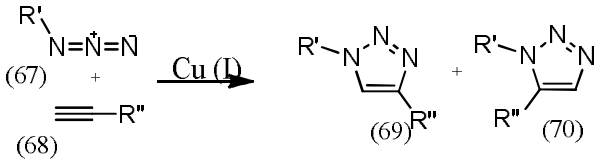

Scheme 1.22

The original version of the Huisgen 1,3-dipolar cycloaddition between an azide (67) and an alkyne (68) furnishes a mixture of the 1,4- and the 1,5-regioisomer and this requires further purification.[118,119]

Copper catalyzed Azide-Alkyne cycloaddition reaction is one of the best click reaction to date.[115-121] It has enormous rate acceleration of 10^7 to 10^8 compared to uncatalyzed 1,3-dipolar cycloaddition reaction. It proceeds over a broad temperature range, insensitive to aqueous conditions, a broad pH range and a plethora of functional groups. A pure product can be isolated by simple filtration or extraction without the need of chromatography or crystallization.

Introduction of a 1,2,3-triazole into the porphyrin impose interesting and different properties to the porphyrin ring. Recently various groups have applied click chemistry for synthesis of novel porphyrins. Coupling of azido zinc porphyrin (71) with ethylnyl phenyl zinc porphyrin (72) led to formation of bisporphyrin (73) (Scheme 1.23).[120] The reactions of azido porphyrins (74) with several terminal alkynes (75) were investigated using different catalytic systems (1.24). Copper carbene (SIMes)CuBr was found to be better catalyst than most of the usual copper complexes used for this transformation (Scheme 1.23).

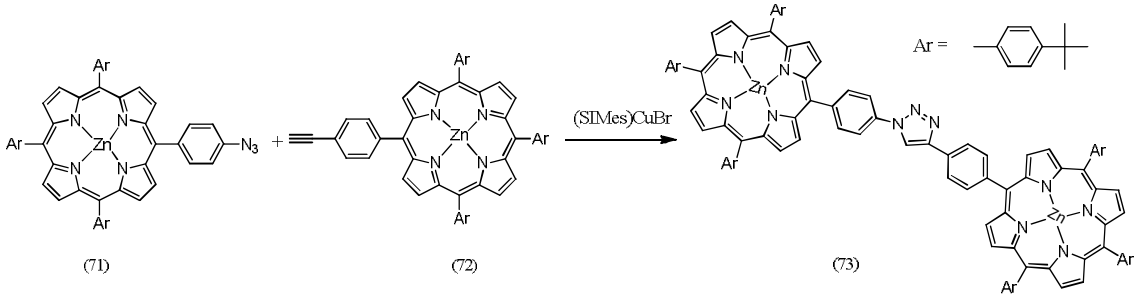

Scheme 1.23

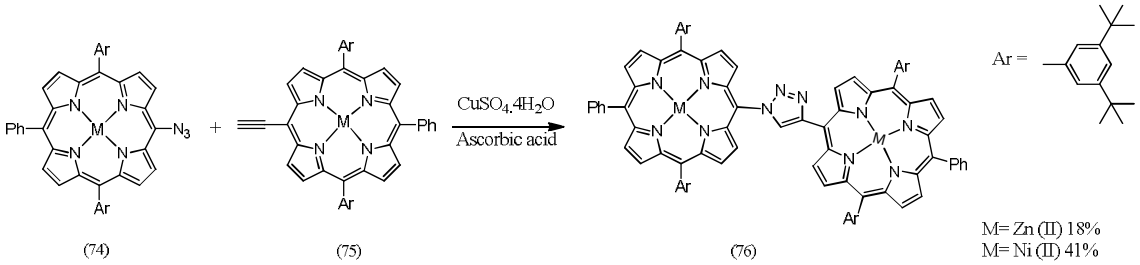

(74) (75) (76)

Scheme 1.24

Cu(I)-catalyzed 1,3-dipolar cycloaddition β-azidotetraarylporphyrins (77) with alkynes (78) have been reported effectively to introduce the triazolyl group into the porphyrin periphery (Scheme 1.25).[121]

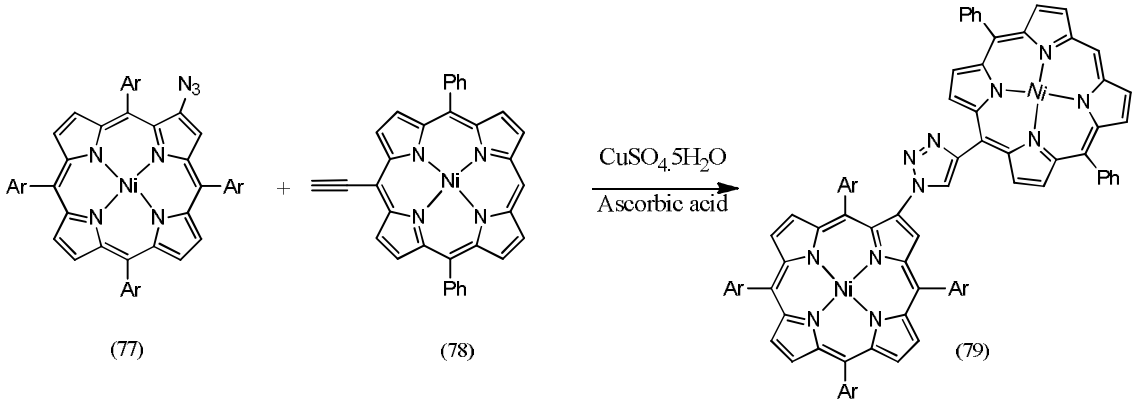

(77) (78) (79)

Scheme 1.25

A triazole-bridged porphyrin dyad containing N_2S_2 porphyrin and N_4 or ZnN_4 porphyrin subunits have been synthesized using click chemistry (Scheme 1.26).[122] The singlet-singlet energy transfer from the N_4 or ZnN_4 porphyrin subunit to the N_2S_2 porphyrin subunit has been demonstrated by fluorescence studies. A triazole ring has been reported to be a better linker for energy transfer from donor to acceptor unit compared to ethyne (Scheme 1.26).

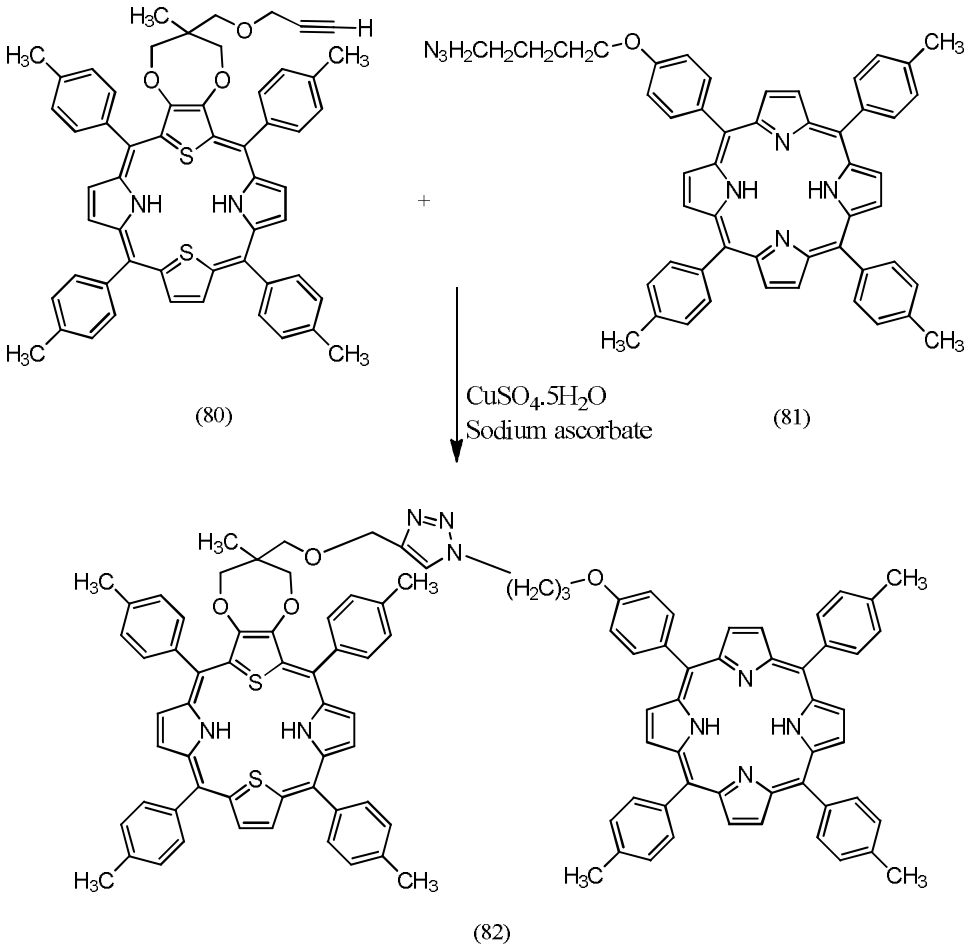

Scheme 1.26

The core modified azido porphyrins (83) have been used to synthesize the triazole-bridged unsymmetrical porphyrin dyads containing two different types of porphyrin sub-units (85) (Scheme 1.27) as well as the triazole-bridged porphyrin-ferrocene conjugates (86) under Cu(I)-catalyzed “click” reaction conditions (Scheme 1.28).

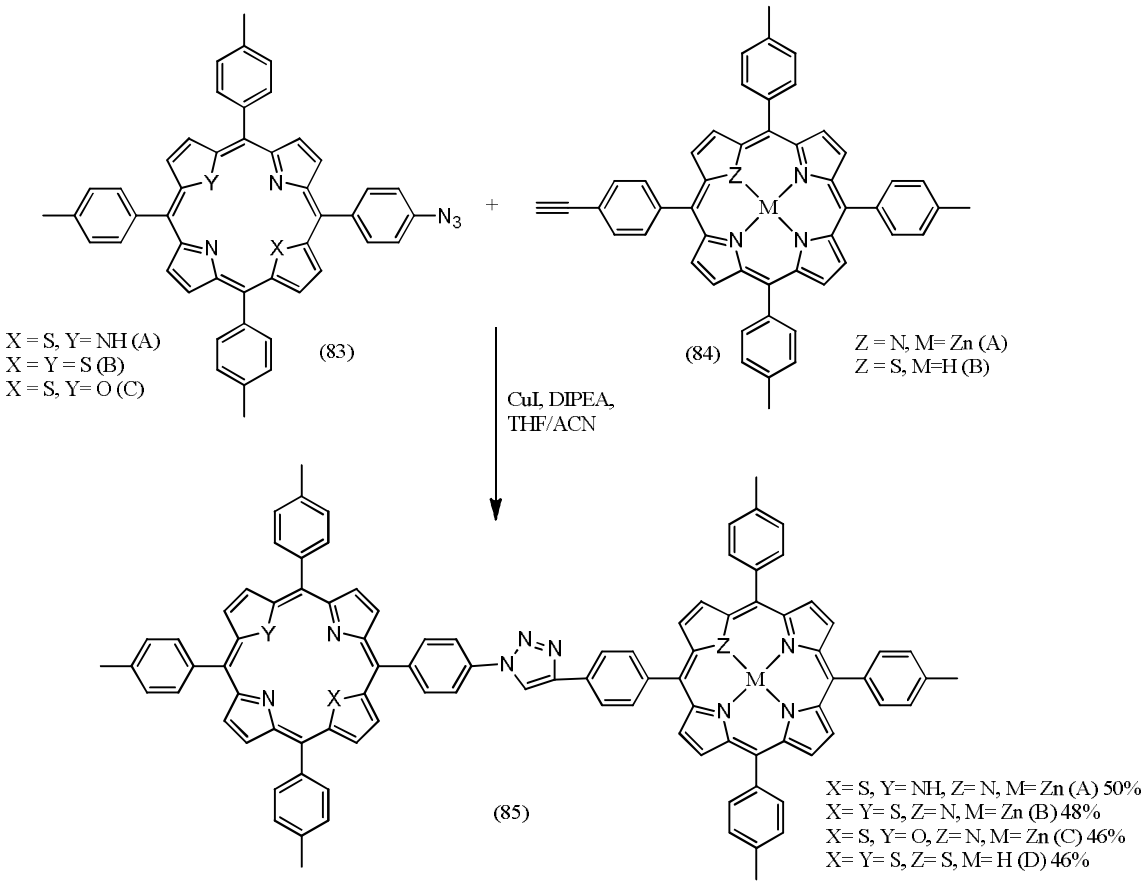

Scheme 1.27

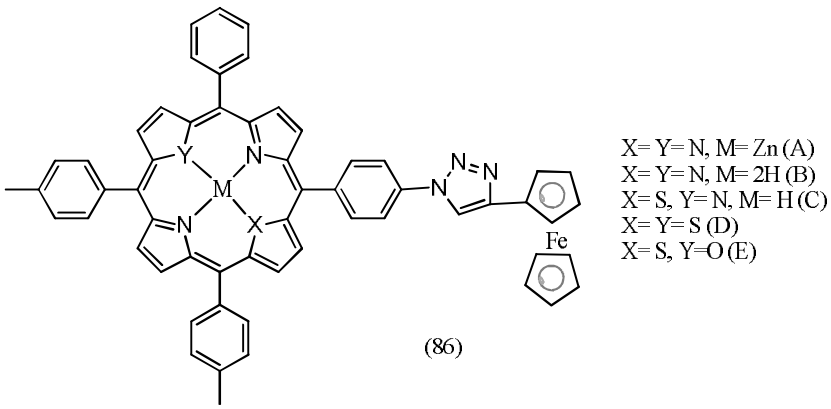

Scheme 1.28

Porphyrin quinolone conjugates with triazole appended porphyrin systems (88) have been prepared *via* 1,3-dipolar cycloaddition of an azidoquinolone to porphyrins bearing alkynyl groups (87). Meso-Tetrakis (pentafluorophenyl)porphyrin reacted with propargyl alcohol to afford porphyrins substituted with one, two, three or four prop-2-yn-1-yloxy groups in the 4-position of the meso-aryl groups (Scheme 1.29).[124]

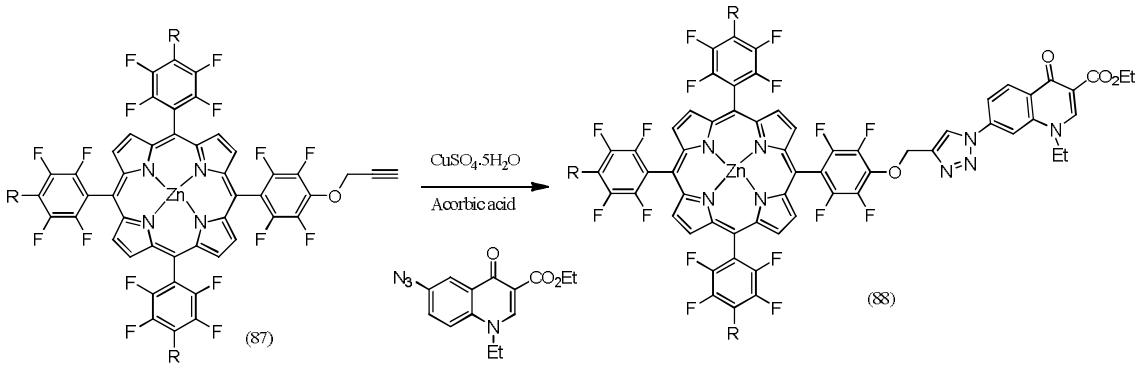

Scheme 1.29

A microwave assisted a sequential "double click" reaction from bis-azide porphyrin (89) where one carbohydrate moiety was introduced (90) followed by addition of a second onto the "latent" azide could be achieved to access a new class of bis-modified 5,10-diglycoporphyrins (91) displaying heterogeneous carbohydrates (Scheme 1.30).[125]

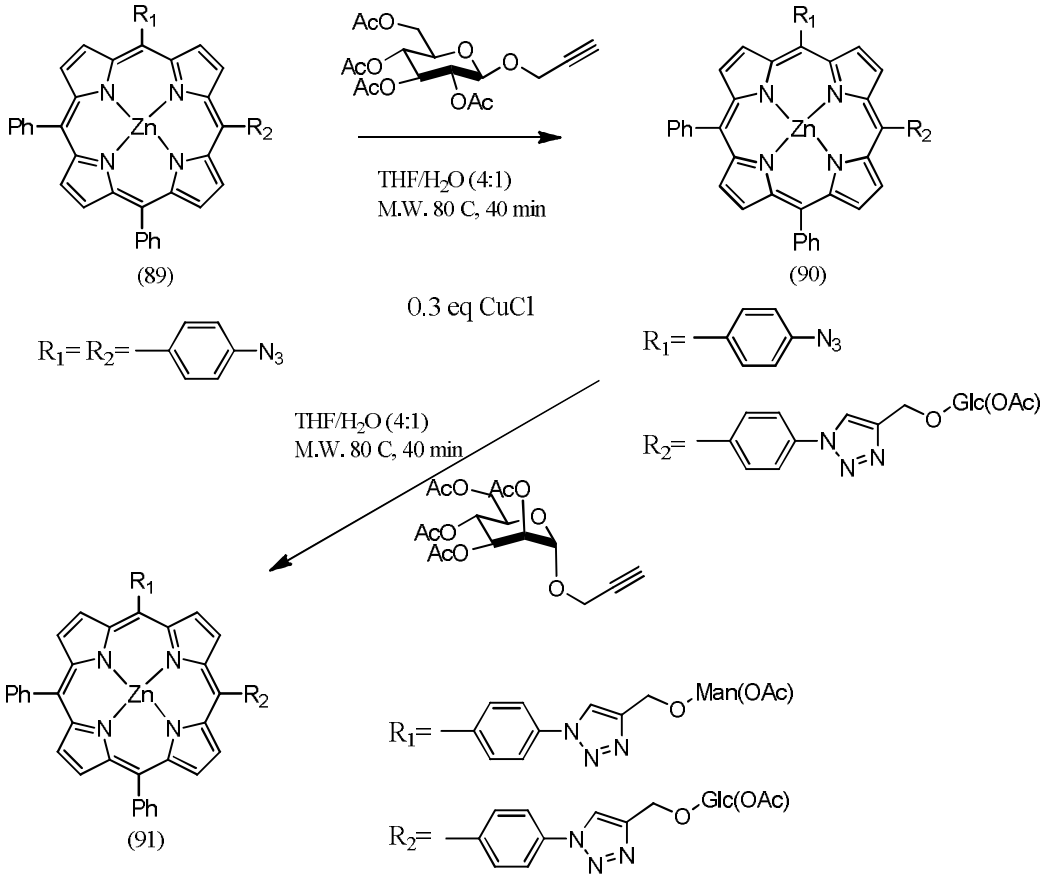

Scheme 1.30

A water-soluble derivative of N-fused porphyrin (NFP) possessing a nona-arginine (R9) peptide tail have been synthesized by a Cu(I)-catalyzed azide-alkyne 'click' reaction starting from N-fused porphyrin (92). Nona-arginine (R9) is a member of peptides showing cell penetrating ability. N-Fused porphyrin (NFP) is a porphyrin analogue with an 18p aromaticity derived from a tetrapyrrolic macrocycle. A notable feature of NFP is its optical property that absorbs NIR light over 1000 nm. Such unusual long wavelength absorption of NFP is supposed to originate from its characteristic tri-pentacylic unit, by which a HOMO–LUMO gap of the macrocycle would become smaller than ordinary porphyrins (Scheme 1.31).[126]

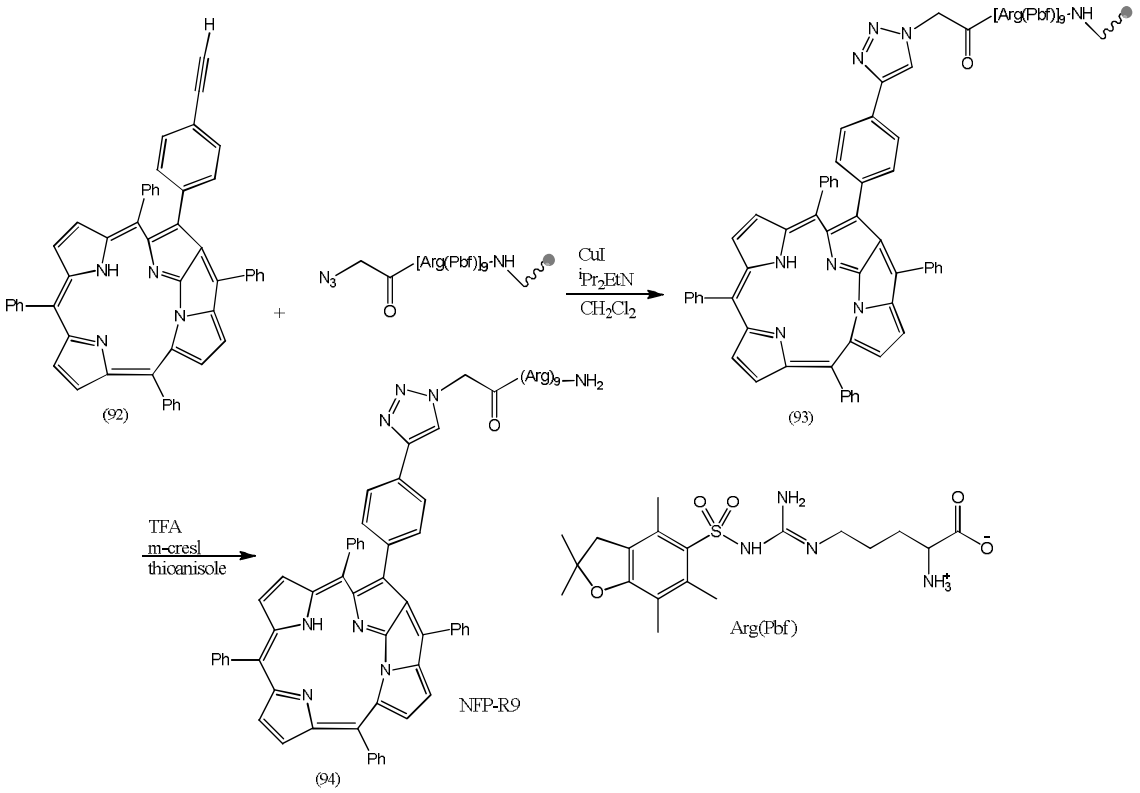

Scheme 1.31

Coupling of azido- Zn porphyrins (95) with single-walled carbon nanotubes (SWNTs) have been reported.[127] SWNT-ZnP, a first-generation dendron bearing two ZnP was chosen, due to its large absorption cross section, for attachment to SWNT. The syntheses of the dendrons were based on click chemistry (Scheme 1.32).

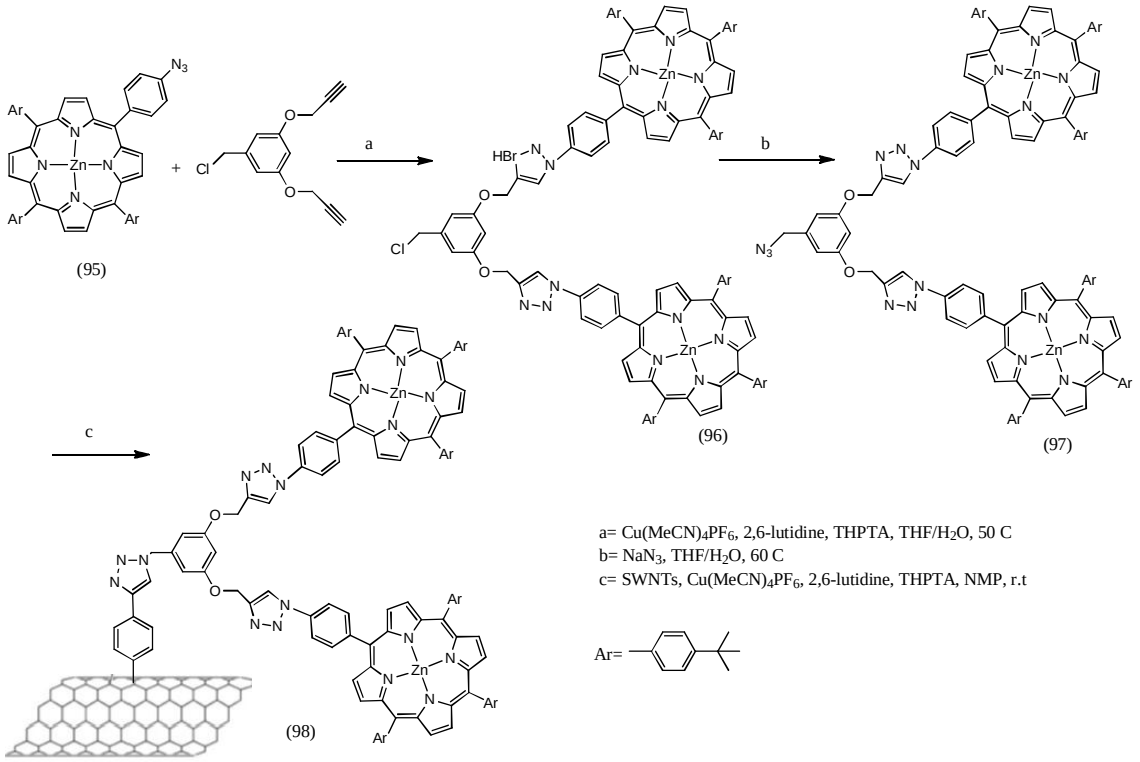

Scheme 1.32

The Cu (I) catalyzed alkyne-azide cycloaddition have also been employed to synthesize dendritic fulleropyrrolidine (101), bearing two bending porphyrins (Scheme 1.33).[128] The electron donor-acceptor conjugate possesses a shape that allows the formation of supramolecular complexes by encapsulation of C_{60} within the jaws of the two porphyrins of another molecules.[128] Chiroselective assembly of a chiral porprhyrins-fullerene dyad have been synthesized by Click reactions.[129] The chirality of amphiphilic D-A dyad plays an important role in generating a supramolecular architecture capable of efficient charge transporter for large distance.[129] Cu (I) catalyzed azide-alkyne cycloaddition reaction has been employed to synthesize donor-acceptor energy transfer arrays with 4,4-difluro-4-bora-3a,4a-diaza-s-indacene and zinc porprhyrins.[130]

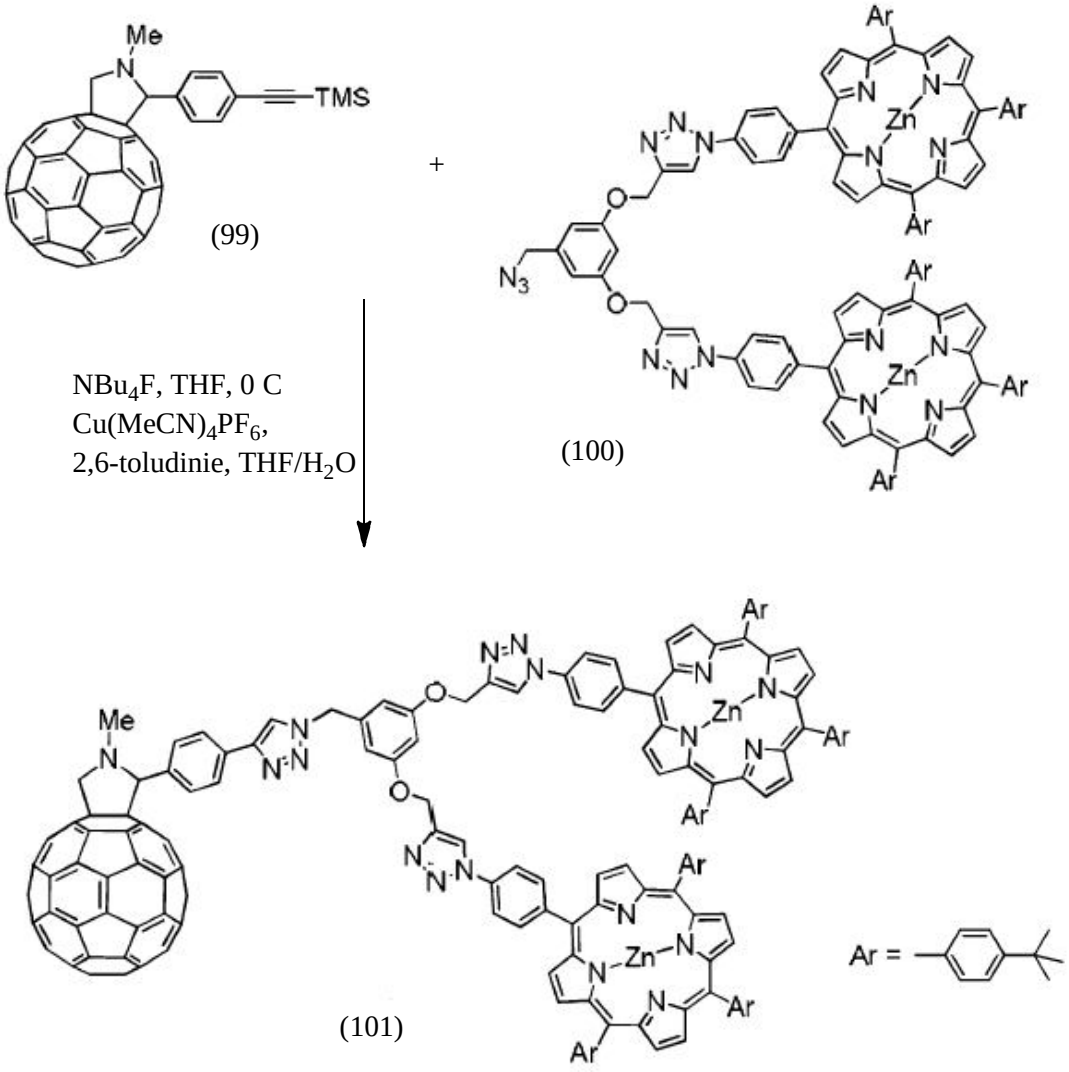

Scheme 1.33

Photophysical characterization and DFT electronic structure modelling of the different arrays are consistent with efficient Foster resonance energy transfer from the BODIPY donors to the zinc-tetraphenyl porphyrin acceptor.[130]

Thus, the above examples of various conjugated of porphyrin with different chromophores have been synthesized by Cu(I) catalyzed alkyene-azide cycloaddition reactions. Hence, Cu(I) catalyzed reactions have been used in the synthesis of various porphyrin derivatives from suitable porphyrin precursors.

REFERENCES

1. A. R. Battersby, *Nat. Prod. Rep.*, **2000**, *17*, 507-526.
2. A. R. M. Soares, D. R. Anderson, V. Chandrashaker and J. S. Lindsey, *New J. Chem.*, **2013**, *37*, 2716-2732.
3. M. Ethirajan, Y. Chen, P. Joshi and R. K. Pandey, *Chem. Soc. Rev.*, **2011**, *40*, 340-362.
4. K. S. Suslick, N. A. Rakow, M. E. Kosal and J. Chou, *J. Porphyrins Phthalocyanines*, **2000**, *4*, 407-413.
5. R. Tanaka and A. Tanaka, *Annu. Rev. Plant Biol.*, **2007**, *58*, 321-346.
6. W. Nam, *Acc. Chem. Res.*, **2007**, *40*, 522-531.
7. I. Radivojevic, A. Varotto, C. Farley and C. M. Drain, *Energy Environ. Sci.*, **2010**, *3*, 1897-1909.
8. M. G. Walter, A. B. Rudine and C. C. Wamser, *J. Porphyrins Phthalocyanines*, **2010**, *14*, 759-792.
9. P. Rothemund, *J. Am. Chem. Soc.*, **1935**, *57*, 2010.
10. A. D. Adler, F. R. Longo, J. D. Finarelli, J. Goldmacher, J. Assour and L. Korsakoff, *J. Org. Chem.*, **1967**, *32*, 476.
11. A. M. d'A. R. Gonsalvez, J. M. T. B. Varejao and M. M. Pereira, *J. Heterocycl. Chem.*, **1991**, *28*, 635.
12. R. A. Johnstone, M. L. Nunes, M. M. Pereira, M. R. Gonsalves and A. C. Serra, *Heterocycles*, **1996**, *43*, 1423.
13. J. S. Lindsey, I. C. Schreiman, H. C. Hsu, P. C. Kearney and A. M. Marguerettaz, *J. Org. Chem.*, **1987**, *52*, 827-836.
14. J. S. Lindsey and R. W. Wagner, *J. Org. Chem.*, **1989**, *54*, 828-836.
15. J. S. Lindsey, *Acc. Chem. Res.*, **2010**, *43*, 300-311.
16. J. K. Laha, S. Dhanalekshmi, M. Taniguchi, A. Ambroise and J. S. Lindsey, *Org. Process Res. Dev.*, **2003**, *7*, 799-812.
17. G. R. Geier, J. B. Callinan, D. P. Rao and J. S. Lindsey, *J. Porphyrins Phthalocyanines*, **2001**, *5*, 810-823.
18. D. K. Dogutan, M. Ptaszek and J. S. Lindsey, *J. Org. Chem.*, **2008**, *73*, 6187-6201.
19. Y. Kita, H. Maekawa, Y. Yamasaki and I. Nishiguchi, *Tetrahedron*, **2001**, *57*, 2095-2102.
20. M. O. Senge, *J. Porphyrins Phthalocyanines*, **2010**, *14*, 557.
21. C. H Lee, J. Y. Park and H. J. Kim, *Bull. Korean. Chem. Soc.*, **2000**, *21*, 97-100.

22. D. K. Dogutan, S. H. H. Zaidi, P. Thamyongkit and J. S. Lindsey, *J. Org. Chem.,* **2007**, *72*, 7701-7714
23. P. D. Rao, S. Dhanalekshmi, B. J. Littler and J. S. Lindsey, *J. Org. Chem.*, **2000**, *65*, 7323-7344.
24. J. I-C. Wu, I. Fernández and P. V. R. Schleyer, *J. Am. Chem. Soc.*, **2013**, *135*, 315-321.
25. A. Kato, R. D. Hartnell, M. Miyasaka, K. Suigiura and D. P. Arnold, *J. Porphyrins Phthalocyanines*, **2004**, *8*, 1222-1227.
26. D. E. Chumakov, A. V. Khoroshutin, A. V. Anisimov and K. I. Kobrakov, *Chem Heterocyclic Compounds*, **2009**, *45*, 259-283.
27. W.J. Kruper, T.A. Chamberlin and M. Kochanny, *J. Org. Chem.*, **1989**, *54*, 2753.
28. N. W. Smith and S. V. Dzyuba, *Arkivoc.*, **2010**, *7*, 10-18.
29. C. A. Busby, R. K. Dinello and D. Dolphin, *Can. J. Chem.*, **1975**, *53*, 1554.
30. T. P. G. Sutter, R. Rahimi, P. Hambright, J. C. Bommer, M. Kumar and P. Neta, *J. Chem. Soc. Faraday Trans.*, **1993**, *89*, 495.
31. E. E. Bonfantini, A. K. Burrell, W. M. Campbell, M. J. Crossley, J. J. Gosper, M. M. Harding, D. L. Officer and D. C. W. Reid, *J. Porphyrins Phthalocyanines*, **2002**, *6*, 708.
32. A. M. G. Silva, M. A. F. Faustino, T. M. P. C. Silva, M. G. P. M. S. Neves, A. C. Tomé, A. M. S. Silva and J. A. S. Cavaleiro, *J. Chem. Soc. Perkin Trans.*, **2002**, *1*, 1774-1777.
33. A. M. G. Silva, A. C. Tomé, M. G. P. M. S. Neves, A. M. S. Silva and J. A. S. Cavaleiro, *J. Org. Chem.*, **2002**, *67*, 726-732.
34. H. Shinokubo and H. Osuka, *Chem. Commun.*, **2009**, 1011-1021.
35. S. Shanmugathasan, C. Edwards and R. W. Boyle, *Tetrahedron*, **2000**, *56*, 1025-1046.
36. J. Setsune, *J. Porphyrins Phthalocyanines*, **2004**, *8*, 93-102.
37. N. Sugita, S. Hayashi, F. Hino and T. Takanami, *J. Org. Chem.*, **2012**, *77*, 10488-10497.
38. H. Yorimitsu and A. Osuka, *Asian J. Org. Chem.*, **2013**, *2*, 356-373.
39. S. Shanmugathasan, C. K. Johnson, C. Edwards, E. K. Mathews, D. Dolphin and R. W. Boyle, *J. Porphyrins Phthalocyanines*, **2000**, *4*, 228-238.
40. O. B. Locos and D. P. Arnold, *Org. Biomol. Chem.*, **2006**, *4*, 902-916.
41. C. Muthiah, M. Ptaszek, T. M. Nguyen, K. M. Flack and J. S. Lindsey, *J. Org. Chem.*, **2007**, *72*, 7736-7749.

42. M. A. Bakar, N. N. Sergeeva, T. Juillard and M. O. Senge, *Organometallics*, **2011**, *30*, 3225-3228.
43. K. Osawa, N. Aratani and A. Osuka, *Tetrahedron Lett.*, **2009**, *50*, 3333
44. S. M. LeCours, S. G. DiMagno and M. J. Therien, *J. Am. Chem. Soc.*, **1996**, *118*, 11854-11864.
45. N. Aratani, H. S. Cho, T. K. Ahn, S. Cho, D. Kim, H. Sumi and A. Osuka, *J. Am. Chem. Soc.*, **2003**, *125*, 9668-9681.
46. D. Fan, M. Taniguchi and J. S. Lindsey, *J. Org. Chem.*, **2007**, *72*, 5350-5357.
47. P. Xing, X. Chu, S. Li, F. Xin, M. Ma and A. Hao, *New J. Chem.*, **2013**, *37*, 3949-3955.
48. S. G. D. Magno, V. S. Y. Lin and M. J. Therien, *J. Org. Chem.*, **1993**, *115*, 2513-2515.
49. J. K. Laha, C. Muthiah, M. Taniguchi and J. S. Lindsey, *J. Org. Chem.*, **2006**, *71*, 7049-7052.
50. N. N. Sergeeva, A. Scala, M. A. Bakar, G. O'Riordan, J. O'Brien, G. Grassi and M. O. Senge, *J. Org. Chem.*, **2009**, *74*, 7140-7147.
51. I. M. Blake, H. L. Anderson, D. Beljonne, J. L. Brédas and W. Clegg, *J. Am. Chem. Soc.*, **1998**, *120*, 10764-10765.
52. T. Takanami, M. Yotsukura, W. Inoue, N. Inoue, F. Hino and K. Suda, *Heterocycles*, **2008**, *76*, 439-453.
53. M. O. Senge, Y. M. Shaker, M. Pintea, C. Ryppa, S. S. Hatscher, A. Ryan and Y. Sergeeva, *Eur. J. Org. Chem.*, **2010**, *2*, 237-257.
54. S. Hatscher and M. O. Senge, *Tetrahedron Lett.*, **2003**, *44*, 157.
55. M. O. Senge, *Acc. Chem. Res.*, **2005**, *38*, 733-743.
56. M. O. Senge, *Chem. Commun.*, **2011**, *47*, 1943-1960
57. D. Shen, C. Liu, X. Chen and Q Chen, *J. Org. Chem.*, **2009**, *74*, 206-211.
58. C. H. Devillers, A. K. D. Dime, H. Cattey and D. Lucas, *Chem. Commun.*, **2011**, *47*, 1893-1895.
59. K. Yamashita, K. Kataoka, M. S. Asano and K. Sugiura, *Org. Lett.*, **2012**, *14*, 190-193.
60. M. K. Panda, K. Ladomenou and A. G. Coutsolelos, *Coord. Chem. Rev.*, **2012**, *256*, 2601-2627.
61. J. Jiang, P. Vairaprakash, K. R. Reddy, T. Sahin, M. P. Pavan, E. Lubian and J. S. Lindsey, *Org. Biomol. Chem.*, **2014**, *12*, 86-103.

62. M. K. Panda, G. D. Sharma, K. R. J. Thomas and A. G. Coutsolelos, *J. Mater. Chem.*, **2012**, *22*, 8092-8102.
63. J. Rochford and E. Galoppini, *Langmuir*, **2008**, *24*, 5366-5374.
64. I. Beletskaya, V. S. Tyurin, A. Y. Tsivadze, R. Guilard and C. Stern, *Chem. Rev.*, **2009**, *109*, 1659-1713.
65. I. Ogoshi and T. Mizutani, *Acc. Chem. Res.*, **1998**, *31*, 81-89.
66. K. Tashiro, K. Konishi and T. Aida, *J. Am. Chem. Soc.*, **2000**, *122*, 7921-7926.
67. V.V. Borovkov, G.A. Hembury and Y. Inoue, *Acc. Chem. Res.*, **2004**, *37*, 449-459.
68. N. Berova, G. Pescitelli, A. G. Petrovic and G. Proni, *Chem. Comm.*, **2009**, 5958-5980.
69. N. Berova, L. D. Bari and G. Pescitelli, *Chem. Soc. Rev.*, **2007**, *36*, 914-931.
70. V. V. Borovkov, I. Fujii, A. Muranaka, G. A. Hembury, T. Tanaka, A. Ceulemans, N. Kobayashi and Y. Inoue, *Angew. Chem. Int. Ed.*, **2004**, *43*, 5481-5485.
71. G. A. Hembury, V. V. Borovkov and Y.Inoue, *Chem. Rev.*, **2008**, *108*, 1-73.
72. V. V. Borovkov and Y. Inoue, *Top. Curr. Chem.*, **2006**, *265*, 89-146.
73. V.V. Borovkov, N. Z. Mamardashvili and Y. Inou, *Russ. Chem. Rev.*, **2006**, *75*, 820-832.
74. J. Etxebarria, A. V. Ferran and P. Ballester, *Chem. Commun.*, **2008**, 5939-5941.
75. S. Brahma, S. A. Ikbal, S. Deya and S. P. Rath, *Chem. Commun.*, **2012**, *48*, 4070-4072.
76. G. Proni, G. Pescitelli, X. Huang, K. Nakanishi and N. Berova, *J. Am. Chem. Soc.*, **2003**, *125*, 12914-12927.
77. A. Chaudhary, S. A. Ikbal, S. Brahma and S. P. Rath, *Polyhedron*, **2013**, *52*, 761.
78. S. Brahma, S. A. Ikbal and S. P. Rath, *Inorg. Chim. Acta.*, **2011**, *372*, 62-70.
79. I. C. Pintre, S. Pierrefixe, A. Hamilton, V. Valderrey, C. Bo and P. Ballester, *Inorg. Chem.*, **2012**, *51*, 4620-4635.
80. X. Li, M. Tanasova, C. Vasileiou and B. Borhan, *J. Am. Chem. Soc.*, **2008**, *130*, 1885-1893.
81. X. Huang, B. H. Rickman, B. Borhan, N. Berova and K. Nakanishi, *J. Am. Chem. Soc.*, **1998**, *120*, 6185-6186.
82. M. Tanasova, C. Vasileiou, O. O. Olumolade and B. Borhan, *Chirality*, **2009**, *21*, 374-382.
83. S. Matile, N. Berova, K. Nakanishi, S. Novkova, I. Philipova and B. Blagoev, *J. Am. Chem. Soc.*, **1995**, *117*, 7021-7022.

84. C. Siering, J. Toräng, H, Kruse, S. Grimme and S. R. Waldvogel, *Chem. Commun.*, **2010**, *46*, 1625-1627.
85. J. Etxebarria, A. V. Ferran and P. Ballester, *Chem. Commun.*, **2008**, 5939-5941.
86. V. V. Borovkov, J. M. Lintuluoto and Y. Inoue, *Org. Lett.*, **2002**, *4*, 169-171.
87. G. Pescitelli, S. Gabriel, Y. Wang, J. Fleischhauer, R. W. Woody and N. Berova, *J. Am. Chem. Soc.*, **2003**, *125*, 7613-7628.
88. D. Arnold, A. W. Johnson and M. Winter, *J. Chem. Soc. Perkin Trans. 1*, **1977**, 1643-1647.
89. V. V. Borovkov, G. A. Hembury and Y. Inoue, *J. Org. Chem.*, **2005**, *70*, 8743-54.
90. A. Chaudhary and S. P. Rath, *Chem. Eur. J.*, **2011**, *17*, 11478.
91. W. J. Kruper, T. A. Chamberlin, M. Kochanny and K. Lang, *J. Org. Chem.*, **1989**, *54*, 2753-2756.
92. J. S. Lindsey, P. A. Brown and D. A. Siesel, *Tetrahedron*, **1989**, *45*, 4845.
93. H. Imahori, K. Hagiwara, A. Masanori, T. Akiyama, S. Taniguchi, T. Okada, M. Shirakawa and Y. Sakata, *J. Am. Chem. Soc.*, **1996**, *118*, 11771.
94. M. A. Fazio, O. P. Lee and D. I. Schuster, *Org. Lett.*, **2008**, *10*, 4979-4982.
95. T. Carofiglio, A. Varotto and U. Tonellato, *J. Org. Chem.*, **2004**, *69*, 8121-8124.
96. G. Blotny, *Tetrahedron*, **2006**, *62*, 9507-9522.
97. G. Blotny, *Tetrahedron Letters*, **2003**, *44*, 1499-1501.
98. T. Carofiglio, E. Lubian, I. Menegazzo, G. Saielli and A. Varotto, *J. Org. Chem.*, **2009**, *74*, 9034-9043.
99. A. G. Petrovic, G. Vantomme, Y. L. N. Abril, E. Lubian, G. Saielli, I. Menegazzo, R. Cordero, G. Proni, K. Nakanishi, T. Carofiglio and N. Berova, *Chirality*, **2011**, *23*, 808-819.
100. M. Gratzel, *Acc. Chem. Res.*, **2009**, *42*, 1788-1798.
101. H. Im, S. Kim, C. Park, S. Jang, C. Kim, K. Kim, N. Park and C. Kim, *Chem. Commun.*, **2010**, *46*, 1335-1337.
102. H. Imahori, Y. Matsubara, H. Iijima, T. Umeyama, Y. Matano, S. Ito, M. Niemi, N. V. Tkachenko and H. Lemmetyinen, *J. Phys. Chem. C*, **2010**, *114*, 10656-10665.
103. T. Bessho, S. M. Zakeeruddin, C. Yeh, E. W. Diau and M. Gratzel, *Angew. Chem. Int. Ed.*, **2010**, *49*, 6646-6649.
104. Y. Chang, C. Wang, T. Pan, S. Hong, C. Lan, H. Kuo, C. Lo, H. Hsu, C. Lin and E. W. Diau, *Chem. Commun.*, **2011**, *47*, 8910-8912.

105. Z. Zeng, B. Zhang, C. Li, X. Peng, X. Liu, S. Meng and Y. Feng, *Dyes and Pigments*, **2014**, *100*, 278-285.
106. G. E. Zervaki, M. S. Roy, M. K. Panda, P. A. Angaridis, E. Chrissos, G. D. Sharma and A. G. Coutsolelos, *Inorg. Chem.*, **2013**, *52*, 9813-9825.
107. L. L. Li and E. W. Diau, *Chem. Soc. Rev.*, **2013**, *42*, 291.
108. H. Imahori, T. Umeyama and S. Ito, *Acc. Chem. Res.*, **2009**, *42*, 1809-1818.
109. C. Y. Lee, C. She, N. C. Jeonga and J. T. Hupp, *Chem. Commun.*, **2010**, 46, 6090-6092.
110. B. E. Hardin, H. J. Snaith and M. D. Mcgehee, *Nat. Photonics*, **2012**, *6*, 162.
111. A. Yella, H. Lee, H. N. Tsao, C. Yi, A. K. Chandiran, M. K. Nazeeruddin, E. W. Diau, C. Yeh, S. M. Zakeeruddin and M. Gratzel, *Science*, **2011**, *334*, 629.
112. B. M. Toast, *Science*, **1991**, *254*, 1471-1477.
113. C. J. Li and B. M. Toast, *Proc. Natl. Acad. Sci.*, **2008**, *105*, 13197-13202.
114. I. T. Horváth and P. T. Anastas, *Chem. Rev.*, **2007**, *107*, 2169-2173.
115. C. W. Tornøe, C. Christensen and M. Meldal, *J. Org. Chem.*, **2002**, *67*, 3057-3064.
116. V. V. Rostovtsev, L. G. Green, V. V. Fokin and K. B. Sharpless, *Angew. Chem. Int. Ed.*, **2002**, *41*, 2596-2599.
117. H. C. Kolb, M. G. Finn and K. B. Sharpless, *Angew. Chem. Int. Ed.*, **2001**, *40*, 2596-2599.
118. J. D. Moses and A. D. Moorhouse, *Chem. Soc. Rev.*, **2007**, *36*, 1249.
119. V. D. Bock, H. Hiemstra and J. H. van Maarseveen, *Eur. J. Org. Chem.*, **2006**, *71*-51.
120. M. Severac, L. Le Pleux, L. A. Scarpaci, E. Blart and F. Odobel, *Tetrahedron Lett.*, **2007**, *48*, 6518-6522.
121. D. M .Shen, C. Liu and Q. Y. Chen, *Eur. J. Org. Chem.*, **2007**, 1419-1422.
122. S. Punidha, J. Sinha, A. Kumar and M. Ravikanth, *J. Org. Chem.*, **2008**, *73*, 323-326.
123. V. S. Shetti and M. Ravikanth, *Eur. J. Org. Chem.*, **2010**, 494-508.
124. F. C. Santos, A. C. Cunha, M. B. V. de Souza, A. C. Tome, V. F. Ferreira, M. G. P. M. S. Neves and J. A. S. Cavaleiro, *Tetrahedron Lett.*, **2008**, *49*, 7268-7270.
125. O.B. Locos, C. C. Heindl, A. Corral, M. O. Senge and E. M. Scanlan, *Eur. J. Org. Chem.*, **2010**, *6*, 1026-1028.
126. Y. Ikawa, H. Harada, M. Toganoh and H. Furuta, *Bioorg. Med. Chem. Lett.*, **2009**, *19*, 2448-2452.

127. T. Palacin, H. L. Khanh, B. Jousselme, P. Jegou, A. Filoramo, C. Ehli, D.M. Guldi and S. Campidelli, *J. Am. Chem. Soc.*, **2009**, *131*, 15394-15402.
128. K. H. L. Ho, I. Hijazi, L. Rivier, C. Gautier, B. Jousselme, G. Miguel, C. Romero-Nieto, D. M. Guldi, B. Heinrich, B. Donnio and S. Campidelli, *Chem. Eur. J.*, **2013**, *19*, 11374-11381.
129. Y. Hizume, K. Tashiro, R. Charvet, Y. Yamamoto, A. Saeki, S. Seki and T. Aida, *J. Am. Chem. Soc.*, **2010**, *132*, 6628-6629.
130. M. J. Leonardi, M. R. Topka and P. H. Dinolfo, *Inorg. Chem.*, **2012**, *51*, 13114-13122.

II Cellulose

2.1 Overview

Cellulose is a naturally occurring renewable biomass which is most abundant material on the Earth.[1,2] A French chemist, Anselme Payen in 1838 first discovered and isolated cellulose from various plant matters.[3] The commercial form cellulose are isolated and purified from the seed hairs of cotton, flax, hemp, sisal, jute and ramie or as wood.[4] Beside green plants, cellulose is also present in bacteria, fungi, algae and some animals. The chemical structure of cellulose consists of linear macromolecular chains, wherein the repeating monomer units of β-D-anhydroglucopyranose (AGU) rings are linked by β-1,4-linkages (Figure 1.3). The number of such repeating units can be up to 20000 in a chain. Sometimes cellulose is also considered a constitutional unit of the polymer cellobiose or two rings of glucopyranose.

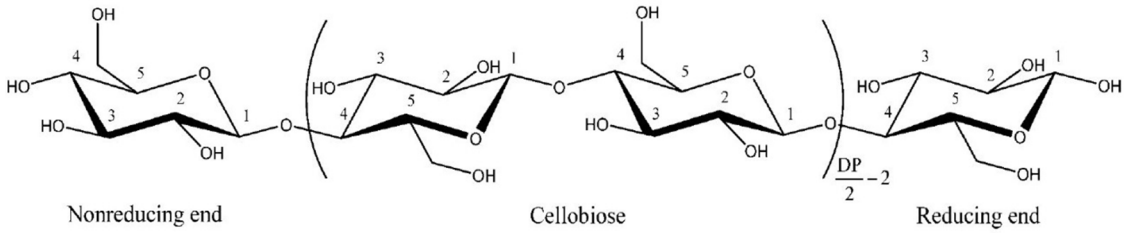

Figure 1.3: Chemical structure of Cellulose

The chemical structure of cellulose contains three different hydroxyl groups, out of which, two hydroxyl group is present at carbon C2 and C3 (secondary, equatorial) and one hydroxyl group is present at carbon C6 (primary). Also, each chain contains a non-reducing end (where C1 forms glycosidic bond) and a reducing end (where C1 binds with a hydroxyl group). The equatorial orientation of these hydroxyl groups in linear structure of cellulose tends to form an extended hydrogen bonding network within molecule. In principle, two types of hydrogen bonding exist in cellulose i.e. intra-molecular and inter-molecular hydrogen bonds. The intra-molecular hydrogen bonding are two kinds of such bonds occur within the same chain such as C3-OH with an endocyclic oxygen and C6-OH (primary) with the C2-OH, while inter-molecular hydrogen bonding are of kind of H-bonds between neighbouring chains C2 and C6 hydroxyl groups.[5] The intra-molecular hydrogen bonding

are responsible for stiff and rigid nature of cellulose molecule. Figure 1.4 depicts the network of the hydrogen bonding present inside cellulose.

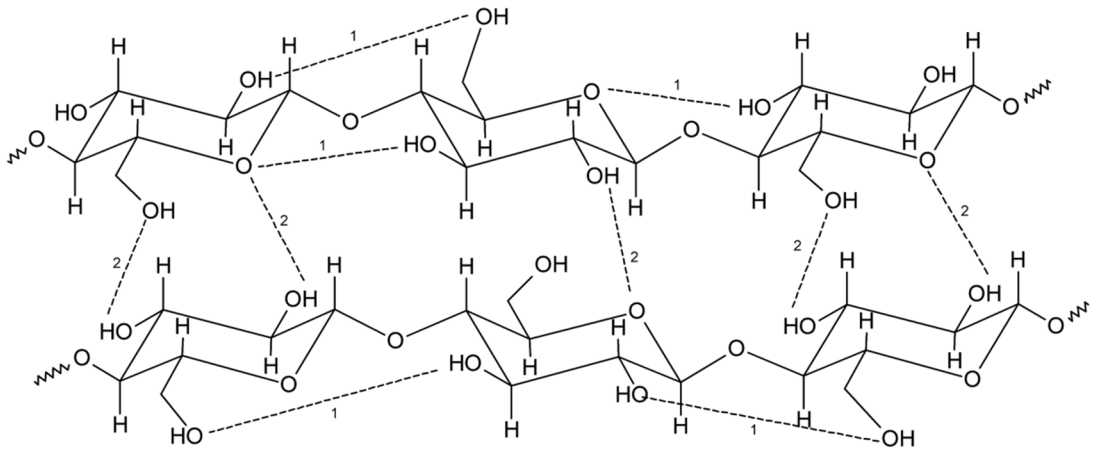

Figure 1.4: Hydrogen bonding in native cellulose[5]

The macromolecular structure of cellulose in its solid state is not uniform in nature and it is often dominated by the regions of high order, which are categorised as crystalline and low order, generally termed as amorphous regions. Figure 1.5 shows the crystalline and amorphous domains present in the cellulose matrix. The strong (intra and inter-) hydrogen bond network is responsible of ordered crystalline domains, while loosely packed regions mainly form the disordered amorphous domains.[6]

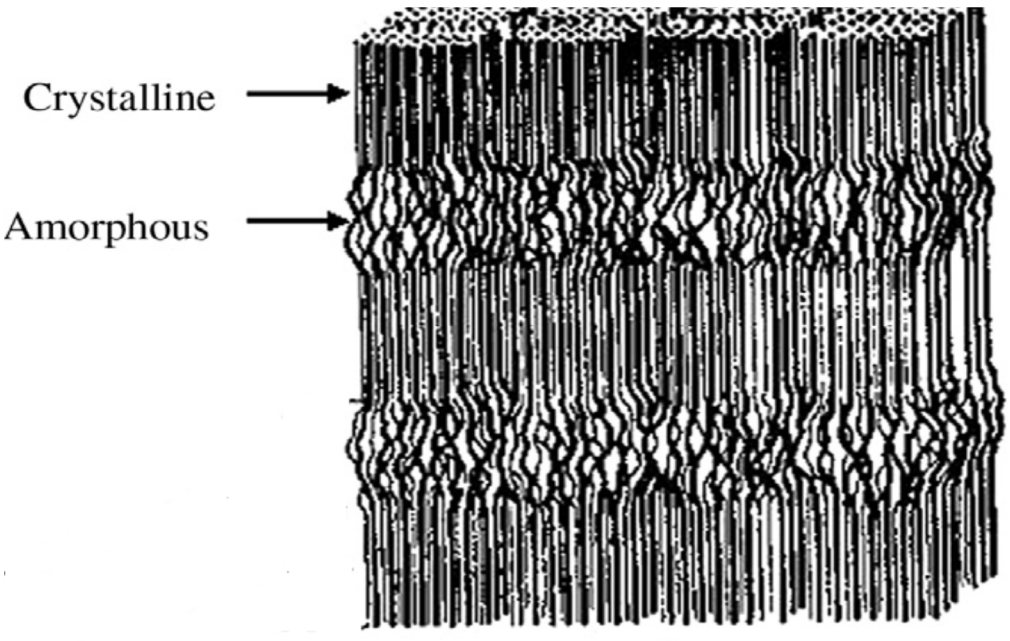

Figure 1.5: Crystalline and amorphous region in cellulose [6]

The degree of crystallinity (DP) of native cellulose varies between 40-60% , which generally depends on the origin and pre-treatment of the sample (Table 1.1).[7,8]

Table 1.1: Average DP of cellulose obtained from different sources.[8]

Source	DP_w (10^3) weight average DP determined by viscosimetric methods
Wood	8-9
Valonia	25-27
Cotton	8-15
Acetobacter xylinum	2-6
Cotton linters	1-5
Flax	7-8
Pulp	2.1
Kapok	9.5
Ramie	9-11

The morphology of cellulose has an intense effect on its reactivity. The hydroxyl (OH) groups located in the low ordered amorphous regions are highly accessible and tend to react readily, whereas those present in high ordered crystalline regions with close packing and strong interchain bonding are completely inaccessible.[9] The source and treatment of the cellulose, can lead to different molecular orientation and hydrogen bonding which give rise to different polymorphs of cellulose.

2.2 Crystal Structure and Polymorphism of Cellulose

Cellulose that is produced by plants is termed to as native cellulose, which exists in two crystalline forms I and II.[10] The cellulose I is considered to be most thermodynamically metastable form of cellulose.[11] In 1984, Atalla & VanderHart,[12] discovered the two sub forms of Cellulose I by NMR, which was later on confirmed as Cellulose Iα and Cellulose Iβ by Wada and co-workers[13] by using electron diffraction). The Iβ form, coincides with

the model of Meyer-Mark-Misch (Figure 1.6) while the Iα corresponds to a crystalline triclinic one-chain unit cell.[14,15]

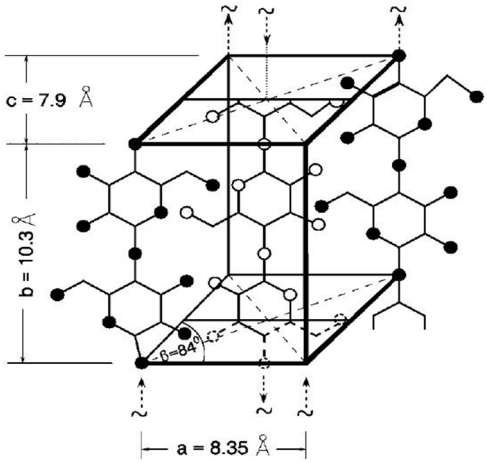

Figure 1.6: Cell native crystalline cellulose (model: Meyer-Mark-Misch)

The form Iα (which is usually present in large amounts in bacterial cellulose) can be converted to metastable form Iβ by annealing at 260 °C, however, it cannot be reversed.

The cellulose II is another crystalline phase that is obtained by chemical regeneration of cellulose I, or by dissolution in an appropriate solvent and re-precipitation in water, or by the process of mercerization with solution of sodium hydroxide.[16-18] The conversion of cellulose I to cellulose II is irreversible.[16-18] The cell type crystal is monoclinic $P2_1$ with different cell parameters as compared to the corresponding native cellulose also two chains are antiparallel to each other and this gives a greater rigidity to the structure. Such great strength of structure makes it suitable for textile and paper industry. Some bacterial species are also reported to produce cellulose II.[19]

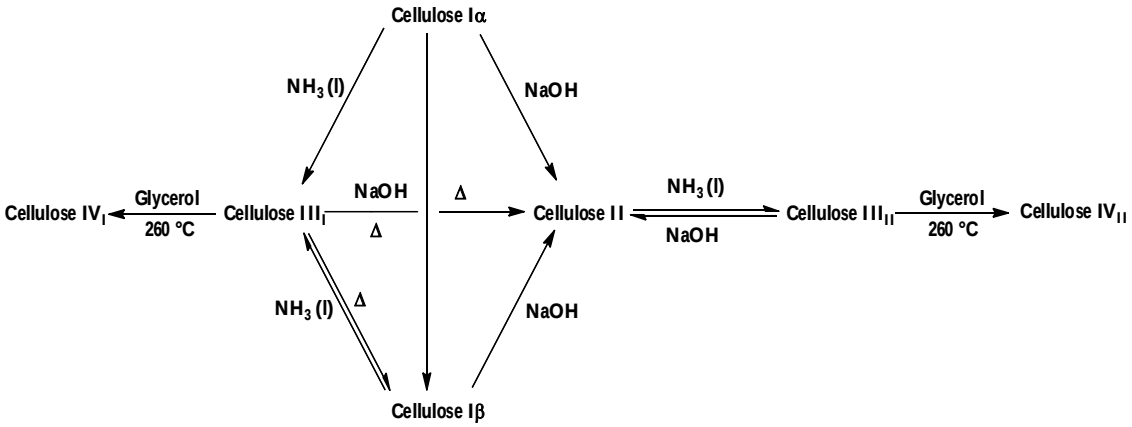

Figure 1.7: Crystalline cellulose phases and its interconversion

Figure 1.7 depicts the schematic interconversion relationship between different phases of cellulose. The cellulose I and II, when treated with ammonia (gas or liquefied) or various amines, generates the cellulose III. In particular, there are two crystalline phases, III_I[20] and III_{II}, although the structure of the phase III_{II} is not yet fully clarified.[21] The phases IV_I and IV_{II} are obtained by heating the cellulose III_I and III_{II} over 260 °C in glycerol and in the similar fashion cellulose III can be reconvert to cellulose I or II. Different plants typically contain cellulose IV in their cell wall.[22-23]

2.3 Hierarchical structure and morphology of the cellulose fibers

In nature, the native cellulose does not exist as a single molecule, but rather in the form of fibers resulting into hierarchical organization (Figure 1.8) of cellulose chains that are essentially product of the biosynthesis process of cellulose.

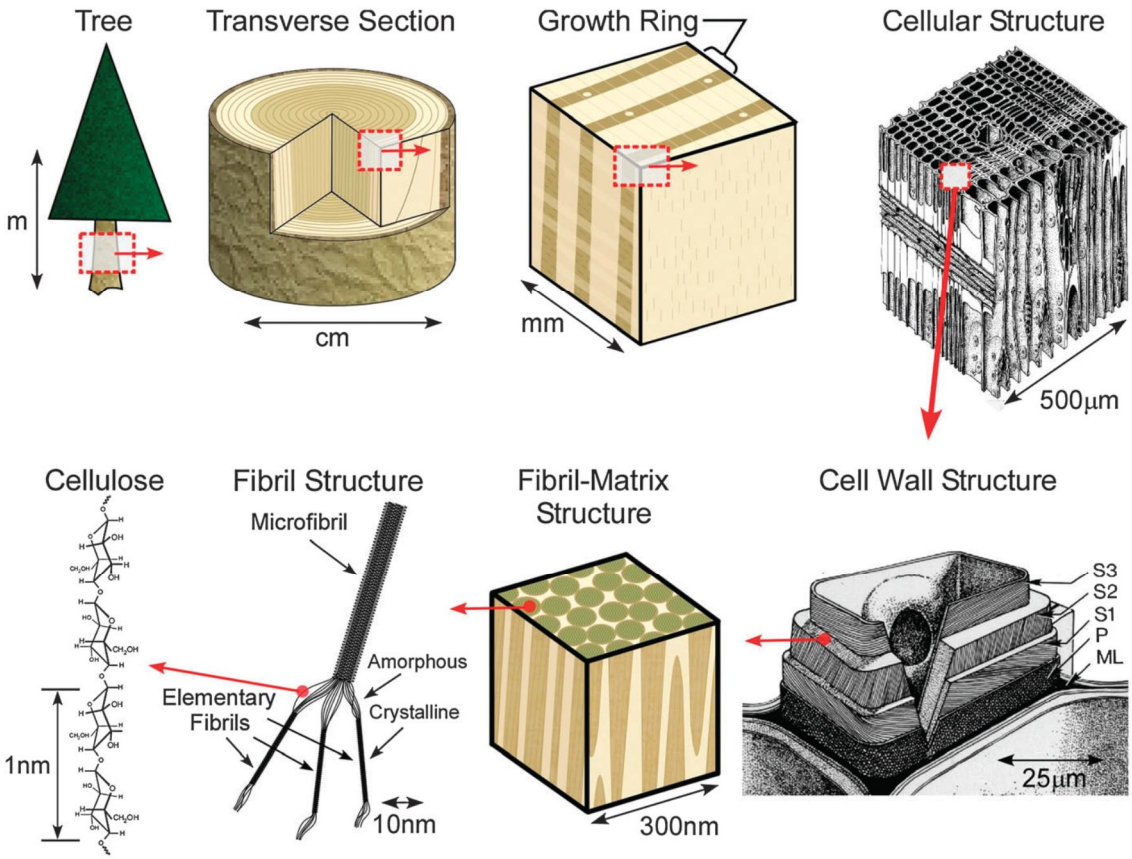

Figure 1.8: Hierarchical organization of a cellulose [24]

Several studies[25-27] have shown that the formation of chains are the result of two processes of polymerization and crystallization, which are carried out by complex enzymatic complex called terminals (terminal complexes, TCs), present in the wall of plant cell. However, the mechanism of this process is not yet fully understood. In plants, typically 36 cellulose chains aggregate to form a larger unit called elementary fibril or proto fibril, which in turn packaging with other elementary fibrils form micro fibrils. These micro fibrils, in turn, form the fibers themselves, which constitute the supporting structure of the plant cell walls. The aggregation of these fibrils due to intra- and inter- molecular Van der Waals forces and hydrogen bonds intra-and inter-molecular. As assessed by electron microscopy and wide-angle X-ray scattering (WAXS), the average diameter of a proto fibril is about 3.5 nm[28] while that of a micro fibril varies between 4 and 35 nm depending on source of cellulose (Table 1.2).[29] The micro fibrils can in turn form the macrofibrils, with a diameter in the range of micrometers.[28]

Table 1.2: Diameter of various cellulose micro fibrils[28]

Sample	Diameter (nm)
Bacterial cellulose	4-7
Cotton linters	7-9
Ramie	10-15
Dissolving pulp	10-30
Valonia cellulose	10-35

The packing of the cellulose chains allows to have an ordered structure with a high crystallinity, though there are areas of para-crystalline or amorphous spread randomly along the microfibrils that result from the distortion of the fibers which reduce the effectiveness of internal forces.[30] These amorphous domains are responsible for the origin of the formation of the nanocrystalline cellulose, which is described in the next paragraphs. These amorphous zones are selectively dismantled by acid hydrolysis, since they are less compact and higher in energy and thus are more reactive than the crystalline counterparts.

3. Nano Crystalline Cellulose

3.1 Overview

The nanocrystalline cellulose or crystalline nanocellulose (NCC) is a type of nanocrystals or nanowhiskers, which can be obtained from the native cellulose from plant cell wall. It is entirely different from bacterial cellulose (BNC or BC) and nanofibrilated cellulose (NFC), by means of its synthesis, morphology and its applications. Their production ranges from top-down methods, which involves different pathway such as enzymatic/chemical/physical process for its isolation from wood and agricultural/forest residues to the bottom-up formation of cellulose nanofibrils from glucose by bacteria.[31] The NCC, produced by chemical modification, is represented in the form of crystalline structures (whiskers), which consists of a rodlike cellulose crystals with diameter of about 10-20 nm and lengths of a few hundred nanometers. The bacterial cellulose produced by organic farming of the *Acetobacter xylinum* bacteria, is nanometer-sized which is similar to the NCC in its morphology but differs in size. The fibrillated nanocellulose is produced by partly chemical and partly mechanical modification(s) with lengths of more than one micrometer.

Depending on crystal size, functions and isolation method, the nanocelluloses are broadly classified into three main categories- Microfibrillated cellulose (MFC), nanocrystalline cellulose (NCC) and bacterial nanocellulose (BNC) (Table 1.3).[31] The terminology used to describe these materials in the scientific literature has not yet been normalized. As a consequence, often synonyms are used to indicate different types of cellulose thus creating confusion and a certain difficulty in literature surveys (Table 1.3). Typical structure of these cellulose types on the nanoscale can be seen in the electron micrographs (Figure 1.9).[31]

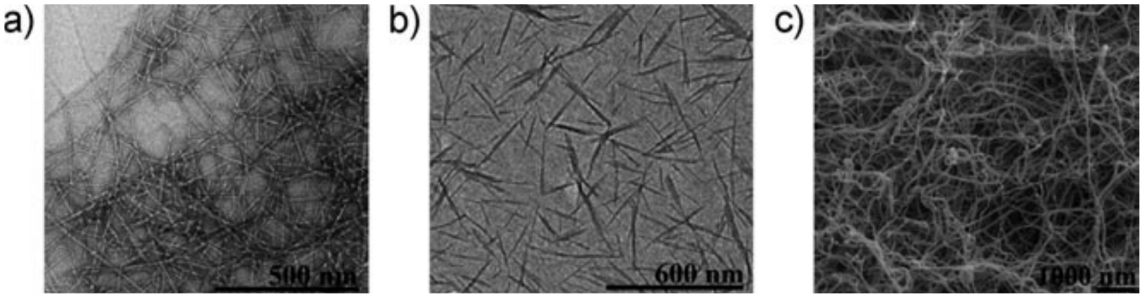

Figure 1.9: Transmission electron micrographs of a) MFC[34] and b) NCC[56] c) scanning electron micrograph of BNC [31]

Table 1.3: The family of nanocellulose materials[31]

Type of nanocellulose	Selected references and synonyms	Typical sources	Formation and average size
microfibrillated cellulose (MFC)	microfibrillated cellulose,[32-35] nanofibrils and microfibrils, nanofibrillated cellulose	wood, sugar beet, potato tuber, hemp, flax	delamination of wood pulp by mechanical pressure before and/or after chemical or enzymatic treatment diameter: 5-60 nm length: several micrometers
nanocrystalline cellulose (NCC)	cellulose nanocrystals, crystallites,[36-41] whiskers,[42-45] rodlike cellulose microcrystals[46]	wood, cotton, hemp, flax, wheat straw, mulberry bark, ramie, Avicel, tunicin, cellulose from algae and bacteria	acid hydrolysis of cellulose from many sources diameter: 5-70 nm length: 100-250 nm (from plant celluloses); 100 nm to several micrometers (from celluloses of tunicates, algae, bacteria)
bacterial nanocellulose (BNC)	bacterial cellulose,[47-52] microbial cellulose,[53-54] biocellulose[55]	low-molecular-weight sugars and alcohols	bacterial synthesis diameter: 20-100 nm; different types of nanofiber networks

3.2 Nanocrystalline Cellulose Production

Cellulose in native form contains both amorphous and crystalline zones. The amorphous domains are responsible for the origin of nanocrystalline cellulose. The amorphous zone, being less compact and higher in energy are more reactive, thus, are more easily attacked by the acid hydrolysis at glycosidic bonds than their crystalline counterparts.[57,58]

The factors which effect in the preparation of the NCC are the following:

- **Temperature**
- **Reaction time**
- **Nature of acid used**
- **Acid-Cellulose ratio**

Firstly, in general the **nature of the acid** affects the colloidal stability of NCC in aqueous environment, its rheological properties and thermal stability. Generally, hydrolysis is carried out using sulphuric acid or hydrochloric acid. In particular, the first acid adds a negative

charge on the NCC, due to formation of sulphuric esters on the surface of the nanocrystals (which are deprotonated at pH>3), and then promotes the dispersion of the product in water to electrostatic repulsion.[59] The mechanism of acid catalysed hydrolysis of cellulose is described in Figure 1.10. However, the NCC obtained by this way has low thermo-stability, thus it behaves like a Newtonian fluid.

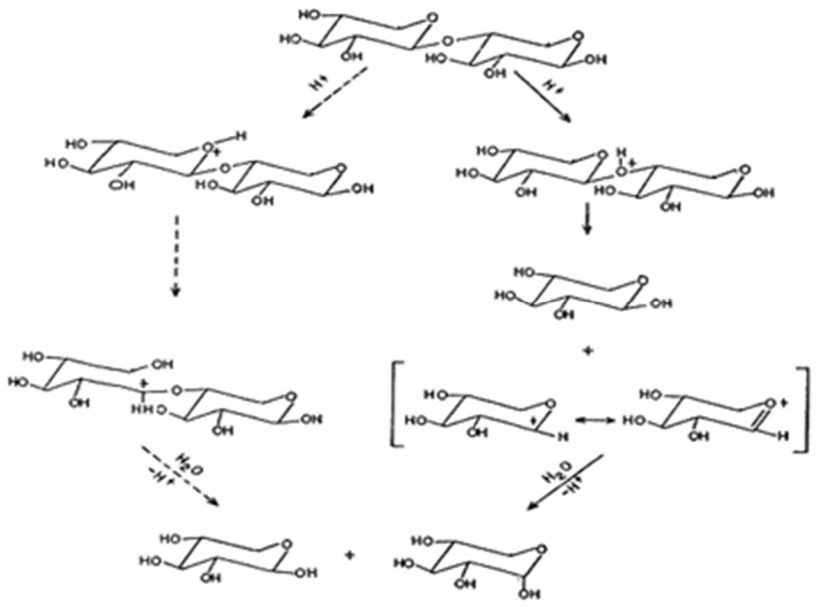

Figure 1.10: Mechanism of cellulose hydrolysis[28]

On the other hand, using hydrochloric acid for the hydrolysis produces a NCC with low dispersibility in water and which has a thixotropic behaviour at concentrations above 0.5% (w/v) and vice-versa below 0.3% (w/v).[60] Generally, the concentration of the sulphuric acid that is used for hydrolysis of the cellulose is 65% by weight. The **temperature** can vary from 25 °C to 70 °C and consequently varies the **reaction time** which will be certainly longer at low temperatures. Bondeson[61] has observed that the prolongation of the reaction time leads to a decrease of the length of nanocrystals of cellulose and an increase of the surface charge. Subsequent studies corroborates that the reaction time and the **ratio of acid-cellulose** has critical role, in formation of the size distribution of the nanocrystals.[62] The temperature also has similar effects to those of the reaction time for obtaining smaller crystals.[63] The NCC can be synthesized through variety of sources, such as cotton, liner, hemp, pulp bleached soft wood and hard wood and microcrystalline cellulose. A higher value of crystallinity in the cellulose origin results in a final product with larger dimensions, since highly crystalline materials have a limited portion of amorphous areas attacked by the acid.[64]

3.3 Morphology and self-organization of nanocrystalline cellulose

The size of the nanocrystals of cellulose depends on the source of cellulose and conditions in which the acid hydrolysis took place. Table 1.4 indicate dimension of few examples of cellulose nanocrystals reported in literature.

Table 1.4: Dimensions of cellulose nanocrystals from various sources.[38]

Cellulose type	Length	Cross section
Tunicate [42,44]	100 nm - several μm	10-20 nm
Bacterial [36,65]	100 nm - several μm	5-10 nm x 30-50 nm
Algal (Valonia) [37,66]	>1000 nm	10-20 nm
Cotton[67]	200-350 nm	5 nm
Wood[60,67]	100-300 nm	3-5 nm diameter

The morphology of the cross section of the crystalline NCC is linked to the mechanism of biosynthesis of cellulose origin. The different geometries of the crystal are the result of the many provisions of the TC that have been observed in plant cell walls.[25] Observations made by TEM shows that the nanocrystals of cellulose produced from *Valonia ventricosa* have a square section, with side mean of almost 18 nm[37] while nanocrystals of cellulose derived from marine organism tunicates have a rectangular cross section of 8.8 nm x 18.2 nm[44]. Thus, the morphology along the chain, the NCC obtained from tunicates and BNC have wrapped helical chains.[63,68] In contrast, NCC originating from plants, have a uniplanar orientation, thus does not possess morphological variation.

In an aqueous suspension at low concentration, NCC produced from sulphuric acid hydrolysis is randomly oriented and tends to form an isotropic phase. When the concentration reaches a critical value, the suspension form a phase called anisotropic, chiral nematic or cholesteric phase, typical form of liquid crystalline fibril of NCC.[59] The cellulose nano particles are aligned along the planes, perpendicular to the main axis of the phase (cholesteric axis), according to a direction that rotates by a certain angle between a plane and the other axis. The plane forms a helical structure with a pitch P between 20 micro-meters and 80 micro-meters (Figure 1.11). The cholesteric phase has the property of changing the plane of polarized light and, when viewed with polarizing filters, it shows the

characteristic domains of birefrigence. Also, the suspension of NCC, separates out spontaneously into two phases: the upper isotropic and the lower anisotropic.

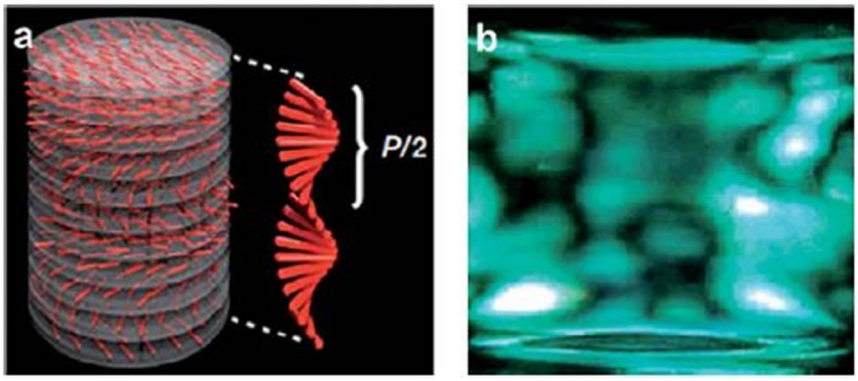

Figure 1.11: Schematic representation[69] of the (a) chiral nematic phase of NCC, P-pitch of the chiral b) birefrigent domains

The anisotropic phases can also be obtained in non-polar solvents, using NCC stabilized with suitable surfactants.[70] These anisotropic phases has the ability to evaporate the solvent and tends to form solid films of iridescent NCC (Figure 1.12), which preserve the structure of the phase chiral and are potentially applicable in the field of decorative materials or security cards (the optical properties of such materials cannot be reproduced by printing or photocopying.)[71]

Figure 1.12: Iridescent films obtained by slow evaporation nanocellulose suspension[72]

In an aqueous solution, the concentration of NCC sulphonated suspension which forms the chiral nematic phase depends on the charge density, which generally varies between 1% and 10% (w/w). Quantitative studies[40,73] have also shown that the presence of electrolytes, as well as their ionic size and concentration, have a considerable effect on properties of the nematic phase. In particular, with the increase in quantity of electrolyte, it decreases the

anisotropic phase and the pitch of the propeller associated therewith. Moreover, as the size of the ion increases the value of critical concentration increases for the formation of the anisotropic phase. Finally, the presence of macromolecules such as dextrans or ionic dyes induces the formation of two phases, an isotropic and the other anisotropic.[74-76] In organic solvents, the chiral phase is observed but the pitch of propeller of chiral phase appears to be much more smaller (4 mM) and it is higher when aqueous suspensions the concentration of NCC is high (up to 36%).[77] Furthermore, the NCC must be suitably functionalized superficially to be dispersible in organic solvents.

3.4 Mechanical properties of Nanocrystalline cellulose

Theoretically, the nanocellulose obtained by acid hydrolysis can be considered as a material consisting of a single crystal of cellulose (degree of crystallinity of 100%) since the hydrolysis removes the amorphous zones. Neverthless, in the reality, hydrolysis of cellulose can never be complete. Typically, the degree of crystallinity varies between 50-90 % depending on the cellulose source.[78] It is difficult to measure the mechanical properties of these nanometer-sized crystals due to variety of factors such as crystal structure, crystallinity index, defects and property of measurement approach.

Sakurada (1962) experimentally analyse the cellulose polymer for the first time by using diffractometer. The value for the elastic modulus of the crystals of cellulose, particularly cellulose I made from Ramie was found to be 138 GPa.[79] The theoretical calculations for cellulose, which were based on molecular mechanics-dynamics models found Young's modulus between 100 and 160 GPa, which are in agreement with studies carried out by Sakurada.[80,81] Similar mechanical values were obtained with nanocellulose extracted from tunicates which was verified via Raman spectroscopy[82] and AFM[83] technique. Table 1.5 indicate mechanical properties of cellulose nanocrystals reported from different sources.[78]

Table 1.5: Properties of cellulose based materials[78]

Material	E_A (GPa)	E_T (GPa)	σ_f (GPa)	ε_f (%)	Technique
WF[84]	14-27	-	0.3-1.4	4-23	Tensile
PF[85-88]	5-45	-	0.3-0.8	1.3-8	Tensile, Raman
MCC [88,89]	25±4	-	-	-	Raman
MFC & NFC	N/A	-	-	-	
CNC					
Plant[90]	57,105	-	-	-	Raman
Wood[91]	-	18-50	-	-	AFM indentation
t-CNC[82]	143	-	-	-	Raman
Acid[a] [83]	151±29	-	-	-	AFM-3pt bend
TEMPO[a] [83]	145±31	-	-	-	AFM-3pt bend
[24]	-	9±3	-	-	AFM indentation
BC[92,93]	78±17	-	-	-	AFM-3pt bend
	114	-	-	-	Raman
E_A-elastic modulus in axial direction, E_T-elastic modulus in transverse direction, σ_f-tensile strength (tensile testing), ε_f= strain to failure(tensile testing). [a]Treated t-CNCs.					

The high rigidity combined with the high tensile strength (7500 MPa), high length-diameter ratio and the high specific surface area (150-250 m^2/g), together with excellent biodegradability opens up the use of cellulose as a substitute of the inorganic fillers used in polymer materials.[94] The improvement of mechanical properties resulted from such filler is caused by the rigid "network" that the NCC is able to form due to hydrogen bonds. The greater adhesion between this hydrogen bond network and the polymer matrix, the higher is the improvement in the properties of NCC. It is possible to maximize the dispersibility of the NCC in the hydrophobic polymer matrix and mitigate its hydrophilic characteristics by insertion of relatively nonpolar organic functionalities on the surface of cellulose. The major limitation of NCC as filler lies in its low thermal stability, since its thermal decomposition is in the range of 200-300 °C.

The NCC is cheap, abundant, natural, renewable, mechanical etc, and that makes it a promising nanomaterial. In order to use NCC for various applications, its functionalization is required. The coming paragraph deals with functionalization of nanocellulose.

3.5 Functionalization of Nanocrystalline cellulose

The NCC has very high number of hydroxyl groups (OH) on the surface that may be involved in many chemical reactions. According to the molecular structure of cellulose, there are two different OH groups. The OH on the carbon atoms at position C2 and C3 are of secondary type while the OH on the carbon in position C6 is primary. If all the hydroxyl group of anhydroglucose unit of cellulose were replaced by a chemical reaction, the degree of substitution (DS) would be equal to 3. However, this situation is not possible, besides cellulose being a trihydric alcohol. Indeed, in cellulose chemical molecular structure, the repeating glucose units are arranged in alternating manner i.e. zig-zag format, so only few OH groups (C6) are accessible, while other OH groups (C2, C3) are not accessible since they are pointing inside the crystal lattice or they submerged in the cellulose chains. The majority of cellulose derivatives are ‘‘very random block”, copolymers,[95] which applies to situation where the degree of substitution (DS) value is neither zero nor 3. In such derivative ‘‘block’’ copolymers, different degrees of substitution of anhydroglucose units will be present in the cellulose chains, along with anhydroglucose units that carry no substituent groups and anhydroglucose units that are fully substituted.[95] The primary OH being more accessible is more reactive than the others, and is the functional group that participates in the chemical reactions for functionalization of the cellulose.

Cellulose is a peculiar polymeric biopolymer that has several attributes such as a fine cross section, the ability to absorb moisture, high strength and durability, high thermal stability, good biocompatibility, relatively low cost and low density yet good mechanical properties.[95] Beside these outstanding properties, cellulose has some inherent drawbacks. These include poor solubility in common solvents, poor resistance, poor dimensional stability, lack of thermoplasticity, high hydrophilicity and lack of antimicrobial properties, which are not desirable for several composite applications.[95] In order to overcome such drawbacks, the controlled physical and/or chemical modification of the cellulose structure is necessary.[96]

3.5.1 Chemical Modification

Firstly, it is pertinent to mention the principle chemical composition of native cellulose are determined by biosynthesis, thus, cannot be altered in the same way as those of synthetic polymer.[95] In order to overcome this problem, Chemical modification is key role for introduction of functional group into cellulose. The functional groups can add new properties to cellulose without disturbing their intrinsic properties.

The main purposes of the chemical reactions on the surface of cellulose are:

- To increase the dispersibilty of the cellulose material in organic solvents and for compatibility with non-polar/hydrophobic matrices
- Introduction of various functional groups which contribute nanocellulose material for potential applications.

From the literature[97] it is known that the chemical modifications do affect the cellulosic surface, but the prolonged time of reactions and/or aggressive reagents may also be detrimental for the crystalline structure of the material thus causing profound morphological changes. So, one has to be cautious while carrying out the chemical modification of cellulose. It should be noted that, while the degree of substitution is enhanced, the structure, morphology and crystalline properties of nanocrystals should be remain intact.

For example, the chemical modification of cellulose carried out by atomic transfer polymerization (ATRP) involves reaction with bromine which introduces the active bromine on the nano crystals of cellulose and these brominated nanocrystals act as macromolecular initiators which promote the monomer free radical polymerization.[98] One key point about these types of reaction between OH (from nano crystals) and Br (from 2-bromoisobutyrylbromide), which is violent since it releases a large amount of heat.[98] Though the reaction may have been carried at low temperature, the properties of original crystals should be preserved. The Figure 1.13 shows the most common surface modifications of the NCC known till now.

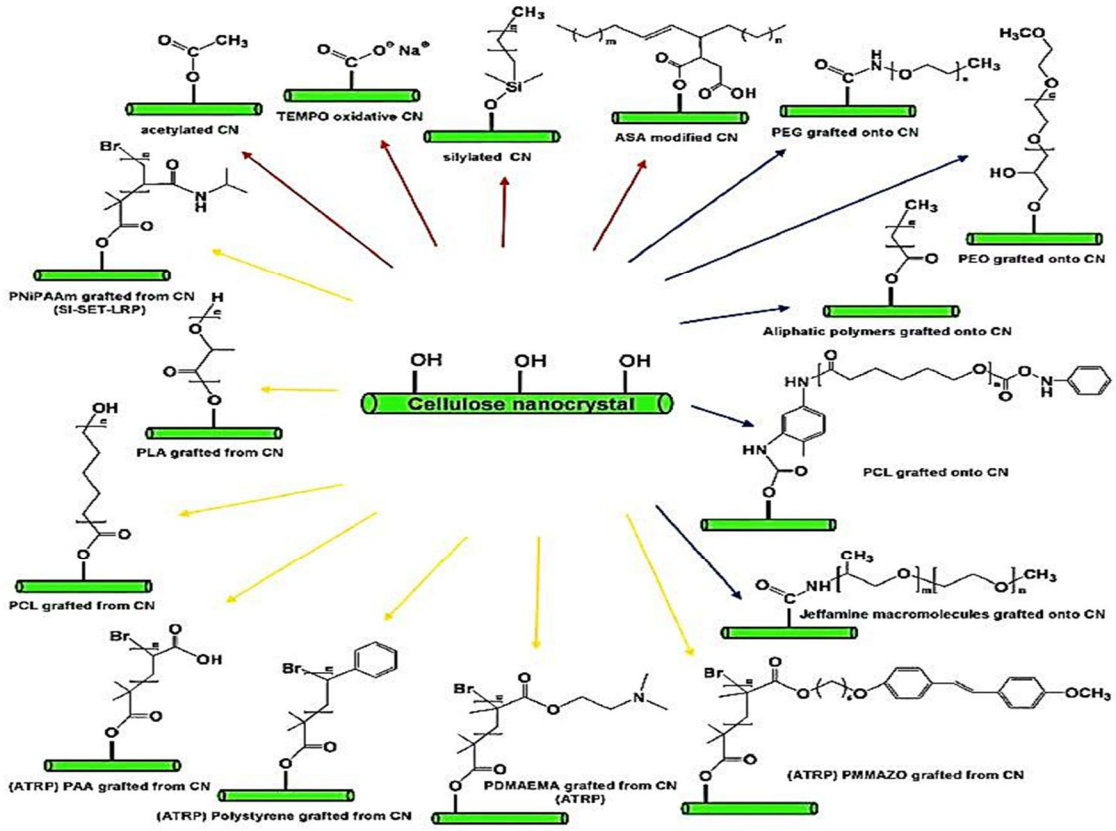

Figure 1.13: Common chemical modification of nanocrystalline cellulose[98]

[PEG: poly(ethylene glycol); PEO: poly(ethylene oxide); PLA: poly(lacticacid); PAA: poly(acrylic acid); PNiPAAm: poly(N-isopropylacrylamide); PDMAEMA: poly(N,N-dimethylaminoethyl methacrylate]

The surface chemical modification of cellulose nanocrystals can be classified in different types. In the figure 1.13, the arrows of different colours indicate the different types of chemical modifications takes place. The red arrows indicate the substitution reactions of OH groups with small molecules (TYPE A), the blue arrows indicate anchoring reactions made of polymer chains with different coupling reagents (TYPE B). Finally, the yellow arrows indicate reactions anchoring polymer chains through polymerization from surface initiators immobilized on the surface (TYPE C). The reactions employed in this thesis belong to the first category. In this regards, the other two types of reactions, may be considered both methodologies of (grafting) anchoring polymers. Specifically, the first one, which is the most exploited, is defined as "grafting-on" while the second is termed as "grafting-from".

Alain Dufresne and coworkers (2008) used the grafting-on approach to anchor chains polycaprolactone (PLC) of various molecular weight to the NCC through coupling reaction via isocyanate group.[99] According to their observations, PLC was able to crystallize on the surface of NCC for higher degrees of functionalization. Also, they grafted the organic halides on the surface of NCC via esterification reaction.[100] The same methodologies were performed using other anchoring functionalization of polyurethane[101], amino-polyethylene glycol (PEG-NH_2) with a nitroxide radical (TEMPO)[102], DNA oligomers[103] and polypropylene maleate[104].

The grafting-from method was used to grow polymer chains on the surface of NCC through the atom transfer radical polymerization (ATRP), which allows a high control on the molecular weight of the polymer. The polymerization process involves two stages: (1) esterification of the OH groups with 2-bromoisobutyrylbromide, (2) followed by polymerization of the monomer. Several studies in the literature reported in the case of grafting-from approach with monomer of styrene[105], azobenezene[106] and N,N-Dimethylaminoethyl Methacrylate (DMAEMA)[107].

As described above, the chemical modification of nanocrystals can be employed for the inclusion of some special functional groups, which results in promising material for various applications. In figure 1.14 shows the different functionalization routes. The functionalization of NCC with fluorescent molecules is useful for the study of cellular uptake and bio-distribution in vivo systems of the nanocrystals of cellulose. Dong and Roman (2007) described a methodology for covalently binding of the fluorescein-5-isothiocyanate (FITC) to the NCC.[108] It involves the insertion of an epoxy functionality on the surface of cellulose by reaction with epichlorohydrin. Subsequently, the epoxy ring is opened by reaction with ammonium hydroxide which introduces a primary amino group (NH_2). Finally, amine reacts with the isothiocyanate group of FITC to form a thiourea. Fluorescent molecules can also bind on the NCC surface, as reported in literature dual florescent labelling of cellulose nanocrystals.[109] In which, first the reaction between the isothiocyanate group of FITC and cellulosic deprotonated OH groups takes place, while another reaction via thiol-ene click chemistry. The dual fluorescent labelling of cellulose nanocrystals was effectively sensitive to the pH change, which can be possibly used in sensing different nanomaterials.

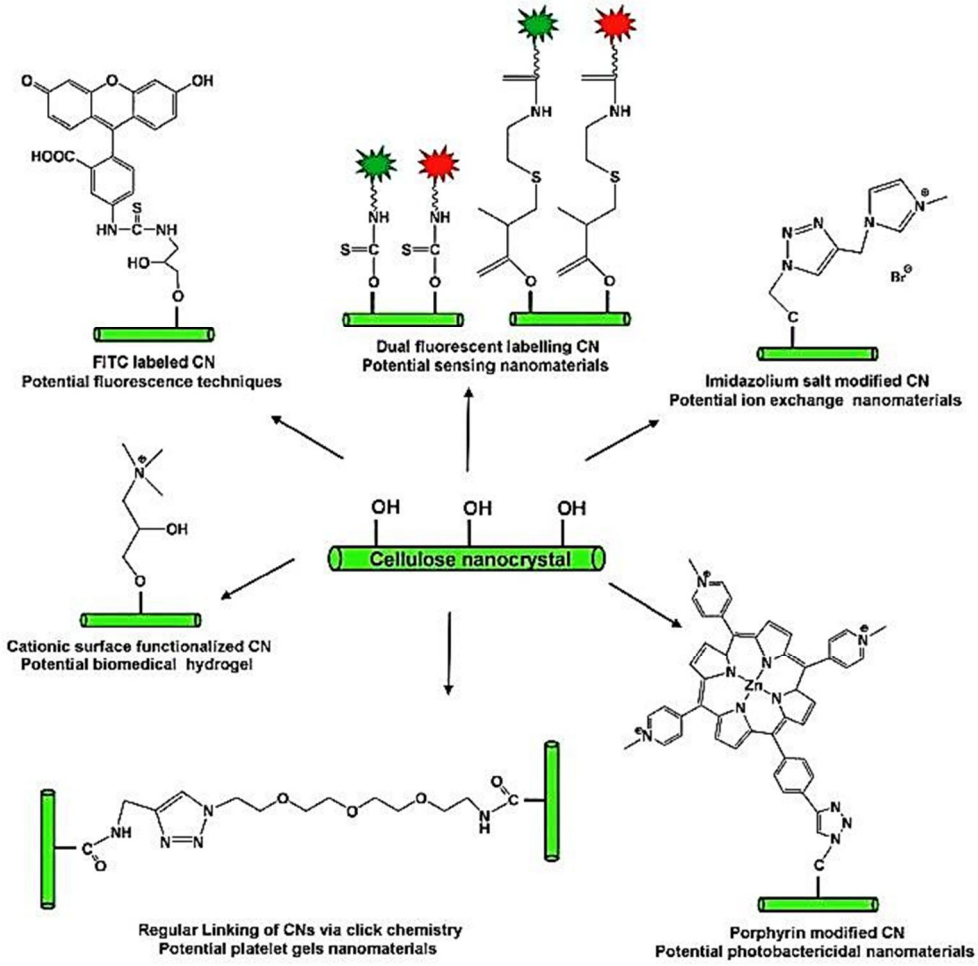

Figure 1.14: Potential applications of nanocrystalline cellulose chemically modified[98]

Other functionalizations are obtained by binding different molecules via click chemistry on the surface of cellulose nanocrystals. For example Argyropoulos and co-workers synthesized a nanoplatelet gel material by grafting amine-terminated monomers on surface modified NCC by click reaction.[110,111] Highly fluorescent chromophore such as porphyrins was also covalently linked on the surface of NCC by click chemistry.[112] This material showed an excellent efficiency against photodynamic inactivation of Mycobacterium smegmatis and Staphylococcus aureus bacterial models. Another aspect of click chemistry was explored by grafting imidazolium salt on the NCC surface, to create nanomaterials potentially employable as ion exchange resins.[113] Others include, cationic functionalization of nanocellulose, which was achieved by surface modification with epoxypropyltrimethylammonium chloride, which induces to form a thixotropic hydrogel.[114]

REFERENCES

1. B. Hinterstoisser and L. Salmen, *Vib. Spectroscopy*, **2000**, *22*, 111-118.
2. A. M. Bochek, *Russ. J. Appl. Chem.*, **2003**, *76*, 1711-1719.
3. A. Payen, *Comptes Rendus*, **1838**, *7*, 1052-1056
4. P. Zugenmaier, *Crystalline Cellulose and Derivatives*, *Berlin Heidelberg*, **2008**, Springer.
5. T. Kondo, *Hydrogen bonds in cellulose and cellulose derivatives In Severian Dumitriu Editor. Polysaccharides, structural diversity and functional versatility,* **2005**, *6995*.
6. D. Bhattacharya, L. T. Germinario and W. T. Winter, *Carbohydrate Polym.*, **2008**, *73*, 371-377.
7. S. Kamel, N. Ali, K. Jahangir, S. M. Shah and A. A. El-Gendy, *eXPRESS Polym. Lett.,* **2008**, *2*, 758-778.
8. A. H. Conner, *Size exclusion chromatography of cellulose and cellulose derivatives. NY, USA: Marcel Dekker,* **1995**, 331-352.
9. E. Sjostrom, *Wood chemistry, fundamentals and applications. Academic Press, New York*, **1993**.
10. S. Kuga and R. M. Brown, *Carbohydr. Res.*, **1988**, *180*, 345-350.
11. B. G. Rånby, *Acta Chem. Scand.*, **1952**, *6*, 128-138.
12. R. H. Atalla and D. L. Vanderhart, *Science*, **1984**, *223*, 283-285.
13. M. Wada, J. Sugiyama and T. Okano, *J. Appl. Polym. Sci.*, **1993**, *49*, 1491-1496.
14. H. Mark, K. H. Meyer and F. Zeits, *Physik. Chemie, B2*, **1929**, *115*.
15. K. H. Meyer and L. Misch, *Helv. Chim. Acta*, **1937**, *20*, 232-244.
16. I. M. Saxena and R. M. Bown, *Ann. Bot.*, **2005**, *96*, 9-21.
17. F. J. Kolpak and J. Blackwell, *Macromolecules*, **1976**, *9*, 273-278.
18. P. Langan, Y. Nishiyama and H. Chanzy, *J. Am. Chem. Soc.*, **1999**, *121*, 9940-9946.
19. S. Kuga, S. Takagi and R. M. Brown, *Polymer*, **1993**, *34*, 3293-3297.
20. M. Wada, H. Chanzy, Y. Nishiyama and P. Langan, *Macromolecules*, **2004**, *37*, 8548-8555.
21. M. Wada, L. Heux, Y. Nishiyama and P. Langan, *Biomacromolecules*, **2009**, *10*, 302-309.
22. H. Chanzy, K. Imada, A. Mollard, R. Vuong and F. Barnoud, *Protoplasma*, **1979**, *100*, 303-316.
23. W. Helbert, J. Sugiyama, M. Ishihara and S. Yamanaka, *Biotechnol.*, **1997**, *57*, 29-37.

24. M. T. Postek, A. Vladár, J. Dagata, N. Farkas, B. Ming, R. Wagner, A. Raman, R. J. Moon, R. Sabo, T. H. Wegner and J. Beecher, *Meas. Sci. Technol.*, **2011**, *22*, 024005.
25. R. M. Brown, *J. Macromol. Sci. Part A: Pure Appl. Chem.*, **1996**, *33*, 1345-1373.
26. R. E. Williamson, J. E. Burn and C. H. Hocart, *Trends Plant Sci.*, **2002**, *7*, 461-467.
27. C. H. Haigler, *In Biosynthesis and Biodegradation of Cellulose, New York,* **1991**.
28. D. Fengel and G. Wegener, *Wood-chemistry, ultrastructure, reactions, Berlin*, **1989**.
29. H. P. Fink, D. Hofmann and H. J. Purz, *Acta Polym.*, **1990**, *41*, 131-137.
30. S. P. Rowland and E. J. Roberts, *J. Polym. Sci. Part A: Polym. Chem.*, **1972**, *10*, 2447-2461.
31. D. Klemm, F. Kramer, S. Moritz, T. Lindström, M. Ankerfors, D. Gray and A. Dorris, *Angew. Chem. Int. Ed.*, **2011**, *50*, 5438-5466.
32. M. Pääkkö, M. Ankerfors, H. Kosonen, A. Nykänen, S. Ahola, M. Österberg, J. Ruokolainen, J. Laine, P. T. Larsson, O. Ikkala and T. Lindström, *Biomacromolecules*, **2007**, *8*, 1934-1941.
33. A. F. Turbak, F. W. Snyder and K. R. Sandberg, *J. Appl. Polym. Sci. Appl. Polym. Symp.*, **1983**, *37*, 815-827.
34. L. Wågberg, G. Decher, M. Norgren, T. Lindström, M. Ankerfors and K. Axnäs, *Langmuir*, **2008**, *24*, 784-795.
35. M. Henriksson, L. A. Berglund, P. Isaksson, T. Lindström and T. Nishino, *Biomacromolecules*, **2008**, *9*, 1579-1585.
36. C. Tokoh, K. Takabe, M. Fujita and H. Saiki, *Cellulose*, **1998**, *5*, 249-261.
37. J. F. Revol, *Carbohydrate Polym.*, **1982**, *2*, 123-134.
38. S. Beck-Candanedo, M. Roman and D. G. Gray, *Biomacromolecules*, **2005**, *6*, 1048-1054.
39. J. Araki, M. Wada, S. Kuga and T. Okano, *J. Wood Sci.*, **1999**, *45*, 258-261.
40. X. M. Dong, T. Kimura, J. F. Revol and D. G. Gray, *Langmuir*, **1996**, *12*, 2076-2082.
41. Y. Habibi, L. A. Lucia and O. J. Rojas, *Chem. Rev.*, **2010**, *110*, 3479-3500.
42. V. Favier, H. Chanzy and J. Y. Cavaillé, *Macromolecules*, **1995**, *28*, 6365-6367.
43. L. Petersson, I. Kvien and K. Oksman, *Compos. Sci. Technol.*, **2007**, *67*, 2535-2544.
44. P. Terech, L. Chazeau and J. Y. Cavaillé, *Macromolecules*, **1999**, *32*, 1872-1875.
45. M. A. S. A. Samir, L. Chazeau, F. Alloin, J. Y. Cavaillé, A. Dufresne and J. Y. Sanchez, *Electrochim. Acta*, **2005**, *50*, 3897-3903.
46. M. M. de Souza Lima and R. Borsali, *Macromol. Rapid Commun.*, **2004**, *25*, 771-787.

47. D. Klemm, B. Heublein, H. P. Fink and A. Bohn, *Angew. Chem.*, **2005**, *117*, 3422-3458.
48. D. Klemm, D. Schumann, F. Kramer, N. Hessler, M. Hornung, H. P. Schmauder and S. Marsch, *Adv. Polym. Sci. (Polysaccharides II), Vol. 205 (Ed.: D. Klemm), Springer, Heidelberg*, **2006**, 49-96.
49. D. Klemm, D. Schumann, F. Kramer, N. Hessler, D. Koth and B. Sultanova, *Macromol. Symp.*, **2009**, *280*, 60-71.
50. D. Klemm, D. Schumann, U. Udhardt and S. Marsch, *Prog. Polym. Sci.*, **2001**, *26*, 1561-1603.
51. S. Yamanaka, K. Watanabe, N. Kitamura, M. Iguchi, S. Mitsuhashi, Y. Nishi and M. Uryu, *J. Mater. Sci.*, **1989**, *24*, 3141-3145.
52. R. E. Cannon and S. M. Anderson, *Crit. Rev. Microbiol.*, **1991**, *17*, 435-447.
53. W. Czaja, A. Krystynowicz, S. Bielecki and R. M. Brown, *Biomaterials*, **2006**, *27*, 145-151.
54. W. K. Czaja, D. J. Young, M. Kawecki and R. M. Brown, *Biomacromolecules*, **2007**, *8*, 1-12.
55. A. Sani and Y. Dahman, *J. Chem. Technol. Biotechnol.*, **2010**, *85*, 151-164.
56. K. Fleming, D. Gray, S. Prasannan and S. Matthews, *J. Am. Chem. Soc.*, **2000**, *122*, 5224-5225.
57. M. N. Anglès and A. Dufresne, *Macromolecules*, **2001**, *34*, 2921-2931.
58. M. M. Ruiz, J. Y. Cavaillé, A. Dufresne, J. F. Gérard and C. Graillat, *Compos. Interfaces*, **2000**, *7*, 117-131.
59. J. F. Revol, H. Bradford, J. Giasson, R. H. Marchessault and D. G. Gray, *Int. J. Biol. Macromol.*, **1992**, *14*, 170-172.
60. J. Araki, M. Wada, S. Kuga and T. Okano, *Colloids Surf. A: Physicochem. Eng. Asp.*, **1998**, *142*, 75-82.
61. D. Bondeson, I. Kvien and K. Oksman, *In Cellulose Nanocomposites: Processing, Characterization, and Properties, ACS Symposium Series 938; American Chemical Society: Washington DC*, **2006**.
62. S. Beck-Candanedo, M. Roman and D. G. Gray, *Biomacromolecules*, **2005**, *6*, 1048-1054.
63. S. Elazzouzi-Hafraoui, Y. Nishiyama, J. L. Putaux, L. Heux, F. Dubreuil and C. Rochas, *Biomacromolecules*, **2008**, *9*, 57-65.
64. M. M. de Souza Lima, J. T. Wong, M. Paillet, R. Borsali and R. Pecora, *Langmuir*, **2003**, *19*, 24-29.

65. M. Grunert and W. T. Winter, *J. Polym. Environ.*, **2002**, *10*, 27-30.
66. S. J. Hanley, J. Giasson, J. F. Revol and D. G. Gray, *Polymer*, **1992**, *33*, 4639-4642.
67. D. Fengel, G. Wegener, *Wood: Chemistry, Ultrastructure, Reactions; Walter de Gruyter: New York*, **1984**.
68. S. J. Hanley, J. F. Revol, L. Godbout and D. G. Gray, *Cellulose*, **1997**, *4*, 209-220.
69. M. A. S. A. Samir, F. Alloin and A. Dufresne, *Biomacromolecules*, **2005**, *6*, 612-626.
70. S. Elazzouzi-Hafraoui, J. L. Putaux and L. Heux, *J. Phys. Chem. B*, **2009**, *113*, 11069-11075.
71. J. F. Revol, J. D. L. Godbout and D. G. Gray, *International Patent WO*, **1995**, 95/21901.
72. C. C. Y. Cheung, M. Giese, J. A. Kelly, W. Y. Hamad and M. J. MacLachlan, *ACS Macro Lett.*, **2013**, *2*, 1016-1020.
73. X. M. Dong and D. G. Gray, *Langmuir*, **1997**, *13*, 2404-2409.
74. S. Beck-Candanedo, D. Viet and D. G. Gray, *Cellulose*, **2006**, *13*, 629-635.
75. S. Beck-Candanedo, D. Viet and D. G. Gray, *Langmuir*, **2006**, *22*, 8690-8695.
76. S. Beck-Candanedo, D. Viet and D. G. Gray, *Macromolecules*, **2007**, *40*, 3429-3436.
77. L. Heux, G. Chauve and C. Bonini, *Langmuir*, **2000**, *16*, 8210-8212.
78. R. J. Moon, A. Martini, J. Nairn, J. Simonsen and J. Youngblood, *Chem. Soc. Rev.*, **2011**, *40*, 3941-3994.
79. I. Sakurada, Y. Nukushina and T. Ito, *J. Polym. Sci.*, **1962**, *57*, 651-660.
80. K. Tashiro and M. Kobayashi, *Polymer*, **1991**, *32*, 1516-1526.
81. R. J. Marhofer, S. Reiling and J. Brickmann, *J. Ber. Bunsen-Ges. Phys. Chem.*, **1996**, *100*, 1350-1354.
82. A. Šturcová, G. R. Davies and S. J. Eichhorn, *Biomacromolecules*, **2005**, *6*, 1055-1061.
83. S. Iwamoto, W. Kai, A. Isogai and T. Iwata, *Biomacromolecules*, **2009**, *10*, 2571-2576.
84. L. Mott, L. Groom and S. Shaler, *Wood Fiber Sci.*, **2002**, *34*, 221-237.
85. S. J. Eichhorn, A. Dufresne, M. Aranguren, N. E. Marcovich, J. R. Capadona, S. J. Rowan, C. Weder, W. Thielemans, M. Roman, S. Renneckar, W. Gindl, S. Veigel, J. Keckes, H. Yano, K. Abe, M. Nogi, A. N. Nakagaito, A. Mangalam, J. Simonsen, A. S. Benight, A. Bismarck, L. A. Berglund and T. Peijs, *J. Mater. Sci.*, **2010**, *45*, 1-33.
86. A. K. Bledzki and J. Gassan, *Prog. Polym. Sci.*, **1999**, *24*, 221-274.

87. S. J. Eichhorn, C. A. Baillie, N. Zafeiropoulos, L. Y. Mwaikambo, M. P. Ansell, A. Dufresne, K. M. Entwistle, P. J. Herrera-Franco, G. C. Escamilla, L. Groom, M. Hughes, C. Hill, T. G. Rials and P. M. Wild, *J. Mater. Sci.*, **2001**, *36*, 2107-2131
88. S. J. Eichhorn, J. Sirichaisit and R. J. Young, *J. Mater. Sci.*, **2001**, *36*, 3129-3135.
89. S. J. Eichhorn and R. J. Young, *Cellulose*, **2001**, *8*, 197-207.
90. R. Rusli and S. J. Eichhorn, *Appl. Phys. Lett.*, **2008**, *93*, 033111.
91. R. R. Lahiji, X. Xu, R. Reifenberger, A. Raman, A. Rudie and R. J. Moon, *Langmuir*, **2010**, *26*, 4480-4488.
92. G. Guhados, W. K. Wan and J. L. Hutter, *Langmuir*, **2005**, *21*, 6642-6646.
93. Y. C. Hsieh, H. Yano, M. Nogi and S. J. Eichhorn, *Cellulose*, **2008**, *15*, 507-513.
94. J. F. Revol, L. Godbout and D. G. Gray, *J. Pulp Pap. Sci.*, **1998**, *24*, 146.
95. D. Roy, M. Semsarilar, J. T. Guthriea and S. Perrier, *Chem. Soc. Rev.*, **2009**, *38*, 2046-2064.
96. A. Hebeish and J. T. Guthrie, *The Chemistry and Technology of Cellulosic Copolymers, Springer-Verlag, Berlin*, **1981**.
97. N. S. Cetin, P. Tingaut, N. Özmen, N. Henry, D. Harper, M. Dadmun and G. Sèbe, *Macromol. Biosci.*, **2009**, *9*, 997-1003.
98. N. Lin, J. Huang and A. Dufresne, *Nanoscale*, **2012**, *4*, 3274-3294.
99. A. J. de Menezes, G. Siqueira, A. A. S. Curvelo and A. Dufresne, *Polymer*, **2009**, *50*, 4552-4563.
100. Y. Habibi and A. Dufresne, *Biomacromolecules*, **2008**, *9*, 1974-1980.
101. X. Cao, Y. Habibi and L. A. Lucia, *J. Mater. Chem.*, **2009**, *19*, 7137-7145.
102. J. Araki, M. Wada and S. Kuga, *Langmuir*, **2001**, *17*, 21-27.
103. A. P. Mangalam, J. Simonsen and A. S. Benight, *Biomacromolecules*, **2009**, *10*, 497-504.
104. F. Azzam, L. Heux, J. L. Putaux and B. Jean, *Biomacromolecules*, **2010**, *11*, 3652-3659.
105. G. Morandi, L. Heath and W. Thielemans, *Langmuir*, **2009**, *25*, 8280-8286.
106. J. Yi, Q. Xu, X. Zhang and H. Zhang, *Polymer*, **2008**, *49*, 4406-4412.
107. J. Yi, Q. Xu, X. Zhang and H. Zhang, *Cellulose*, **2009**, *16*, 989-997.
108. S. Dong and M. Roman, *J. Am. Chem. Soc.*, **2007**, *129*, 13810-13811.
109. L. J. Nielsen, S. Eyley, W. Thielemans and J. W. Aylott, *Chem. Commun.*, **2010**, 8929-8931.
110. I. Filpponen and D. S. Argyropoulos, *Biomacromolecules*, **2010**, *11*, 1060-1066.

111. H. Sadeghifar, I. Filpponen, S. P. Clarke, D. F. Brougham and D. S. Argyropoulos, *J. Mater. Sci.*, **2011**, *46*, 7344-7355.
112. E. Feese, H. Sadeghifar, H. S. Gracz, D. S. Argyropoulos and R. A. Ghiladi, *Biomacromolecules*, **2011**, *12*, 3528-3539.
113. S. Eyley and W. Thielemans, *Chem. Commun.*, **2011**, 4177-4179.
114. M. Hasani, E. D. Cranston, G. Westman and D. G. Gray, *Soft Matter*, **2008**, *4*, 2238-2244.

Chapter-2

OUTLINE OF THE RESEARCH

This Thesis has been divided in two sections: Porphyrins and Nanocrystalline cellulose.

I) Porphyrins

To acquire the necessary skills needed for synthesis, purification and characterization of porphyrin derivatives, the experimental part of this Thesis begun with the preparation of some compounds of interest for the ongoing research in the group. More precisely:

1. **Reference porphyrin chromophores for DSSC applications:** The development of new sensitizer for DSSC requires comparing its performances with those of state of the art derivatives. Thus, the following two porphyrins have been prepared.

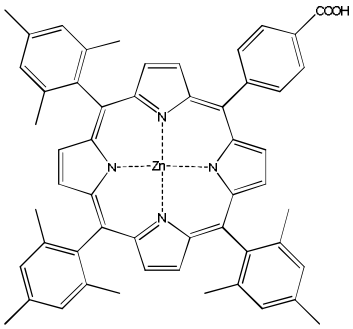

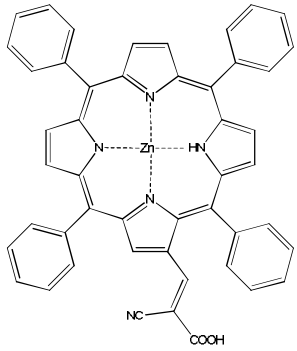

2. **Melamine bridged porphyrin dyads as sensors for diamines:** Recently, the group in which this Thesis has been carried out reported a new methodology for the synthesis of porphyrin-porphyrin dimers based on the use of trichlorotriazine as linking agent. These derivatives showed interesting properties as optical sensors for diamines. In addition, they have been used, in collaboration with Professor Nina Berova at Columbia University, for the determination of the absolute configuration of chiral molecules by circular dichroism. Thus, two new batches of dimers and a new one have been prepared. Their structures were the following:

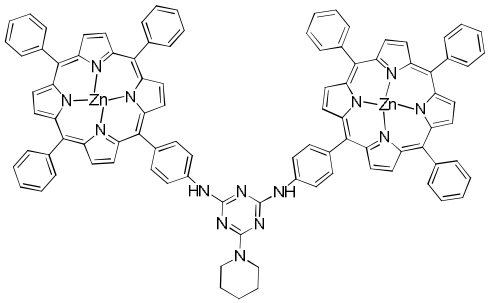

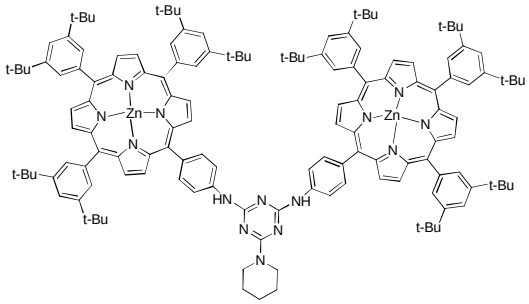

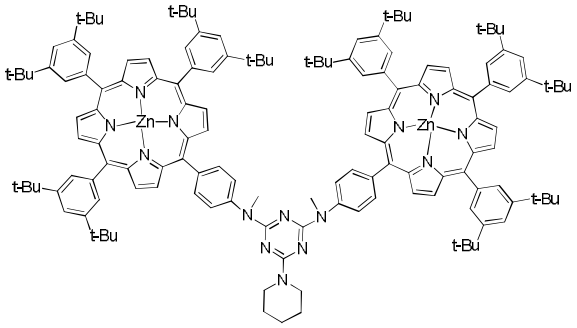

3. **New project involving the use of "click chemistry" for the functionalization of porphyrin derivatives and their conjugation to other molecular compounds (i.e. carbon nanostructures, cyclodextrins), polymeric materials (i.e. nanocrystalline cellulose, resins), metallic and metal oxide nanoparticles (i.e. titania, gold nanoparticles)**. The use of Huisgen reaction (1,3-dipolar addition of an azide to a terminal alkyne) represents a modern approach for the preparation of functional materials. The two derivatives prepared are reported below.

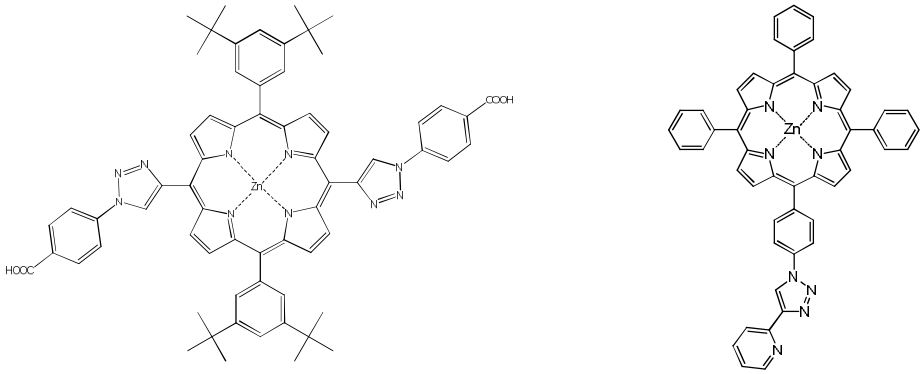

Further, attempts were being made for synthesis of 1,2,3-triazole porphyrin complexes with Palladium and Ruthenium metals.

II) Nanocrystalline cellulose: Cellulose, the most ubiquitous and renewable biomass on Earth, is biosynthesized in the form of fibrils with alternating crystalline and amorphous domains. This unique structure permits the top-down production of a valuable nanomaterial generally known as nanocrystalline cellulose (NCC). It bears many hydroxyl groups that can be used to tailor its surface properties through the attachment of a variety of organic functionalities, according to the well-consolidated polysaccharide chemistry. Many reports focus on the creation of advanced, cellulose based functional nanomaterials have been recently flourishing in the literature. Some notable examples are in the field of

catalysis, electronic and magnetic materials, drug delivery, photodynamic therapy, and regenerative medicine. The production of state of the art NCC is not trivial. Therefore, It has been necessary to set up the following steps:

4. **Preparation of nanocrystalline cellulose (NCC)**: it requires the hydrolysis of a cellulose source. Two starting materials were considered, namely microcrystalline cellulose and filter paper. Also, purification of NCC requires a considerable amount of operations such as washing and fractionation by ultracentrifugation, dialysis and lyophilization. The characterization of the NCC is carried out by multiple techniques such as microscopy (TEM, SEM, AFM), elemental analysis, thermogravimetry, infrared spectroscopy, dynamic light scattering and z-potential.

5. **Functionalization of NCC**: The availability of a large amount of hydroxyl groups on the surface of nanocrystals allows for the conjugation of functional molecules. The following has been attached by this was to produce a pH sensitive material for optical sensing purposes.

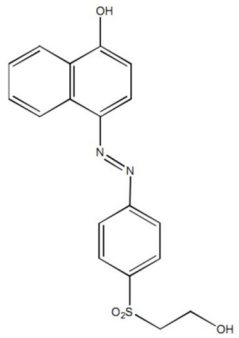

Nevertheless, the hydroxyl chemistry can be not adequate or versatile enough for more elaborate conjugations. Therefore it has been considered the decoration of NCC surface with amino groups or carboxylic acid units. The determination of the extent of functionalization required the set-up of analytical techniques for the quantification of these groups such as infrared spectroscopy, UV-Vis analysis (via the formation of a blue compound using the Kaiser test), conductometric titration, and elemental analysis.

6. **Nanocrystalline cellulose-Porphyrin Hybrid**: This activity culminated with the preparation of a hybrid NCC-porphyrin that showed **NCC** can be used as a scaffold to covalently appending chromophores without impairing their photophysical properties. This material holds promises for applications such as photodynamic therapy.

7. **Nanocrystalline cellulose-Nitrobenzene Hybrid:** Nitro derivative N-(3-aminopropyl)-3-(trifluoromethyl)-4-nitrobenzenamine was introduced on the surface of NCC. This NCC-Nitro hybrid material has ability to release NO radical upon illumination, which can be used for various therapeutic applications.

Chapter-3

RESULTS AND DISCUSSION

I Porphyrin

As anticipated in the Introduction, porphyrins exhibit extremely interesting properties which make them attractive moieties for various applications. In this Thesis porphyrins were prepared as reference materials for application in Dye sensitized solar cells (DSSC), as well as sensors for the detection of diamines and chirality probes. In addition, new porphyrin derivatives were synthesized using "Click-chemistry" strategy. All these aspects are detailed in the sections below.

1. Porphyrin as chromophore for DSSC

In literature, numerous porphyrin carboxylic acid derivatives have been reported as a chromophore for dye sensitized solar cells.[1] The reason for the presence of the carboxylic functionality in the porphyrin framework is due to the affinity of this functionality for titania employed in DSSC photo-anodes. Galoppini and co-workers have investigated the various binding modes of porphyrin sensitizers (Figure 3.1) with carboxylic acid as an anchoring groups.[1] Apart from carboxylic acid functionality, other functionalities such as phosphonic acids have also been used for chemisorption of dyes, although not as frequently as carboxylic ones.

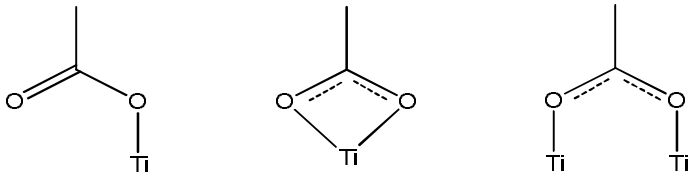

Figure 3.1: Modes of chemisorption of dye to TiO_2 surface

In this thesis, three different porphyrin derivatives containing carboxylic functionality have been synthesized, which will be discussed in the next sub-section.

1.1 Porphyrin chromophore (1) [5-(4-Carboxyphenyl)-10,15,20-tris(2,4,6-trimethyl phenyl) porphyrinato zinc(II)] (TPMC-Zn)

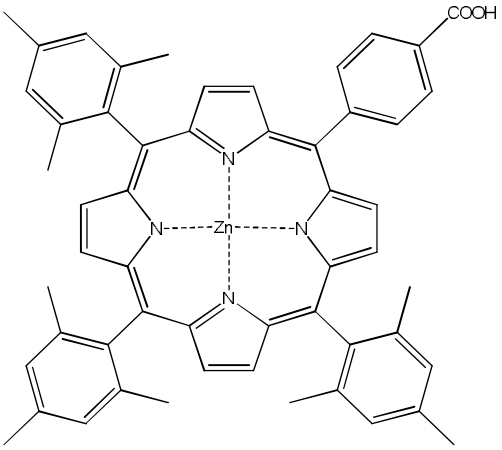

Figure 3.2: Structure of porphyrin chromophore (1) for DSSC

This compound was prepared by following the literature procedure described by Yoshikawa and co-workers[2] by mixed condensation of aldehydes and pyrrole to get the porphyrin methyl ester. The latter was further hydrolysed with potassium hydroxide to obtain the corresponding carboxylic acid derivative. Finally, metallation with zinc acetate led to formation of target compound. The synthetic approach of this porphyrin chromophore has been discussed below.

1.1.1 Synthesis of 5-(4-Methoxycarbonylphenyl)-10,15,20-tris(2,4,6-trimethyl phenyl) porphyrin (TPMM)

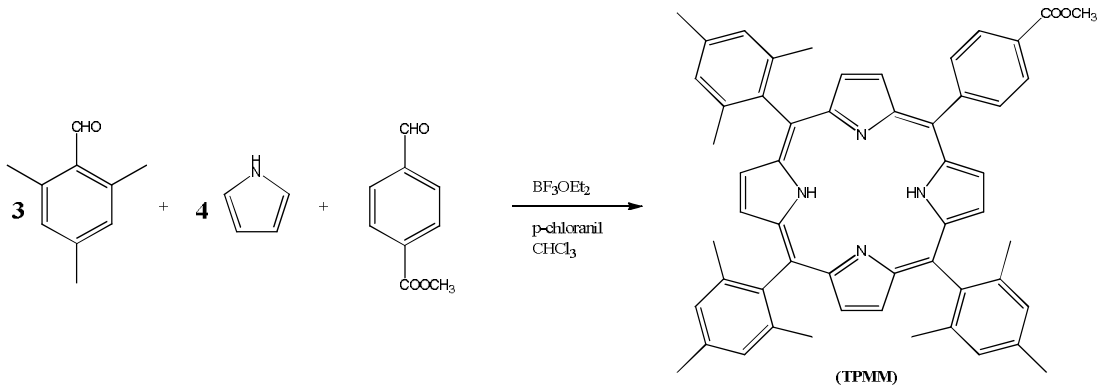

Scheme 3.1: Synthesis of 5-(4-Methoxycarbonylphenyl)-10,15,20-tris(2,4,6-trimethyl phenyl) porphyrin (TPMM)

The construction of the porphyrin ring was carried out by mixed condensation of pyrrole and the two aldehydes (i.e. methyl 4-formylbenzoate and 2,4,6-trimethylbenzaldehyde) in a 1:3 ratio. Thus, to a solution of 2,4,6-trimethylbenzaldehyde in chloroform, methyl 4-formyl benzoate and pyrrole were added. The mixture was stirred at room temperature for 10 minutes. Then, BF_3 etherate solution was added to the reaction mixture and it was stirred for another 2 hours at room temperature. It was followed by addition of p-chloranil as an oxidant. The purple solution so obtained was stirred at room temperature for 1 hour. The reaction mixture was then neutralized by addition of triethyl amine and the solvent was removed in vacuo. The solid residue thus obtained was subjected to purification by column chromatography. The undesired tetra mesityl porphyrin was eluted first using only dichloromethane as eluent. Later, the desired A_3B type porphyrin was eluted using a CH_2Cl_2/hexane (1:1) mixture as eluent. The solvent was evaporated giving a red solid of the target porphyrin. The product was analysed by ESI spectrometry. The observation of a signal m/z 799 confirmed the formation of desired compound (TPMM). The ^1H NMR shows the expected peak at desired position as reported in the literature[2].

1.1.2 Synthesis of 5-(4-Carboxyphenyl)-10,15,20-tris(2,4,6-trimethylphenyl) porphyrin (TPMC)

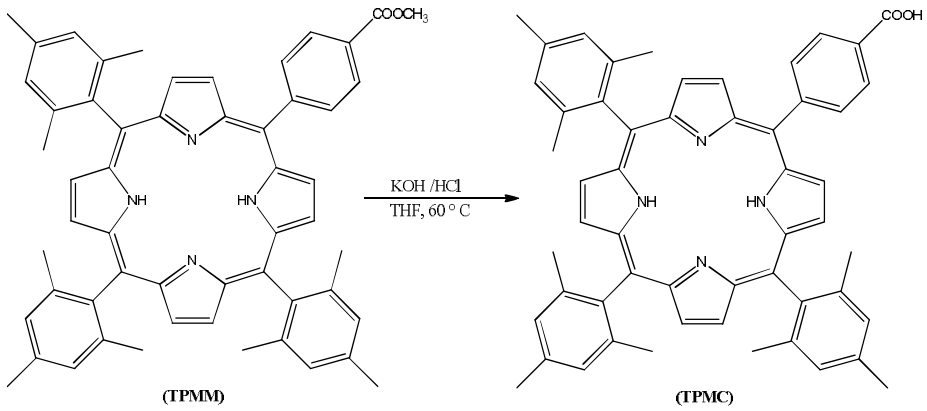

Scheme 3.2: Synthesis of 5-(4-Carboxyphenyl)-10,15,20-tris(2,4,6-trimethylphenyl) porphyrin (TPMC)

The ester group on porphyrin was converted to corresponding carboxylic group by hydrolysis with potassium hydroxide (KOH). For this purpose, a solution of TPMM porphyrin in THF was treated with an aqueous solution of KOH and the solution was refluxed for 2 hours at 65 °C. The progress of the reaction was monitored by TLC using dichloromethane/ethyl acetate (8:2) as eluent. The reaction mixture was allowed to attain

the room temperature, followed by neutralization with an aqueous solution of 1M HCl. The product was extracted with dichloromethane and the organic phase was washed extensively with water. The organic phase was dried over sodium sulfate and the solvent was evaporated giving a red-purple solid as the desired target porphyrin. The product was characterized by ESI spectrometry, the observation of a peak at m/z 786 confirmed the formation of desired porphyrin (TPMC). The ^{1}H NMR was in consistent with the literature values[2], wherein the resonance signals of methyl ester group were no more visible.

1.1.3 Synthesis of [5-(4-Carboxyphenyl)-10,15,20-tris(2,4,6-trimethyl phenyl) porphyrinato zinc (II)](TPMC-Zn)

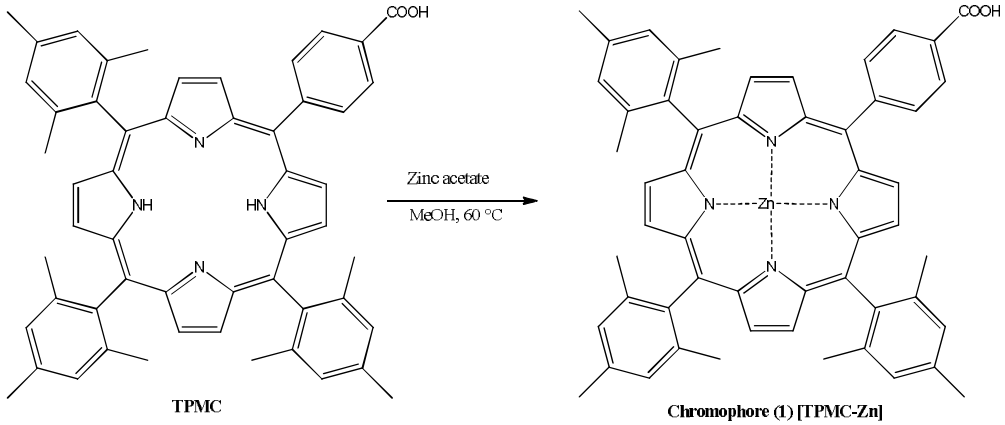

Scheme 3.3: Synthesis of chromophore (1) [5-(4-Carboxyphenyl)-10,15,20-tris(2,4,6-trimethyl phenyl) porphyrinato zinc (II)] (TPMC-Zn)

The metallation of porphyrin was carried out using zinc acetate. For this purpose, a methanolic solution of zinc acetate was added to a solution of TPMC in chloroform. The reaction mixture was refluxed for 1 hour at 60° C. The progress of reaction was monitored by TLC using CH_2Cl_2 as eluent. After complete disappearance of starting material on TLC, the reaction mixture was poured in water and extracted with CH_2Cl_2. The organic layer was separated and dried over sodium sulfate. The solvent was removed under vacuum giving a deep red solid (TPMC-Zn). The product was analysed by ESI spectrometry and the appearance of a peak at m/z 849 confirmed the formation of the target porphyrin. It was further characterized by ^{1}H-NMR, wherein all the hydrogen signals were in accordance with the literature values[2].

The synthesis of this porphyrin enabled me to acquire the requisite skills related to the synthesis, recovery and purification as well as the characterization of porphyrins derivatives. This further helped me to prepare a more complex porphyrin molecule which has been reported to be very effective for DSSC by Gratzel and coworkers.[3]

1.2 Porphyrin chromophore (2) [2-Cyano-3-(2'-(5',10',15',20'-tetraphenyl porphyrinato zinc-(II))yl)acrylic Acid]

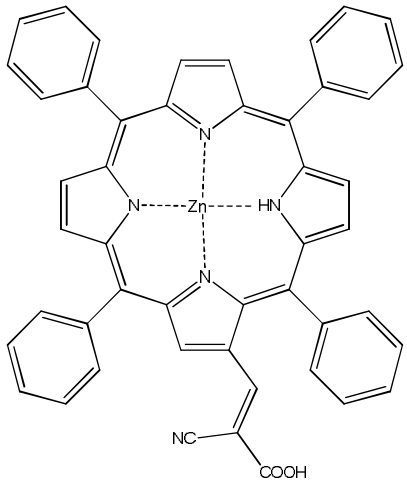

Figure 3.3: Structure of porphyrin chromophore (2) for DSSC

The target porphyrin was synthesized by modification of commercially available tetra phenyl porphyrin. At first, the porphyrin ring was complexed with copper metal using a solution of copper acetate. This was followed by introduction of aldehyde group at β-position of porphyrin by using phosphoryl chloride as a formylating agent. Further, formylated porphyrin derivative was metallated using zinc acetate. Finally, the treatment with cyanoacetic acid resulted in the formation of desired target porphyrin. The synthetic details are discussed in the following sub-sections.

1.2.1 Synthesis of Copper (II) tetra phenyl porphyrin (Cu-TPP)

In order to protect the internal hydrogen of pyrrolic ring for the subsequent formylation reaction, the tetraphenyl porphyrin was metallated with copper(II).[4]

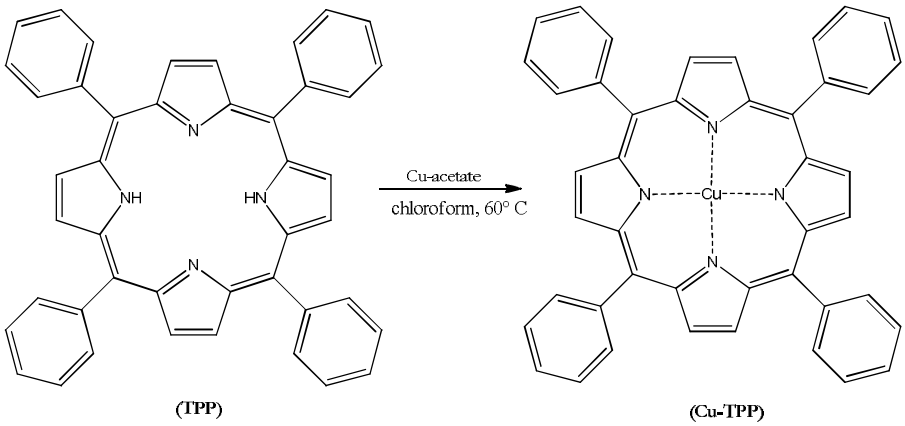

Scheme 3.4: Synthetic approach for Cu-TPP

To a solution of tetraphenyl porphyrin (TPP) in chloroform, a solution of copper acetate in methanol was added. The reaction mixture was refluxed for 1.5 hours at 60° C. The progress of the reaction was monitored by TLC using diethyl ether /chloroform (6:4) as eluent. The formation of a new spot at R_f = 0.7 was observed on TLC. After the complete disappearance of starting tetraphenyl porphyrin on TLC, the desired product was recovered by column chromatography using a mixture of diethyl ether and chloroform as eluent. The fractions containing the product were evaporated and Cu-TPP was obtained as orange solid crystals in nearly quantitative yield.

1.2.2 Synthesis of 2-Formyl-5,10,15,20-tetraphenylporphyrin (CHO-TPP)

The introduction of aldehydic group in the periphery of porphyrin macrocycle was accomplished by the use of phosphoryl chloride ($POCl_3$) as a formylating agent.[5]

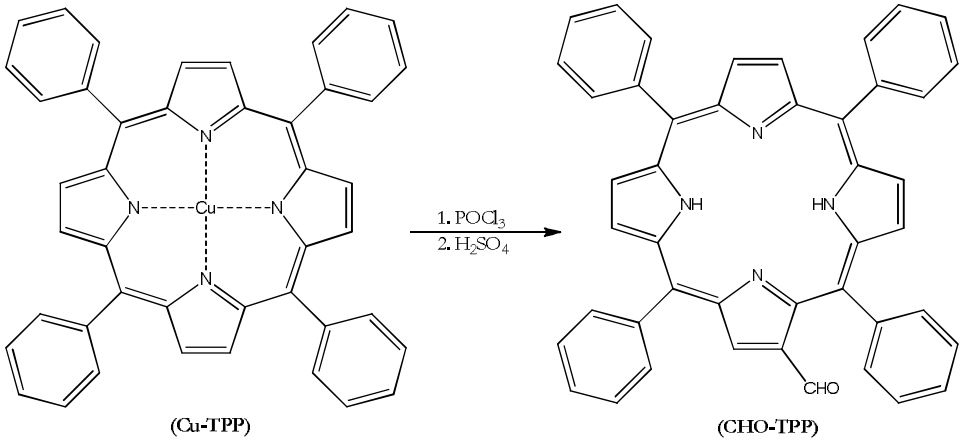

Scheme 3.5: Synthetic approach for CHO-TPP

The reaction was carried out under inert atmosphere. Phosphoryl chloride ($POCl_3$) was solubilized in dry DMF and cooled down to 0 °C. A solution of Cu-TPP was prepared in dry dichloromethane and this was added to $POCl_3$ solution prepared above. After stirring for 15 minutes at room temperature, the reaction mixture was refluxed for 5 hours. The progress of reaction was monitored by TLC and reaction showed disappearance of starting material Cu-TPP. In order to remove copper (II) from the porphyrin ring, concentrated sulphuric acid was added to the reaction and stirred for 10 minutes. Then, the reaction mixture was poured on ice and neutralized with a solution of sodium hydroxide. The target product was collected by extraction with chloroform. The organic layer was separated using separating funnel and washed with a sodium bicarbonate solution. The organic layer was dried over sodium sulfate and the solvent was evaporated. The desired product was purified by column chromatography using CH_2Cl_2/Toluene (2:1) as eluent. The solvent was removed under vacuum and the solid obtained was the desired CHO-TPP porphyrin. The product was characterized by ESI spectrometry, wherein the observation of a peak at m/z 642 confirmed the formation of the product. The formation of product was further confirmed by ^1H NMR, which shows the expected signals at appropriate positions as reported in literature[5].

1.2.3 Synthesis of 2-Formyl-5,10,15,20-tetraphenyl porphyrinato zinc (II) (CHO-Zn-TPP)

The introduction of zinc metal to the formylated porphyrin ring was carried out using zinc acetate.[3]

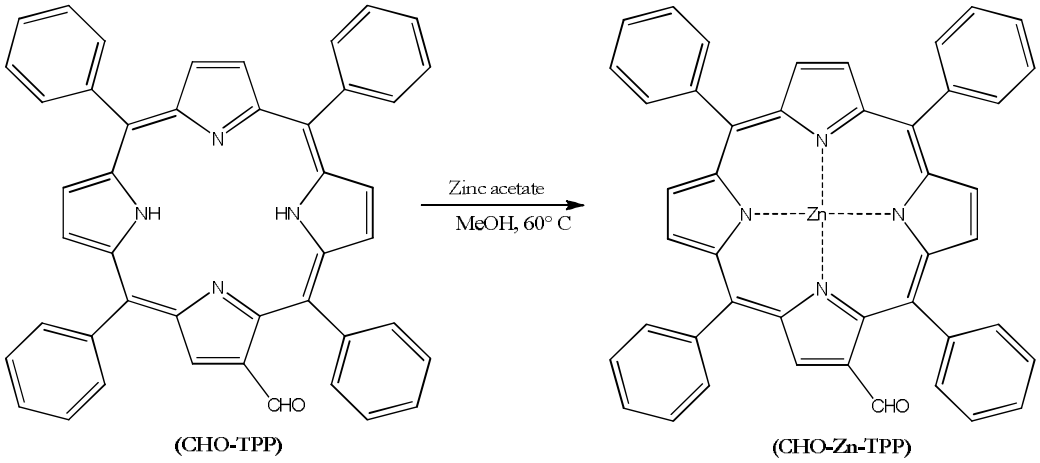

(CHO-TPP) (CHO-Zn-TPP)

Scheme 3.6: Synthesis of 2-formyl-5,10,15,20-tetra phenyl porphyrinato Zinc (II) (CHO-Zn-TPP)

A solution of zinc acetate in methanol was added to a solution of CHO-TPP prepared in chloroform. The reaction mixture was refluxed for 1 hour at 60° C. The progress of the reaction was monitored by TLC using CH_2Cl_2/Toluene (2:1) as an eluent. After the complete disappearance of starting material on TLC, the reaction mixture was poured in water. The organic layer was separated using separating funnel, washed with water and dried over sodium sulfate. The solvent was evaporated giving a purple solid as desired porphyrin (CHO-Zn-TPP). The product was analysed by ESI spectrometry, wherein the formation of corresponding zinc complex was confirmed by mass peak m/z 704. The ^1H NMR spectra was similar to the non-metallated complex, except the proton signals originating from internal hydrogens were not evident in metallated complex.

1.2.4 Synthesis of [2-Cyano-3-(2'-(5',10',15',20'-tetraphenyl porphyrinato zinc-(II))yl)acrylic Acid]

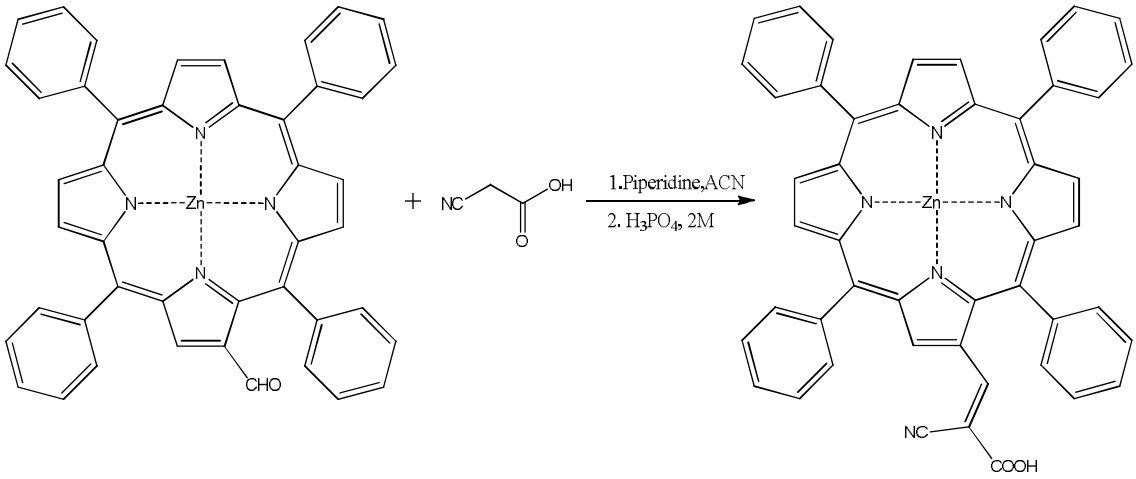

(CHO-Zn-TPP) Chromphore (2)

Scheme 3.7: Synthesis of chromophore (2) [2-Cyano-3-(2'-(5',10',15',20'-tetraphenyl porphyrinato Zinc-(II))yl) acrylic Acid]

The final target cyano-carboxylate porphyrin was prepared in two steps as reported in literature.[3] Firstly, acrylic acid was introduced by reacting the aldehyde moiety of formylated Zn(II) porphyrin with cyanoacetic acid. To this purpose, a solution of porphyrin (CHO-Zn-TPP), cyanoacetic acid and piperidine was prepared in acetonitrile. The reaction mixture was refluxed for 1 hour at 80 °C. After cooling to room temperature, the resulting green precipitate of the target molecule was collected by filtration and thoroughly rinsed with acetonitrile. The precipitate was re-dissolved in DMSO-water-chloroform mixture.

Secondly, a solution of 2M H_3PO_4 was added to this mixture (pH≈2) and stirred vigorously for 10 minutes at room temperature. The organic layer was separated by using separating funnel, washed extensively with water and dried over sodium sulfate. The solvent was evaporated giving a green solid of desired target porphyrin. The product was analysed by ESI spectrometry and ^1H NMR spectroscopy. The observation of a signal at m/z 771 and the expected proton peaks in NMR analysis, confirmed the formation of the desired porphyrin complex.

2. Melamine bridged porphyrin dyads as sensors for diamine

As reported in the Introduction section of this Thesis, the significant application of porphyrins as optical sensors includes their sensing ability to bind to diamine ligands. In particular, dimeric metalloporphyrin hosts with tweezer-like structures, have been specifically designed to effectively complex bifunctional guests through a ditopic interaction. The prominent examples is the dimeric metalloporphyrin host made up of two achiral zinc- or magnesium- porphyrins linked by a flexible covalent tether,[6-10] and melamine bridged zinc tweezer.[11] These tweezers have been exploited to assess the absolute stereochemical configuration of chiral amines, alcohols, and carboxylic acids through the sign of the exciton-coupled circular dichroism in the porphyrin spectrum.

In our laboratory, a convenient one pot synthetic methodology has been developed in order to synthesize bis-porphyrin dyads.[11] This procedure involves the use of cyanuric chloride or trichloro triazine (TCT) as an essential building block and takes advantage of its temperature-dependent stepwise nucleophilic substitution at the chlorine atoms by an amino porphyrin.[12]

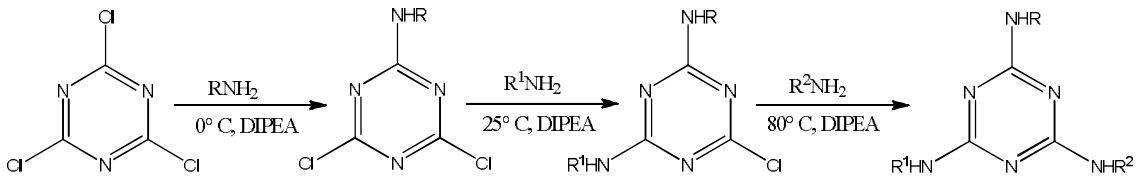

Figure 3.4: Reactivity of cyanuric chloride

Indeed, trichloro triazine (TCT) undergoes a rapid nucleophilic substitution of its first chlorine atom at 0 °C, and undergoes second substitution at room temperature or moderate heating. In order to displace the third chlorine atom, harsher conditions are required (temperature >80 °C for multiple hours). Thus, it is feasible to conduct one pot reaction for varying substitution of TCT in a sequential manner owing to the nearly quantitative yield of each substitution steps. The advantage of this synthetic methodology could be exploited in the design of porphyrin dyads. In this, the overall stereo electronic diversity can be generated by a proper synthesis/selection of the isolated components in a homodimer arrangement, by the combination of these within a heterodimeric structure, and/or by differential metallation of the porphyrin.[13]

Herein, three different porphyrin dyads were synthesized, the details of which will be discussed in the following sub-sections.

2.1 Bis-phenyl porphyrin zinc (II) dimer (3)

The bis-phenyl porphyrin zinc (II) dimer depicted in Figure 3.5 is known to act as a molecular tweezer for diamine ligands. Indeed, a marked colour variation from purple to blue was consistently observed upon adding aliphatic diamines of general formula $H_2N(CH_2)_nNH_2$ (n=4-8) to a dichloromethane solution of these bis-phenyl porphyrin-Zn(II) receptors.[11,13] Due to this property, there is a wide scope of using them as optical sensors. The next three sections will deal with the porphryin dimers I prepared for some ongoing collaborations of the group.

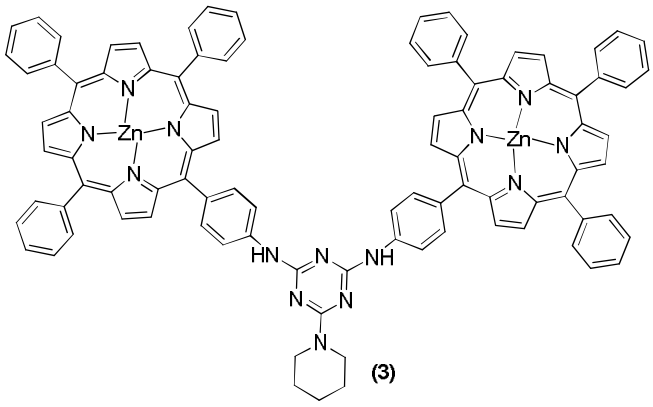

Figure 3.5: Structure of bis-phenyl porphyrin zinc (II) dimer (3)

2.1.1 Synthesis of bis-phenyl porphyrin adduct (PTP)

The preparation of bis-phenyl porphyrin adducts requires the preliminary synthesis of amino tetra phenyl porphyin (TPP-NH_2) which will be discussed in section 6.1.2 of the thesis.

Two moles of TPP-NH_2 were reacted with cyanuric chloride to give the bis-phenyl porphyrin adduct as shown in scheme 3.8.

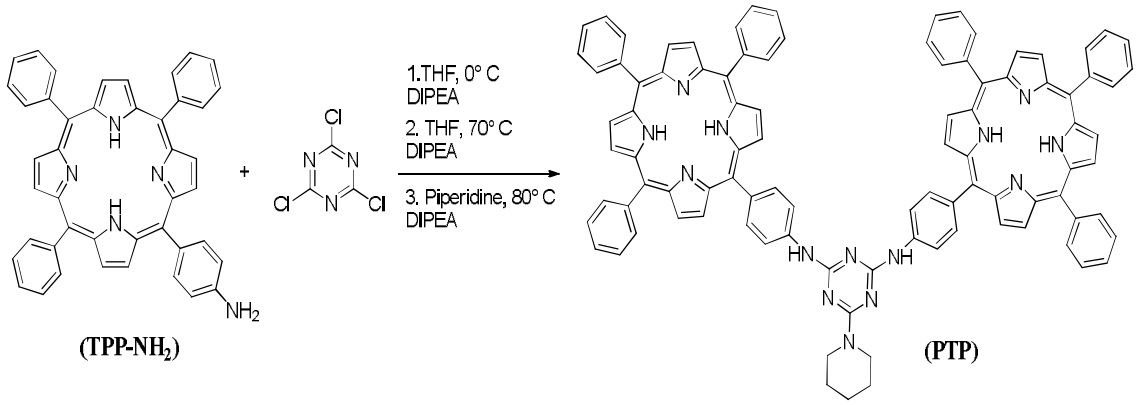

Scheme 3.8: Synthesis of bis-phenyl porphyrin adduct (PTP)

A solution of amino porphyrin (TPP-NH_2) in THF was reacted with one equivalent of trichloro triazine at 0° C in the presence of 1.2 equivalent of diisopropylethylamine (DIPEA) as a base. The reaction mixture was stirred at room temperature and monitored by TLC analysis (using petroleum ether/ethyl acetate 3:2 v/v as eluent) which indicated the complete disappearance of starting material (TPP-NH_2) and formation of the mono adduct. At this point, another equivalent of amino porphyrin was added, together with 1.2 equivalent of DIPEA and the reaction mixture was stirred at 70°C for 3 hours to afford the corresponding bis-phenyl porphyrin adduct. Finally, the third chloride atom was replaced by treatment with an excess of piperidine at 80 °C. After 3 hours, the solvent was evaporated and the solid was subjected to flash column chromatography (eluent: petroleum ether/ethyl acetate 3:2) to recover the desired bis-phenyl porphyrin adduct (PTP) as purple solid. The product so formed showed a single spot on TLC. The peak at m/z 1420 as obtained in ESI spectrometry confirmed the formation of the desired product, which was also confirmed by ^{1}H NMR analysis where the proton signals were in accordance with the literature values.

2.1.2 Synthesis of bis-phenyl porphyrin zinc (II) dimer (3)

The bisphenyl porphyrin adduct (PTP) prepared in the previous sub-section was subjected to metallation using zinc acetate.

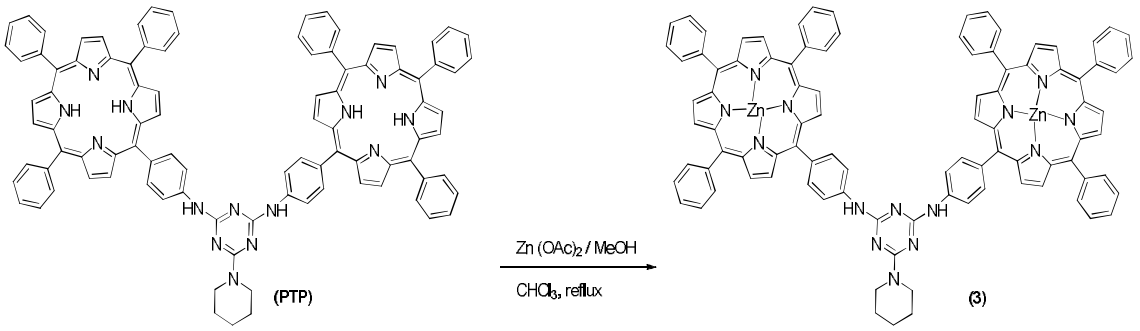

Scheme 3.9: Synthesis of bis-phenyl porphyrin zinc (II) dimer (3)

A solution of zinc acetate in methanol was added to a solution of porphyrin adduct (PTP) in chloroform. The reaction mixture was refluxed for 1 hour at 60° C. The progress of the reaction was monitored by TLC using mixture of CH_2Cl_2/Toluene (2:1) as the eluent. After the complete disappearance of starting material on TLC, the reaction mixture was poured in water. The organic layer was separated using separating funnel and dried over sodium sulfate. The solvent was evaporated yielding a quantitative amount of purple solid as desired bis-phenyl porphyrin zinc (II) dimer (3). The observation of a peak at m/z 1546 in ESI spectrometry confirmed the formation of the corresponding zinc complex (3). Further, the ^{1}H NMR analysis does not show the signals originating from internal hydrogens of porphyrin, which were evident in non-metallated complex.

2.2 Bis-(3,5-di-tert-butylphenyl-porphyrin) zinc (II) dimer (4)

In the past years, dimeric metal porphyrin hosts (tweezers) have been used as chirality probes for determination of the absolute configuration (AC) for a large variety of natural products and synthetic compounds.[14-17] The tweezer (4) depicted in Figure 3.6 demonstrated a better molecular recognition, a stronger circular dichroism (CD) response and a broader utility, than commercially available probes.[18,19]

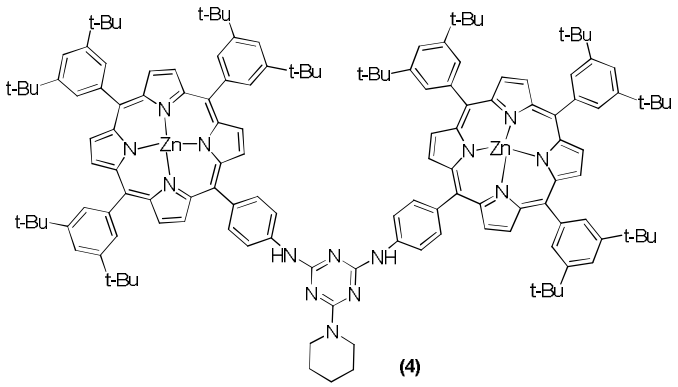

Figure 3.6: Structure of bis-(3,5-di-tert-butylphenyl-porphyrin) zinc (II) dimer (4)

By using this tweezer, various classes of chiral guests such as diamines, α-amino-amides, α-amino-alcohols and secondary mono alcohols were studied. The main advantages of this tweezer are:

i) correct assignment of the AC

ii) univocal sign of the CD couplet regardless of solvent polarity

iii) sensitivity of the tweezer host estimated by the minimum number of equivalents of chiral guest needed to reach the maximum CD response.

As a part of collaboration with Prof Nina Berova at University of Columbia, the synthesis of porphyrin tweezer (4) was repeated. In order to prepare this, the procedure reported by Berova and co-workers was followed.[20]

First of all, the preparation of the tweezer (4) requires the preliminary synthesis of 5-(4-aminophenyl)-10,15,20-(3,5-tert-butylphenyl)porphyrin in accordance with the procedure reported by Schuster and coworkers.[21]

2.2.1 Synthesis of 5-(4-acetamidophenyl)-10,15,20-tri-(3,5-di-tert-butylphenyl) porphyrin (t-butyl-Ac-TPP)

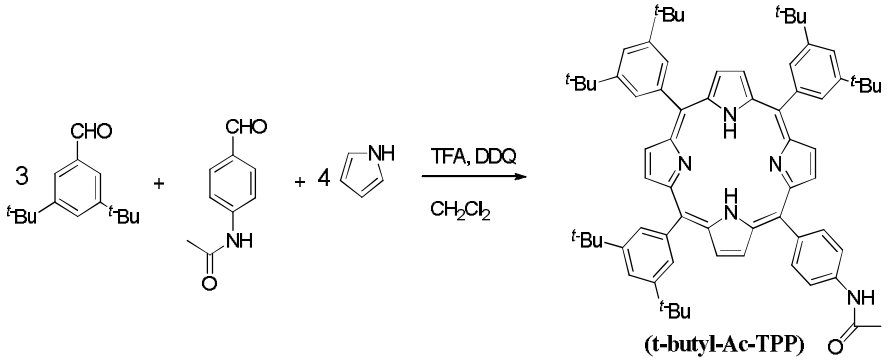

Scheme 3.10: Synthesis of 5-(4-acetamidophenyl)-10,15,20-tri-(3,5-di-tert-butyl phenyl) porphyrin (t-butyl-Ac-TPP)

The construction of porphyrin macrocycle was done using pyrrole and a mixture of acetamido benzaldehyde, 3,5-di-tert-butylbenzaldehyde in 1:3 ratio in dichloromethane. After stirring the mixture at room temperature for 10 minutes, TFA was added to the reaction mixture and stirred for another 2 hours at room temperature. In order to oxidize the porphyrinogen to the corresponding porphyrin, DDQ was added and stirred at room temperature during 1 hour. Further, to neutralize the reaction mixture, triethyl amine was added. The solvent was removed in vacuo and solid thus obtained was subjected to column chromatography. First, the tetra substituted porphyrin was eluted using dichloromethane. Then, the desired A_3B porphyrin was eluted using a mixture of CH_2Cl_2/EtOAc (8:2). The solvent was evaporated yielding a purple solid as desired target porphyrin (t-butyl-Ac-TPP). The product was analysed by ESI spectrometry, the observation of a peak at m/z 1006 confirmed the formation of the desired porphyrin. The formation of porphyrin was further confirmed using ^{1}H NMR spectroscopy, wherein all the expected peaks were at its usual position as reported in literature.

The next step was the hydrolysis of acetamido porphyrin (t-butyl-Ac-TPP) to get the amino porphyrin.

2.2.2 Synthesis of 5-(4-aminophenyl)-10,15,20-tri-(3,5-di-tert-butylphenyl) porphyrin (t-butyl-TPP-NH_2)

The hydrolysis of acetamido porphyrin with concentrated hydrochloric acid resulted in the formation of corresponding amino porphyrin.

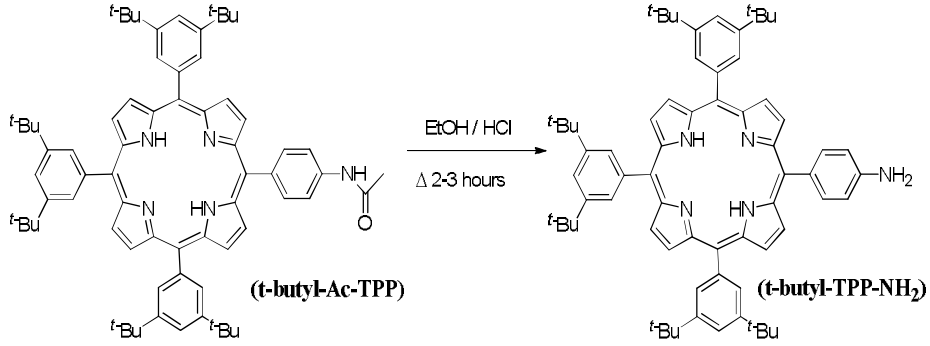

Scheme 3.11: Synthesis of 5-(4-aminophenyl)-10,15,20-tri-(3,5-di-tert-butylphenyl) porphyrin (t-butyl-TPP-NH_2)

A solution of p-acetamido porphyrin (t-butyl-Ac-TPP) was prepared in ethanol. Concentrated HCl was added to the reaction mixture and then refluxed for 17 hours. The crude mixture was diluted with water and extracted with dichloromethane. The organic layer was washed with water and then with saturated $NaHCO_3$ solution. The organic layers were dried over Na_2SO_4. The solvent was removed under vacuum and subjected to flash chromatography using dichloromethane as eluent that afforded the desired amino porphyrin (t-butyl-TPP-NH_2). The formation of amino porphyrin was confirmed by ^1H NMR analysis where all the proton values was similar as reported in literature

2.2.3 Synthesis of bis-(3,5-di-tert-butylphenyl-porphyrin) adduct (BTB)

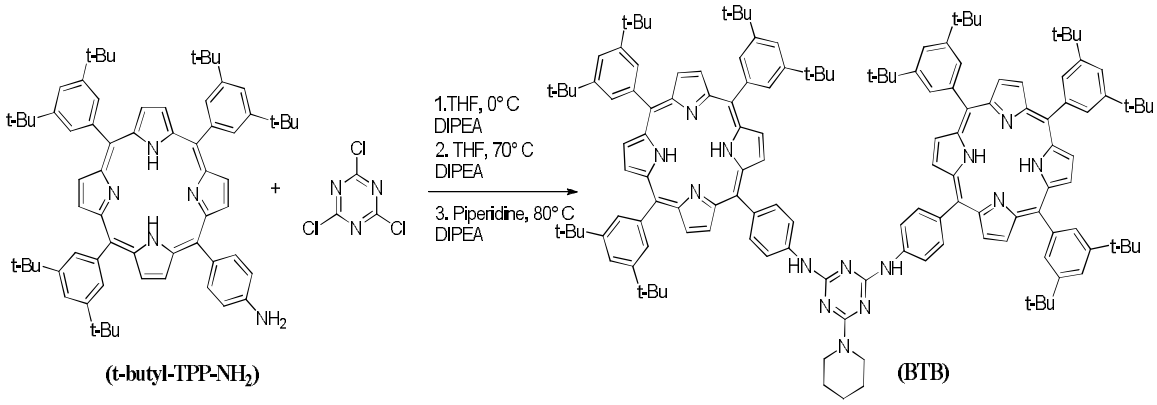

Scheme 3.12: Synthesis of bis-(3,5-di-tert-butylphenyl-porphyrin) adduct (BTB)

The synthetic procedure of bis-porphyrin adduct (BTB) was almost identical as described above using TCT one pot methodology.

A solution of 5-(4-aminophenyl)-10,15,20-tri-(3,5-di-tert-butylphenyl) porphyrin in THF was cooled at 0 °C followed by addition of 1 equivalent of cyanuric chloride and 1.2 equivalents of DIPEA. After stirring for 10 minutes at 0 °C, the solution was allowed to attain room temperature. The formation of mono adduct was complete, as witnessed from TLC analysis (ether/ethyl acetate 3:2 v/v), that showed the disappearance of starting amino porphyrin (R_f = 0.31) and the formation of a new spot at R_f = 0.63. A second equivalent of amino porphyrin was then added together with 1.2 equivalents of DIPEA and the reaction mixture was stirred at 70 °C for 24 hours. After observing a almost complete formation of the bis-adduct (R_f = 0.73), an excess of piperidine was added together with 1.2 equivalents of DIPEA and the reaction mixture was further stirred at 80 °C for 3 hours. The solvent was evaporated and the residue was purified by flash chromatography (petroleum ether/ethyl acetate, 3:2 v/v), thereby affording porphyrin adduct (BTB). The product was analysed by ESI spectrometry, the observation of a peak at m/z 2093 confirmed the formation of the desired porphyrin adduct.

2.2.4 Synthesis of bis-(3,5-di-tert-butylphenyl-porphyrin) zinc (II) dimer (4)

The bisphenyl porphyrin adduct (BTB) prepared in the previous sub-section was subjected to metallation using zinc acetate.

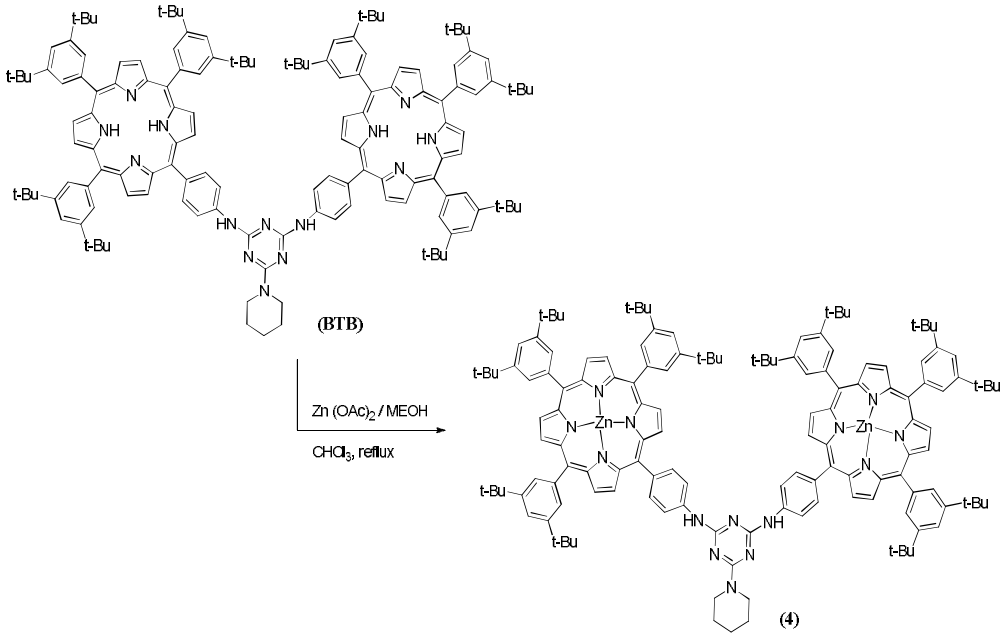

Scheme 3.13: Synthesis of bis-(3,5-di-tert-butylphenyl-porphyrin) zinc (II) dimer (4)

A solution of zinc acetate in methanol was added to a solution of bis-porphyrin adduct (BTB) in chloroform. The reaction mixture was refluxed for 1 hour at 60° C. The progress of reaction was monitored by TLC using CH_2Cl_2/Toluene (2:1) as the eluent. After complete disappearance of starting material, the reaction mixture was poured into water. The organic layer was collected and dried over Na_2SO_4. The solvent was evaporated giving a purple solid as desired bis-(3,5-di-tert-butylphenyl-porphyrin) zinc(II) dimer (4) in quantitative yield. The product was analysed by ESI spectrometry, the observation of a peak at m/z 2221 confirmed the formation of corresponding zinc complex (4). The product was further characterized by NMR analysis, which showed peaks almost similar to non-metallated complex except the proton peak originating from internal hydrogens were not evident in metallated form.

The most recent synthetic task required from our partners was to modify this tweezer by introduction of methyl group on melamine bridge tweezer and study if whether or not a stereochemical hindering of the linker would affect the tweezer properties in comparison with the already reported tweezers. For this purpose, synthesis of N-methylated tweezer was explored and the results are documented in the coming section.

2.3 N-methyl bis-(3,5-di-tert-butylphenyl-porphyrin) zinc (II) dimer (5)

The introduction of methyl group was done on the trichloro triazine building block to get modified tweezer as shown in Figure 3.7.

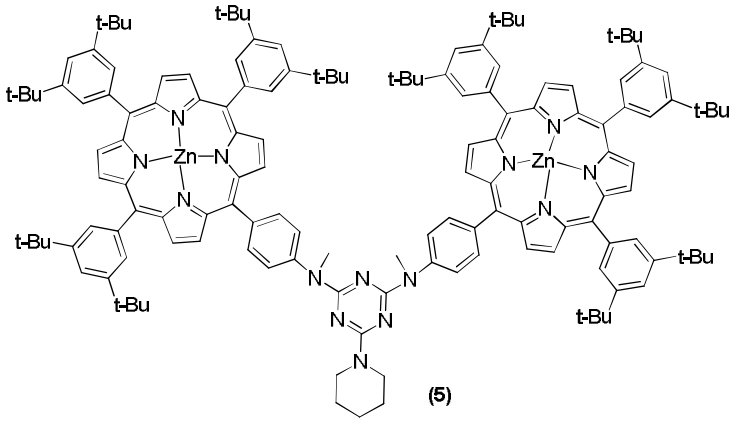

Figure 3.7: Structure of N-methyl bis-(3,5-di-tert-butylphenyl-porphyrin) zinc (II) dimer (5)

Due to the reactivity issues of cyanuric chloride towards methylation, the incorporation of the N-methyl moiety directly on the triazine linker was not considered promising. Thus, it was decided to introduce the N-methyl group on the porphyrin molecule instead. Hence, during the construction of porphyrin ring, the methylation could be done on the specific aldehyde group as described in the following sub-section.

2.3.1 Synthesis of N-methyl p-acetamido benzaldehyde (6)

The introduction of methyl group on p-acetamido benzaldehyde can be performed by treatment with iodomethane as reported in literature by Pike and co-workers.[22]

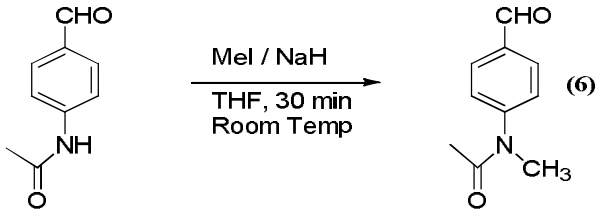

Scheme 3.14: Synthesis of N-methyl p-acetamido benzaldehyde (6)

Firstly, sodium hydride (NaH) was added to a magnetically stirred solution of p-acetamido benzaldehyde in anhydrous THF, followed by the dropwise addition of iodomethane. The reaction mixture was maintained for 0.5 hour at below 5 °C and then stirred at room temperature. The reaction was monitored by TLC. After the reaction was complete, the mixture was partitioned between saturated aqueous ammonium chloride and ethyl acetate. The organic layer was separated and the aqueous layer was extracted with ethyl acetate. The combined organic layers were washed with water and dried over sodium sulfate. The solvent was evaporated and the residue was purified by flash chromatography using a mixture of petroleum ether/ethyl acetate as the eluent to give the desired product (6). The product was analysed by ESI spectrometry, the observation of peak at m/z 178 confirmed the formation of N-methyl p-acetamido benzaldehyde. The next step was to construct the porphyrin ring.

2.3.2 Synthesis of 5-(N-methyl-4-acetamidophenyl)-10,15,20-tri-(3,5-di-tert-butylphenyl) porphyrin (N-met-t-butyl-Ac-TPP)

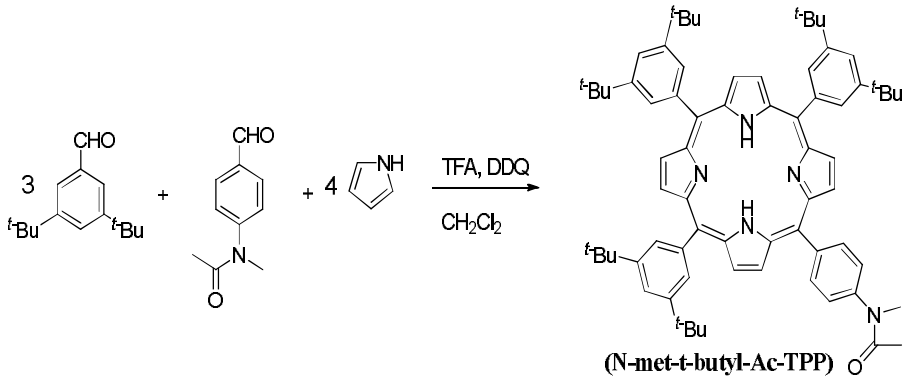

Scheme 3.15: Synthesis of 5-(N-methyl-4-acetamidophenyl)-10,15,20-tri-(3,5-di-tert-butylphenyl) porphyrin (N-met-t-butyl-Ac-TPP)

The construction of porphyrin ring was carried using pyrrole and a mixture of N-methyl p-acetamido benzaldehyde, and 3,5-di-tert-butylbenzaldehyde in 1:3 ratio in dichloromethane. The mixture was stirred at room temperature for 10 minutes then TFA was added to start the cyclization process. The reaction mixture was stirred for another 2 hours at room temperature. Then, DDQ was added and stirred at room temperature for further 1 hour. Further, to neutralize the reaction mixture, triethyl amine was added. The solvent was then removed in vacuo and the residue was subjected to column chromatography. The elution was started using dichloromethane to obtain the tetra substituted porphyrin and then with a mixture of CH_2Cl_2/EtOAc (8:2) as eluent, in order to obtain the desired A_3B porphyrin. The solvent was evaporated yielding a purple solid as (N-met-t-butyl-Ac-TPP) porphyrin. The product so formed was characterized by ESI spectrometry and ^{1}H NMR spectroscopy techniques.

The ESI spectrometry (figure 3.8) shows peak at m/z 1022 corresponding to M+1 molecular ion peak of (N-met-t-butyl-Ac-TPP) porphyrin. The ^{1}H NMR spectra (figure 3.9) was in agreement with expected proton resonances specially the N-methyl protons were easily visible at 3.5 ppm.

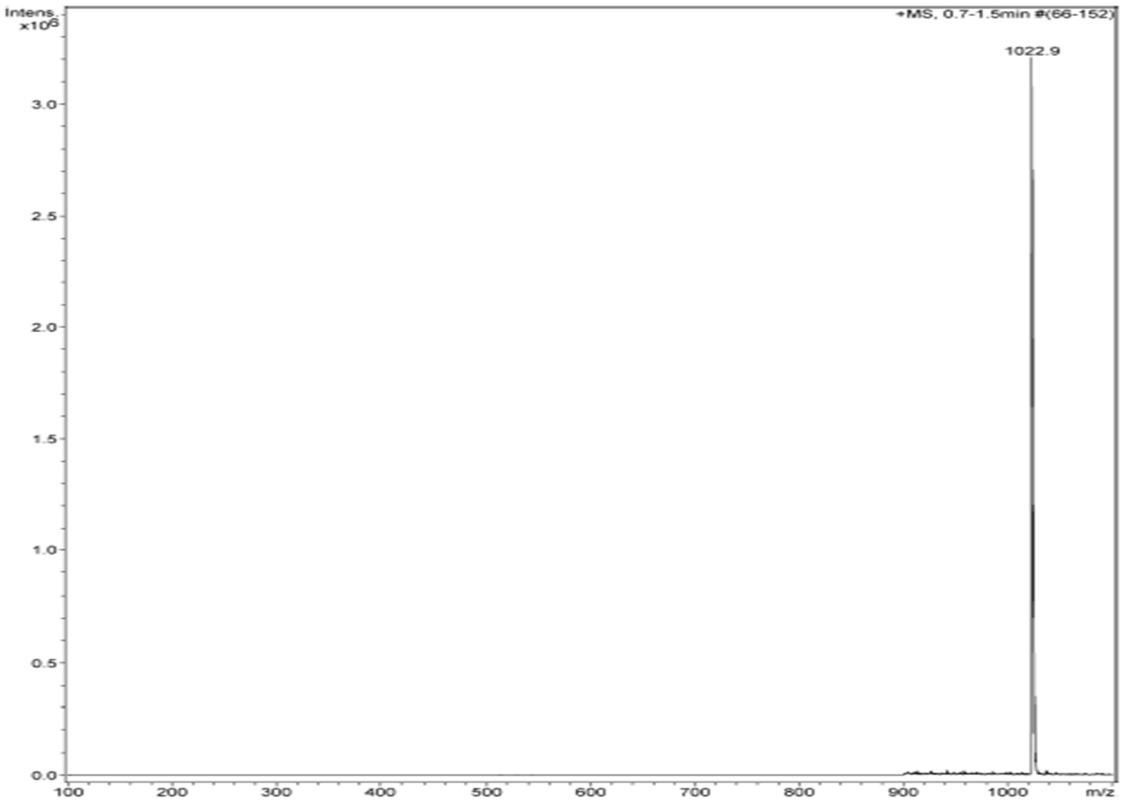

Figure 3.8: ESI-MS (ACN) spectrum of (N-met-t-butyl-Ac-TPP) porphyrin

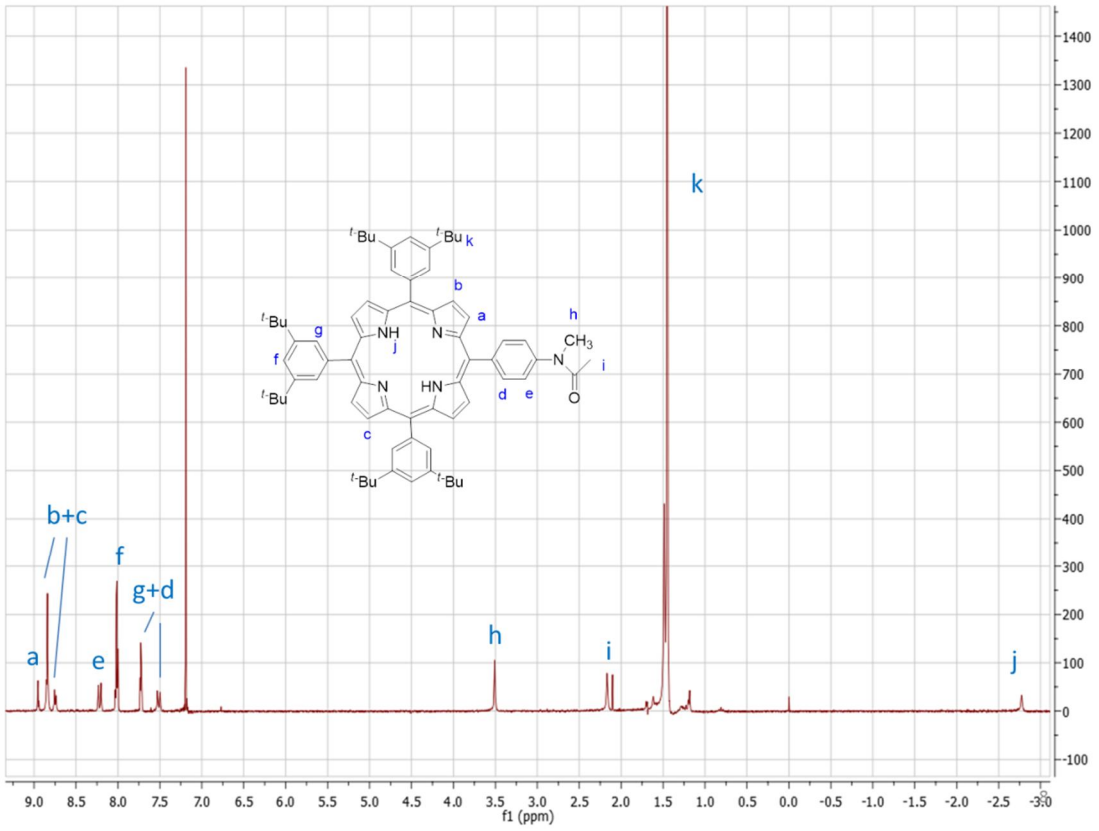

Figure 3.9: ^{1}H-NMR $(CDCl)_3$ spectrum of (N-met-t-butyl-Ac-TPP) porphyrin

The next step was the hydrolysis of acetamido porphyrin (N-met-t-butyl-Ac-TPP) to get the corresponding amino porphyrin.

2.3.3 Synthesis of 5-(N-methyl-4-aminophenyl)-10,15,20-tri-(3,5-di-tert-butylphenyl) porphyrin (N-met-t-butyl-TPP-NH_2)

The hydrolysis of acetamido porphyrin with concentrated hydrochloric acid resulted in the formation of N-methyl-amino porphyrin as shown in Scheme 3.16.

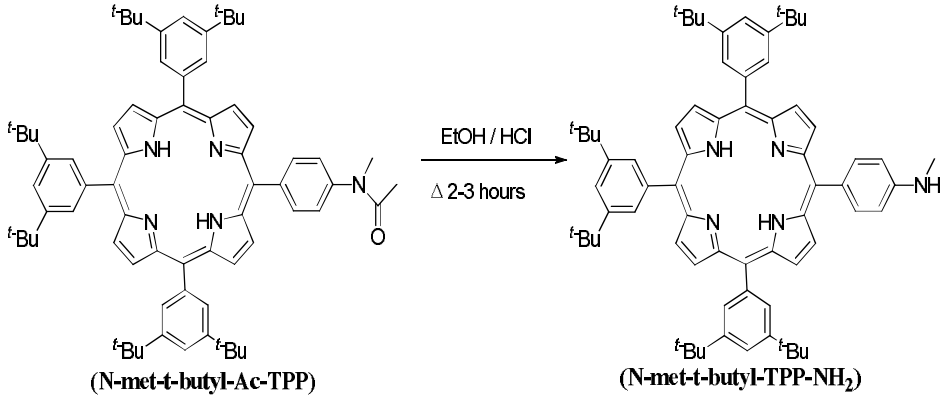

Scheme 3.16: Synthesis of 5-(N-methyl-4-aminophenyl)-10,15,20-tri-(3,5-di-tert-butylphenyl) porphyrin (N-met-t-butyl-TPP-NH_2)

A solution of p-acetamido porphyrin was prepared in ethanol. To this, concentrated HCl was added and the solution was refluxed for 17 hours. The crude mixture was diluted with water and extracted with dichloromethane. The organic layer was washed with water and then with saturated $NaHCO_3$ solution. The pooled organic layers were dried over Na_2SO_4. The solvent was removed under vacuum and subjected to flash chromatography using dichloromethane as eluent that afforded the desired amino porphyrin (N-met-t-butyl-TPP-NH_2). The product so formed was characterized by ESI spectrometry and ^1H NMR spectroscopy techniques.

The ESI spectrometry shows two peaks at m/z 981 and 491 corresponding to $[MH]^+$ and $[MH_2]^{2+}$ molecular ions of (N-met-t-butyl-Ac-TPP) porphyrin respectively. The ^1H NMR spectra was in agreement with the expected proton signals specially the N-methyl and N-H protons were well evident at 3.0 and 4.5 ppm respectively.

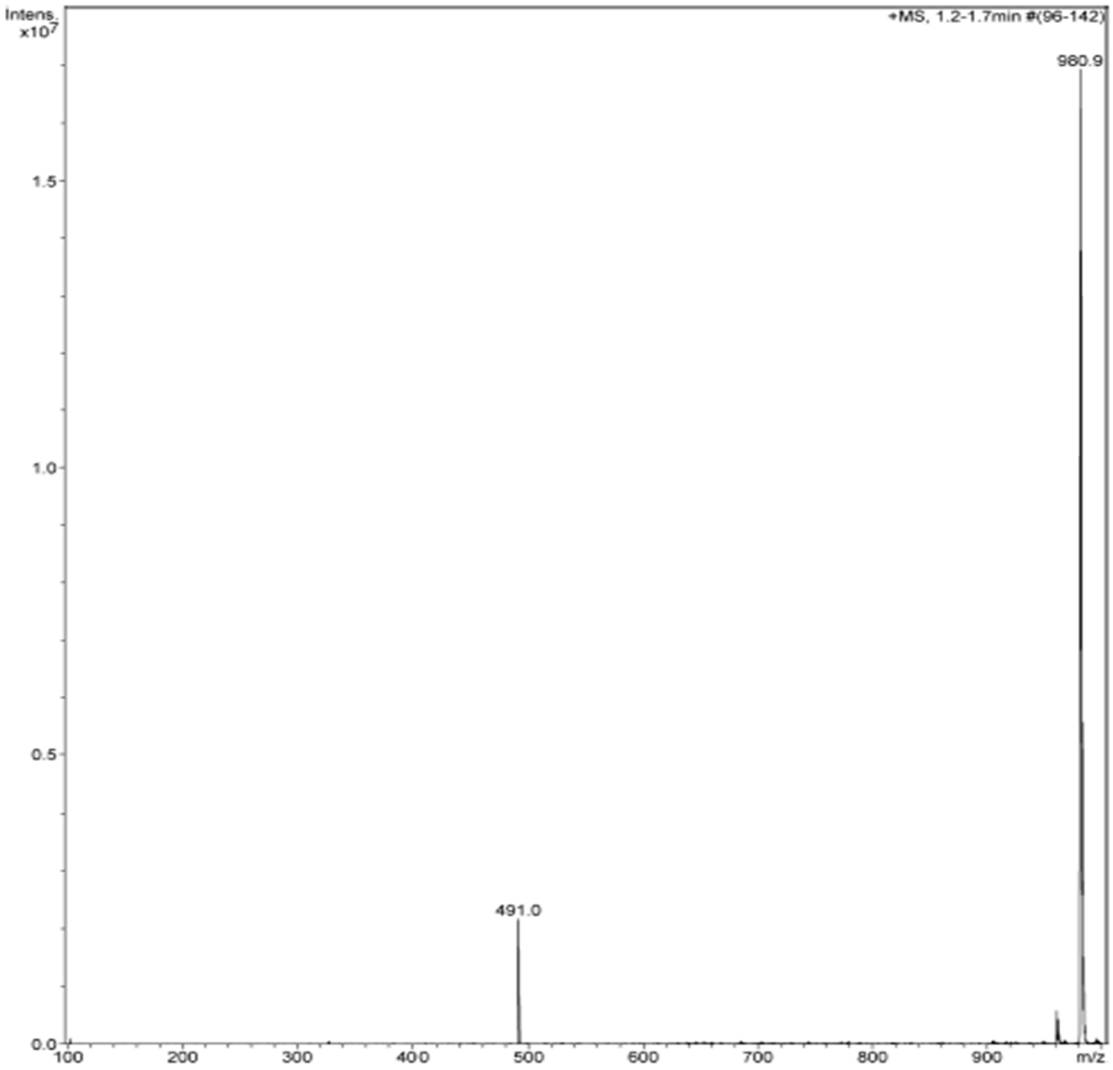

Figure 3.10: ESI-MS (ACN) spectrum of (N-met-t-butyl-TPP-NH_2) porphyrin

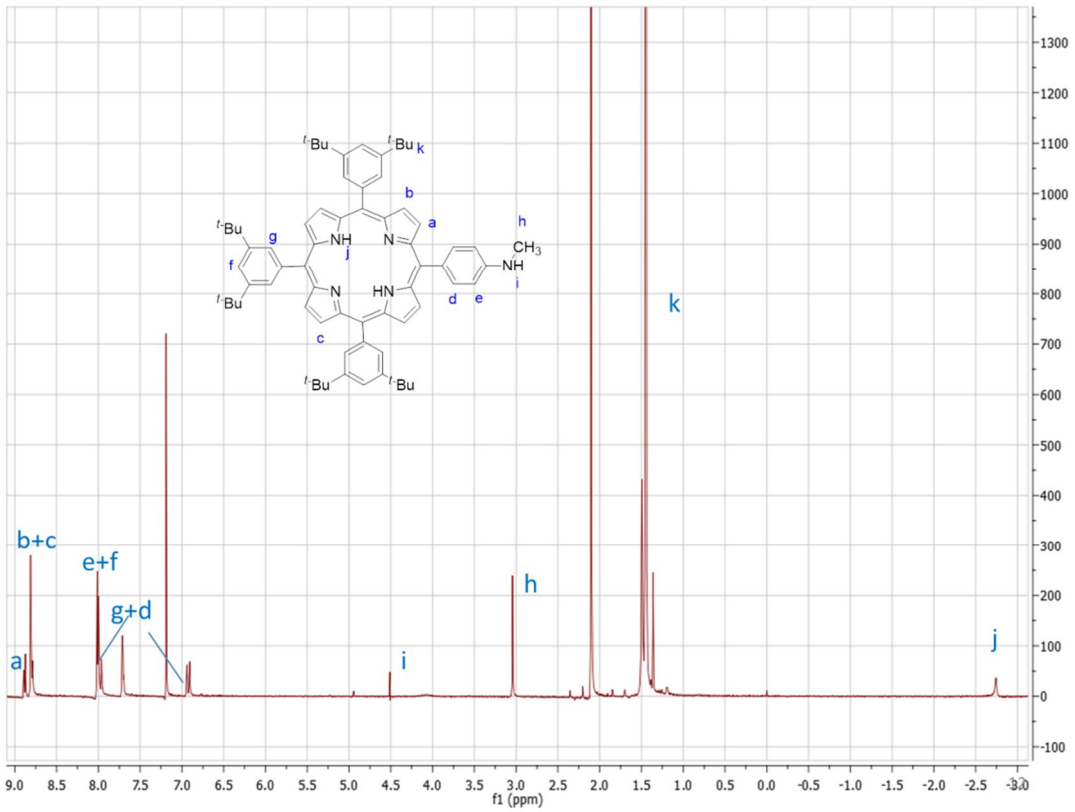

Figure 3.11: ^{1}H-NMR $(CDCl)_3$ spectrum of (N-met-t-butyl-TPP-NH_2) porphyrin

2.3.4 Synthesis of N-methyl bis-(3,5-di-tert-butylphenyl-porphyrin) adduct (N-BTB)

The synthetic procedure of bis-porphyrin adduct (N-BTB) was almost similar as described above using TCT one pot methodology.

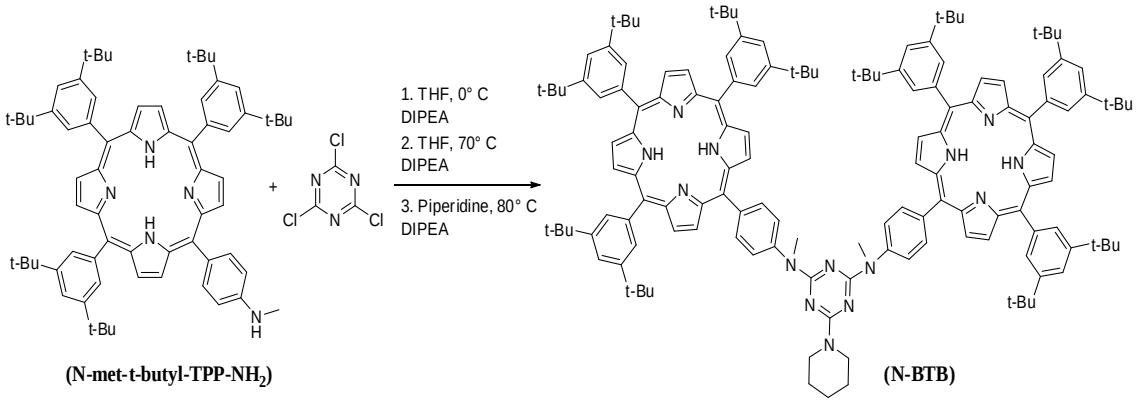

Scheme 3.17: Synthesis of N-methyl bis-(3,5-di-tert-butylphenyl-porphyrin) adduct (N-BTB)

To a solution of (N-met-t-butyl-TPP-NH_2) porphyrin in THF cooled at 0 °C, trichloro triazine (1 equivalent) and DIPEA (1.2 equivalent) were added. After stirring for 10 minutes at 0 °C, the solution was allowed to attain the room temperature. The reaction was complete, as evident from the TLC analysis (petroleum ether/ethyl acetate, 3:2 v/v) showing the disappearance of starting porphyrin (R_f = 0.40) and the formation of a new spot at R_f = 0.65 corresponding to the porphyrin mono-adduct. At this moment, a second equivalent of amino porphyrin was added together with 1.2 equivalent of DIPEA. The reaction was further stirred at 70 °C for 24 hours. After observing almost complete formation of the bis-adduct (R_f = 0.80), an excess of piperidine was added together with 1.2 equivalents of DIPEA and the mixture was further stirred at 80 °C for 3 hours. After removal of the solvent by evaporation, the residue was purified by flash chromatography (petroleum ether/ethyl acetate 3:2 v/v) affording the desired (N-BTB) porphyrin adduct. The product was characterized by ESI spectroscopy technique.

The ESI spectrometry shows a main peak at m/z 2121 which corresponds to M+1 molecular ion peak of porphyrin adduct (N-BTB).

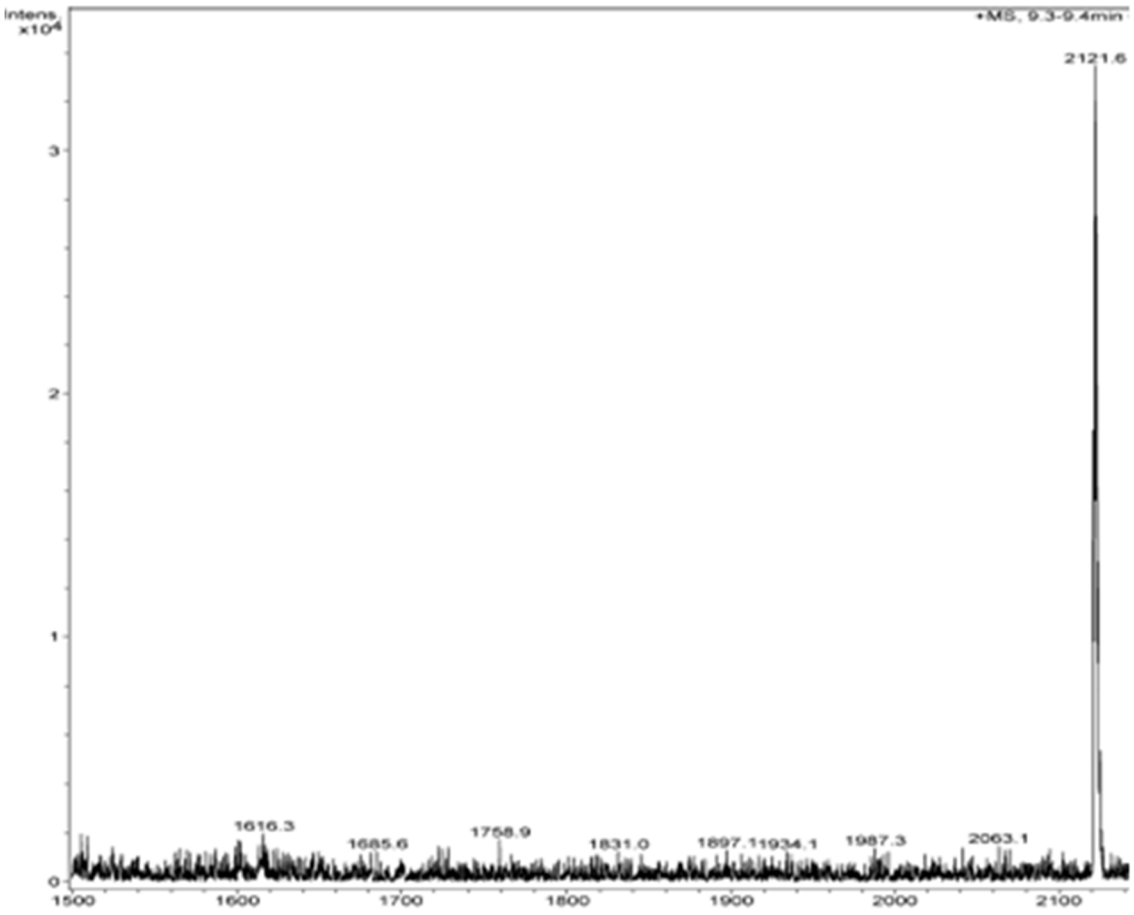

Figure 3.12: ESI-MS (ACN) spectrum of porphyrin adduct (N-BTB)

2.3.5 Synthesis of N-methyl bis-(3,5-di-tert-butylphenyl-porphyrin) zinc (II) dimer (5)

The bisphenyl porphyrin adduct (N-BTB) prepared in the previous sub-section was subjected to metallation using zinc acetate as shown in Scheme 3.18.

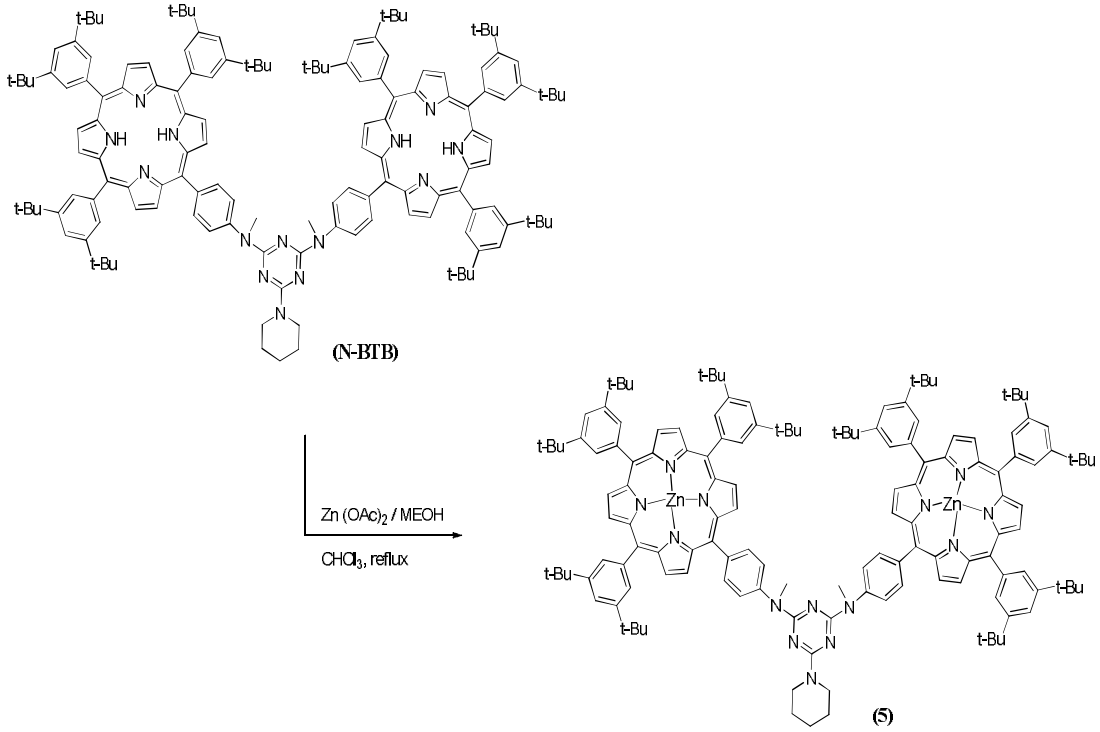

Scheme 3.18: Synthesis of N-methyl bis-(3,5-di-tert-butylphenyl-porphyrin) zinc (II) dimer (5)

A solution of zinc acetate in methanol was added to a solution of bis-porphyrin adduct (N-BTB) in chloroform. The reaction mixture was refluxed for 1 hour at 60° C. The progress of the reaction was monitored by TLC using CH_2Cl_2/Toluene (2:1) as eluent. As evident from the TLC analysis, after the complete disappearance of starting material the reaction mixture was poured into water. The organic layer was separated using separating funnel and dried over sodium sulfate. The solvent was evaporated yielding a purple solid as desired porphyrin dimer (5). The product so formed was characterized by ESI spectrometry and ^{1}H NMR spectroscopy techniques.

The ESI spectrometry shows a peak at m/z 2243 corresponding to M+1 molecular ion peak of porphyrin dimer (5). The ^{1}H NMR spectra was in well agreement with the expected proton peaks and the representation of the same has been done in the experimental part of the thesis.

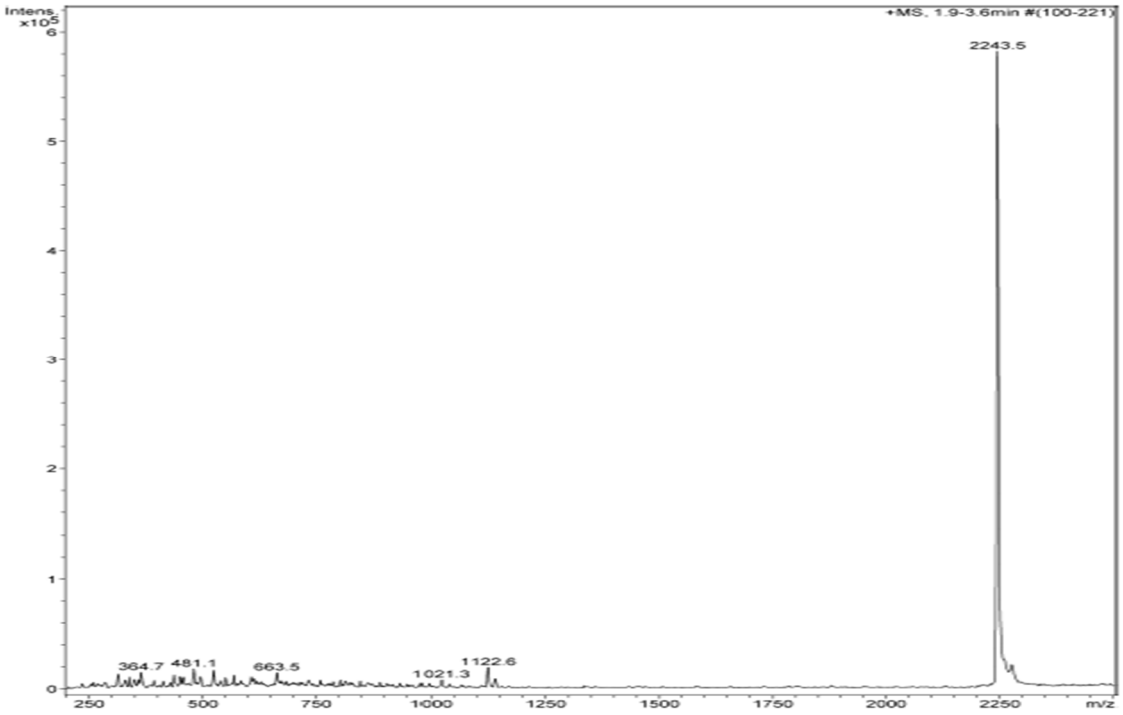

Figure 3.13: ESI-MS (ACN) spectrum of porphyrin dimer (5)

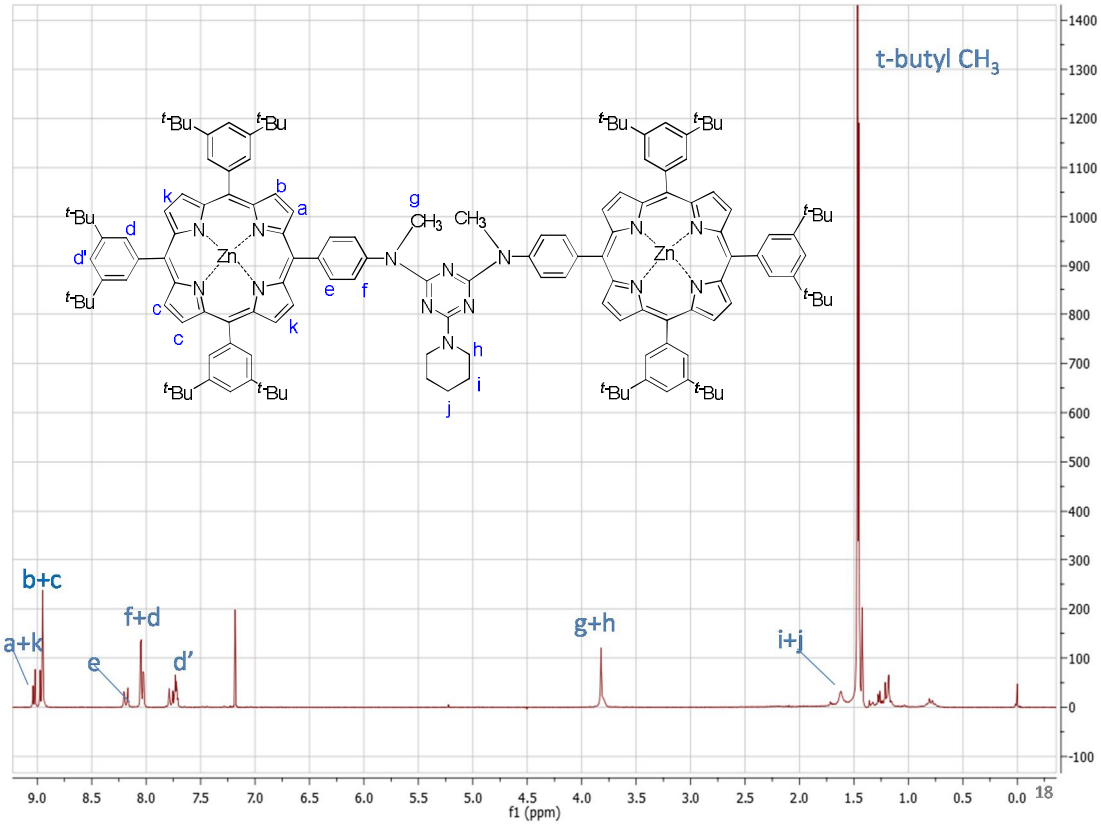

Figure 3.14: ^{1}H-NMR $(CDCl)_3$ spectrum of porphyrin dimer (5)

3. Synthesis of Porphyrin derivative using Click chemistry

Since a complex bis-porphyrin dyad was synthesized in the above sub-section, the next task was to synthesize a novel porphyrin chromophore for DSSC involving triazole moiety. In order to achieve this, "click chemistry" approach was used, which has only few reports in literature involving porphyrin structures.[24,25]

3.1 Porphyrin chromophore (7) [Meso Triazole clicked Porphyrin]

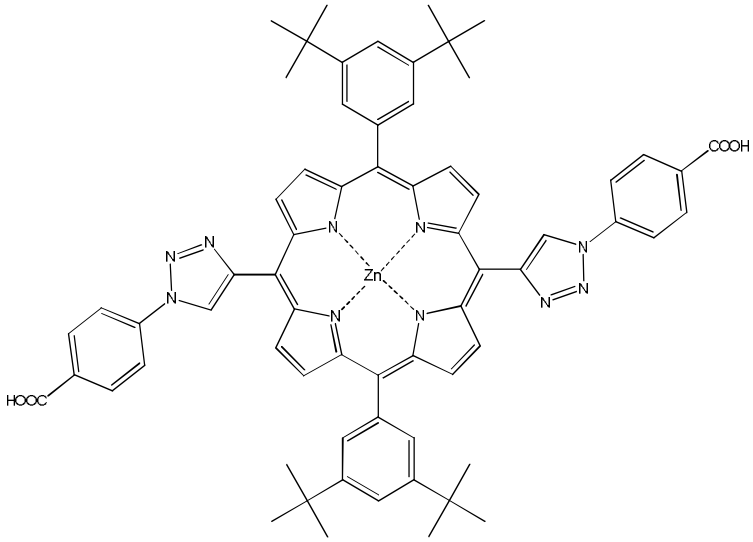

Figure 3.15: Structure of porphyrin chromophore (7) for DSSC

The above porphyrin derivative was synthesized using "Click chemistry". The click reaction (Huisgen reaction), is a 1,3-dipolar addition of an azide to a terminal alkyne which has demonstrated a great potential in many fields of chemistry.[23] This reaction is promoted by using copper(I) salt that produces a 1,2,3-triazole substituted in 1,4 and 1,5-positions.

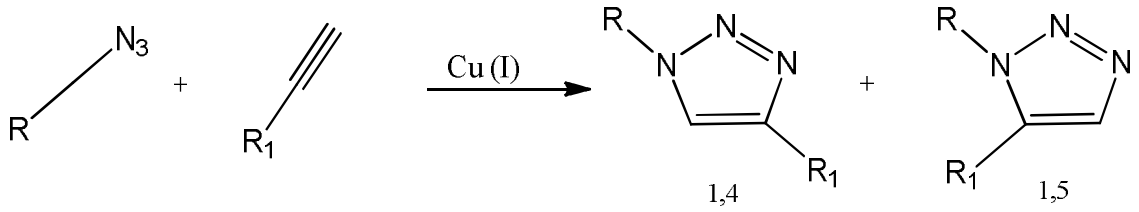

Scheme 3.19: Huisgen reaction

Due to the substitution pattern of the target molecule (7), the porphyrin framework cannot be prepared according the procedures described above. On the contrary, it is more convenient to follow the "dipyrromethane" approach invented by Lindsey.[26]

For this purpose, the dipyrromethane was synthesized by reacting pyrrole with paraformaldehyde. This derivative was then reacted with 3,5-di-butyl benzaldehyde in the presence of DDQ/TFA to accomplish the formation of the porphyrin ring. Further treatment with N-Bromosuccinimide (NBS) yielded the corresponding di-bromo porphyrin. This was followed by palladium catalyzed coupling of dibrominated porphyrin with trimethylsilyl acetylene, which was subjected to removal of silyl group using tetra-n-butylammonium fluoride (TBAF), thereby resulting in bis(ethynyl)porphyrin. This was finally treated with an azido derivative under classical click-chemistry conditions (i.e. in the presence of copper sulfate and sodium L-ascorbate) followed by hydrolysis to get the target molecule. The detailed synthetic pathway will be discussed in the following sub-section.

3.1.1 Synthesis of Dipyrromethane (8)

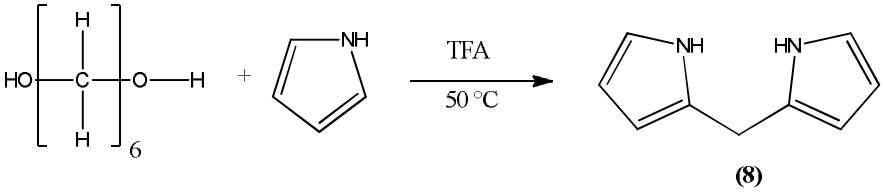

(8)

Scheme 3.20: Synthesis of dipyrromethane (8)

The dipyrromethane was synthesized using literature pathway described by Lindsey and co-workers.[26]

Firstly, the pyrrole was purified by passing it through a plug of alumina. Then, paraformaldehyde and pyrrole were stirred in a round bottomed flask. The mixture was heated to 50 °C for 15 minutes, followed by addition of trifluoro acetic acid (TFA). After stirring for 5 minutes, the reaction mixture was quenched with 0.1M sodium hydroxide solution. The product was extracted with ethyl acetate and the organic layer was washed extensively with water. The organic layer was then dried over sodium sulfate and the solvent was removed in vacuum to afford an orange oil, which was subjected to bulb-to-bulb distillation to obtain white crystals of dipyrromethane. The product was analysed by

ESI spectrometry, the observation of a peak at m/z 146 confirmed the formation of the desired product.

3.1.2 Synthesis of 5,15-Bis-(3,5-bis-tert-butylphenyl)porphyrin (9)

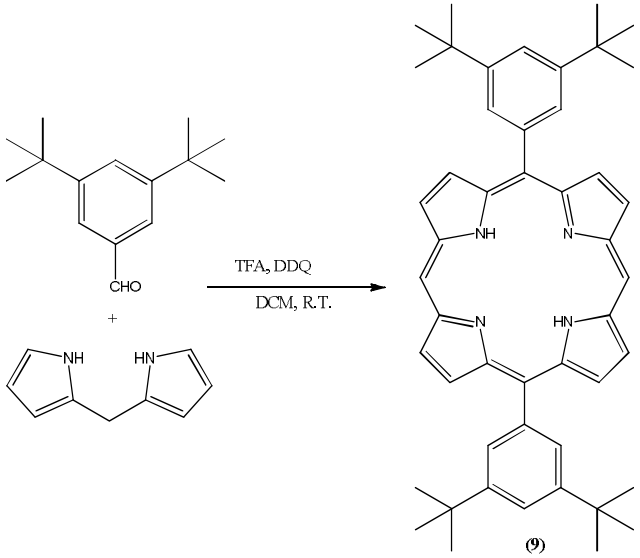

Scheme 3.21: Synthesis of 5,15-Bis-(3,5-bis-tert-butylphenyl)porphyrin (9)

The porphyrin macrocycle was constructed using the procedure described by Bourhill and co-workers.[27] A mixture of dipyrromethane (8) and 3,5-di-tert-butyl benzaldehyde in dichloromethane was stirred at room temperature for 10 minutes under nitrogen atmosphere. The reaction was initiated by addition of TFA. After stirring the reaction mixture for 2 hours, the porphyrin was formed by addition of DDQ as an oxidant. The mixture was then neutralized with triethyl amine (Et_3N). The desired product was purified by passing through short column of silica using dichloromethane as eluent. After removal of solvent, the desired porphyrin derivative (9) was obtained as a purple solid. The product was analysed by ESI spectrometry, the observation of a peak at m/z 687 confirmed the formation of the desired product. The product appeared to be pure enough and hence was used in the next step without any purification.

3.1.3 Synthesis of 5,15-bis-(3,5-bis-tert-butylphenyl)porphinato zinc (II) (10)

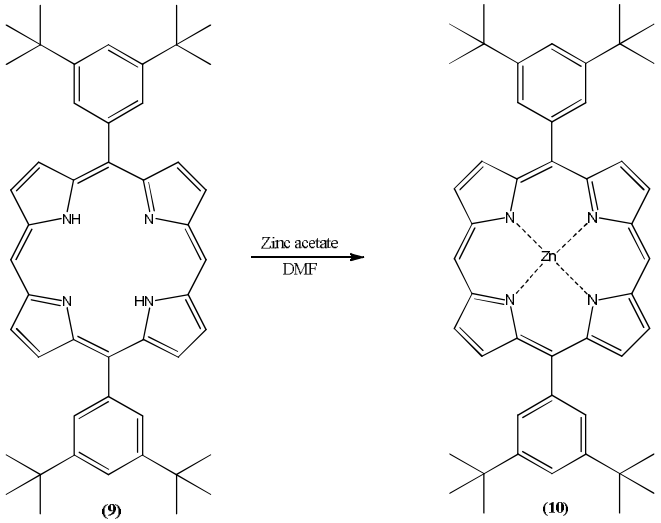

Scheme 3.22: Synthesis of 5,15-bis-(3,5-bis-tert-butylphenyl)porphinato zinc (II) (10)

The metallation of porphyrin (9) was carried out by using zinc acetate.[27] The free porphyrin derivative (9) was dissolved in DMF and to this, an aqueous solution of zinc acetate was added. The reaction mixture was refluxed for 3 hours. Later, more water was added to obtain the porphyrin precipitate. The solid was filtered followed by washing with MeOH and acetone. The product was purified by dissolution with chloroform and re-precipitation with MeOH to produce purple solid of porphyrin derivative (10). The product was analysed by ESI spectrometry, the observation of a peak at m/z 749 confirmed the product formation. As expected, the ^{1}H NMR analysis does not show the signals originating from internal hydrogens of the porphyrin ring.

3.1.4 Synthesis of 5,15-bis-bromo-10,20-bis(3,5-bis-tert-butylphenyl)porphinato zinc (II) (11)

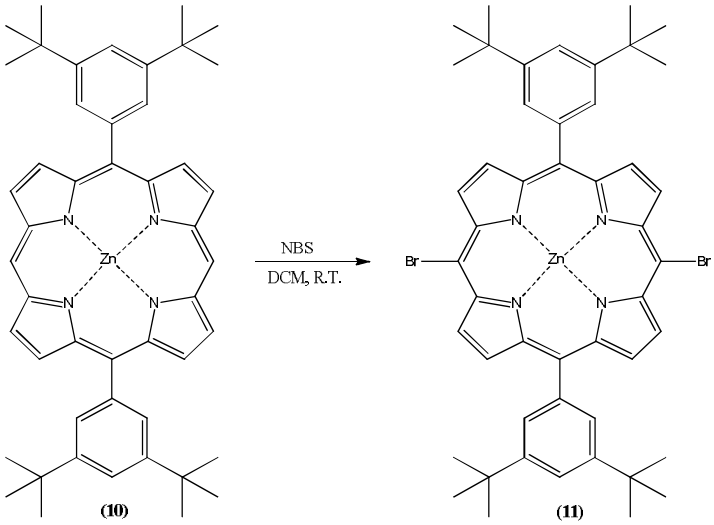

Scheme 3.23: Synthesis of 5,15-bis-bromo-10,20-bis(3,5-bis-tert-butylphenyl)porphinato zinc (II) (11)

The bromination of porphyrin was carried out by using N-Bromosuccinimide (NBS) as brominating agent.[27] For this purpose, NBS was added to a stirred solution of porphyrin (10) in dichloromethane. After stirring for 5 minutes at room temperature, the reaction was quenched by addition of acetone. The solvent was evaporated to obtain solid which was then triturated in MeOH. The suspension was then filtered and the residue was washed with MeOH to give the desired dibromo porphyrin derivative (11) in quantitative yield. The product was analysed by ESI spectrometry, the observation of a peak at m/z 927/929/931 confirmed the formation of the desired product. The product so formed showed a single spot on TLC using THF/petroleum ether (8:2) as eluent. It was pure enough to be used for the next step without any purification.

3.1.5 Synthesis of 5,15-bis(3,5-bis-tert-butylphenyl)-10,20-bis-tri-methylsilylethynyl porphinato zinc (II) (12)

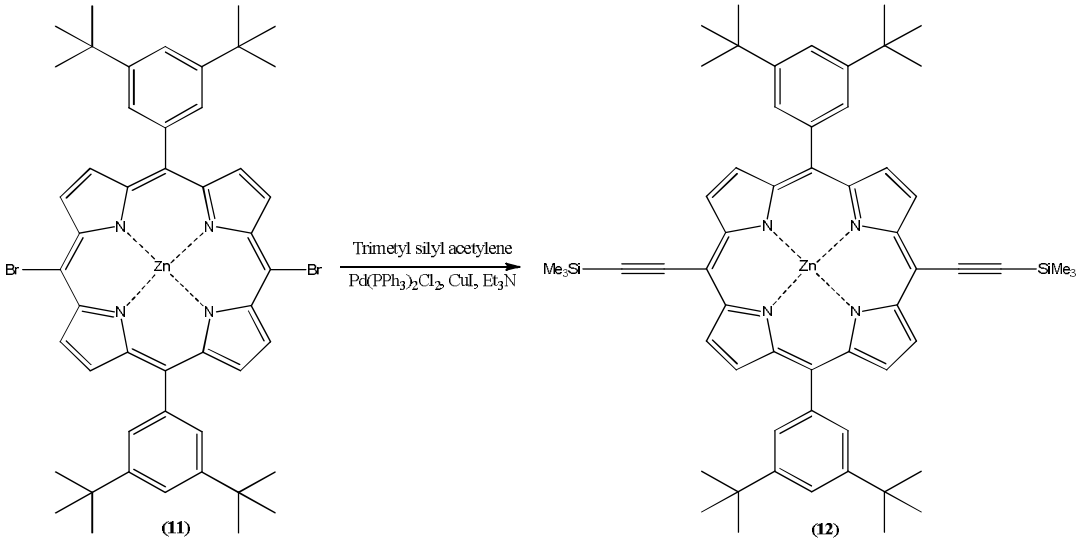

Scheme 3.24: Synthesis of 5,15-bis(3,5-bis-tert-butylphenyl)-10,20-bis-tri-methylsilylethynyl porphinato zinc (II) (12)

Palladium catalyzed coupling of dibromo porphyrin (11) was carried out with trimethylsilyl acetylene in order to get the corresponding silyl derivative.[27] At first, freshly distilled triethyl amine was added to a solution of dibromo porphyrin (11) in THF under nitrogen atmosphere. To this reaction mixture, trimethylsilylacetylene, $Pd(PPh_3)_2Cl_2$ and copper iodide were added. The reaction mixture was stirred for 16 hours at room temperature. The

solvent was removed under reduced pressure to obtain a residue which was re-dissolved in a mixture CH_2Cl_2 /petroleum ether (1:1). The resulting solution was passed through a short plug of silica. The residue was recrystallized from CH_2Cl_2/acetonitrile to get a deep purple solid as porphyrin derivative (12). The product was analysed by ESI spectrometry, the observation of a peak at m/z 941 confirmed the formation of the desired product. The product so formed was further transformed without any purification.

3.1.6 Synthesis of 10,20-bis(3,5-bis-tert-butylphenyl)-5,15-bis-ethynylporphinato zinc (II) (13)

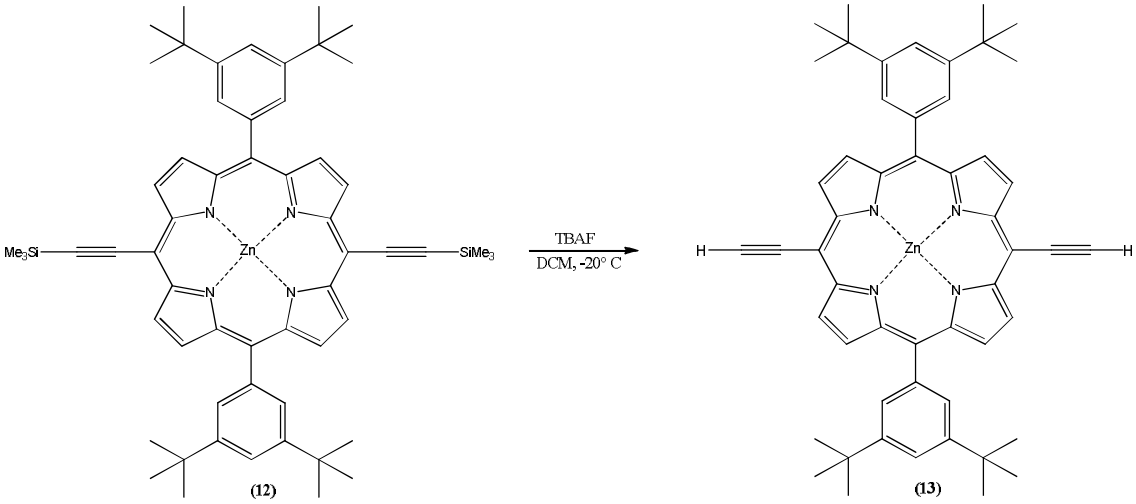

Scheme 3.25: Synthesis of 10,20-bis(3,5-bis-tert-butylphenyl)-5,15-bis-ethynylporphinato zinc (II) (13)

In order to synthesize bis(ethynyl)porphyrin derivative (13), the silyl group was removed by using tetrabutylammonium fluoride (TBAF).[27] To this purpose, TBAF was added at -20 °C to a solution of porphyrin derivative (12) in dichloromethane. After 5 minutes, acetic acid and methanol were added to the reaction mixture. Then, after 1 hour, the precipitate formation was observed, which was filtered off and washed with methanol to give the desired bis(ethynyl)porphyrin derivative (13) in quantitative yield. The product was characterized by ESI spectrometry, wherein the signal at m/z 798 corresponds to M+1 peak of the desired product thereby confirming its formation. The product so formed showed a single spot on TLC using CH_2Cl_2/petroleum ether (8:2) as eluent. It was used as such for the next step without any purification.

3.1.7 Synthesis of Porphyrin chromophore (7) [Meso Triazole clicked Porphyrin]

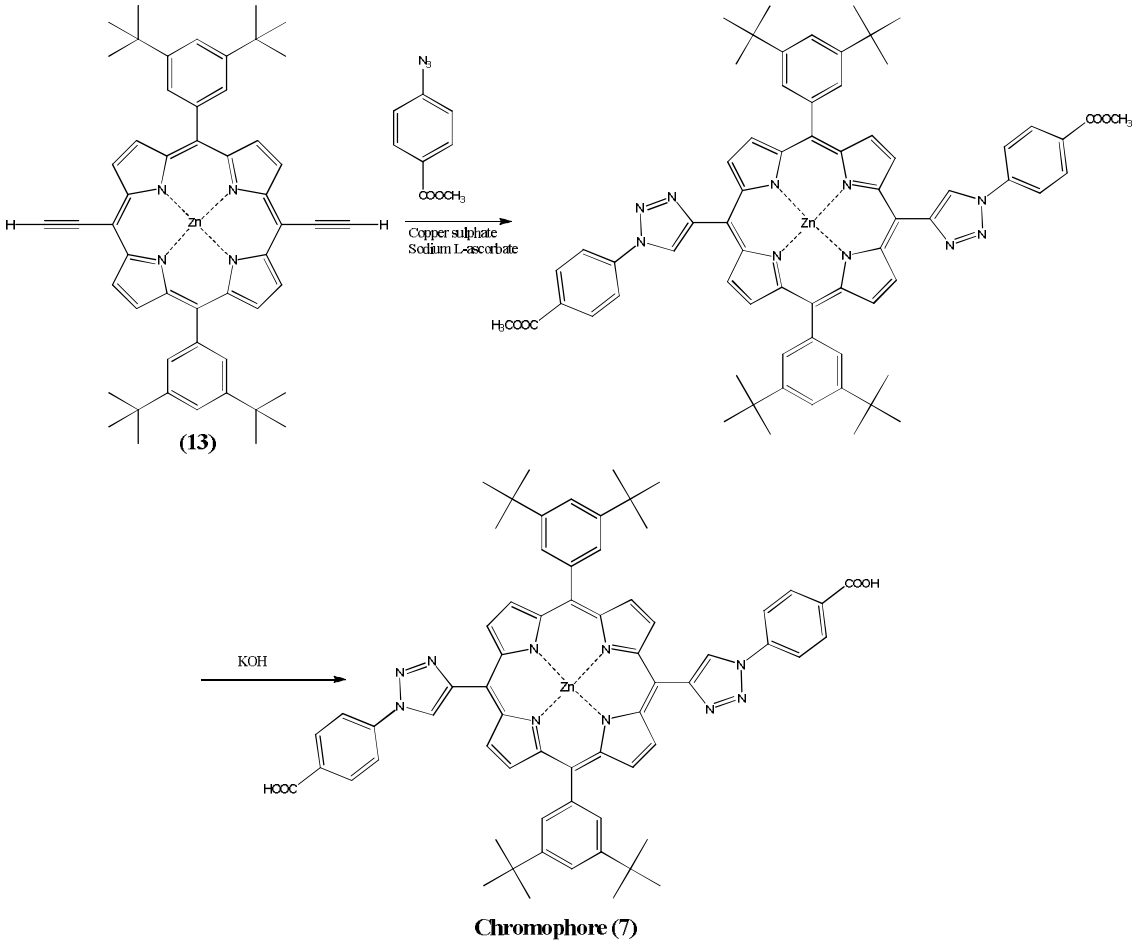

Scheme 3.26: Synthesis of Porphyrin chromophore (7) [Meso Triazole clicked Porphyrin]

The meso triazole clicked porphyrin was synthesized in a similar manner as reported by Zimmerman and co-workers.[28] This reaction involved two steps- i) click reaction between ethynyl porphyrin and methyl 4-azidobenzoate and ii) the hydrolysis of ester i.e. conversion of ester group to corresponding carboxylic functionality.

To a stirred solution of porphyrin (13) in dichloromethane, methyl 4-azidobenzoate was added. After stirring for 10 minutes at room temperature, an aqueous solution of copper(II) sulfate and sodium L-ascorbate was added to the reaction mixture. The reaction was stirred for 3 days, then the mixture was diluted with water and extracted with dichloromethane. The organic phase was separated using separating funnel, dried over sodium sulfate and the solvent was removed under vacuum.

The hydrolysis of methyl ester was carried out by KOH treatment. This was achieved by adding an aqueous solution of KOH to porphyrin methyl ester in THF. The solution was refluxed for 2 hours at 65 °C. The progress of the reaction was monitored by TLC using

dichloromethane/ethyl acetate (8:2) as eluent. When the TLC showed complete disappearance of starting material, the reaction mixture was cooled to room temperature and aqueous 1M HCl was added to it. The product was extracted with dichloromethane and washed with water. The organic layer was dried over sodium sulfate and the solvent was removed under vaccum to get a purple solid of porphyrin derivative (7).

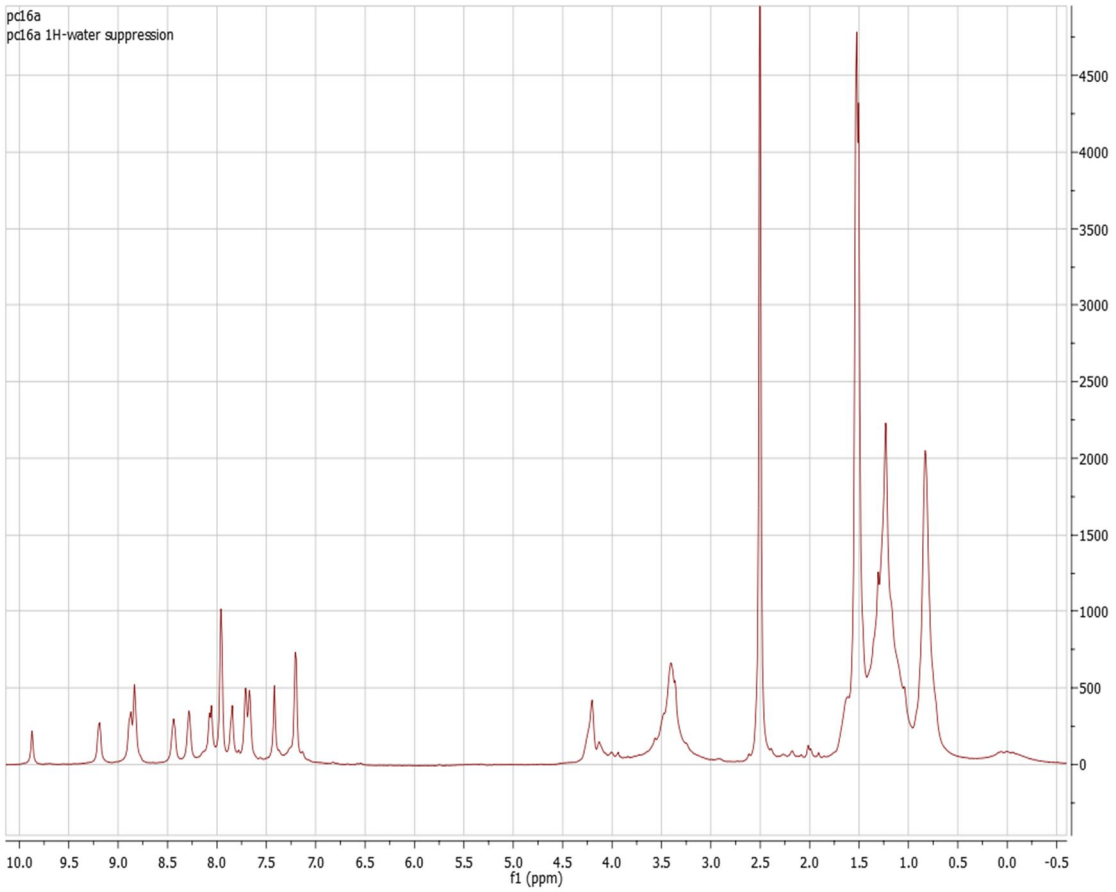

Figure 3.16: ^{1}H NMR spectra of porphyrin chromophore (7)

The product so obtained could not be analysed by ESI spectrometry owing to its poor solubility in organic solvents. In addition, TLC indicated the presence of many impurities, which could also be seen in the ^{1}H NMR spectra (Figure 3.16). Unfortunately, the purification of target porphyrin was not possible by any attempt of column chromatography and/or re-crystallization, so this product was discarded.

In the present section, porphyrin derivative was prepared by reacting the alkynyl-porphyrin with the azide derivative. However, in the next section, the other option was considered, namely reacting azide-porphyrin with an alkynyl derivative.

3.2 Synthesis of triazole linked porphyrin

The present section deals with porphyrin synthesis via click reaction, in which the azide functionality was attached to the porphyrin periphery. Using this methodology, triazole ring could be incorporated in the porphyrin macrocycle. Once this porphyrin derivative was prepared, it was used as a ligand to complex with different metal salts. All the aspects are covered in the following sub-sections.

3.2.1 Synthesis of azido zinc(II) porphyrin (14)

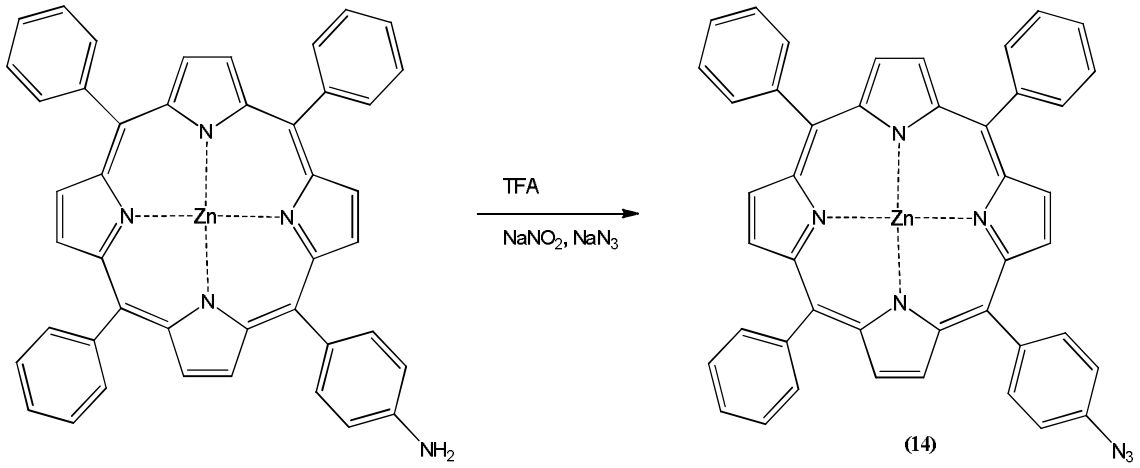

Scheme 3.27: Synthesis of azido zinc(II) porphyrin (14)

The azido porphyrin could be synthesized from an amino porphyrin by reacting it with sodium azide and sodium nitrite. In order to carry to out this modification, the required starting porphyrin (amino tetraphenyl porphyrin) was synthesized in laboratory, whose synthetic pathway will be discussed later in section 6.1.2 of the thesis.

Using the literature procedure, zinc metal complex was formed by treatment with zinc acetate.[29] A solution of zinc amino porphyrin in TFA was prepared at 0 °C and an aqueous solution of sodium nitrite was added. After stirring for 10 minutes at 0 °C, an aqueous solution of sodium azide was added drop wise to the reaction mixture and stirred for further 45 minutes. Then, the solution was diluted with water and extracted with dichloromethane. The organic layer was collected and washed with a solution of $NaHCO_3$. After removing the solvent, a purple solid was obtained. The metallation reaction was carried out using zinc acetate solution in chloroform for 1 hour at reflux temperature. The solvent was removed and residue was dissolved in dichloromethane. The solution was

passed through a small plug of silica. The solvent was removed under vacuum to yield a deep purple solid. The product was analysed by ESI spectrometry, the observation of a peak m/z 717 confirmed the formation of desired azido zinc (II) porphyrin (14). Further the porphyrin was analysed by ^{1}H NMR wherein all the signals were consistent with the literature values.

3.2.2 Synthesis of triazole porphyrin derivative (15)

The azido zinc (II) porphyrin was subjected to Huisgen reaction with an alkyne i.e. 2-ethynylpyridine.

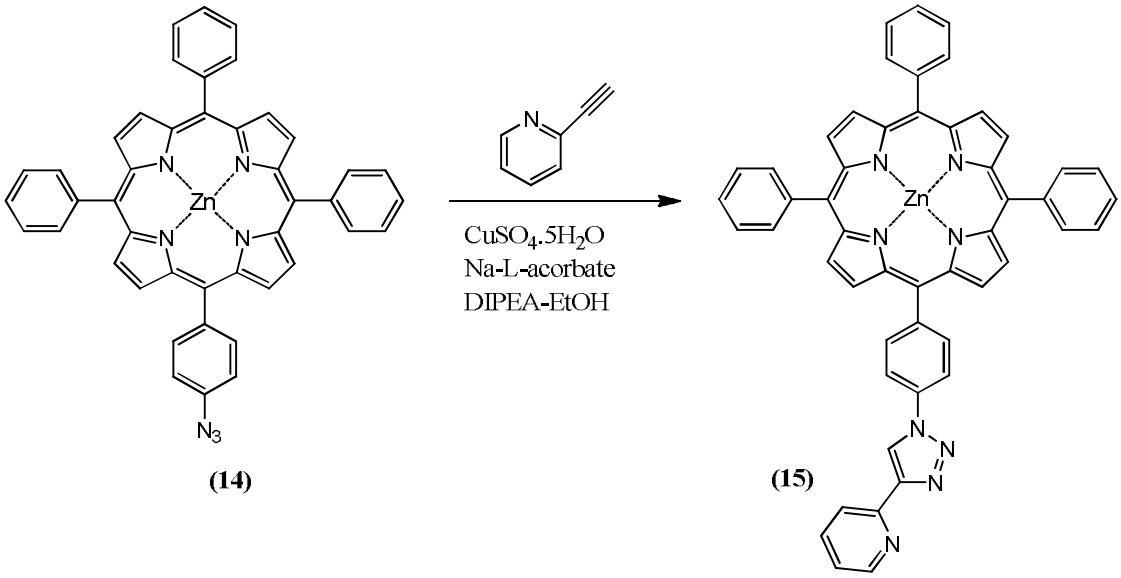

Scheme 3.28: Synthesis of triazole porphyrin derivative (15)

The click reaction between the two was accomplished using the procedure described in literature for similar Huisgen reaction.[30] The synthetic details are discussed as follows.

2-ethynyl pyridine was added to a solution of zinc-azido porphyrin (14) in THF and the reaction mixture was de-aerated with nitrogen. After stirring for 10 minutes, a saturated solution of copper sulfate and sodium-L-ascorbate was added to the reaction mixture using a syringe. Further, 1 mL solution of (1:1 DIPEA/EtOH) was added to reaction mixture. After stirring for 3 days, the mixture was diluted with water and extracted with dichloromethane. The organic layer was dried with sodium sulfate, filtered, and concentrated under vacuum. The crude residue was purified by column chromatography (silica gel, 8:2 CH_2Cl_2/EtOAc). The solvent was removed under vacuum to yield a deep

purple solid (15). The product so formed was further characterized by the ESI, UV, 1D NMR, 2D NMR-COSY and 2D NMR-HMQC techniques.

The ESI spectrometry shows a signal at m/z 821 corresponding to M+1 molecular ion peak of porphyrin derivative (15). The UV-visible spectrum shows an absorption band at 422 nm which corresponds to Soret band of porphyrin while two Q-bands at 570 and 594 highlighted the corresponding metallated porphyrin. The ^{1}H NMR spectra was in well agreement with the expected proton peaks (especially the triazole proton signal is well evident at 8.9 ppm) and the representation of the same has been done in the experimental part of the thesis. The characterization was also further confirmed by proton-proton correlation i.e. 2D-COSY and proton-carbon correlation i.e. 2D-HMQC NMR techniques.

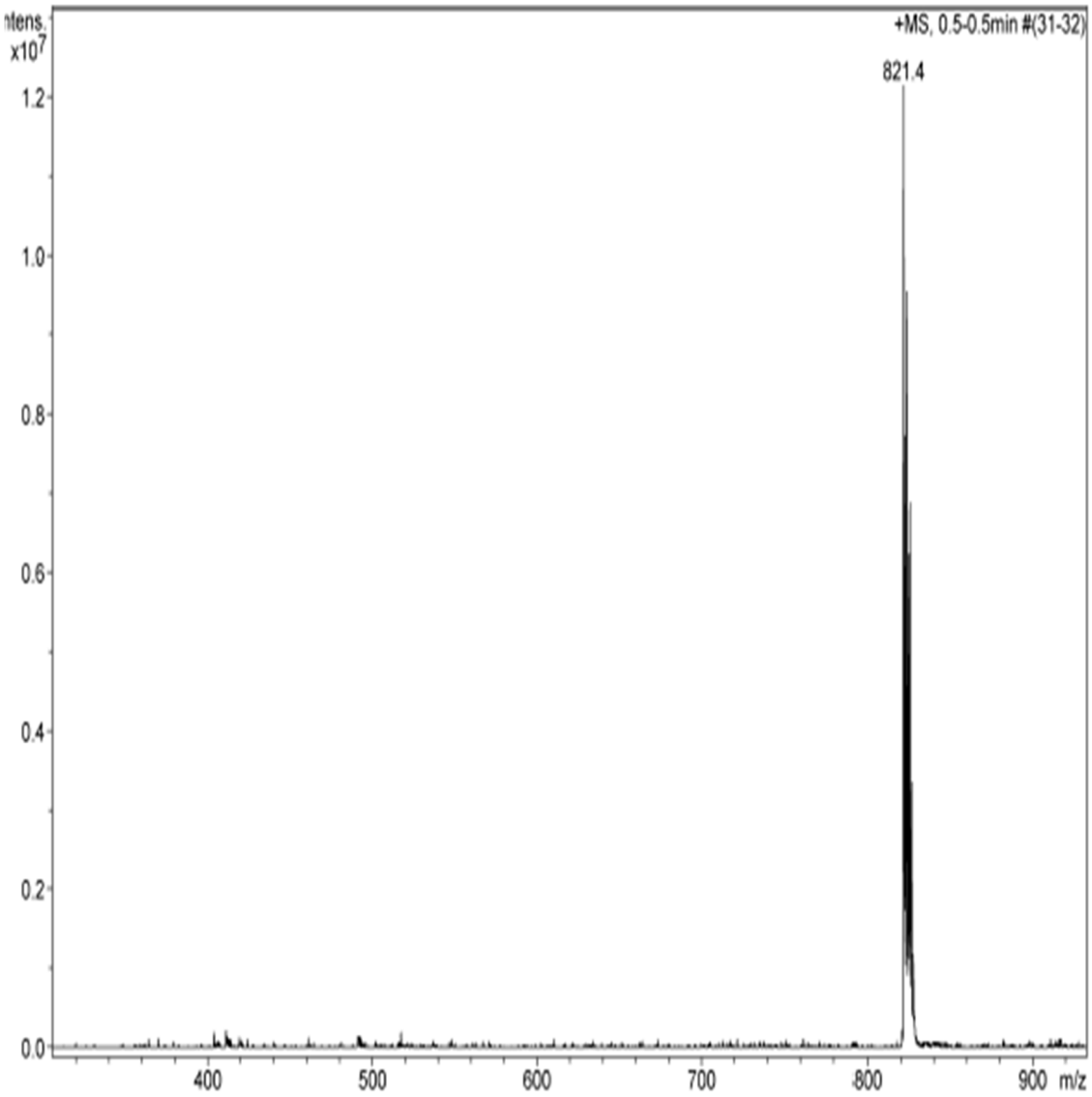

Figure 3.17: ESI-MS (ACN) spectrum of porphyrin derivative (15)

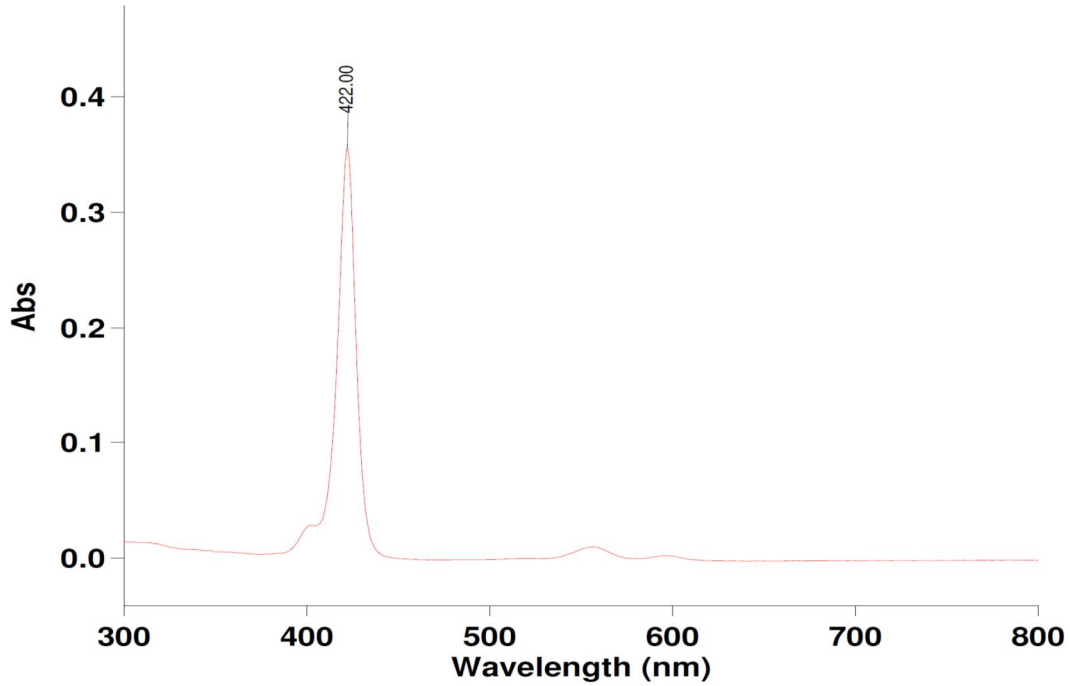

Figure 3.18: UV-visible (DCM) spectrum of porphyrin derivative (15)

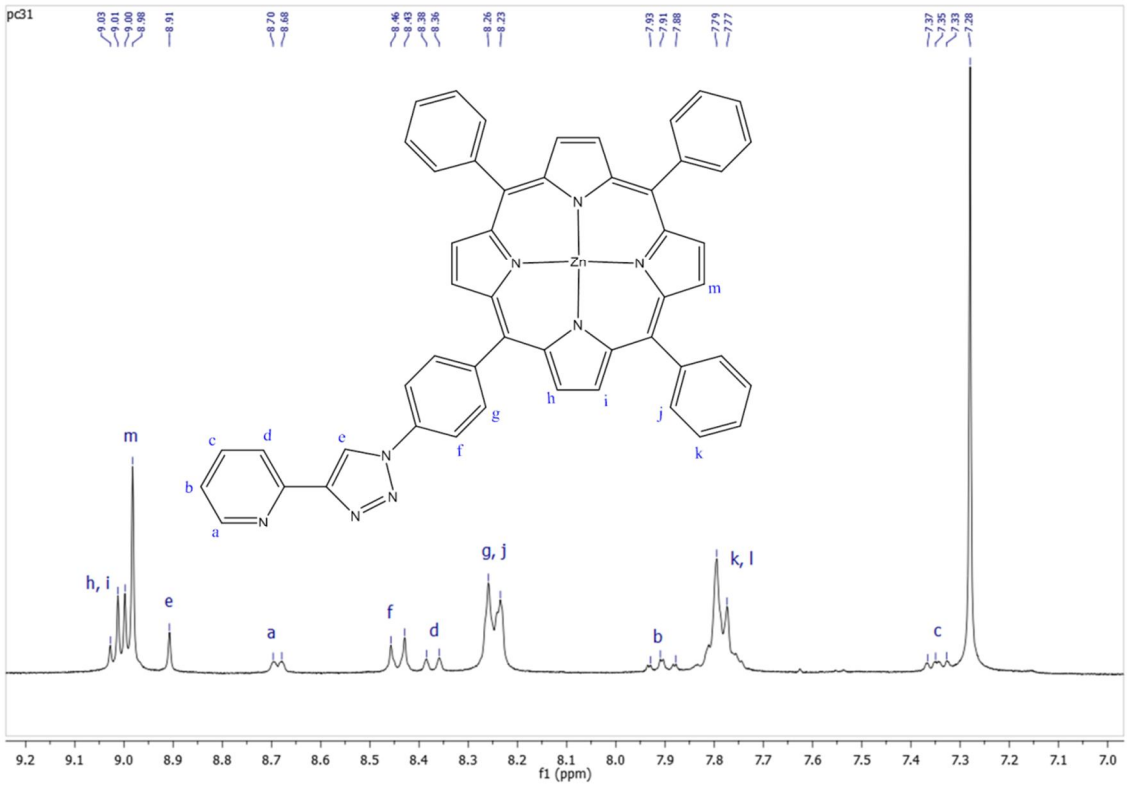

Figure 3.19: ^{1}H-NMR ($CDCl_3$) spectrum of porphyrin derivative (15)

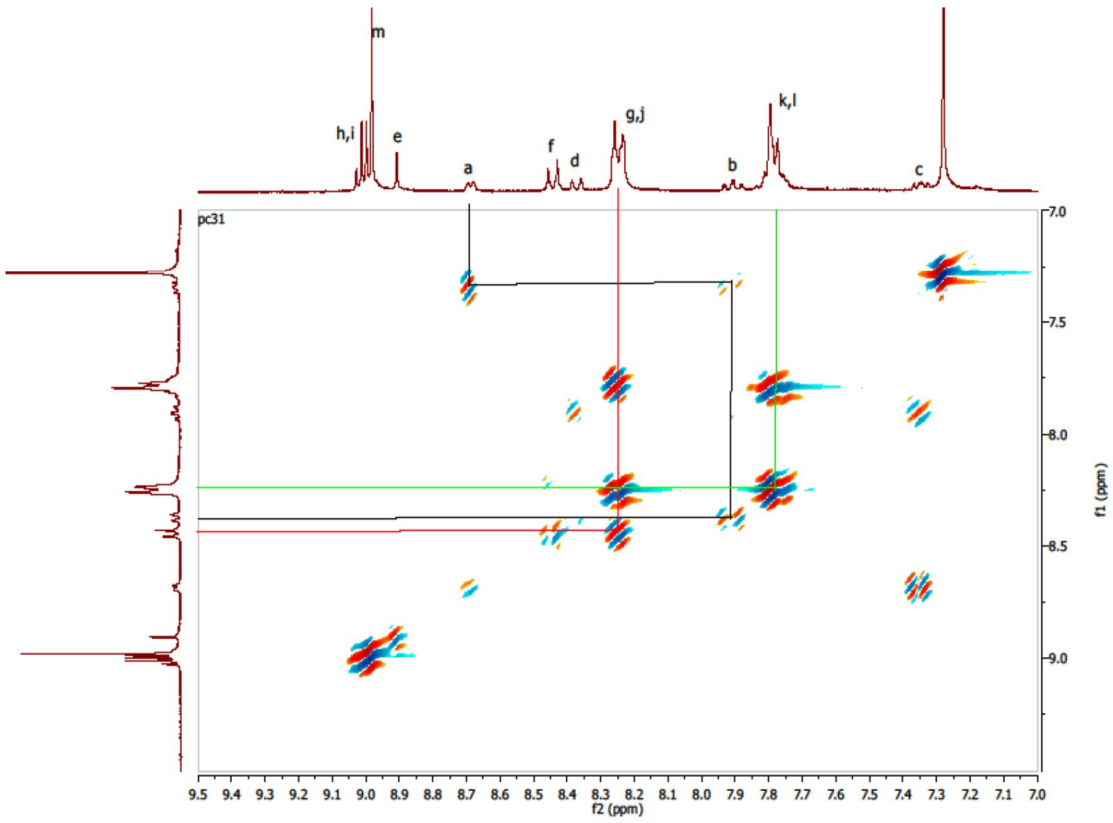

Figure 3.20: 2D-COSY NMR ($CDCl_3$) spectrum of porphyrin derivative (15)

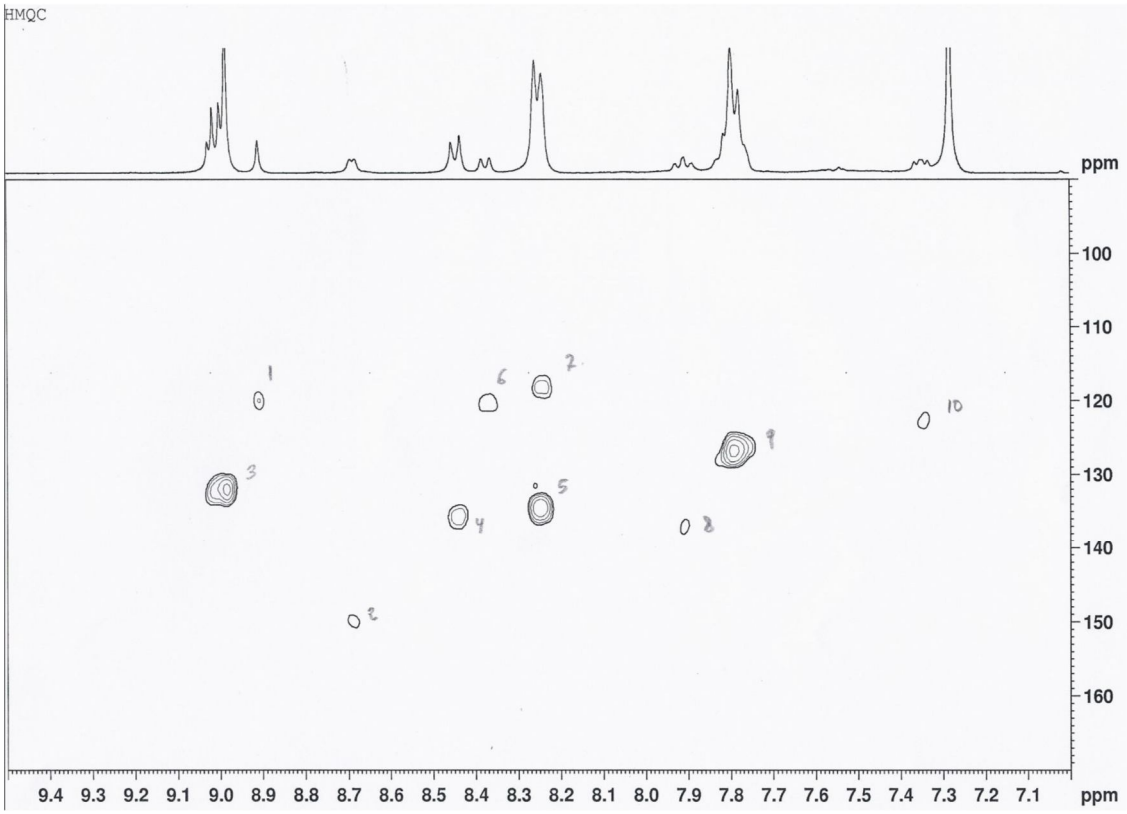

Peak	ν(F2) [ppm]	ν(F1) [ppm]	Intensity
3	8.9956	131.8000	237791.98
1	8.9078	120.0000	48575.10
2	8.6883	150.0000	39286.13
4	8.4413	135.6000	74484.21
6	8.3727	120.0000	41395.84
7	8.2492	117.8000	59720.44
5	8.2464	134.6000	272501.82
8	7.9089	137.0000	35974.14
9	7.7909	126.8000	354368.39
10	7.3463	122.6000	37960.86

Figure 3.21: 2D-HMQC NMR ($CDCl_3$) spectrum and peak intensities of porphyrin derivative (15)

The crystal structure of porphyrin derivative (15) was determined by X-ray crystallography technique. In order to obtain porphyrin crystals for X-ray analysis, crystallization was performed using dichloromethane/methanol solution. The resulting x-rays structure obtained from this method is shown below, wherein the grey circle corresponds to carbon atom, blue circles for nitrogen atom, red for zinc atom of porphyrin derivative (15). Therefore, the crystal structure was in well agreement with expected structure.

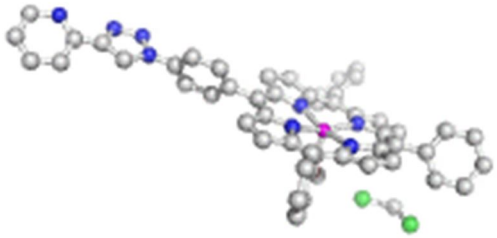

Figure 3.22: X-ray crystal structure of porphyrin derivative (15)

In conclusion, a novel porphyrin derivative (15) was successfully synthesized by using click reaction and was characterized by various techniques.

3.2.3 Synthesis of 1,2,3-Triazole porphyrin Complexes

The triazole unit formed by click chemistry reaction starting from the porphyrin derivative (15) is known from the literature to be able to form coordination complexes with various metal ions with a behaviour reminiscent of bipyridyl ligands. In order to investigate the possibility of this, the following preliminary studies were performed.

The complexation with palladium metal salts such as palladium acetate, was performed using a similar procedure reported by Li and co-workers.[31]

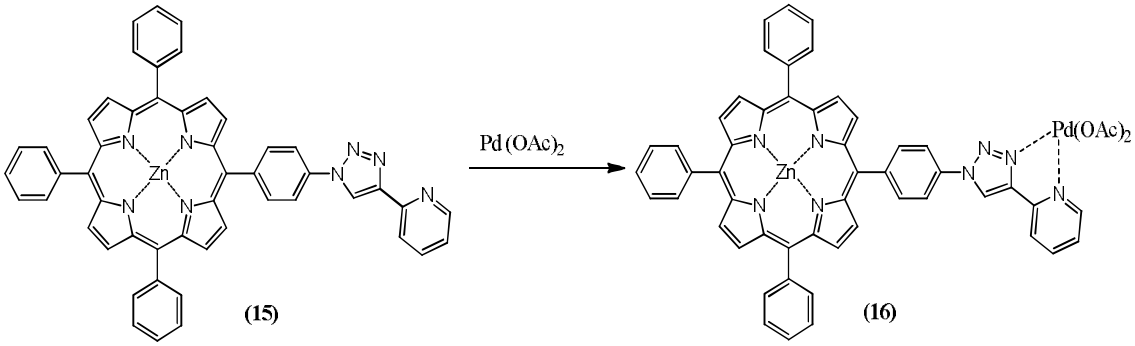

Scheme 3.29: Synthesis of palladium complexed porphyrin derivative (16)

The derivative of porphyrin (15) was first dissolved in toluene and palladium acetate was added with stirring for 1 hour at room temperature. The reaction was monitored by TLC analysis which shows complete disappearance of starting material. After, evaporation of solvent, the product was subjected to column chromatography. However, even with the use of highly polar solvent, the product did not eluted, so this reaction was dismissed.

Another attempt was done, to prepare a complex of porphyrin derivative (15) with Ru(II) salt. Thus, using the same procedure reported by Tam and co-workers, the reaction was carried as follows.[32]

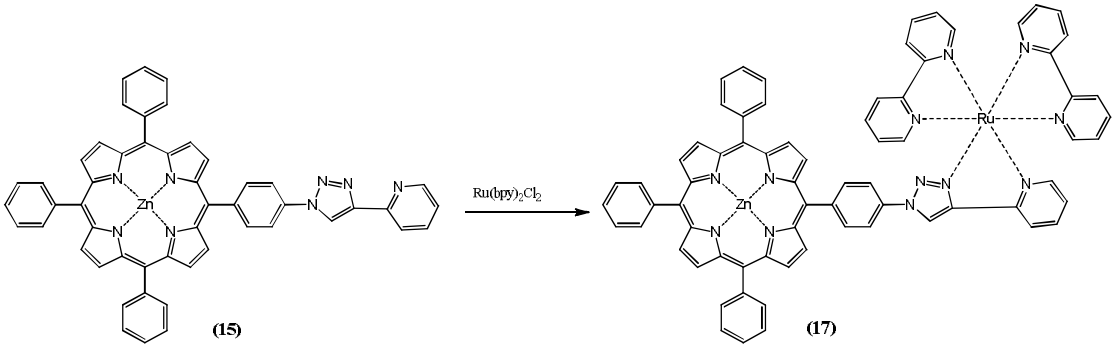

Scheme 3.30: Synthesis of ruthenium complexed porphyrin derivative (17)

The porphyrin derivative (15) was dissolved in ethanol and cis-Ru(bpy)$_2$Cl$_2$ was added to it. The reaction mixture was stirred for 3 hours at 78 °C. The solvent was evaporated and the solid thus obtained was subjected to column chromatography over alumina using dichloromethane/methanol (9:1) as eluent. The product so obtained was analyzed by ESI spectrometry as shown below.

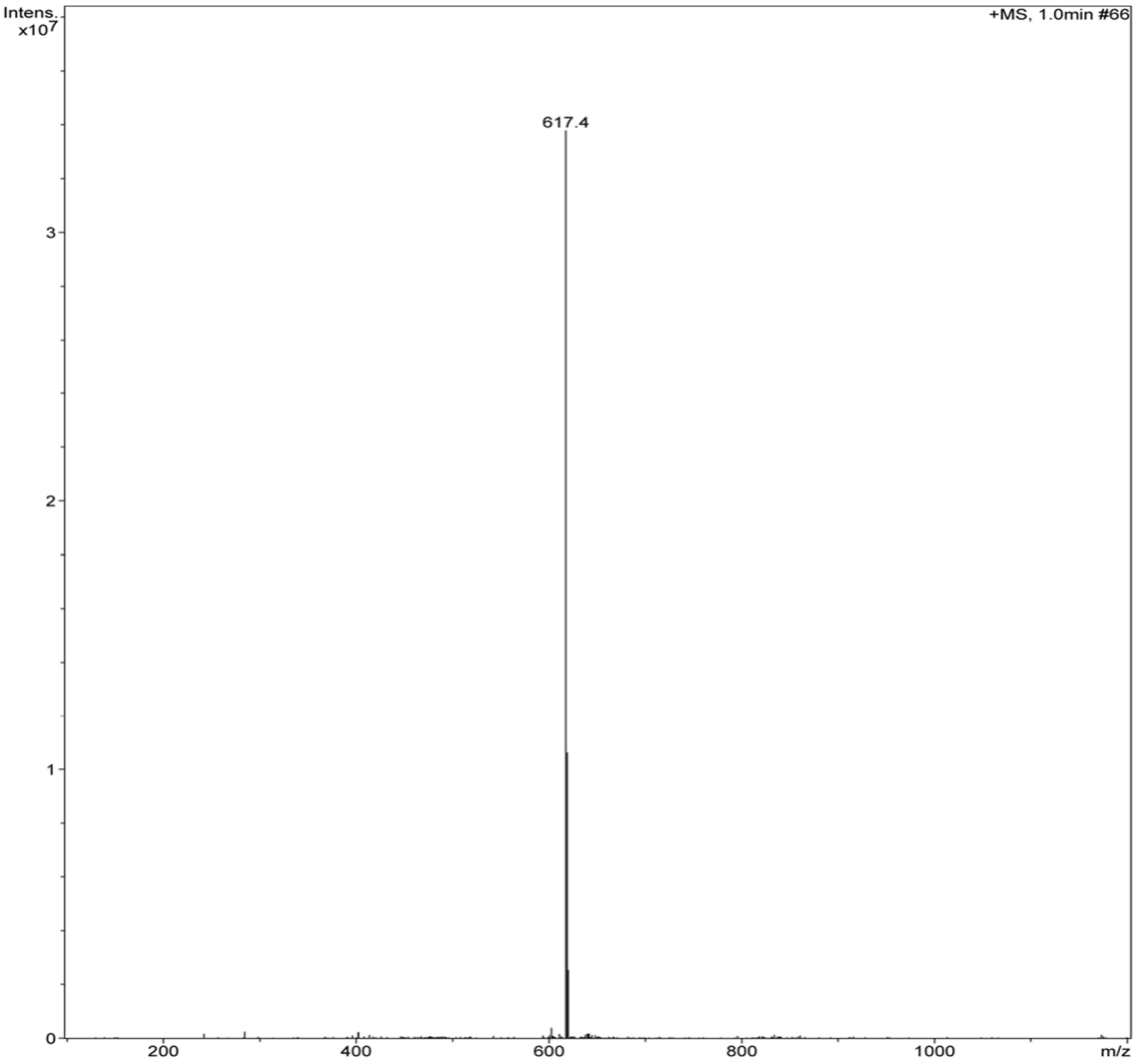

Figure 3.23: ESI-MS spectrum of ruthenium metal complexed porphyrin derivative (17)

As evident from ESI analysis, the peak at m/z 617 $[MH_2]^{2+}$ indicates the formation of clicked-porphyrin-Ru-(bpy) complex. Although, ESI analysis gave an idea of formation of Ru-complex, however, it could not be established by NMR technique due to its poor solubility in various deuterated solvents. Therefore, once again it was difficult to fully characterize and purify the complex so formed.

Hence, we explored another procedure for formation of Ruthenium complex as described by Skoglund and co-workers.[33]

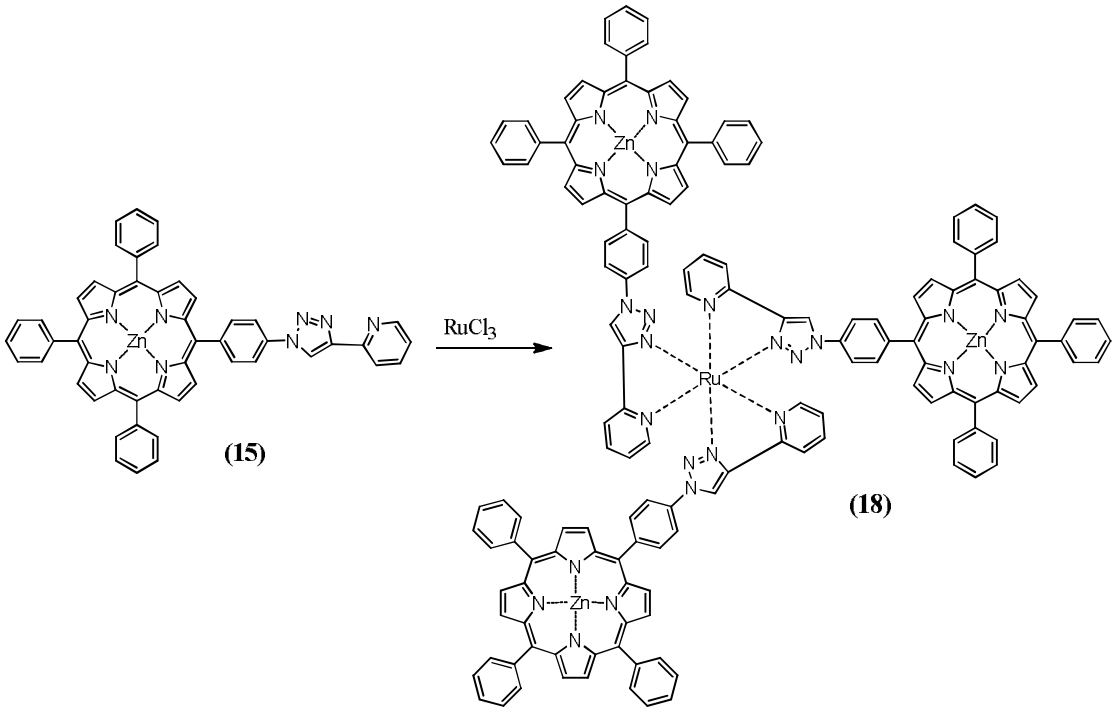

Scheme 3.31: Synthesis of ruthenium complexed porphyrin derivative (18)

The porphyrin derivative (15) was dissolved in ethanol and ruthenium chloride ($RuCl_3$) was added to it. The reaction mixture was stirred for 4 hours at 78 °C. The solvent was evaporated and the solid thus obtained was subject to column chromatography over alumina using chloroform/methanol (9:1) as eluent. The product so obtained was analyzed by ESI spectrometry as shown below.

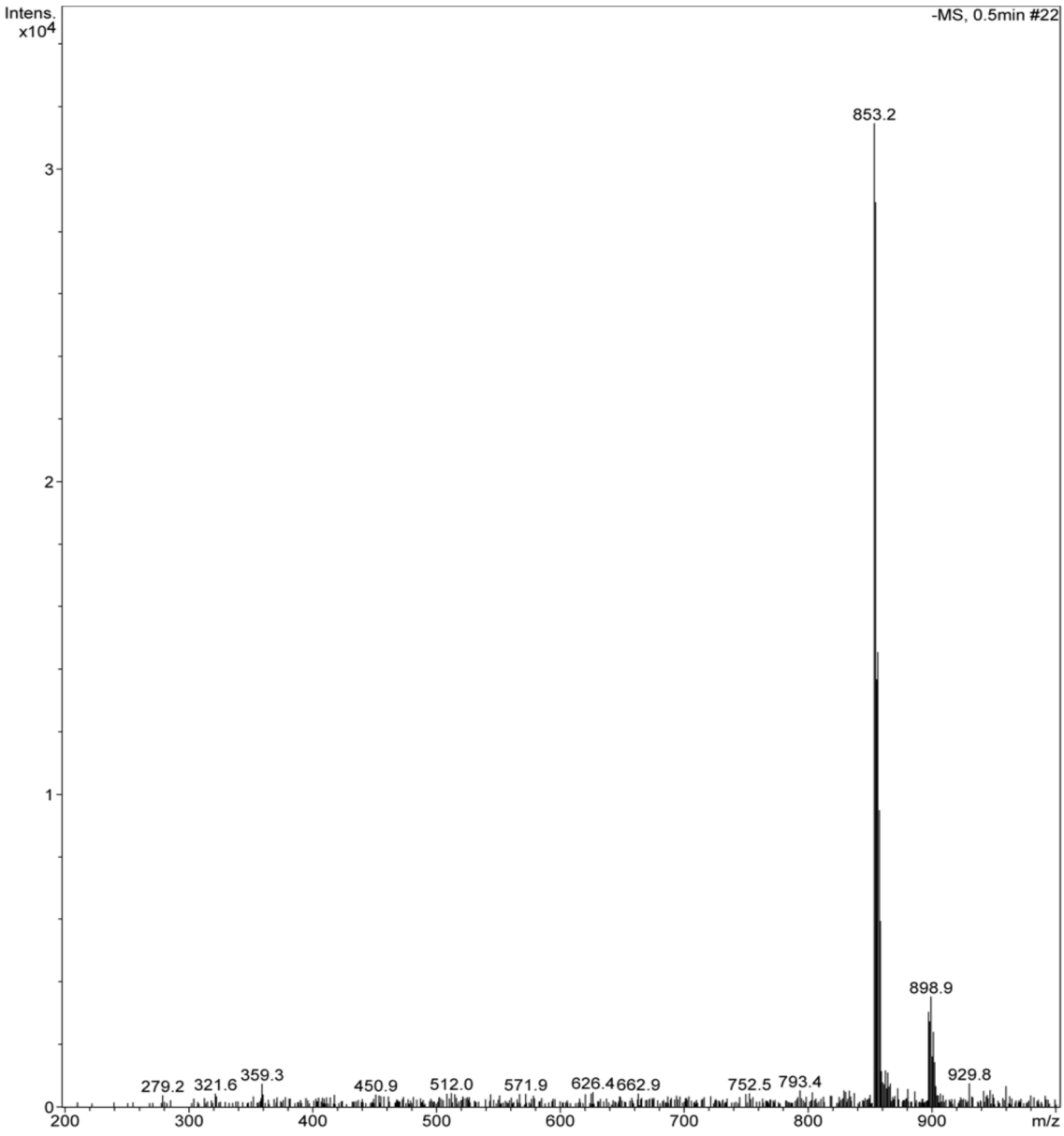

Figure 3.24: ESI-MS spectrum of ruthenium metal complexed porphyrin derivative (18)

As evident from ESI analysis, the peak m/z 853 $[MH_3]^{3+}$ indicates the formation of clicked-porphyrin-Ru complex (18). Although, ESI analysis gave an idea of formation of Ru-complex, however, it could not be established by NMR technique due to its poor solubility in various deuterated solvents.

In conclusion, a novel 1,2,3-triazole porphyrin (15) was synthesized by using click reaction. It was characterized by various spectroscopic techniques namely ESI, UV Visible, 1D NMR, 2D COSY and HMQC NMR and X-ray crystallography. However, the poor solubility of the metal complexes proved to be detrimental and frustrated in the following experiments. For this reason, it was decided to develop another research line based on the nanocrystalline cellulose that will be described in detail in the following paragraphs.

II Nano Crystalline Cellulose

As mentioned earlier in the introductory part of the thesis, the crystalline nanocellulose (NCC) can be prepared by acid hydrolysis from any cellulose containing material by a hydrolysis based top to down approach. NCC bears many hydroxyl groups and its properties can be altered by several ways, one can utilize the reactive -OH groups available on the surface of NCC directly to attach pH sensitive dye through covalent linkage. Another way is to functionalize the NCC with groups more versatile than hydroxyl groups, for example, amino group or a carboxylic acid in it. It was found that introduction of carboxylic acid group on NCC was easy, convenient and provided a much higher degree of functionalization. Finally, this carboxylic nanocellulose was further used as scaffold to prepare different hybrids such as with porphyrin and nitrobenzene derivative for different applications. All these aspects will be discussed in the following sub sections.

4. General procedure for nano crystalline cellulose (NCC) preparation

Cellulose from different sources was treated with an acid solution to get nano crystalline cellulose. The role of the acid is to dismantle the amorphous part in the cellulosic material (by forming the corresponding hydrolysed product such as glucose and other by-products) thus, giving rise to a suspension of individual nano crystallites as depicted in Figure 3.25.

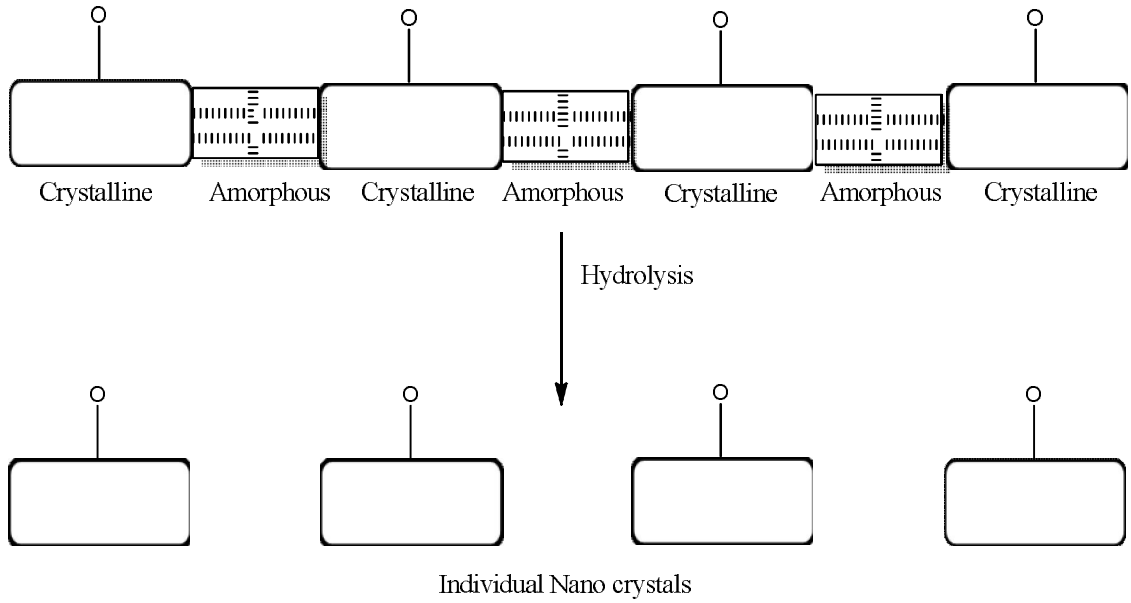

Figure 3.25: Formation of nano crystals of cellulose

Usually, sulphuric acid is used for hydrolysis of cellulose at a concentration around 64 %.[34] The acid solution was preheated at 45° C followed by the addition of cellulose. The suspension was further stirred for 2 hours. The hydrolysis reaction was terminated by a 10-folds dilution with distilled water and allowed to settle down overnight. The product was washed with distilled water by means of several cycles of centrifugations, until neutral pH was achieved in the suspension. The solid was re-suspended in minimum amount of distilled water and transferred in dialysis tubes and dialysed for several days against pure water in order to remove any salts or by-products. The solid product of nanocellulose was recovered by lyophilization.

Different cellulose material sources were explored to get the best quality of nanocellulose.

4.1 From cotton

The household cotton as cellulose starting material was used for preparation of nano crystalline cellulose as described in the literature.[35] However, as soon as the cotton came in contact with the acid solution, the clear acid solution turned black, also some burning like odour was observed and tar/burned residue of cotton was seen. It could be due to the quality of cotton that was purchased from local store that may contain some heterogeneous material such as cotton seeds. Thus, it was decided to dismiss the cotton source and choose another cellulose form such as Whatman® filter paper grade 1, which has been reported in literature as a valuable starting material.

4.2 From Whatman® filter paper grade 1

Since the commercial Whatman® filter paper was available in 1 cm diameter disks, a pre-soaking in water for one day with continuous stirring at room temperature was done with the purpose to obtain the paper pulp. After this, most of the water was removed by filtration. Then, the cellulose was treated for hydrolysis, as described in the literature by Dufresne and co-workers, with sulphuric acid concentration of 63% at 45° C for 2 hours.[36] At the initial stage of the hydrolysis, the white suspension of the cellulose was rather thick, but after 30 minutes the suspension was more fluid and some change in colour to light yellow was observed.

The suspension was diluted with 10 folds of water in order to quench the hydrolysis reaction of cellulose. Most of the supernatant of the suspension was decanted off and the remaining suspension was centrifuged at 4000 rpm (5 minutes) in order to remove the remaining acid solution. The solid product was resuspended in deionized water and centrifuged at 7500 rpm (5 minutes). This procedure was repeated several times until the pH of the suspension turn neutral. The suspension was subjected to dialysis against milliQ water to remove any salts and by-products (if any). The product so obtained was characterized as follows.

The infra-red spectrum of nanocrystalline cellulose carried out in KBr which was almost identical to that of Whatman® filter paper as shown in Figure 3.26. Thus, no specific information was obtained through this technique.

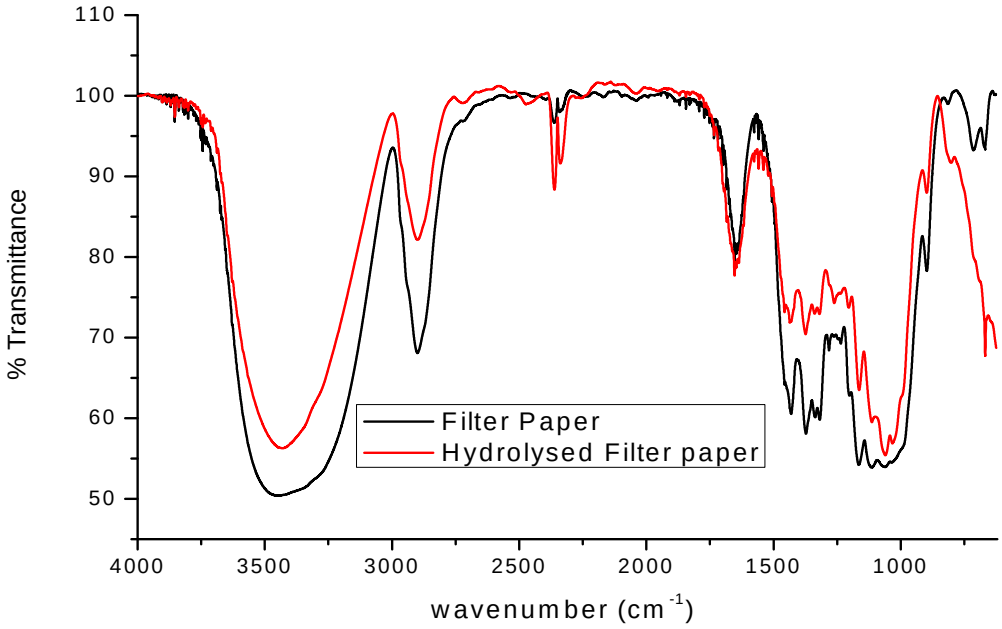

Figure 3.26: Infra-red spectrum of hydrolysed product obtained from Whatman® filter paper

In order to know the morphology of the hydrolysed product so obtained, the TEM analysis was performed. The following images (Figure 3.27) were obtained in an aqueous suspension of 1mg/ml hydrolysed product from Whatman® filter paper.

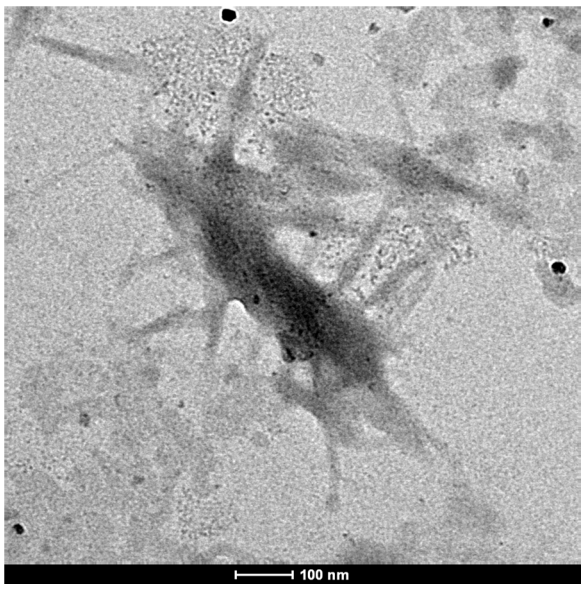

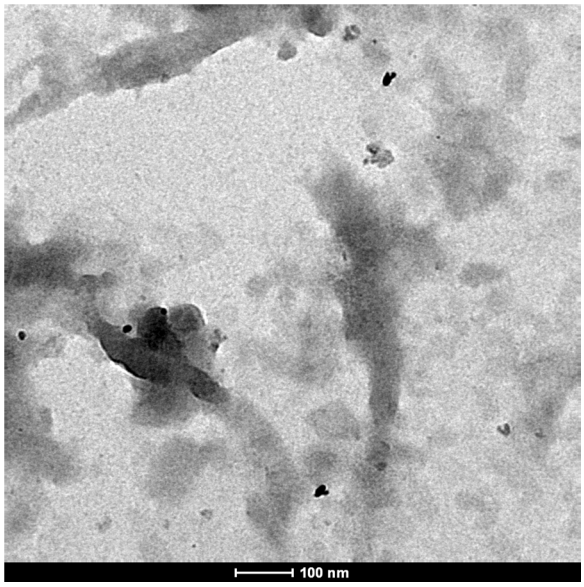

Figure 3.27: TEM images of hydrolysed product from Whatman® filter paper

The TEM images so obtained were not showing the characteristic whisker-like morphology of nanocellulose, but large aggregates/agglomerates of cellulose were well evident. For this reason, it was decided to seek another cellulose source, which should form the desired NCC.

4.3 From Micro crystalline cellulose (MCC)

In order to achieve the target nano sized cellulose, we explored the use of the commercially available microcrystalline cellulose of 20µm dimension range. The major advantage of this type of cellulose is its high crystallinity index of 66%, so good quality nanocellulose can be expected from this cellulose source.

The typical hydrolysis conditions (63% H_2SO_4, 2 hours at 45° C) as described by C. Danumah and H. Fenniri were used for microcrystalline cellulose.[34] The suspension was diluted 10 fold with water, in order to stop the on-going hydrolysis. A low speed centrifugation at 4000 rpm was carried out to remove most of the acidic supernatant. Then, the washings with distilled water and high speed centrifugations at 7500 rpm for 5 minutes was performed, until neutral pH was observed in the supernatant. Finally, the cellulose suspension was transferred in dialysis tube and treated first against tap water (6 days), then against milliQ water (2 days). The final product was recovered by lyophilization and characterized as follows.

A suspension of NCC in water (0.34 mg/mL) was used for TEM analysis. The image (Figure 3.28) shows the morphology of fibrils, which are characteristic of nanocellulose (NCC).

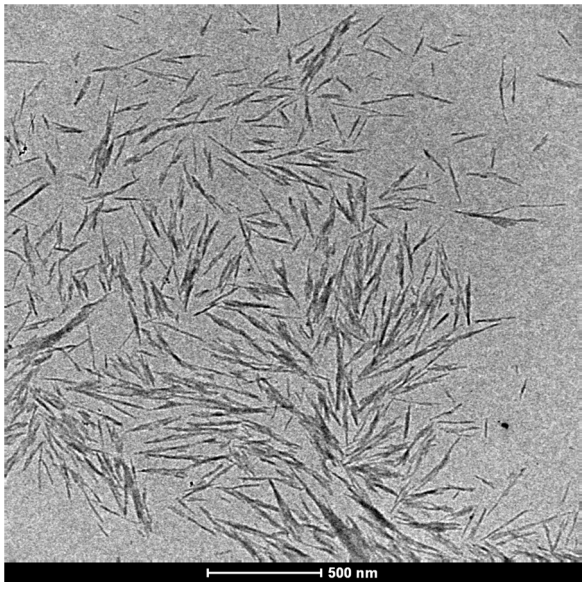

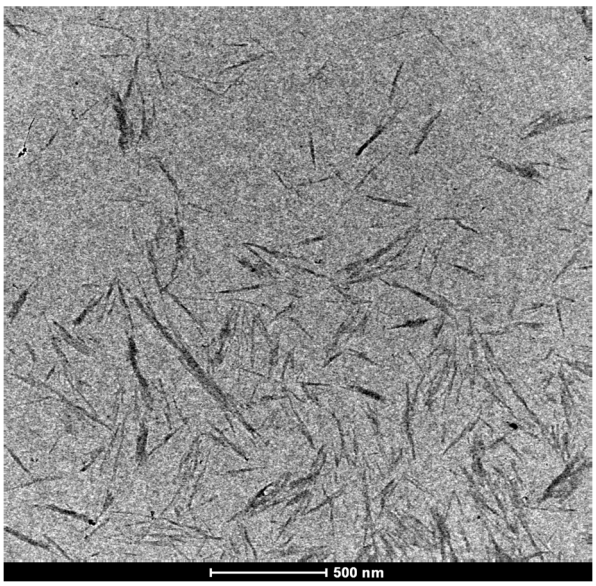

Figure 3.28: TEM images of NCC prepared from MCC

In order to obtain the average sizes of the fibrils, 70 different measurements were randomly taken in the digital image and analyzed using graphical (imageJ) software.

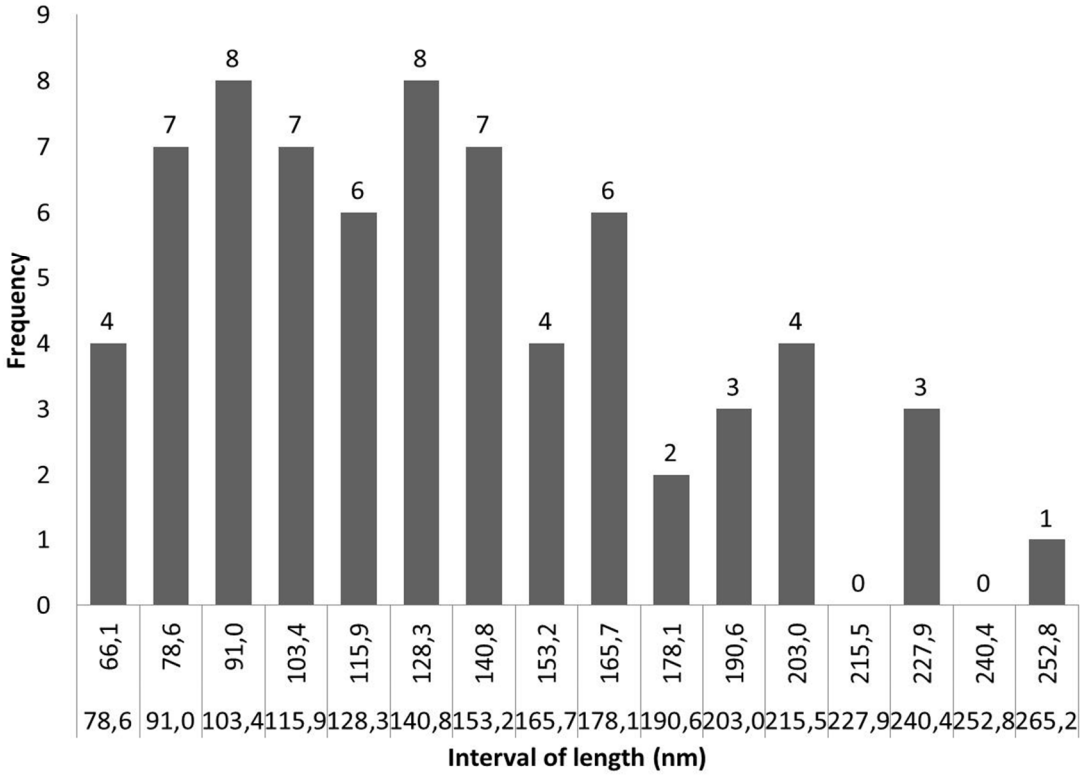

Figure 3.29: Histogram of length for NCC

The arithmetic mean of 70 measurements in the histogram (Figure 3.29) provided a value of 137±46 nm. Although, the number of data was not large enough to conduct a statistical analysis, but it confirmed the nanometer size range of the NCC fibrils were produced and the data were in accordance with literature values.[34]

The NCC was further characterized by elemental analysis. As expected, only in the case of NCC sample, the sulphur content was of 0.54 % due to the formation of sulfate esters during the hydrolysis. The Table 3.1 shows various elemental compositions in NCC and MCC sample.

Table 3.1: Elemental composition of MCC and NCC

Micro Crystalline Cellulose	Composition %	Nano Crystalline Cellulose	Composition %
C	42.89	C	39.75
H	6.62	H	6.47
N	/	N	/
S	/	S	0.54

The NCC samples were analyzed by Z-potential and Dynamic Light Scattering techniques (DLS). The Z-potential measurement for an aqueous suspensions of NCC (0.53 mg/mL) gave an average value of (-14.1 ± 0.8) mV. This confirmed the presence of a negative charge on the surface of NCC, which was due to the anionic sulfates. A morphological study of the particle size of NCC was also accomplished by DLS measurements. The size values obtained for the nanocrystals should be considered as hydrodynamic radii, which also take account of the sphere of hydration. The DLS measurements of NCC sample provided an average diameter of (103.9 ± 9.0) nm, which was in the nano meter range of dimension.

Once again, the infra-red spectrum (Figure 3.30) of NCC sample (KBr) did not provide any specific information as it was nearly identical to that of pristine cellulose. This was as expected since any specific chemical modification was done on NCC. On the other hand, the IR spectrum does not show any typical signal regarding the stretching band of sulfate group at 1360, 1150 or 540 cm^{-1}. This was probably due to the limited amount of sulfate ester groups present on the surface of NCC. This observation was consistent with the elemental analysis data wherein very low sulphur content was observed.

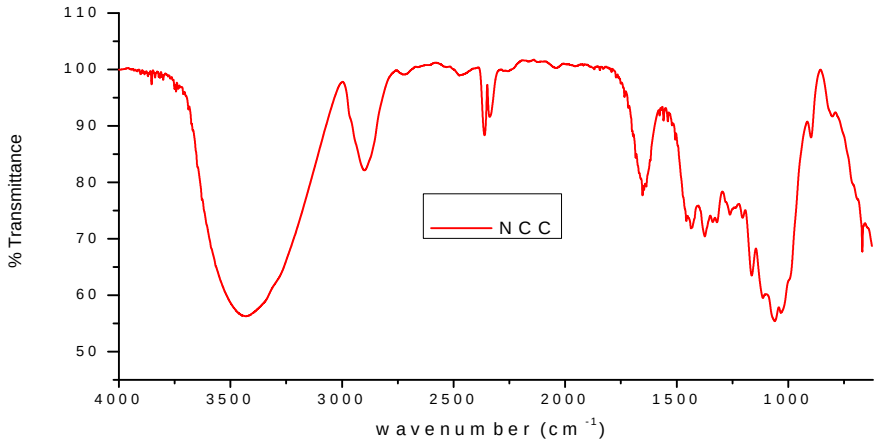

Figure 3.30: Infra-red spectrum of NCC

The NCC sample was further characterized by the thermogravimetric analysis (TGA) technique. The figure 3.31 reports the thermogram of nanocrystalline cellulose when the thermal analysis was carried out in an atmosphere of nitrogen or in air. The NCC showed a main thermal decomposition at about 250 °C and its decomposition took place in several stages. The starting material MCC had a thermal decomposition of 325 °C. Thus, the thermal stability of NCC was lower than that of MCC, which was likely to be due to the presence of sulfate group on the surface of NCC.

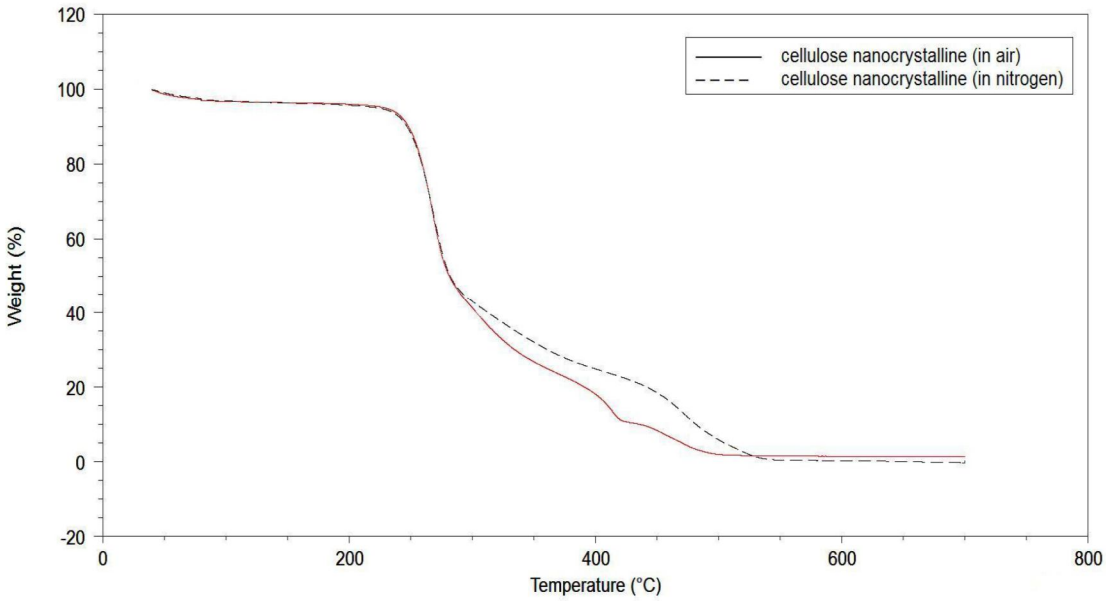

Figure 3.31: TGA of NCC

The nanocellulose produced from micro crystalline cellulose source was of high yield and showed the characteristics fibril like morphology of NCC as compared material obtained from cotton and Whatman® filter paper. Therefore, nanocellulose produced from MCC was explored further to its functionalization in the following subsection.

5. Functionalization of Nanocellulose

5.1 Covalent attachment of pH sensitive dye to NCC

Once it was possible to produce good quality nanocrystalline cellulose, the next step was to functionalize its surface with functional molecules. The first attempt was directed to utilize the reactive -OH groups available on the surface of NCC. As a model reaction we attached a pH sensitive dye to NCC that has been specifically designed to link to cellulose, as reported in a previous paper published in our laboratory.[37] The chemical structure of the pH sensitive dye is shown in Figure 3.32.

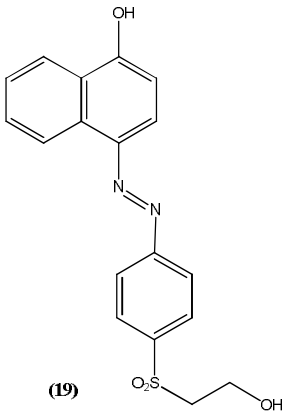

(19)

Figure 3.32: Structure of pH sensitive dye (19)

This azo-dye is characterized by the presence of a 2-hydroxyethylsulfonyl moiety which provides a handle for the covalent attachment of the dye onto supports bearing nucleophilic groups through the formation of a vinysulfone reactive group via the chemical steps reported in Scheme 3.32.

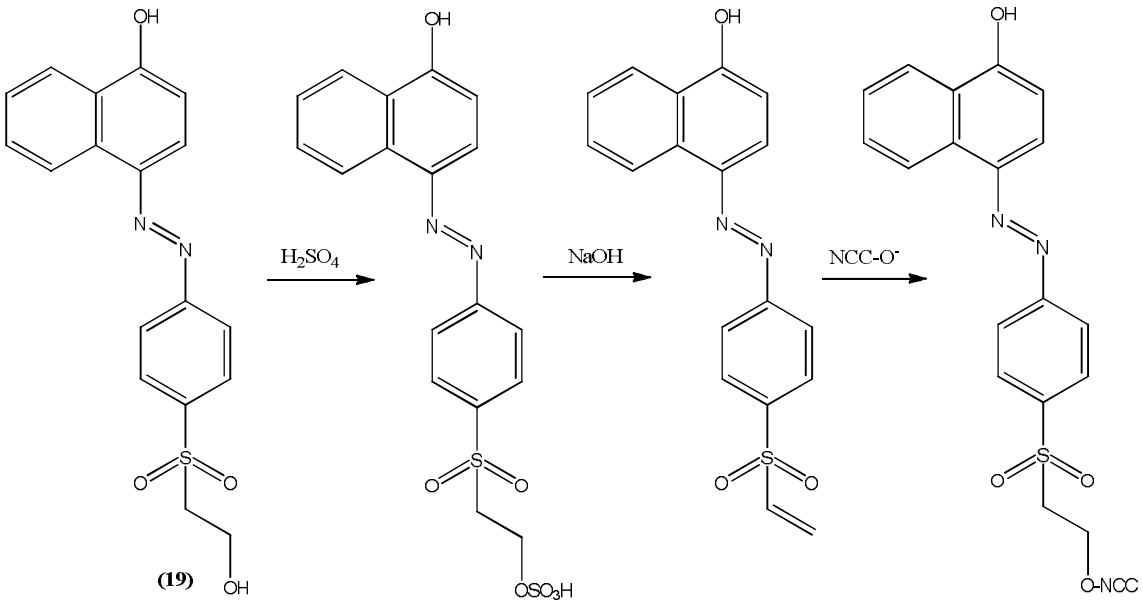

Scheme 3.32: Synthesis of NCC-dye

The NCC was dyied by the following method. First, the dye (19) was dissolved in a small quantity of 96% sulphuric acid and stirred for 30 minutes at ambient temperature. By this way, the sulphonyl ester group was formed from the 2-hydroxyethylsulphonyl group present in the dye. Then, it was diluted with deionized water and the solution was neutralized with sodium hydroxide. After 5 minutes, an appropriate quantity of sodium carbonate was added to the solution, in order to make the reaction medium sufficiently alkaline for the formation of vinyl sulfonic derivative of dye. To this, a basic suspension of nanocellulose was added and stirred overnight at room temperature. The solid was isolated by centrifugation at 7500 rpm for 15 minutes, re-suspended in water and centrifuged again. The suspension/centrifugation steps were repeated five times with sonication. The final suspension of NCC-dye was subjected to dialysis against distilled water until a neutral pH was obtained inside the dialysis membranes (3 days). The solid was recovered by lyophilization. The product so obtained was characterized as follows.

The NCC-dye was analyzed by the thermogravimetric analysis (TGA) technique. The thermograms of three different samples are shown in Figure 3.33: NCC (blue), dye (blue) and NCC-dye (red). It is evident from the thermogram that NCC is more thermally stable in comparison to NCC-dye. In addition, the thermogram of NCC-dye does not reach the 0% value, probably due to the presence of salt contaminants.

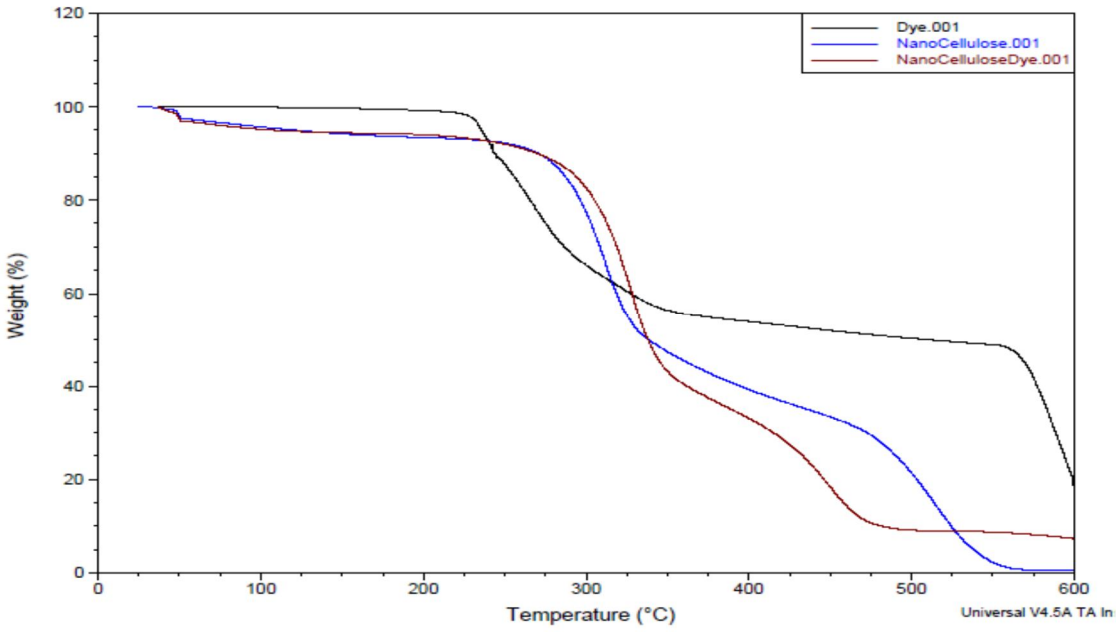

Figure 3.33: TGA of NCC-dye

The UV visible absorption spectra were recorded starting from an aqueous suspension of NCC-dye (0.5 mg /mL) in a sodium phosphate buffer of different pH values. The different colours observed in the NCC-dye suspension at different pH are shown in figure 3.34. The colour changes in suspension are: yellow in presence of an acid, where the protonation of naphthol in dye attached to NCC takes place, pink in presence of base where deprotonation of the same takes place.

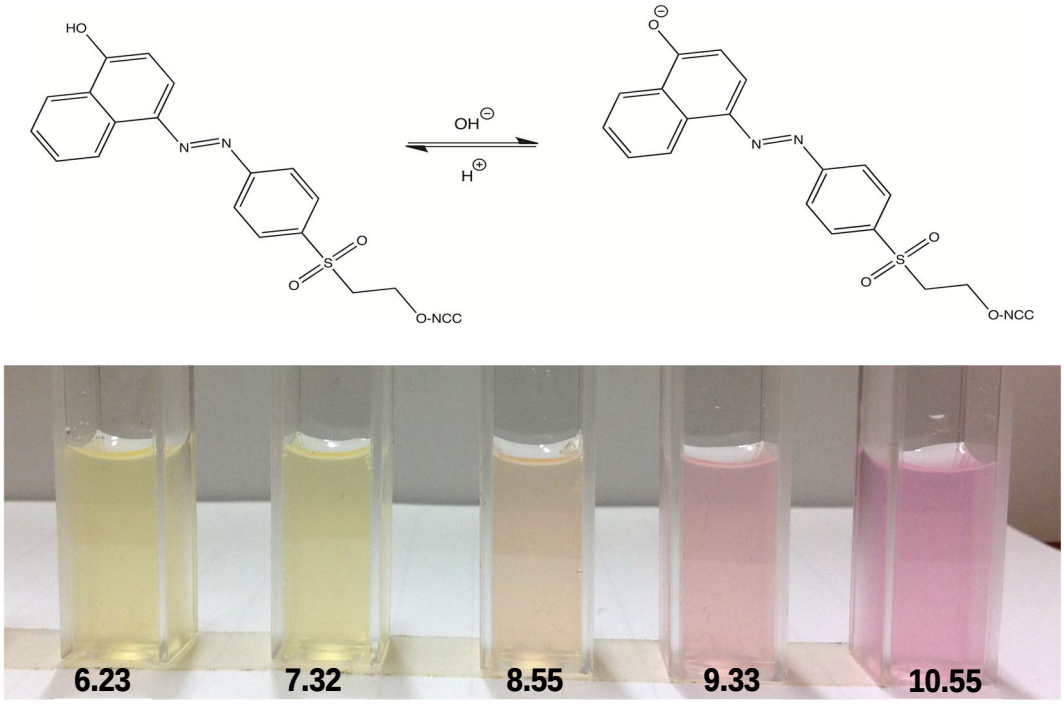

Figure 3.34: Suspension of NCC-dye at different pH

The suspension showed maximum absorbance at 453 nm and 545 nm for acid and base form NCC-dye as depicted in figure 3.35. Further, using the absorbance values obtained from UV-visible spectra, pk_a values were calculated. The pk_a values were determined from fitting the acid and base form curves were found to be 8.5 and 9.1 respectively, in good agreement each others.

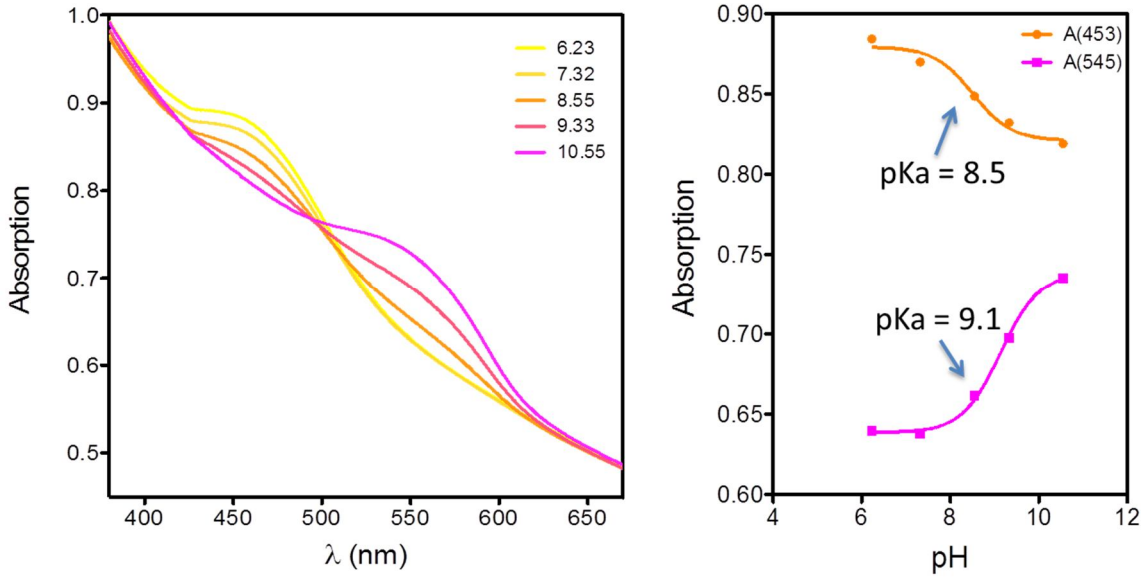

Figure 3.35: UV-visible of NCC-dye at different pH.

In order to further confirm the dye was covalently linked to the NCC surface, it was decided to do UV analysis using a NCC-dye membrane. In this, first a membrane of NCC-dye was constructed (Figure 3.36) using a Bi-adhesive tape and incorporated inside the surface of a plastic cuvette. As expected, different colours of NCC-dye membrane were observed for acid and basic form as depicted in figure 3.36.

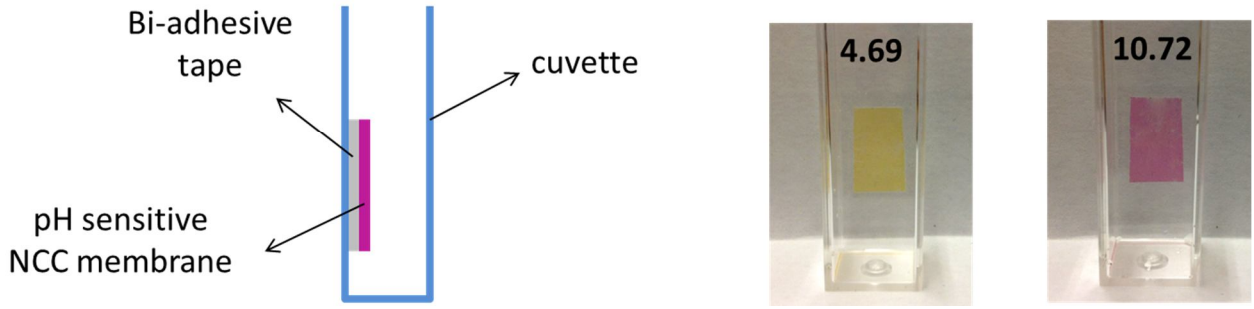

Figure 3.36: NCC-dye membrane

Similar UV visible spectra (Figure 3.37) were observed as in the case, when NCC-dye was in suspension. This result proves that the dye was covalently linked to NCC surface and even after several washing with water/buffer solution it does not alter the UV visible spectrum.

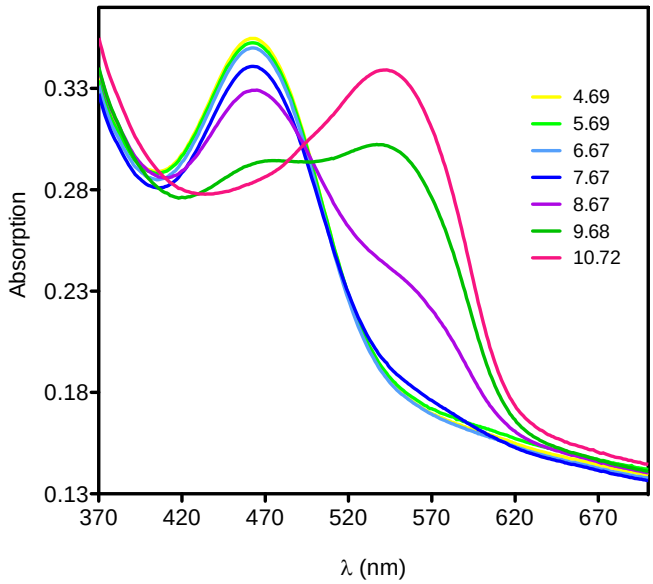

Figure 3.37: UV-visible of NCC-dye membrane

NCC-dye sensor was further evaluated in a reasonable timeframe by using a digital image analysis in a high-throughout approach. To this purpose NCC-dye a suspension was spotted in different places of a Whatman® filter paper, then each spot was covered with a drop of buffer at a different pH. The image of spotted filter was then acquired using a plane scanner. The color on the digital image, in term of RGB values, was carried out using Photoshop as described previously.[37]

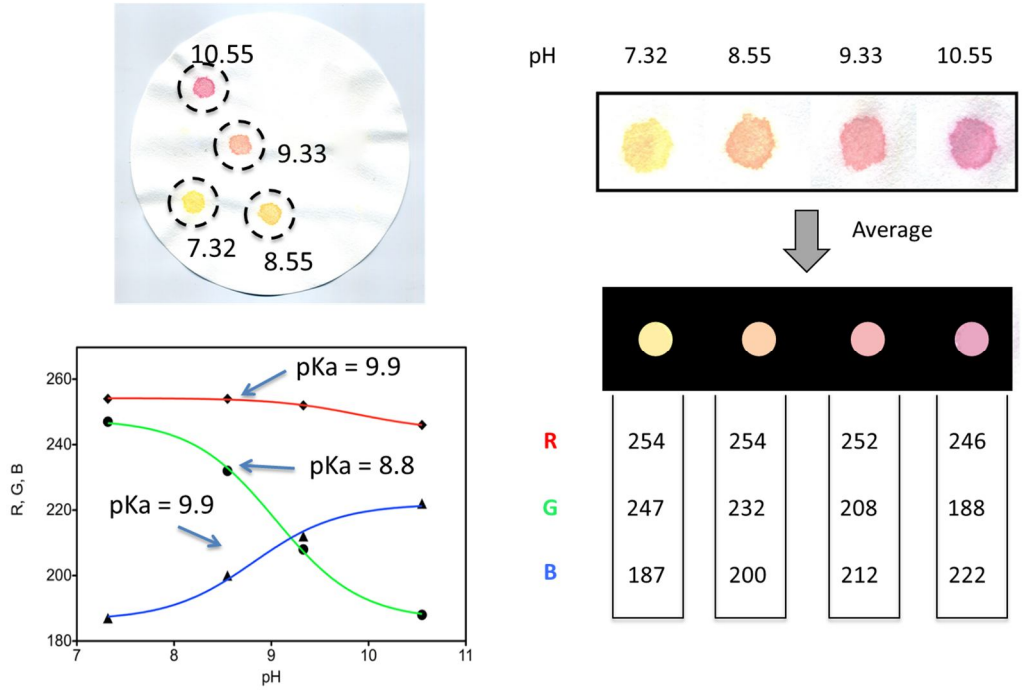

Figure 3.38: NCC-dye membrane and its RGB values

The figure 3.38 shows plot of R, G, B values by the variation of pH. The fitting of the curves gave a pk_a of 9.9 for Red, 8.8 for Green and 9.9 for Blue respectively, in good agreement with the results obtained for the suspension and for the membrane reported above.

Despite the success of this functionalization, the chemistry of hydroxylic groups is not very versatile. Therefore, we considered the functionalization of NCC surface with other groups that open up other kind of interactions or chemistries to be exploited. In the following paragraphs are the results obtained.

5.2 Synthesis of cationic nanocellulose (NCC-CAT)

An interesting way to functionalize nanocrystalline cellulose was described by Gray and co-workers.[38] It was based on the reaction of NCC with 2,3-epoxypropyl trimethyl ammonium chloride (EPTMAC) which allows for the introduction of cationic groups on the surface of NCC.

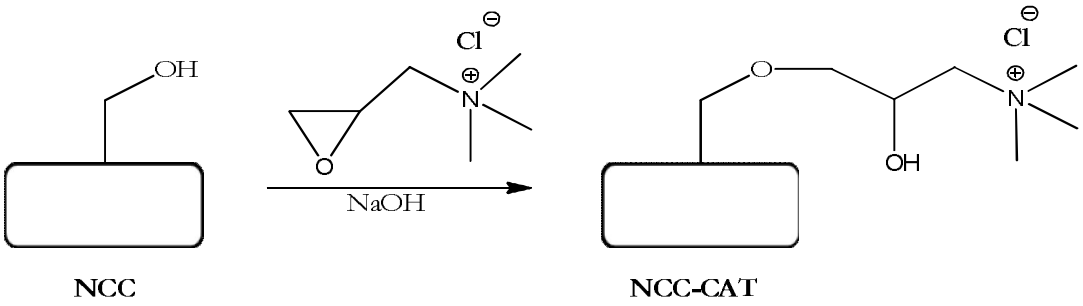

NCC NCC-CAT

Scheme 3.33: Synthesis of cationic nanocellulose (NCC-CAT)

For this purpose, sodium hydroxide (NaOH) was dissolved in milliQ water. The nanocrystalline cellulose (NCC) was added to the solution and sonicated for 15 minutes. After stirring for 30 minutes at room temperature, EPTMAC was added and the mixture was further stirred at 65°C. After 5 hours, the reaction mixture was diluted 5-fold with water and dialyzed against purified water for 7 days. The final product was recovered by lyophilisation. The product so obtained was characterized as follows.

First of all, the measurement of the Z-potential of an aqueous suspension of NCC-CAT (0.19 mg/mL) gave an average value of (23.4 ± 0.4) mV, indicating the presence of a positive charge due to the cationic species on the NCC particles. It should be pointed out that the basic conditions of the cationization reaction are known to promote the hydrolysis of sulfate ester, so the charged observed was real and not just an excess of positive charge since the anionic charges were not present anymore. The morphological study of the particle size of NCC was accomplished by DLS measurements. The DLS analysis provided an average diameter of (103.9 ± 9.0) nm, which confirms that chemically modified NCC maintains the nano meter dimension of crystals.

The number of trimethylammonium chloride groups in the cationic nanocellulose was estimated by conductometric titration of chloride ions with an aqueous silver nitrate solution (Figure 3.39), assuming the presence of one chloride counter ion per trimethylammonium group. In particular, 50 mL of 1% w/w NCC-CAT suspension was titrated with 0.01 M $AgNO_3$ (aq) solution by adding approximately 0.5 mL at 30 seconds time intervals. The corresponding degree of substitution was found to be 0.084 mmol per g of NCC which are in accordance with literature values.[38]

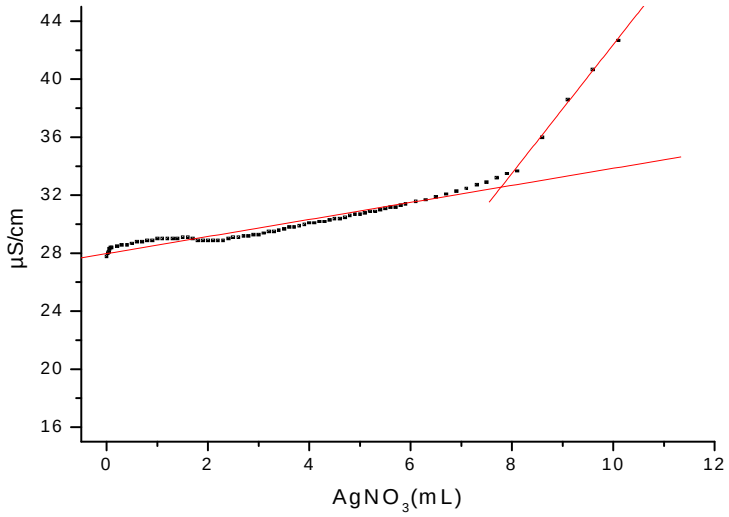

Figure 3.39: Conductometric titration of NCC-CAT

The positive charge introduced on NCC surface was tested as a support for anionic porphyrins owing to the electrostatic interaction. Supporting porphyrins is of potential interest in many fields, for example in catalysis and material science. The occurrence of the interation between NCC-CAT and the tetrasulphonatophenyl porphyrin ($TPPS_4$) was demonstrated by UV-Visible absorption spectroscopy according the following procedure.

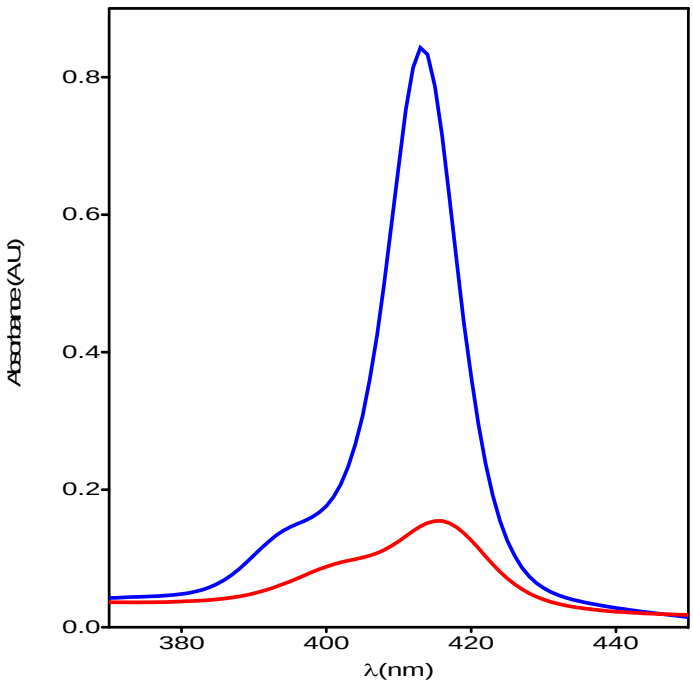

Figure 3.40: UV-visible spectrum of NCC-CAT and anionic porphyrin

A known amount of a $TPPS_4$ solution of 2.18 µM concentration was introduced into a cuvette and the corresponding UV-Vis spectrum was recorded. To this, a known amount of NCC-CAT (4.1 mg) was added and the suspension was shaken for 5 minutes. Then, the suspension was centrifuged at 13000 rpm and the supernatant was analyzed by UV-Vis spectroscopy. A decrease in absorbance of $TPPS_4$ was well evident as shown in Figure 3.40 and the new concentration of $TPPS_4$ (0.40 µM) was calculated from the molar extinction coefficient. This decrease can be attributed to the fact that the electrostatic interaction between the cationic cellulose and nanocellulose reduces the overall porphyrin content in the solution.

The electrostatic interaction between cationic nanocellulose and anionic porphyrin was further studied by z-potential measurements.

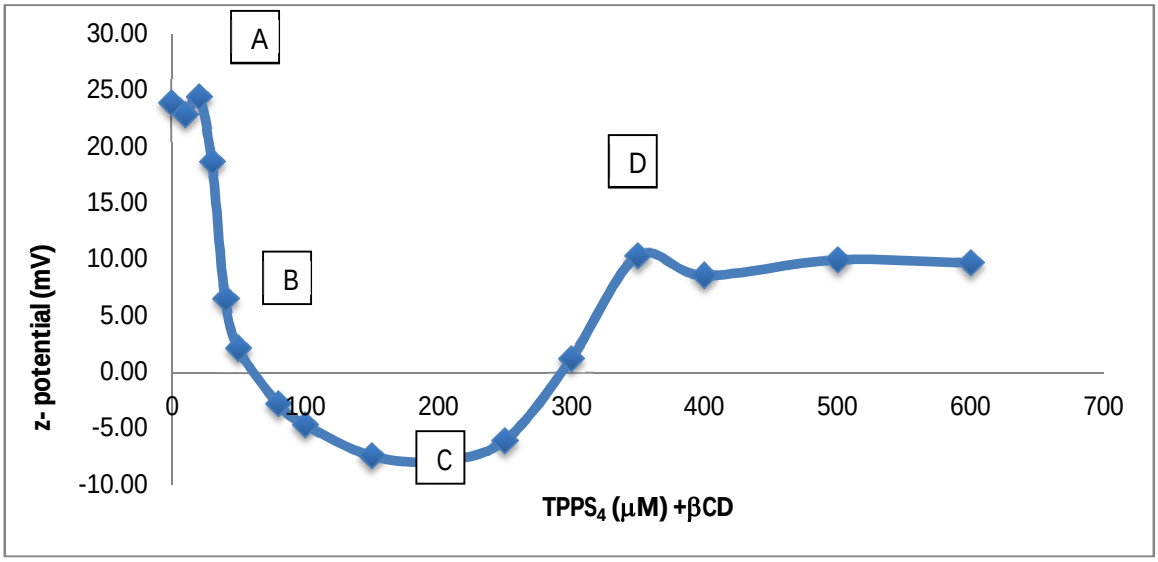

Figure 3.41: Z-potential of NCC-CAT and anionic porphyrin

To this purpose, a known amount of cationic cellulose (4.1 mg) was suspended in water and z-potential was recorded (point A) as shown in Figure 3.41. Then, anionic porphyrin $TPPS_4$ (mother solution 0.03 mM) was added to cationic nanocellulose suspension in small aliquots. A decreasing of z-potential was observed, due to the occurrence of electrostatic interaction between the two charged. At point B, it can be assumed that the cationic nanocellulose surface was decorated with an equivalent amount of anionic porphyrin, since the z-potential was zero at this point. A further addition of anionic porphyrin led to a further increasing of the negative z-potential due to the well documented Π–Π–interactions between porphyrins. It has previously reported by our laboratory that tetra-sulfonated porphyrins and permethylated beta-cyclodextrin form a very strong host-guest complex with a porphyrin:cyclodextrin 1:2 stoichiometry. Thus, starting from the z-

potential situation at the point C, increasing amounts of permethylated beta-cyclodextrin were added to the suspension. As expected, an increase in potential was observed (point D) since the permethylated cyclodextrin was first disrupting the porphyrin-porphryin interaction, then removing the porphyrin electrostatically bonded to the NCC-CAT. However, z-potential did not recover the initial value so some porphyrin-NCC-CAT interactions were still operative. That could be due to a partial aggregation of porphyrin-NCC-CAT that hiddens some porphyrins making them not accessible to permethylated beta-cyclodextrin.

These experiments demonstrated that positive charged functional groups were well incorporated on NCC, which was confirmed by UV visible and z-potential studies. After successful introduction of cationic groups on the surface of NCC, the next chemical modification taken in consideration was the introduction of amino functional groups on the surface of nanocrystalline cellulose.

5.3 Synthesis of Amino Nanocellulose (NCC-NH_2)

Reactive amino groups can be introduced on the surface of nanocellulose using epichlorohydrin according to the procedure described by S. Dong and M. Roman (Scheme 3.34).[39]

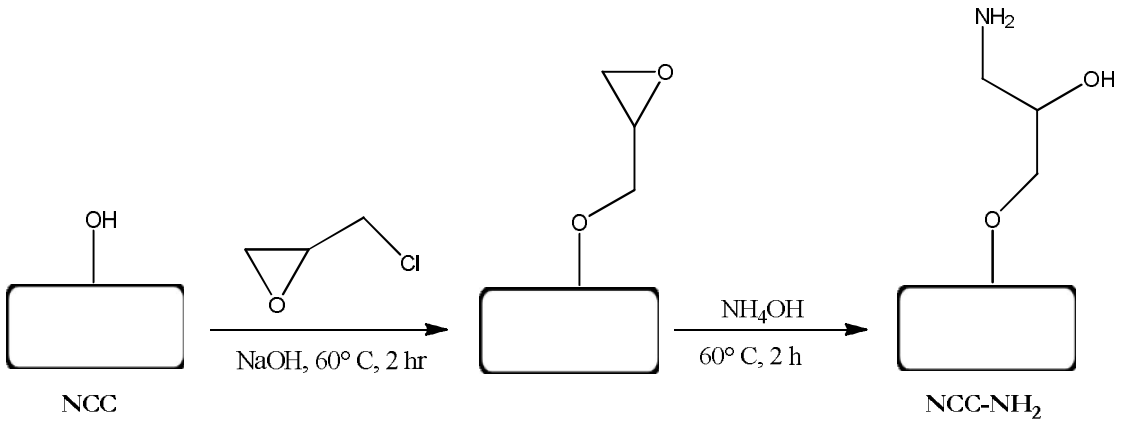

Scheme 3.34: Synthesis of Amino Nanocellulose (NCC-NH_2)

Scheme 3.35 reports the mechanism of the reaction, which involves the ring opening of epoxide of epichlorohydrin by the alkoxide of NCC followed by removal of chlorine through an intra-molecular cyclization step. The NCC suspension was made basic with NaOH solution and reacted with epichlorohydrin for 2 hours with constant stirring at 60° C. The solid was washed with water by means of centrifugation/re-dispersion steps, in order to remove the excess of epichlorohydrin. Further, the epoxide ring thus formed was opened in basic environment in presence of ammonium hydroxide to obtain the amino group.

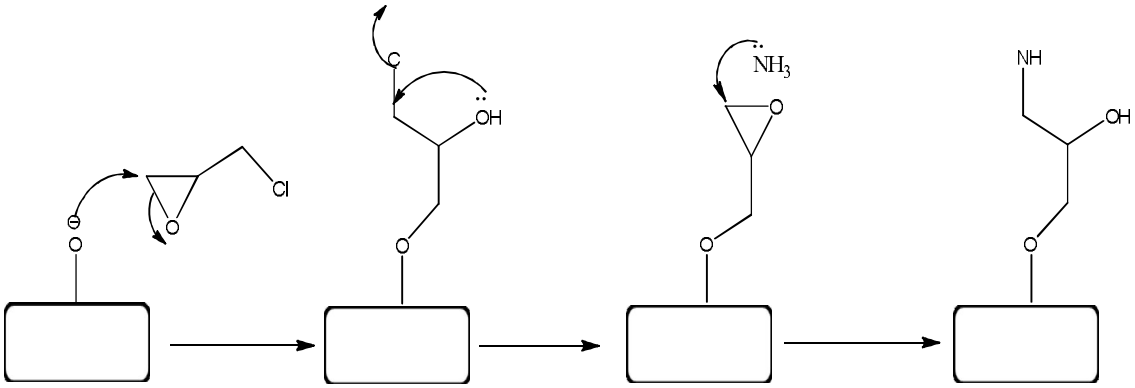

Scheme 3.35: Reaction of NCC with epichlorohydrin

To this purpose, the pH was adjusted to 12 using a concentrated NaOH solution, then ammonium hydroxide was added to the suspension and further stirred for 2 hours at 60° C. The suspension so obtained was washed with distilled water and centrifuged at 7500 rpm (5 minutes) until the pH was neutral. The product was subjected to dialysis against milliQ water (3 days) to remove the salts. The solid product was recovered by lyophilization and characterized as follows.

The product was first analyzed by Kaiser test, which is a simple ninhydrin test that was developed for the detection of primary amine groups in an organic compound. The reactions involved in Kaiser are depicted in Scheme 3.36.

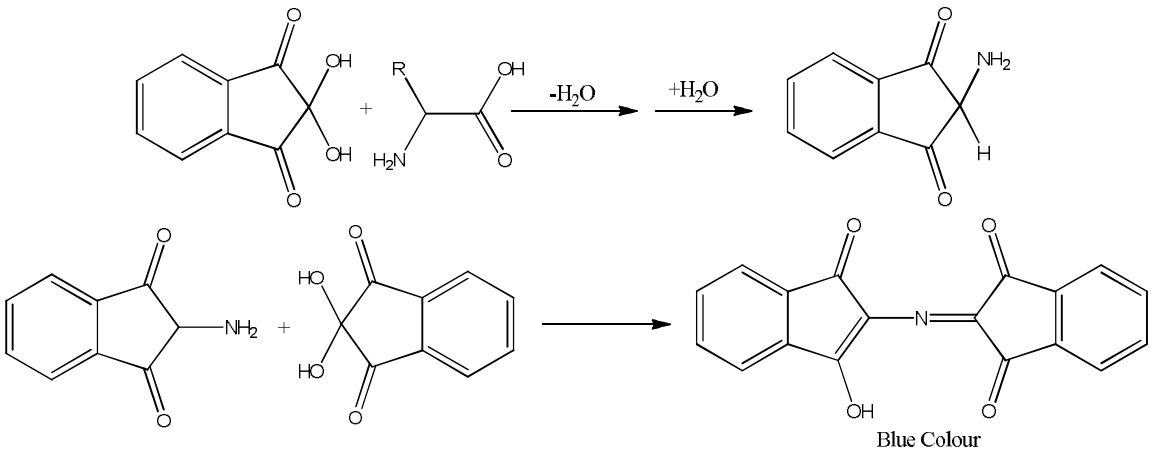

Scheme 3.36: Kaiser test for detection of primary amines

The development of a blue colour testifies the presence of a primary amino group. The same test can be also used to quantify the amino groups exploiting the absorption peak in the UV- visible spectrum at 570. According to Lambert-Beer law, absorbance can be associated with concentration of free amino as follows:

$$\frac{mmol}{g} = \frac{(Abs\ sample - Abs\ blank) \times dilution\ (mL) \times\ 10^3}{Extinction\ coefficient\ \times Sample\ weight\ (mg)}$$

Where **Abs sample** is absorbance of the ninhydrin complex, **Abs blank** is the absorbance of the blank (mix of ethanolic solution of phenol, KCN in pyridine and ethanolic solution of ninhydrin) recorded at 570 nm. The extinction coefficient reported in literature is 15000 m^{-1} cm^{-1}.[40]

In order to determine the degree of substitution, 3.3 mg of amino nanocellulose were subjected to Kaiser test and the corresponding absorption spectrum for the formation of blue ninhydrin complex was recorded.

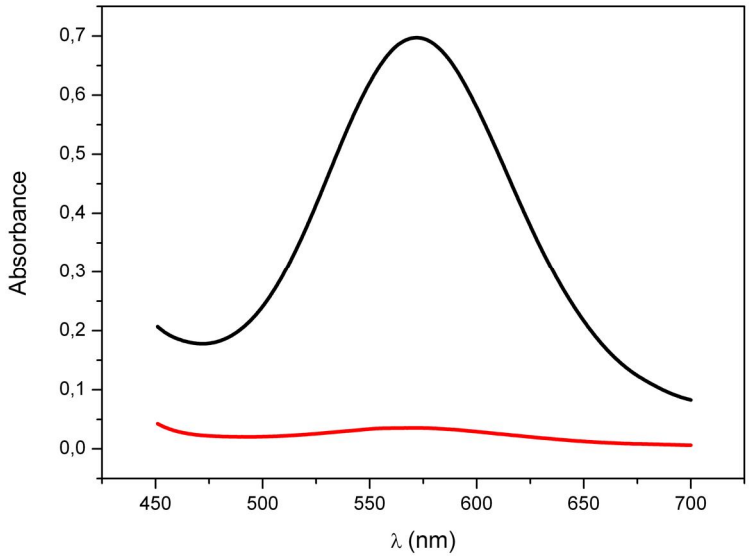

Figure 3.42: UV-visible spectrum of NCC-NH_2 kaiser test

In Figure 3.42, the black line represents the absorbance of ninhydrin complex formed with corresponding absorbance of 0.699 at 570nm while red line is the blank sample having absorbance of 0.0355. Using the above equation, the degree of substitution of amino group was calculated to be 0.04 mmol per gram of nanocellulose, which was in accordance with literature values.

The NCC-NH_2 sample was analysed by transmission electron microscopy. An aqueous suspension of amino nanocellulose (1mg/mL) was used for TEM analysis.

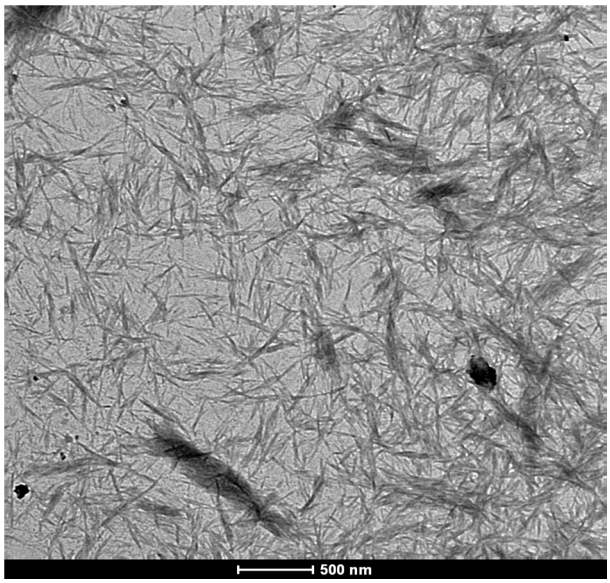

Figure 3.43: TEM image of NCC-NH_2

The analysis by TEM, showed nanosized particles of cellulose which allowed confirming that chemical functionalization with epichlorohydrin does not affect the morphology of nanocellulose. Further, the infra-red spectrum of NCC-NH_2 sample was recorded in KBr. It didn't show any significant signal in NH_2 stretching region, probably because the degree of substitution was very low.

To further confirm the presence of amino groups on the surface of nanocellulose, it was decided to covalently attach two different chromophores such as Fluorescein and Porphyrin.

5.3.1 Fluorescein labelled nanocellulose

In order to further confirm the amino modification, the primary amino groups of nanocellulose were reacted with fluorescein isothiocyanate (FITC) that is considered to be a specific label for amino groups (Scheme 3.37).

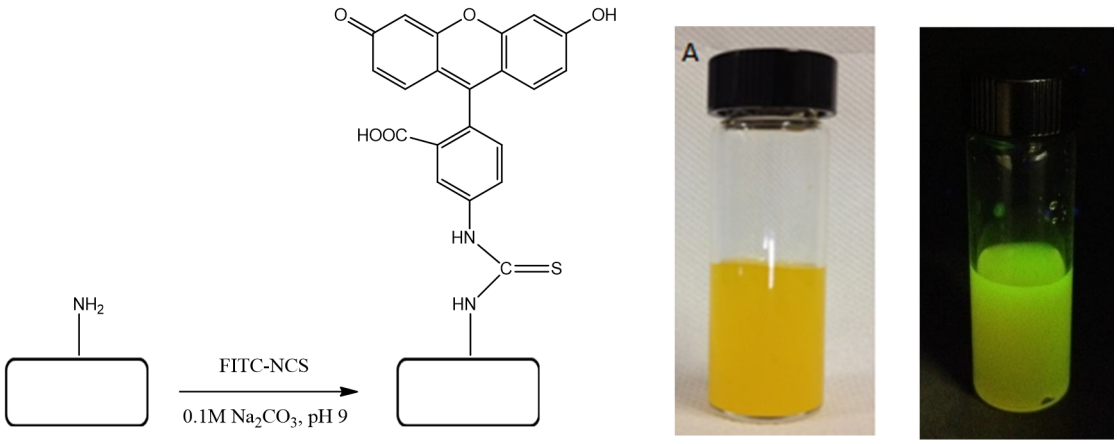

Scheme 3.37: Synthesis of fluorescein labelled nanocellulose

To this purpose, the amino nanocellulose was suspended in a 50mM sodium borate buffer solution, containing ethylene glycol tetra acetic acid, sodium chloride and sucrose. The suspension was stirred at room temperature for 15 minutes to form a stable homogenous suspension. The pH of the suspension was adjusted to 9 and FITC was added. The reaction mixture was stirred overnight in the dark by covering with an aluminium foil. The yellow suspension was transferred in a dialysis bag and dialysed for 5 days. Thus, the yellow colour of the suspension (Scheme 3.37, Figure A) and the fluorescence observed under UV lamp (Scheme 3.37, Figure B) confirmed the successful covalent bonding of FITC on the surface of amino nanocellulose.

The TEM analysis was done using an aqueous suspension of 1 mg/mL NCC-NH_2.

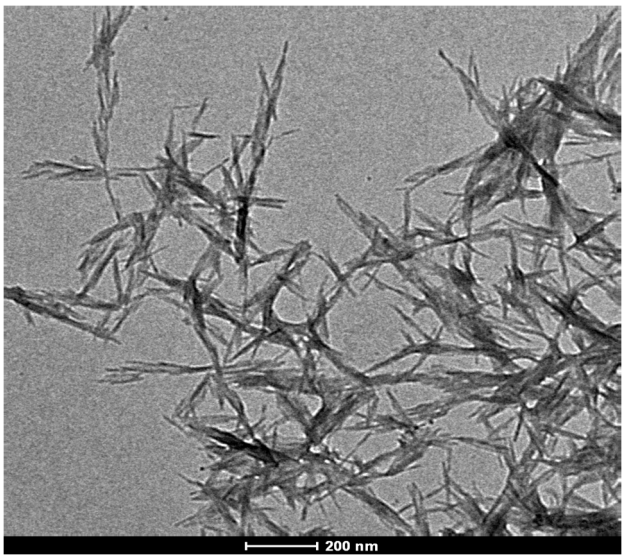

Figure 3.44: TEM image of Fluorescein labelled nanocellulose

The TEM analysis confirmed that whisker-like nano sized particles were present, which allows concluding that functionalization with FITC doesn't affect the morphology of amino nanocellulose.

Another test to confirm the presence the amino group on nanocellulose was performed by introduction of highly coloured porphyrin exploiting the trichloro triazine chemistry.

5.3.2 Porphyrin labelled nanocellulose

Covalent attachment of amino tetraphenyl porphyrin on the surface of amino nanocellulose was performed using Trichloro triazine (TCT) strategy (Scheme 3.38).

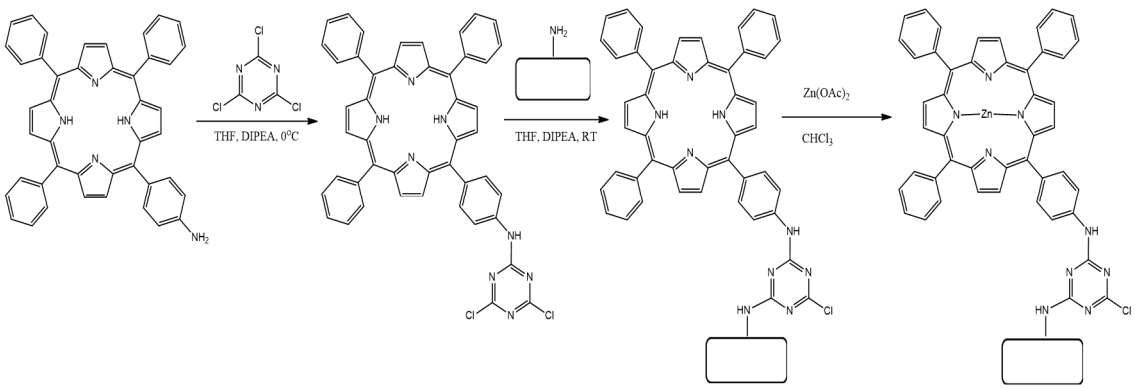

Scheme 3.38: Synthesis of porphyrin labelled nanocellulose

The replacement of chlorine atom in cyanuric chloride was first performed by reaction of amino-tetra phenyl porphyrin, which led to formation of mono-adduct of porphyrin. Later, mono adduct was reacted with amino nanocellulose. More precisely, the amino-tetra phenyl porphyrin (TPP-NH_2) was reacted with 1 equivalent of cyanuric chloride in THF at 0°C in the presence of 1.2 equivalent diisopropylethylamine (DIPEA). The reaction was stirred at room temperature until TLC analysis (PET/EtOAc, 6:4 as eluent) indicated the complete disappearance of the starting material (TPP-NH_2) and the formation of the corresponding mono-adduct. At this point, one equivalent of amino nanocellulose (NCC-NH_2) was added together with 1.2 equivalent of DIPEA and the reaction mixture was stirred at 80°C for 24 hours. After this time, the suspension was washed by the centrifugation method with THF, to remove excess porphyrin monomer adduct, and then with MeOH. The metallation with Zn (II) was performed by treatment with a saturated solution of zinc acetate in MeOH at 60° C for 3 hours. The TPP-NCC (Zn) adduct was recovered by centrifugation and washed with MeOH for 3 times. The solid was finally dried under a flow of nitrogen.

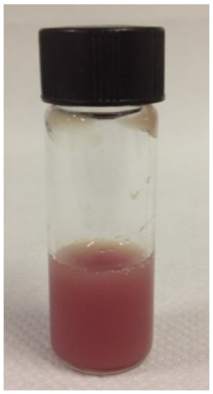

Figure 3.45: Suspension of porphyrin labelled nanocellulose

The red colour of the suspension visually confirms the covalent attachment of amino porphyrin on the surface of amino nanocellulose. Other evidences for the attachment are discussed below.

The covalent linkage of porphyrin monomer adduct on the surface of amino nanocellulose was confirmed by UV-visible spectrometry. The Figure 3.46 shows the UV-Vis spectra of 0.5 mg/ml aqueous suspensions of TPP-NCC (black line) and TPP-NCC (Zn) (red line) at neutral pH. The typical UV-Vis spectroscopic signatures for porphyrinic compounds were observed. In particular, for TPP-NCC, a Soret band around 423 nm and four Q-bands at 521, 563, 604, 654 nm were observed. Upon metallation with Zn(II) acetate, the corresponding TPP-NCC (Zn) adduct was formed as confirmed by the expected red shift

of the Soret band to 429 nm and the reduction of the Q-bands from four to two at 565 and 608 nm

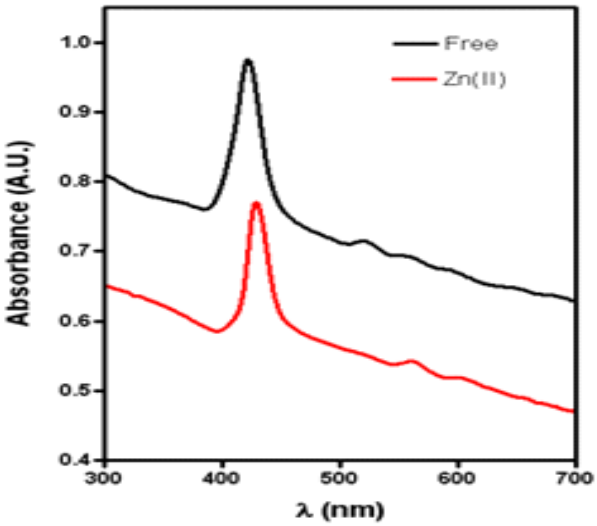

Figure 3.46: UV-visible spectrum of porphyrin labelled nanocellulose

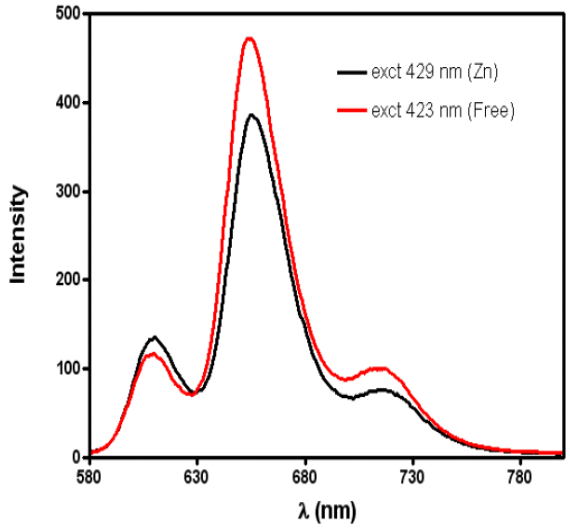

Figure 3.47: Fluorescence spectrum of porphyrin labelled nanocellulose

Upon excitation at 423 nm, the fluorescence spectrum of TPP-NCC (black line) shows three emission bands at 609, 656 and 719 nm (Figure 3.47). On the other hand, excitation at 429 nm produces the fluorescence spectrum of TPP-NCC (Zn) (red line) with three emission bands at 611, 658 and 722 nm.

Hence, the epichlorohydrin procedure for introduction of amino group on NCC was successfully confirmed by covalent linkage of functional materials such as Fluorescein and Porphyrin.

5.4 Amino nanocrystalline cellulose by tosylation (NCC-TNH$_2$)

A further chemical modification that was considered to introduce amino groups on the surface of NCC was the tosylation strategy described by Blackwell and co-workers and depicted in Scheme 3.39.[41]

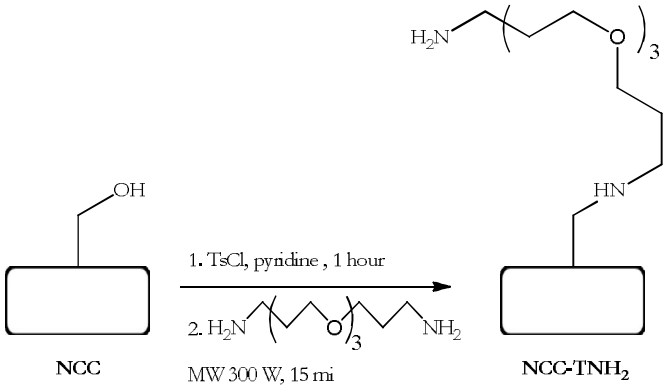

Scheme 3.39: Synthesis of Amino nanocrystalline cellulose by tosylation (NCC-TNH$_2$)

According to this procedure, the hydroxyl groups of nanocellulose were converted to corresponding tosyl group by reaction with a 2M solution of tosyl chloride in pyridine. After stirring for 1 hour at room temperature, the NCC suspension was washed 3 times with ethanol by centrifugation. Then, the cellulose suspension was placed in a microwave tube and 4,7,10-trioxa-1,13-tridecanediamine was added. The reaction mixture was subjected to microwave heating at 20 W power for 15 minutes at 120° C with continuous stirring. After cooling to ambient temperature, the suspension was washed with following solvents: DMF (2 times), EtOH (2 times), NaOH and finally with distilled water until neutral pH. The solid product NCC-TNH$_2$ was obtained by lyophilization and was characterized as follows.

As expected, in the elemental analysis of NCC-TNH_2 the presence of nitrogen confirmed the successful chemical functionalization.

Table 3.2: Elemental analysis of NCC and NCC-TNH_2

NCC	Composition %	NCC-TNH_2	Composition %
C	32.72	C	40.39
H	6.30	H	6.14
N	/	N	0.36
S	0.82	S	0.67

The product was further analysed by Infra-red spectroscopy. The IR spectrum did not show any peak ascribable to the amino group in comparison to pristine nanocellulose, since due to a low degree of amination.

Further, the Kaiser test for detection of primary amino groups was performed on few mg of NCC-TNH_2. Only the appearance of yellow colour was observed. Hence, no free amino group were detected using this test, in contrast with elemental analysis. So, this chemical way of modification was abandoned and another chemical modification was attempted as described in the next section.

5.5 Silane amino nanocrystalline cellulose (NCC-Si-NH_2)

Amino groups could also be introduced on surface of nanocellulose by treatment with 3-aminopropyltrimethoxysilane (APS) (Scheme 40) as described by Q. Yang and X. Pan.[42]

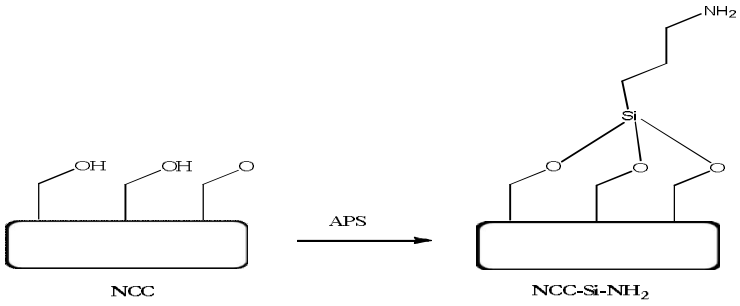

Scheme 3.40: Synthesis of silane amino nanocrystalline cellulose (NCC-Si-NH_2)

Firstly, a homogenous suspension of nanocellulose was prepared in anhydrous DMF by sonication for 10 minutes. Then, a solution of 3-aminopropyltrimethoxysilane (APS) was added under a flow of nitrogen. The reaction mixture was stirred at room temperature for 2 hours. Then, the suspension was first washed by centrifugation with DMF (3 times), to remove the excess of APS, followed by several washings with acetone. The residue was dried under flow of nitrogen to obtain a powder. The product so obtained was characterized as follows.

As evident from the elemental composition, the nitrogen content can be seen in the NCC-Si-NH_2 sample. Thus, it confirms the successful introduction of amino group on the surface of nanocellulose.

Table 3.3: Elemental analysis of NCC and NCC-Si-NH_2

NCC	Composition %	NCC-Si-NH_2	Composition %
C	32.72	C	39.45
H	6.30	H	6.14
N	/	N	0.42
S	0.67	S	0.60

Further, the Kaiser test was performed on NCC-Si-NH_2. The appearance of blue colour was observed thereby confirming the presence of free amino group on nanocellulose surface. The UV visible absorption spectrum of ninhydrin complex formed (blue colour) was recorded. The evaluation of absorption value of complex at 570 nm gave a degree of substitution of 0.2 mmol NH_2 per gram of nanocellulose which was less as compared to literature values.

The product was further analyzed by XPS. The deconvolution of the C 1s levels gives three peaks (C-1, C-2, C-3). These values were in good agreement with data of the literature.[43] The C-1 (*ca.* 285 eV) corresponds to a carbon atom bound only to other carbon atoms and/or hydrogen atoms. The C-2 (286.7–8 eV) belongs to a carbon bound to a single non carbonyl oxygen atom, which has been shown to be mainly derived from cellulose.[43] The C-3 peak (288.2–3 eV) was related to carbon atom bound to one carbonyl oxygen or to two non-carbonyl oxygen atoms.

Table 3.4: XPS data of NCC-Si-NH_2

	C 1s	O 1s	Si 2p	N 1s	O/C	Si/C	Si/N
CNC	284.6 (56%) 286.9 (35%) 288.3 (9%)	533.0			0.43		
CNCSiNH2	284.8 (76%) 286.9 (19%) 288.2 (5%)	533.0	102.8	400.4	0.25	3.12	0.04

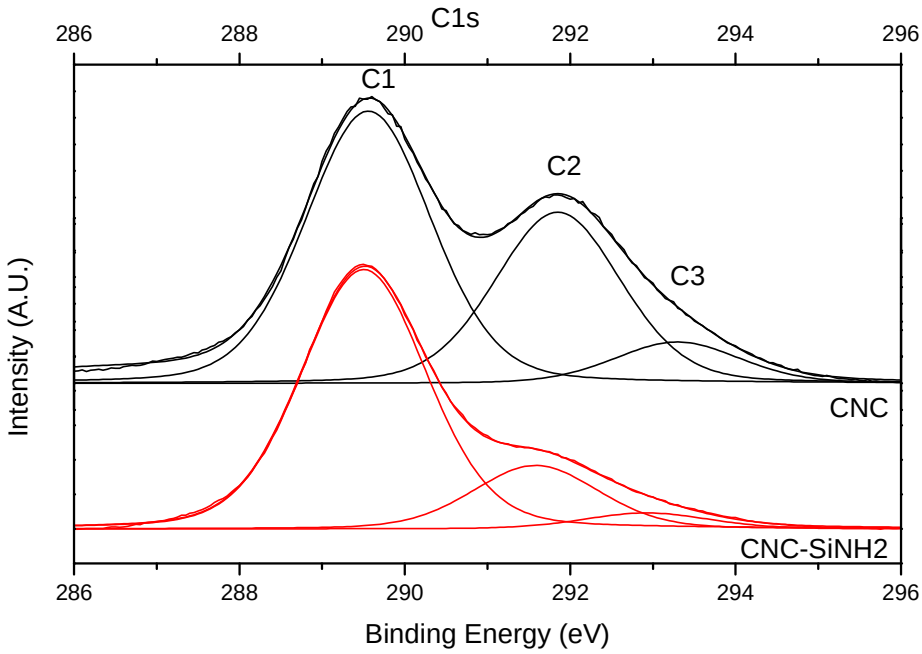

Figure 3.48: XPS analysis of NCC-Si-NH_2

In the NCC-Si-NH_2 sample, there was an increase in the intensity of total Carbon with respect to Oxygen, especially an increasing of the C1 component that was probably due to the propyl moiety bounded to silica. The presence of both silicon and nitrogen further indicate that the functionalization process was successful.

In the coming section, other NCC functionalization pathway for introduction of carboxyl group will be studied.

5.6 Carboxylated nanocrystalline cellulose by oxidation from ammonium persulfate (NCC-APS-COOH)

While we were looking to a way to functionalize the surface of NCC with groups more versatile than hydroxyls, a report appeared in literature by Luong and coworkers[44] that described a direct oxidative procedure, starting from microcellulose, allowed to prepare in one pot both the nanocellulose and produce carboxylic groups on the surface of the nanocrystals (Scheme 3.41). That seemed very interesting and convenient to us so, we decided to repeat it.

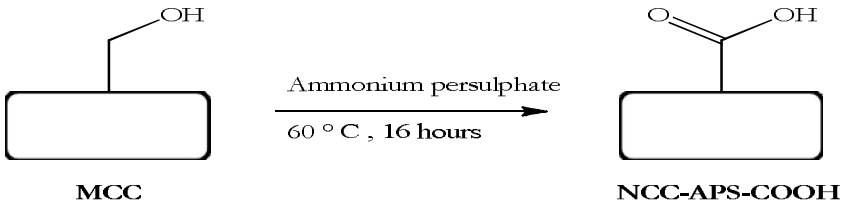

Scheme 3.41: Synthesis of Carboxylated nanocrystalline cellulose from oxidation by ammonium persulfate (NCC-APS-COOH)

According this procedure, the microcrystalline cellulose was added to 1M solution of ammonium persulfate, which resulted in the formation of a suspension. The oxidation of cellulose was carried out by heating the suspension at 60° C for 16 hours with continuous stirring. Then, the suspension was centrifuged at 12,000 rpm for 10 minutes. The solution was decanted and water was added to the cellulose pellet, followed by 5 minutes of vigorous mixing and repeated centrifugation. The centrifugation/washing cycles were repeated 4 times until the suspension pH was around 4. The suspension was lyophilized to yield a white material (NCC-APS-COOH). The product was characterized as follows.

The product was analysed by Infra-red spectrometry in KBr. The IR spectrum (Figure 3.49) showed an absorption band at 1720 cm^{-1} corresponding to the stretching of carboxyl group. Hence, it confirmed the successful introduction of carboxyl group on the surface of cellulose.

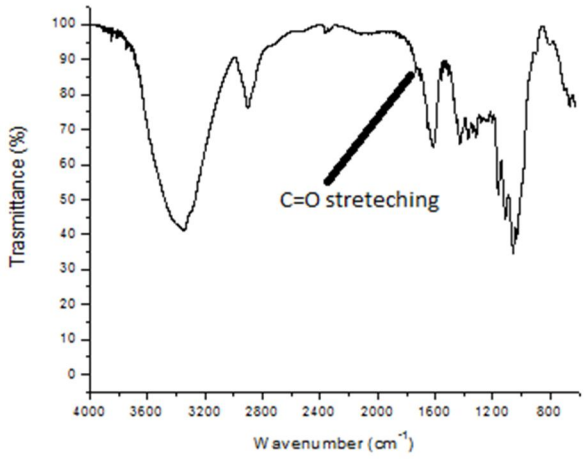

Figure 3.49: Infra-red spectrum of NCC-APS-COOH

Further, the measurement of the Z-potential analysis of an aqueous suspensions of NCC-APS-COOH (0.24 mg/mL) gave an average value of (-21.4 ± 0.4) mV that confirmed the expected presence of a negative charge due to the carboxylate anions present on the particles of NCC. The morphological study of the particle size of NCC was also accomplished by DLS measurements. The DLS measures provided an average diameter of (281 ± 7.0) nm.

The degree of oxidation could be also determinated by conductometric titration with sodium hydroxide.

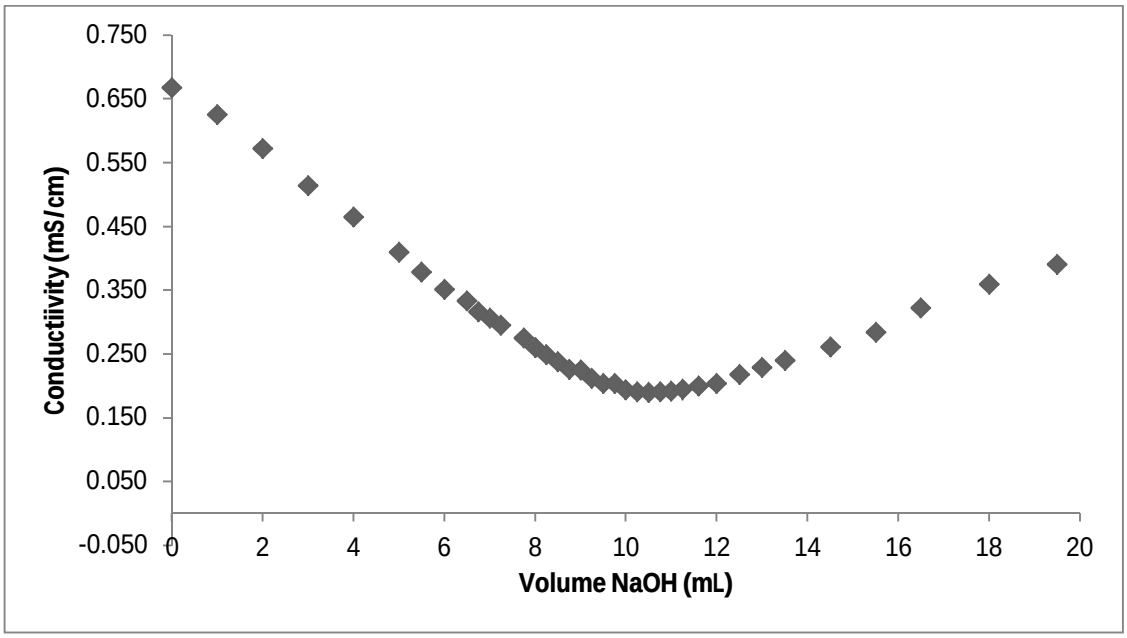

Figure 3.50: Conductometric titration of NCC-APS-COOH

To this purpose, a known amount of NCC-APS-COOH was suspended in a known volume of 0.01M HCl solution and it was titrated against NaOH. The change in conductivity was measured by a conductivity meter. The titration curve showed three different regions. First, the negative slope region due to the titration with NaOH by strong acid HCl (V_1) which was in excess. Subsequently, the conductivity did not change due to the titration carboxylic groups of NCC-COOH (V_2). Finally, the conductivity increased again due to the presence of excess NaOH.

Using the formula, degree of oxidation (DO) could be calculated as follows:

$$\mathrm{DO} = \frac{162(V_2 - V_1)C}{w - 14(V_2 - V_1)C}$$

where w is weight of sample in grams, C is concentration of NaOH and 162 is molecular weight of glycoside unit. This value can be expressed as mmol of COOH groups for gram of NCC.

Using the conductometric titration curve data, for 0.0249g of NCC-APS-COOH sample, V_1 and V3 were found to be 0.00931 and 0.01152, respectively. Applying these values in above formula, the degree of oxidation was found to be 0.146, which was equivalent to 0.09 mmol COOH per g NCC.

Due to the fairly low value of degree of oxidation achieved as compared to literature value, other oxidation procedures for introduction of carboxyl group on surface of nanocellulose were explored.

5.7 TEMPO mediated oxidation of nanocellulose (NCC-COOH)

A survey of the literature convinced us that the oxidation of cellulose nanocrystals to form carboxylic groups on the surface of the particles is a robust methodology of functionalization.

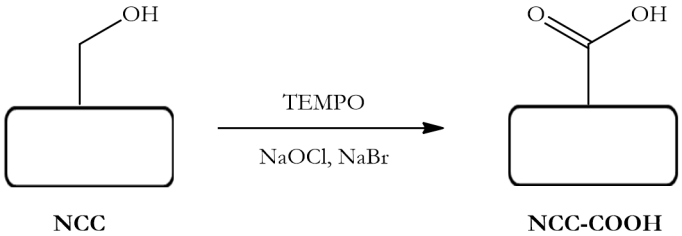

Scheme 3.42: Synthesis of TEMPO mediated oxidation of nanocellulose (NCC-COOH)

The oxidation of nanocellulose using TEMPO was carried out according the procedure described by Dufresne and co-workers (Scheme 3.42).[45] The mechanism for the TEMPO mediated oxidation of primary hydroxyl groups on NCC to the corresponding carboxylic groups is the follow (Scheme 3.43):

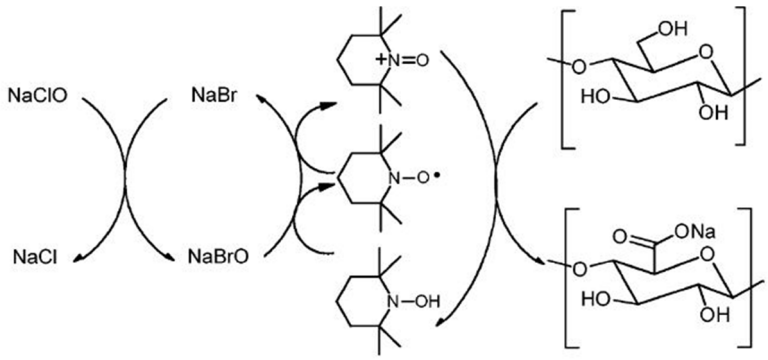

Scheme 3.43: Mechanism of TEMPO mediated oxidation

By this method, the nanocellulose was treated with an aqueous solution containing TEMPO, sodium hypochlorite, and sodium bromide. The pH was adjusted to 10 using 1M NaOH solution and the suspension was stirred at room temperature for 3 hours. The oxidation of cellulose was quenched by the addition of ethanol. Finally, the pH was neutralized with 0.5 M HCl solution. The solid was collected by centrifugation at 13000 rpm for 10 minutes and then washed by 3 cycles of suspension/sonication/centrifugation in water. The final product was recovered by lyophilization and characterized as follows.

The Infra-red spectrometry was used to analyse the NCC-COOH sample in KBr. In the spectrum two carboxyl group peaks were detected, namely the stretching C=O at 1730 cm^{-1} and the stretching of carboxylate anion at 1616 cm^{-1}. These results confirmed the presence of carboxyl group in the sample.

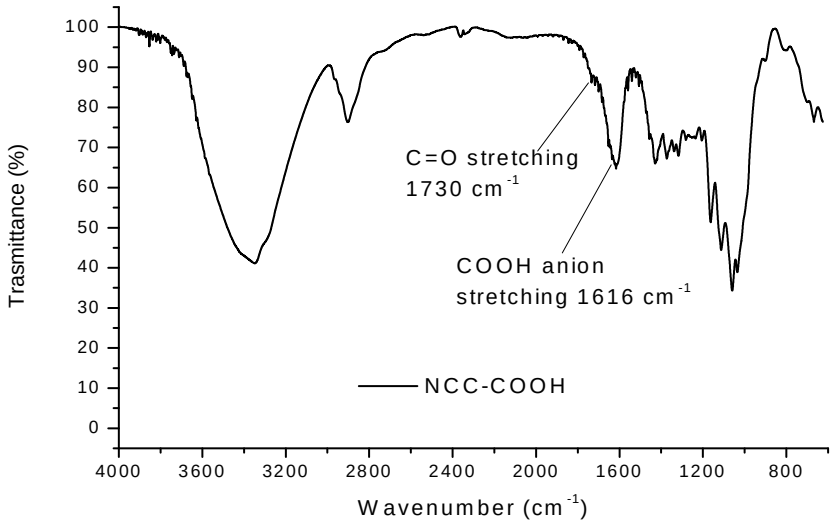

Figure 3.51: Infra-red spectrum of NCC-COOH

A suspension of NCC-COOH in water (0.53 mg/mL) was used for TEM analysis. The image (Figure 3.52) obtained shows the morphology of NCC whiskers, which allowed us to conclude that chemical modification of NCC with TEMPO did not affect the morphology of the nanocrystals.

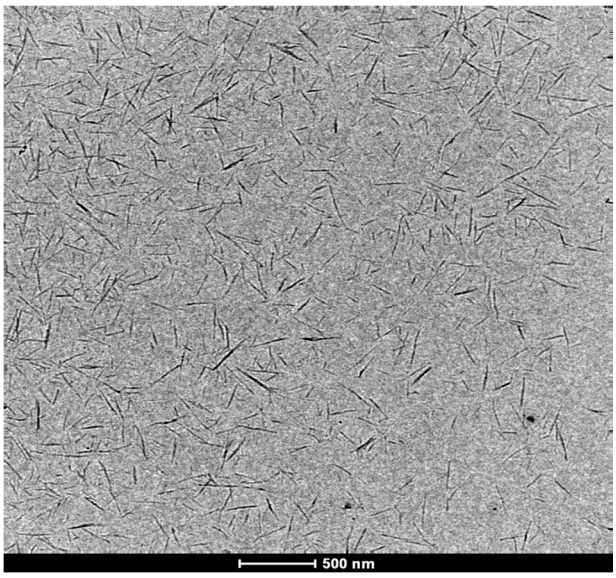

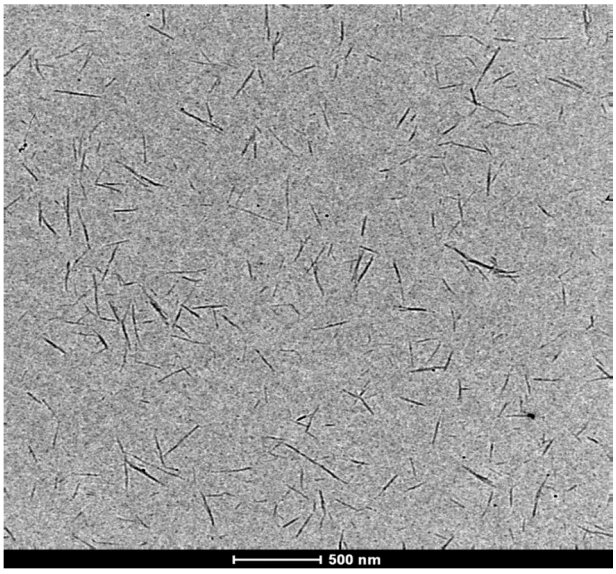

Figure 3.52: TEM images of NCC-COOH

A series of random 150 measurements were performed on the TEM image. The arithmetic mean of these measurements provided an average value of 159 ± 50 nm, similar to the average value obtained for the sample of NCC.

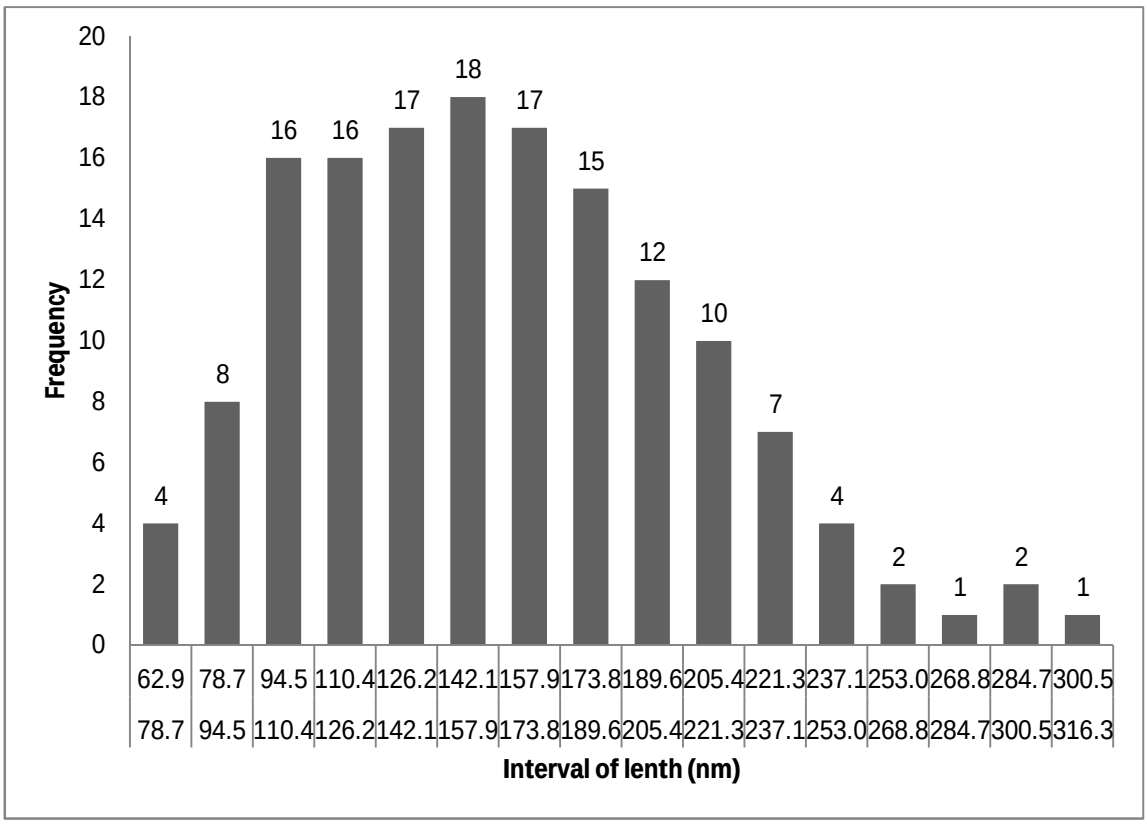

Figure 3.53: Histogram of length for NCC-COOH

A suspension of NCC-COOH in water (0.54 mg/mL) gave a z-potential of -33 ±1 mV. This potential originated only from the carboxylic acid groups since the basic conditions of synthesis of NCC-COOH led to hydrolysis of sulfonated esters. The corresponding DLS measurement provides an average diameter of 125.3±8.0 nm, which was larger in comparison to the corresponding sample of NCC. This also confirmed that NCC still maintains the nano sized dimensions.

The thermogram of NCC-COOH sample (Figure 3.54) showed a slight decrease in thermal stability with respect to NCC, since the starting temperature of decomposition for NCC-COOH is 225 °C, to compare with that of NCC which is around 250 °C. In addition, the thermogram does not reach the 0% value, which is likely due to the formation of oxides (for example "NaO" from the sodium salt of the carboxylic group) or from impurities in the sample.

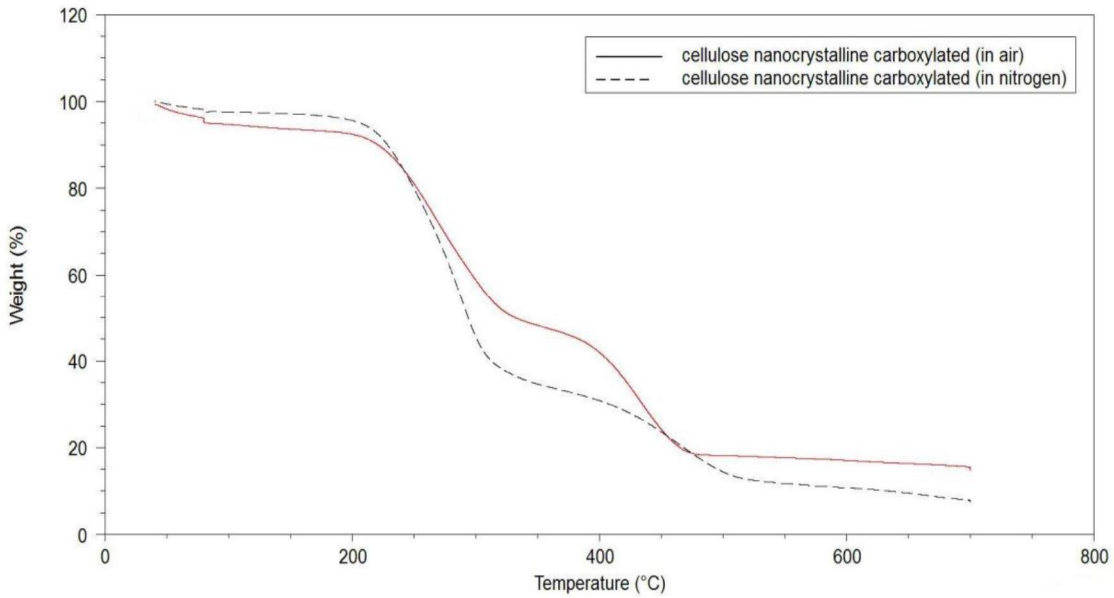

Figure 3.54: TGA of NCC-COOH

In order to estimate the carboxylate content in the sample, a conductometric titration with sodium hydroxide was carried out.

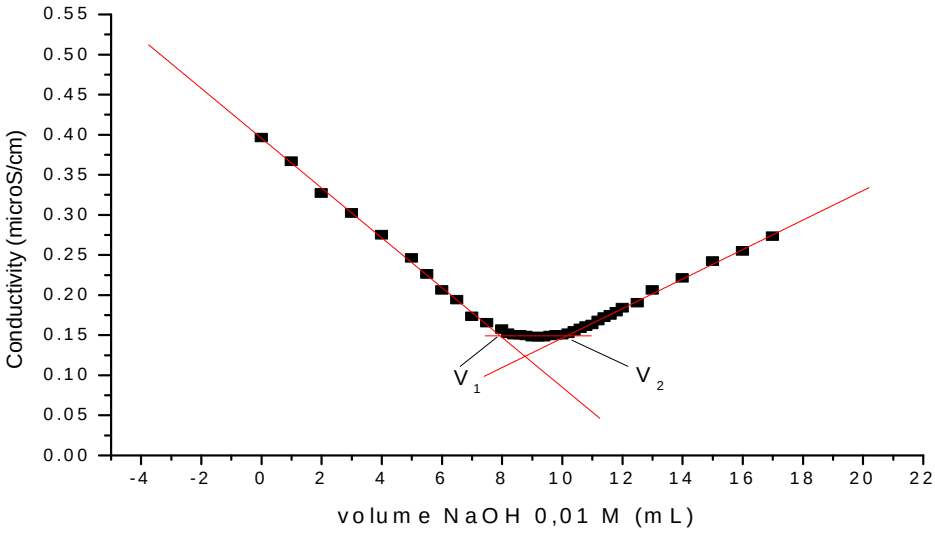

Figure 3.55: Conductometric titration of NCC-COOH

To this purpose a known amount of NCC-COOH (0.027 g) was mixed with a known volume of 0.01M HCl (10 mL) solution and it was titrated with NaOH solution. The change in conductivity of solution was measured by a conductivity-meter. The titration curve showed three different slopes. First a negative slope was observed due to the titration by NaOH with an excess HCl (V_1 =0.007954). Subsequently, the horizontal tract of the titration curve was due to the titration of the weak acid (i.e. COOH from NCC-COOH) (V_2= 0.0101491). Lastly, the conductivity increased again due to the presence of excess NaOH. Using the formula, degree of oxidation (DO) can be calculated

$$\mathrm{DO} = \frac{162(V_2 - V_1)C}{w - 14(V_2 - V_1)C}$$

where w is weight of sample in grams, C is concentration of NaOH and 162 is molecular weight of glycoside unit. The value can be expressed as mmol of COOH groups for gram of NCC. The degree of oxidation was found to be 0.13, which corresponds to 0.82 mmol COOH per g NCC, which is in accordance with literature values.

Out of various chemical modifications carried out on NCC, the TEMPO mediated carboxylation for introduction of carboxyl group on NCC was proved to be easy, convenient and even resulted in high degree of functionalization. Hence, this modification was further explored in order to achieve different hybrid materials of NCC.

6. Nanocrystalline cellulose-Porphyrin Hybrid

After having decided to move forward with carboxylate nanocellulose and with the knowledge that to date only two studies[46,47] have been reported that describe covalent linkage of porphyrin derivative onto a NCC scaffold and its use in light promoted inactivation of bacteria, we decided to investigate attachments of water-soluble amino tetraphenyl porphyrin onto carboxylate NCC using carbodiimide chemistry.

Our choice of using a water-soluble amino tetra phenyl porphyrin was due to the fact that carbodiimide chemistry works well in aqueous medium. In order to achieve this, first the synthesis of water-soluble amino porphyrin will be discussed.

6.1 Synthesis of 5-(4-Aminophenyl)-10,15,20-tris(4-sulfonatophenyl)porphyrin, trisodium salt (TPPS-NH_2)

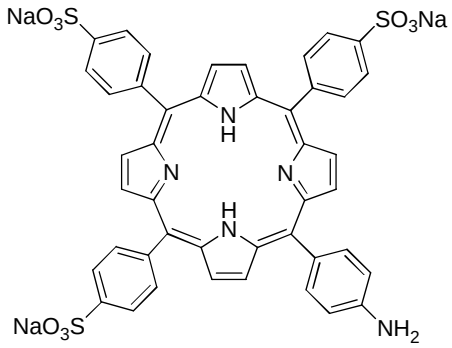

Figure 3.56: Structure of 5-(4-Aminophenyl)-10,15,20-tris(4-sulfonatophenyl)porphyrin, trisodium salt (TPPS-NH_2)

Due to the A_3B substitution pattern of the target porphyrin, first the porphyrin ring was constructed by usual Lindsey conditions to get an acetamido porphyrin derivative. Hydrolysis with concentrated hydrochloric acid results to corresponding amino porphyrin and finally sulphonation with concentrated sulphuric acids led to formation of target (TPPS-NH_2) porphyrin. The detailed synthetic approach has been discussed below.

6.1.1 Synthesis of 5-(4-acetamidophenyl)-10,15,20-triphenyl porphyrin (Ac-NH-TPP)

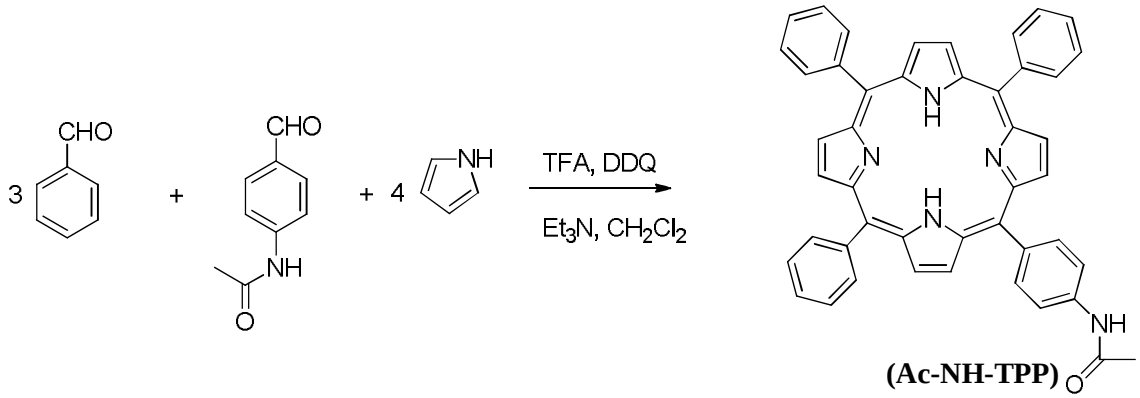

Scheme 3.44: Synthesis of 5-(4-acetamidophenyl)-10,15,20-triphenyl porphyrin (Ac-NH-TPP)

Using the usual procedure described by Lindsey and co-workers, benzaldehyde and p-acetamidobenzaldehyde were dissolved in dichloromethane.[48] The flask was purged with nitrogen for 10 minutes before adding freshly-distilled pyrrole. It was stirred for another 10 minutes, and then the reaction was initiated by the injection of TFA. The reaction was stirred at room temperature for 1.5 hours. To the reaction mixture, DDQ was added and stirred for further 1 hour at room temperature followed by neutralization with triethylamine. The crude mixture was purified with silica gel flash chromatography and elution with CH_2Cl_2 was able to remove all tetraphenyl porphyrin derivatives. Successively, the desired A_3B porphyrin was eluted with 20% EtOAc in CH_2Cl_2. The solvent was removed under vacuum, affording a purple solid of the target porphyrin. The product was analysed by ESI spectrometry, the observation of m/z 671 confirmed the formation of the acetamido porphyin.

6.1.2 Synthesis of 5-(4-aminophenyl)-10,15,20-triphenyl porphyrin (TPP-NH_2)

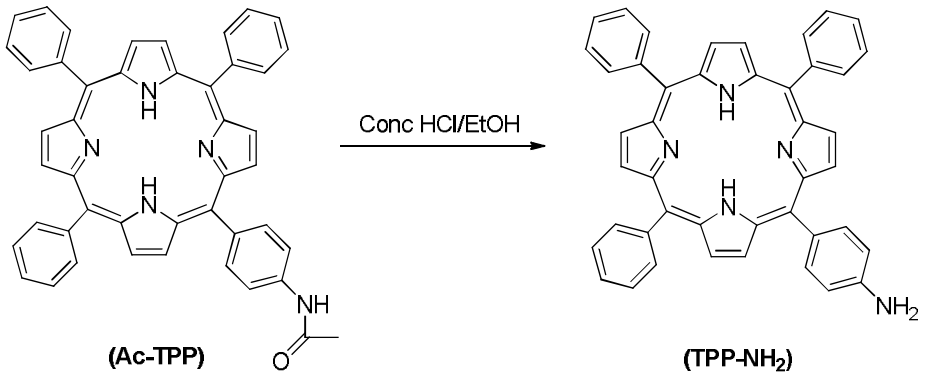

Scheme 3.45: Synthesis of 5-(4-aminophenyl)-10,15,20-triphenyl porphyrin (TPP-NH_2)

The hydrolysis of acetamido porphyrin with concentrated hydrochloric acid resulted in the formation of corresponding amino porphyrin.

A solution of p-acetamidophenyl porphyrin was prepared in ethanol. To this, concentrated HCl was added and refluxed for 17 hours. The crude mixture was diluted with water and extracted with dichloromethane. The organic layer was washed with water and then with saturated $NaHCO_3$ solution. The pooled organic layers were dried over Na_2SO_4 and the solvent was removed under vacuum. Then flash chromatography was done with dichloromethane that afforded the desired amino tetraphenyl porphyrin. The product was analysed by ESI spectrometry, the observation of m/z 629 confirmed the formation of the amino porphyrin (TPP-NH_2).

6.1.3 Synthesis of 5-(4-Aminophenyl)-10,15,20-tris(4-sulfonatophenyl)porphyrin, trisodium salt (TPPS-NH_2)

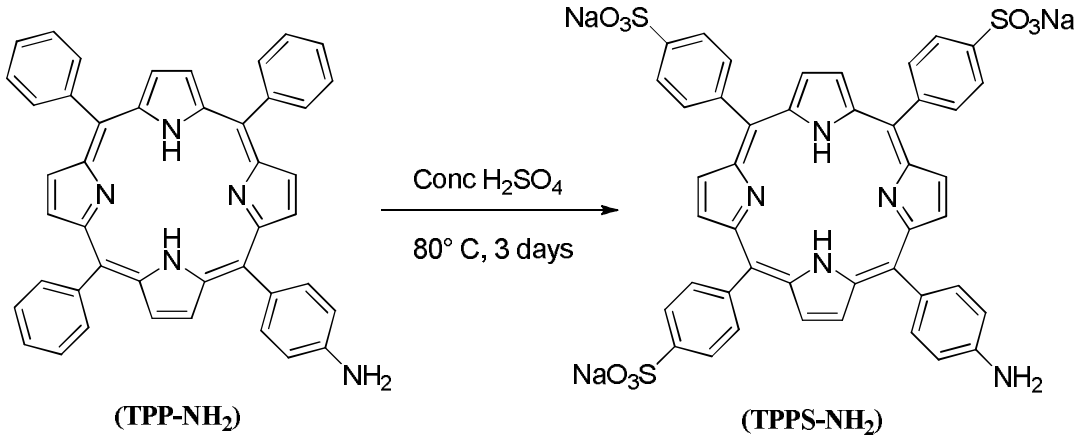

Scheme 3.46: Synthesis of 5-(4-Aminophenyl)-10,15,20-tris(4-sulfonatophenyl)porphyrin, trisodium salt (TPPS-NH_2)

The target sulphonated porphyrin could be achieved by sulphonation of amino porphyrin with concentrated sulphuric acid as described by Mahy and co-workers.[49]

Amino tetraphenyl porphyrin (TPP-NH_2) was treated with concentrated H_2SO_4 and was heated at 80°C under nitrogen atmosphere for 3 days. After cooling down to room temperature, it was poured into an ice/water mixture giving a suspension that was centrifuged four times, by replacing each time the supernatant with neutral water until pH was around 3-4. The solid residue was then dissolved in ammonium hydroxide and the solvent was removed by evaporation. The solid was dissolved in a minimum amount of

water and applied to a Na^+-activated cation exchange column. The product so obtained was lyophilized and analysed by ESI and MALDI spectrometry. The observation of m/z 869 confirmed the formation of tri-sulphonated amino porphyrin (TPPS-NH_2).

6.2 Synthesis of Porphyin-Cellulose Adduct

The conjugation of water soluble (amino trisulphonated) porphyrin to carboxylated nanocellulose *via* amidic linkage was performed using carbodiimide chemistry (Scheme 3.47) as described in literature.[50]

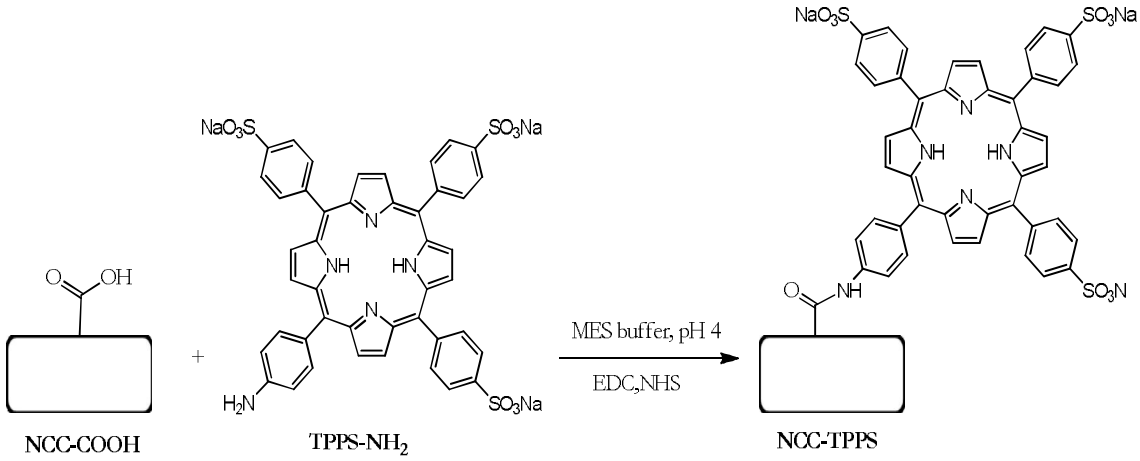

Scheme 3.47: Synthesis of Porphyin-Cellulose Adduct

Firstly, the carboxylated nanocellulose was suspended in an aqueous of solution of 2-(N-morpholino)-ethanesulfonic acid (MES, 50 mM, pH = 4) in the presence of N-(3-dimethylaminopropyl)-N'-ethylcarbodiimide hydrochloride (EDC.HCl) and N-hydroxy succinimide (NHS). To this, amino tri-sulphonated porphyrin was added and stirred at room temperature for 3 days at room temperature. Then, the NCC-TPPS adduct was recovered by ultracentrifugation at 13000 rpm and washed extensively with water, and then subjected to dialysis first against a saturated solution of NaCl (1 day) then against milli-Q water (6 days). An intensely green coloured solid was obtained after lyophilization. The product so obtained was characterized as follows.

The IR analysis of NCC-TPPS adduct in KBr does not provide useful information because it is very similar to the NCC-COOH sample. There are still clearly visible bands of the COOH groups (Figure 3.57), while no bands are seen corresponding to the amide group. This is due to the low percentage of conversion of carboxyl groups to amide derivatives.

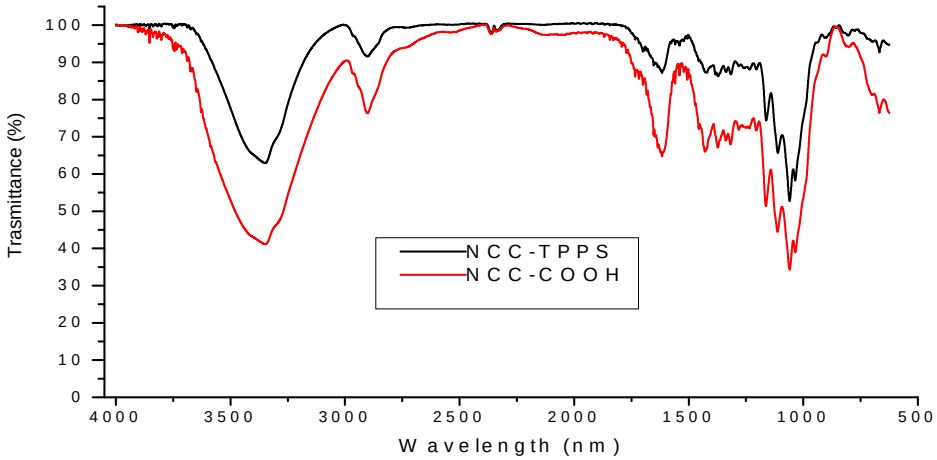

Figure 3.57: Infra-red spectrum of NCC-TPPS

The thermogram of NCC-TPPS adduct, showed a further decrease of the temperature of thermal degradation (approximately 210 °C) as compared to the starting material NCC-COOH. The thermogram of NCC-TPPS (Figure 3.58) adduct is reported in air and in nitrogen.

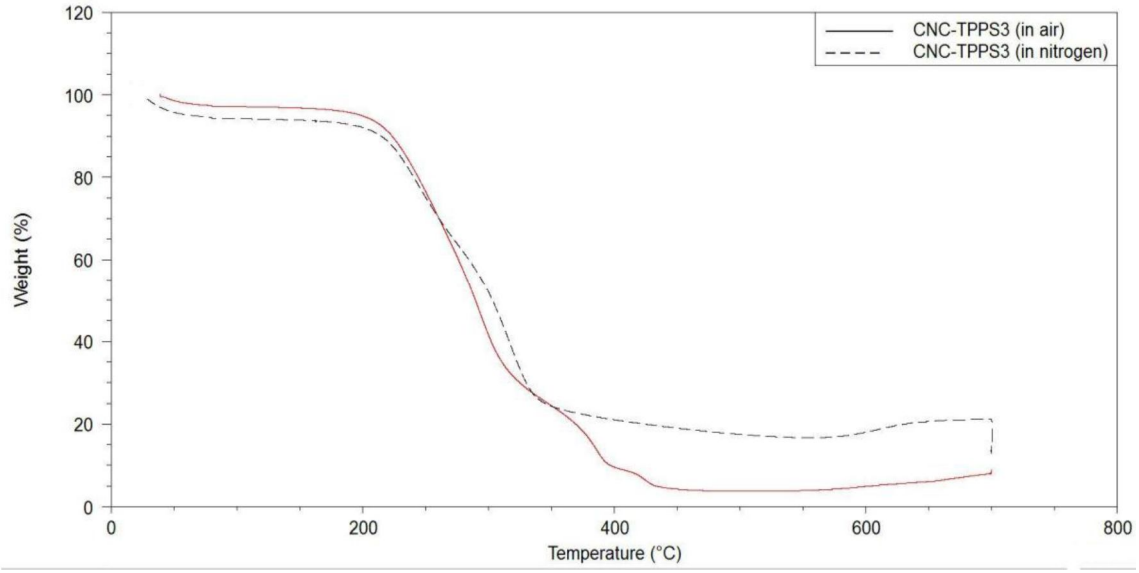

Figure 3.58: TGA of NCC-TPPS

The NCC-TPPS adduct was further analyzed by UV-visible spectroscopy wherein an aqueous suspension containing 0.25 mg /mL of NCC-TPPS was used.

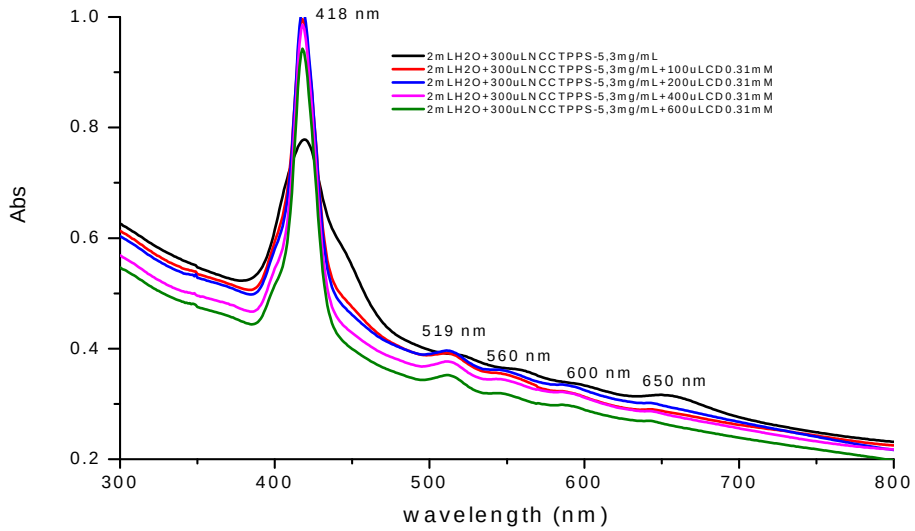

Figure 3.59: UV-visible spectra of NCC-TPPS

2,3,6-trimethyl-β-cyclodextrin (TMβCD) are known to form host guest complex with porphyrin. To this purpose, an increasing amount of TMβCD (0.31 mM) was added to NCC-TPPS suspension. The UV-Visible analysis showed two characteristic absorptions of the porphyrin macrocycle: the Soret band at 418 nm and four Q-bands at 519 nm, 560 nm, 600 nm and 650 nm. The formation of the inclusion complex with the TMβCD led to an increase in the intensity of the Soret band, inspite of the presence of the phenomenon of scattering of light radiation. It was mainly due to the fact that it was a colloidal suspension rather than a homogeneous solution.

Similarly, the fluorescence study was also made on this sample. The fluorescence spectra were recorded with an aqueous suspension containing 0.052 mg/mL of NCC-TPPS (Figure 3.60). An increasing amount of TMβCD (0.31 mM) was added to NCC-TPPS suspension, leading to a marked increase in fluorescence. This fact is consistent with the inclusion of the porphyrin in the cyclodextrin cavity.

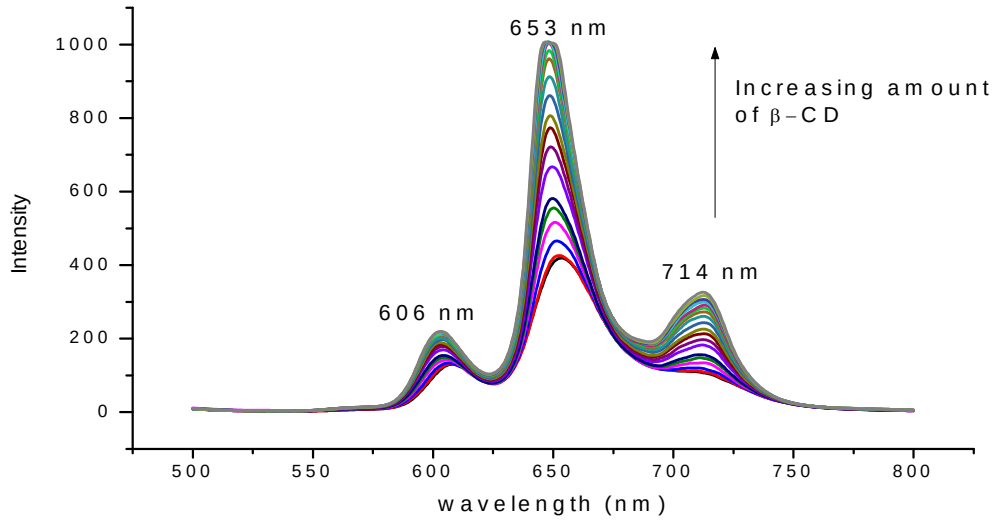

Figure 3.60: Fluorescence spectra of NCC-TPPS

In order to investigate the binding constant between host:guest complex, from the fluorescence data it was possible to construct the graph of the degree of binding θ as a function of free concentration in solution of TMβCD (Figure 3.60).

The initial fluorescence at 653 nm represented the F_0 value. The value of fluorescence F at 653 nm, was recorded after each addition of TMβCD. The addition of TMβCD was continued until a constant value (plateau) of fluorescence was observed. This value was the so-called F_∞. The degree of binding, θ was calculated according the formula:

$$\theta = \frac{F - F_0}{F_\infty - F_0}$$

Values of θ in the range 0.2-0.8 were plotted versus [TMβCD] (concentration was corrected to account for dilution) and subjected to nonlinear fitting using the typical binding isotherm for a 1:1 binding model in the form:

$$\theta = \frac{B_{max} \cdot [TM\beta CD]}{K_d + [TM\beta CD]}$$

where B_{max} is the maximum specific binding parameter and K_d is the equilibrium dissociation constant (i.e. the reciprocal of the binding constant) defined as:

$$K_d = \frac{[TM\beta CD] \cdot [NCCTPPS_3]}{[TM\beta CD - NCCTPPS_3]} = \frac{1}{K_d}$$

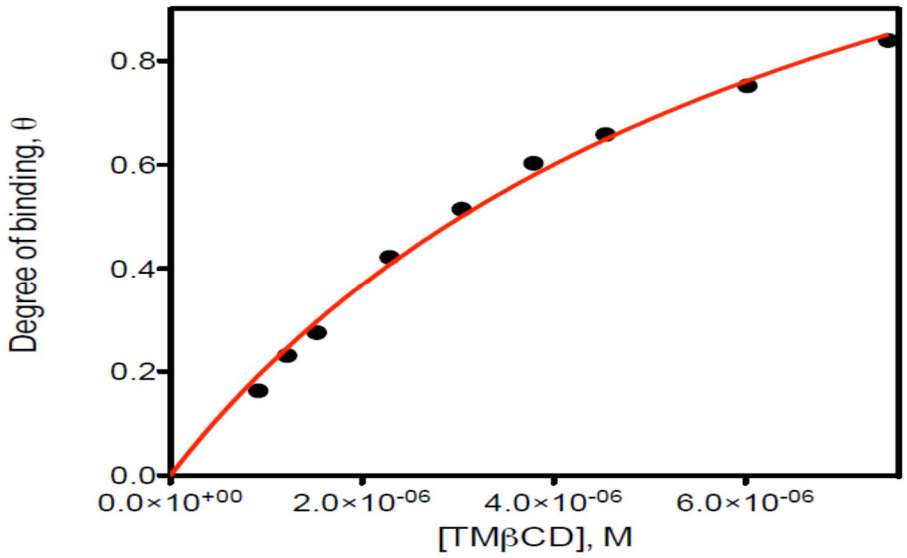

Figure 3.61: Degree of binding θ

The binding model assumes that only a small fraction of TMβCD binds to NCC-TPPS, so TMβCD at the equilibrium can be considered identical to the total concentration of TMβCD.

The titration data was analysed according to a simple 1:1 binding model in order to calculate the corresponding association constant. The non-linear fitting gave a constant value of (1.4 ± 0.2) x 10^5 M^{-1} in agreement with the values reported in the literature for similar host : guest adducts.[51,52] In addition, the fair fitting parameter (R^2 = 0.997) indicates that the 1:1 model describes an adequate binding (Figure 3.61). As a consequence, the porphyrin units can be considered sufficiently far away from each other to act independently.

The NCC-TPPS sample was analyzed by TEM analysis. The sample for the TEM images, were prepared starting from an aqueous suspension of NCC-TPPS (0.1 mg/mL).

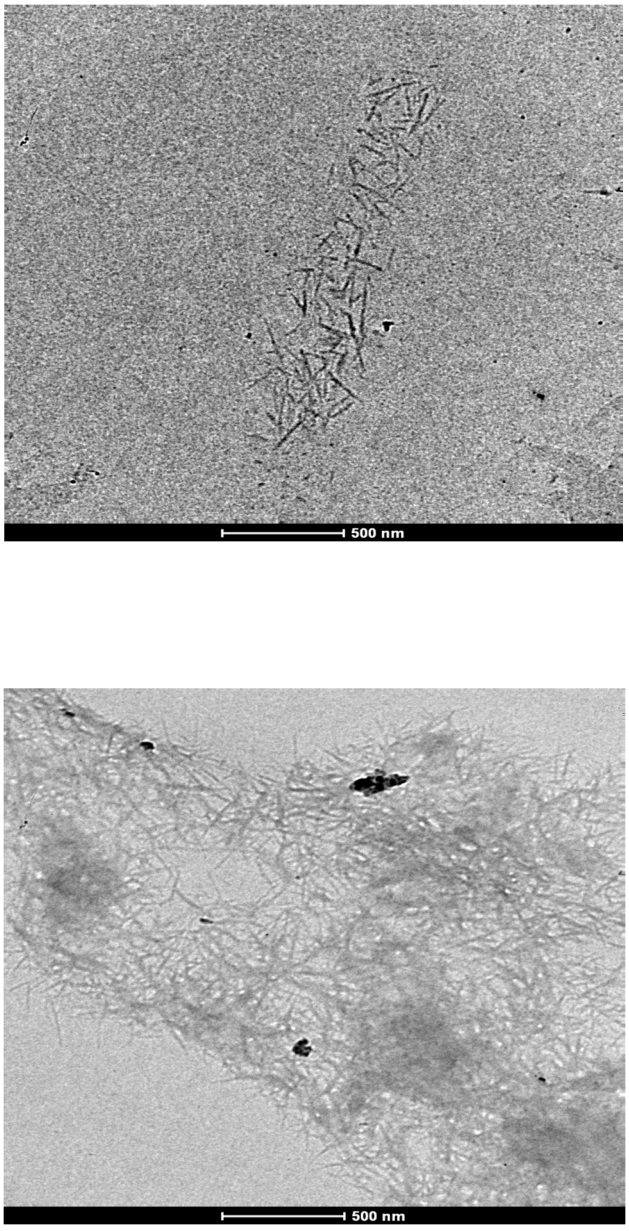

Figure 3.62: TEM images of NCC-TPPS

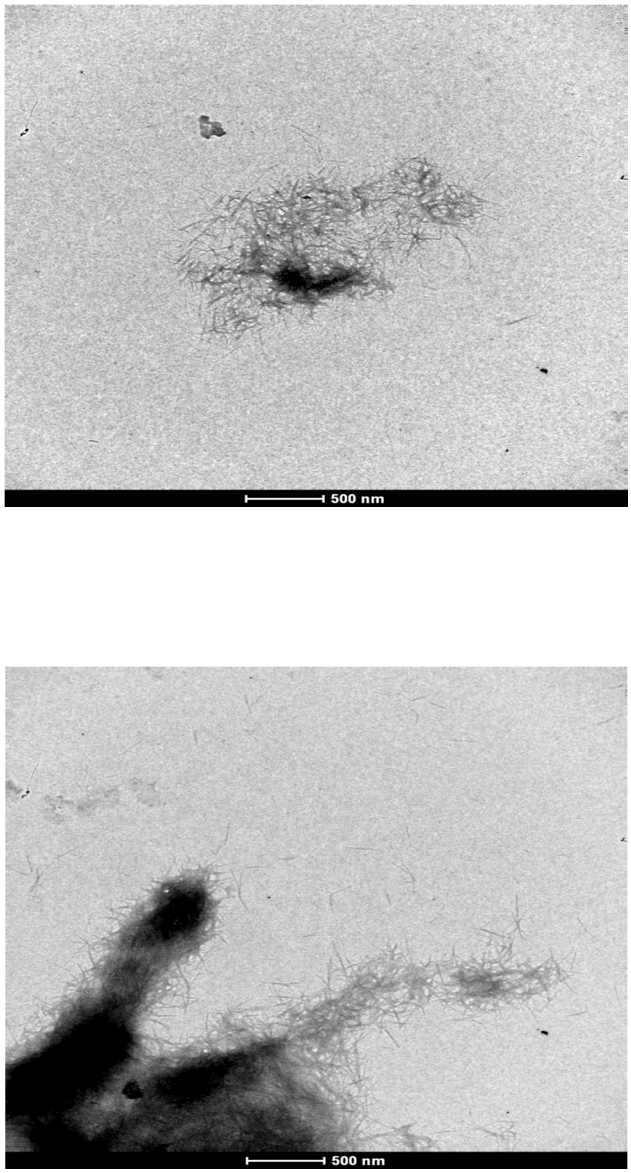

Figure 3.63: TEM images of NCC-TPPS with TMβCD

The observation made by TEM analysis, showed a certain tendency to the formation of aggregates of nanocrystals, which was not mitigated even by the presence of β cyclodextrin (150 μL, 0.31 mM). This fact has complicated the identification of a sufficient number of isolate nanocrystals for the construction of a histogram of the lengths. The aggregation of nanocrystals was observed and this phenomenon can be ascribed from porphyrin-porphyrin interaction.

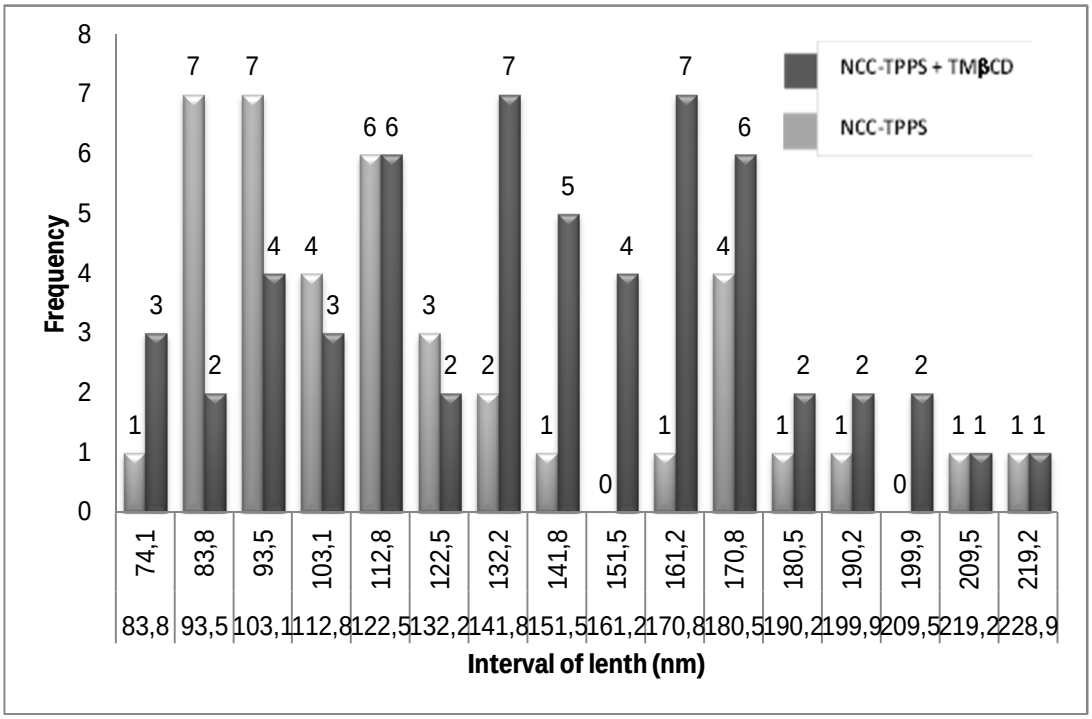

Figure 3.64: Histograms of length for NCC-TPPS

The average arithmetic mean of lengths of NCC-TPPS for 40 measurements (Figure 3.64) was found to be 144 ± 37 nm and for 57 measurements of NCC-TPPS + TMβCD for was found to be 132 ± 53 nm. The low number of measurement in histogram does not allow obtaining a Gaussian distribution and the arithmetic mean so calculated represents the whole area.

Further, the UV-Visible absorption spectrometry was used to quantify the porphyrin loading on the NCC. The procedure requires the availability of a reference porphyrin which has a molar extinction coefficient similar to that of porphyrin attached to NCC. To this purpose two porphyrin models were considered: the TPPS-NH_2 porphyrin, used for the preparation of the NCC-TPPS and the $TPPS_4$ porphyrin, a commercially available water-soluble porphyrin.

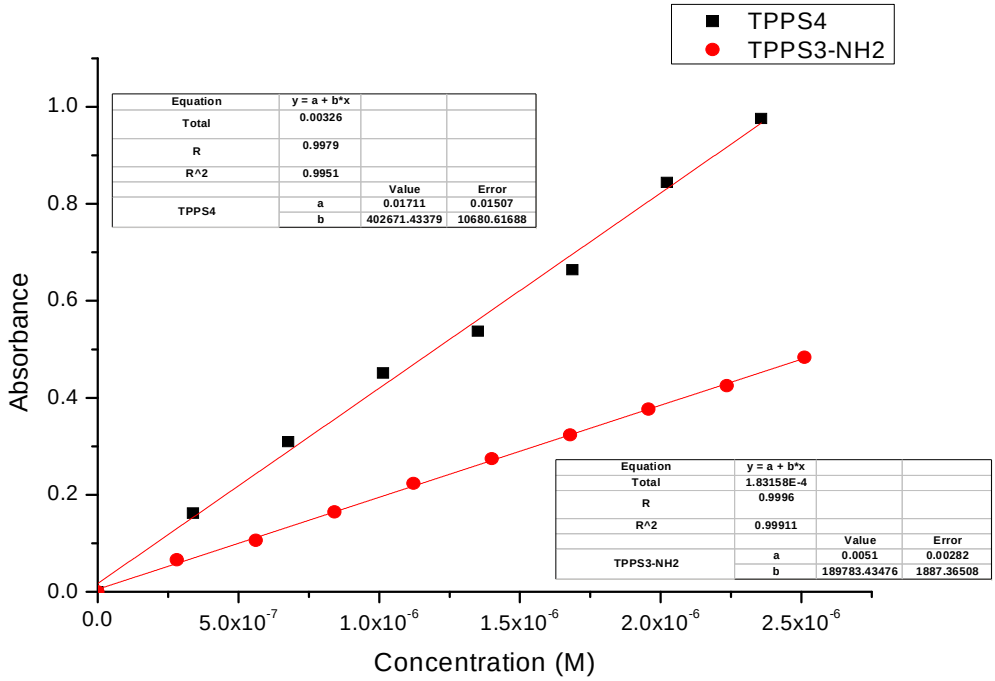

Figure 3.65: UV-visible spectra of TPPS-NH_2 and $TPPS_4$.

In Figure 3.65, two calibration lines could be observed which were obtained by plotting the absorbance at the Soret band of porphyrin in buffer solution of sodium phosphate dibasic (pH 7) with an increasing concentration. It was also evident that even the slight variations in the porphyrin structure might led to significant difference i.e. slope of the two calibration lines. Therefore, reference compound more similar to the NCC-TPPS, namely a compound TPPS-NH_2 covalently linked to a cyclodextrin could be considered as a fragment of cellulose.

Using the molar absorptivity of this compound model (ε = 190400 Soret Band) as a reference and measuring the absorbance of a suspension containing a known amount of NCC-TPPS (0.13 mg / mL), the loading of porphyrin was found to be (3.100 ± 0.015) x 10^{-3} mmol / g NCC.

The loading of porphyrin, if compared to the degree of oxidation of NCC-COOH, is the 0.38%. In other words, only 1 out of every 263 carboxyl groups has reacted with porphyrin to form an amide bond. This could be the result of esters formed between intramolecular carboxylic groups and the OH of the NCC during the reaction, favoured by the low nucleophilicity of the amino group of the aromatic porphyrin.

6.3 Synthesis of metallated Porphyin-Cellulose Adduct

The corresponding zinc metal complex of NCC-TPPS can be formed by treatment with zinc acetate.

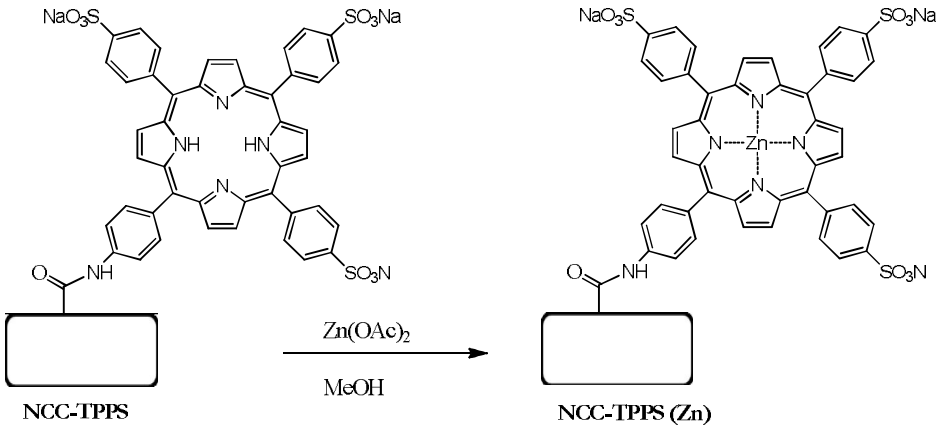

Scheme 3.48: Synthesis of metallated Porphyin-Cellulose Adduct

NCC-TPPS was suspended in methanol by sonication for 10 minutes. To this, a saturated solution of zinc acetate in methanol was added. The suspension was stirred at 30°C for 3 hours. The solid was recovered by centrifugation at 12000 rpm for 5 minutes then washed first with methanol (3 times) and then with water (2 times). The product was recovered by lyophilization thereby obtaining a dark green solid. The product so obtained was characterized as follows.

The infrared analysis NCC-TPPS (Zn) in KBr was almost similar to that of NCC-TPPS (Figure 3.66). No specific information can be determined by IR analysis

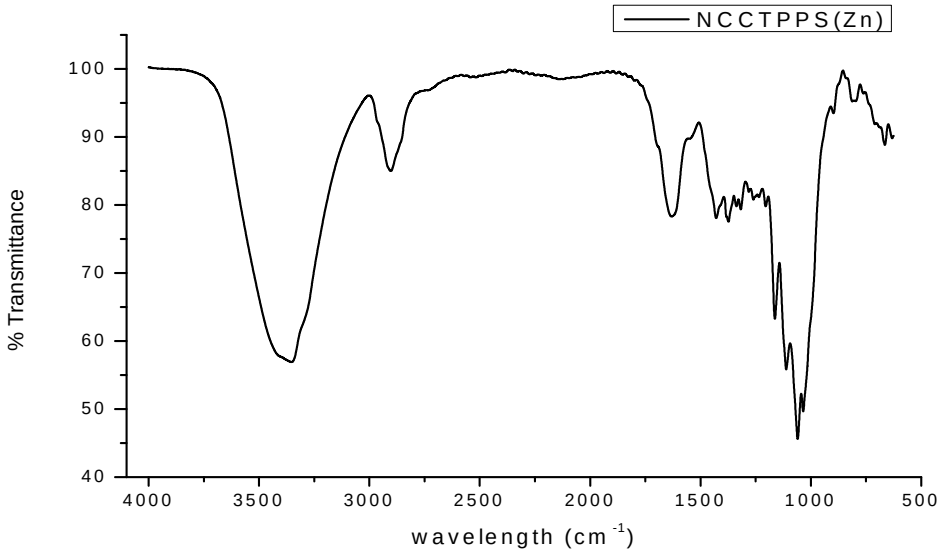

Figure 3.66: Infra-red spectrum of NCC-TPPS (Zn)

The NCC-TPPS (Zn) product was further characterized by transmission electron microscopy (TEM). The samples for the TEM analysis were prepared in an aqueous suspension of NCC-TPPS (Zn) (0.1 mg/mL).

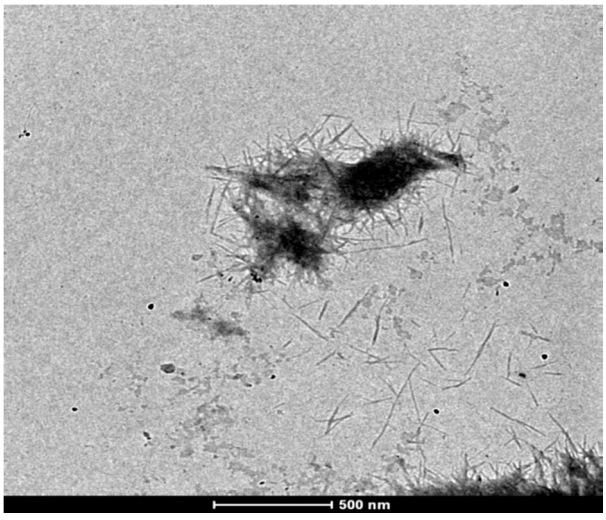

Figure 3.67: TEM image of NCC-TPPS (Zn)

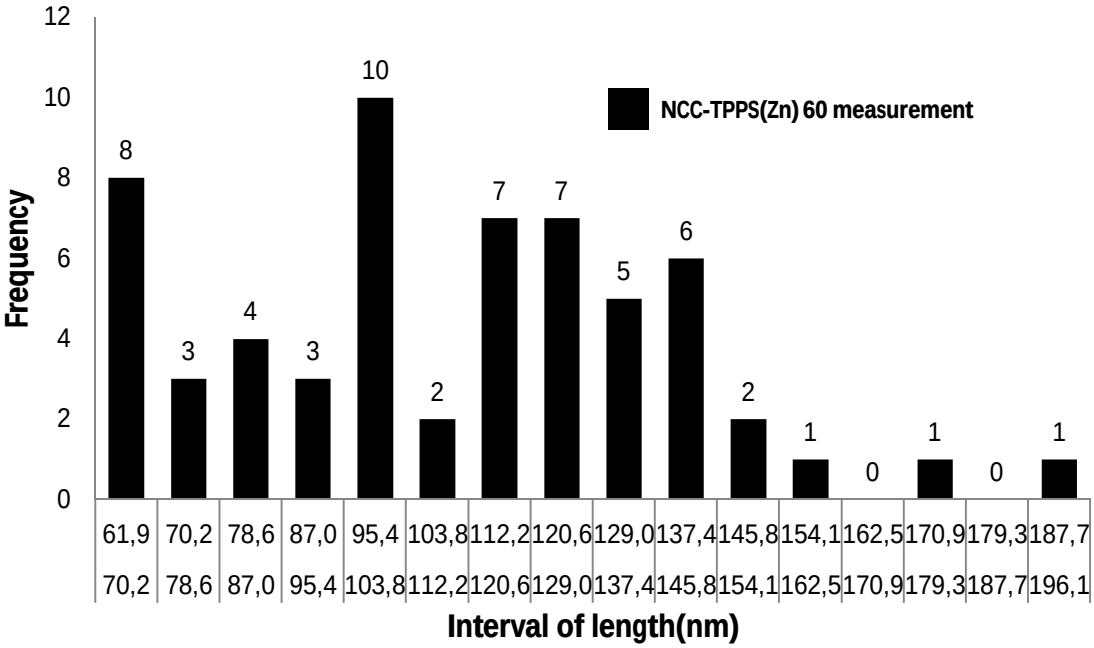

Figure 3.68: Histogram of length for NCC-TPPS (Zn)

Using random 60 measurements, the corresponding histogram was constructed (Figure 3.68), the arithmetic mean of the data gave a value of (110 ± 30) nm for NCC-TPPS (Zn). The aggregation of nanocrystals was observed and this phenomenon can be ascribed from porphyrin-porphyrin interaction. Unfortunately, due to problem in the preparation of the sample with TMβCD, it was not possible to record the images.

The NCC-TPPS (Zn) sample was further analyzed by UV visible spectroscopy.

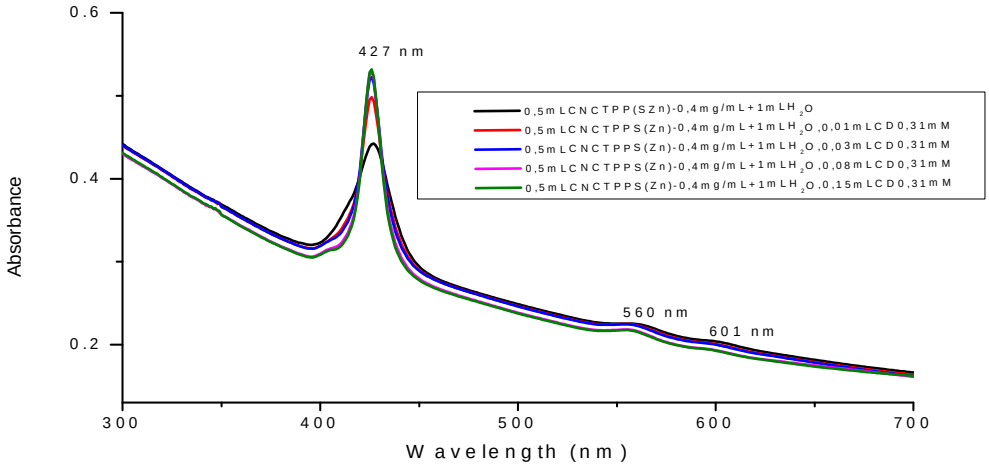

Figure 3.69: UV-visible spectra of NCC-TPPS (Zn)

The UV visible absorption spectra were recorded from an aqueous suspension of NCC-TPPS (Zn) (0.13 mg/mL). This colloidal suspension has a deeper green colour than the corresponding solution of the compound which was not metallated. The spectrum UV-Vis (Figure 3.69) shows the Soret band at 427 nm and two Q bands at 560 nm and 601 nm respectively. The addition of TMβCD to the NCC-TPPS (Zn) suspension produces the same effects as described above in the case of non metallated counterpart.

The fluorescence spectra (Figure 3.70) show two bands, one at 602 nm and the other at 652 nm wherein the latter corresponds to the Q-band. It is not clear attribution of the band at 602 nm. As expected, the relationship between the integral of the intensity of fluorescence of the hybrid NCC-TPPS and the corresponding integral for the hybrid NCC-TPPS (Zn), in the range 550-800 nm at the same concentration, it was found that fluorescence of the non-metallated hybrid in water is 6.7 times greater than that of the metallated adduct.

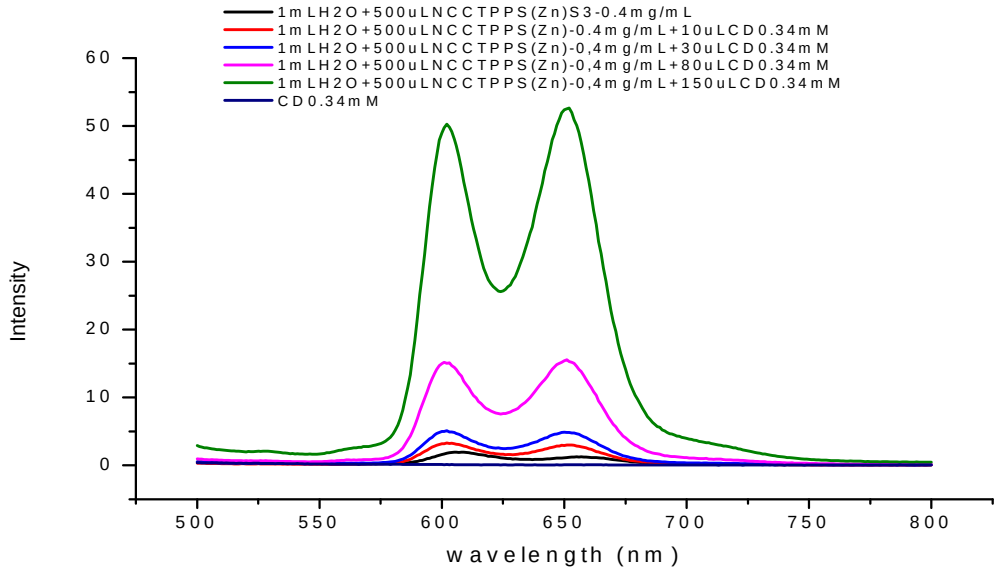

Figure 3.70: Fluorescence spectra of NCC-TPPS (Zn)

The NCC-TPPS (Zn) was further analyzed by XPS analysis (Figure 3.71). The signals for nitrogen, sulphur and zinc are present, together with the oxygen and carbon signals which belong both to NCC and porphyrin ring. This result should be considered only qualitatively since the escape depth for XPS experiment is typically many times the thickness of a single nanocrystal, so the analysis is not true for the nanocrystal surface. Nevertheless, it should be reasonable to compare Zn (1.26%) and N (1.57%) since they come only from the porphyrin moiety. Thus, after considering that %N contains also the contribute from the

amide linked to NCC, it is possible to calculate a N/Zn ratio of 4.62, which was only slightly larger than the theoretical value of 4.

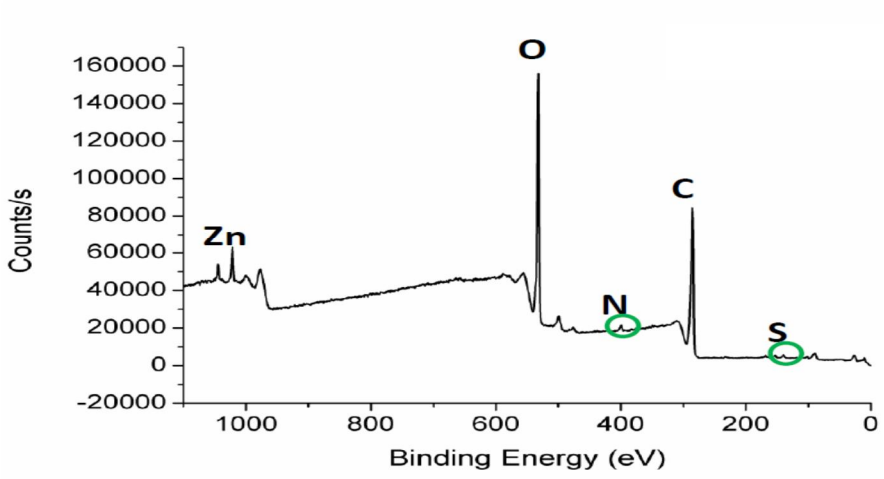

Figure 3.71: XPS spectrum of NCC-TPPS (Zn)

Delighted with successful attempt to synthesize NCC-porphyrin hybrid, we decided to investigate internal properties such as ability to generate singlet oxygen, thus discussed as follows.

6.4 Determination of Singlet Oxygen

The ability of NCC-TPPS adduct for generation of singlet oxygen was verified through two chemical methods:

6.4.1 Photo oxidation of L-methionine methyl ester

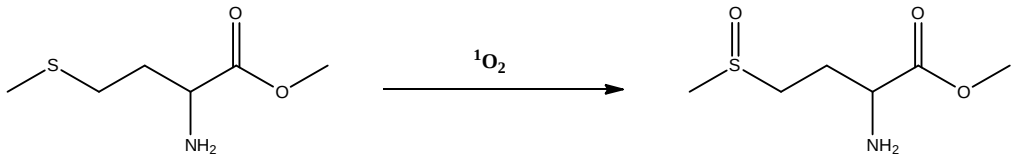

Scheme 3.49: Photo oxidation of L-methionine methyl ester

NCC-TPPS (1.5 mg) was suspended in D_2O (1.5 mL), sonicated to obtain a stable suspension followed by addition of the L-methionine methyl ester (54 mg). The suspension was divided in two identical portions and introduced into two quartz cuvettes. In one cuvette (herein referred as "**1**") a solution of TMβCD in D_2O ($5.8x10^{-2}$mM, 153 µL) was added whereas an equal amount of D_2O (153 µL) was added to the second cuvette (herein referred as "**2**"). Both the cuvettes were capped with a septum and saturated with oxygen, then they are exposed for 75 minutes to a 500 W Xe-Hg lamp through a filter that cuts off

wavelengths <365 nm. The suspension was then centrifuged to remove NCC-TPPS and analyzed by ^{1}H-NMR spectrometry (Figure 3.72, 3.73).

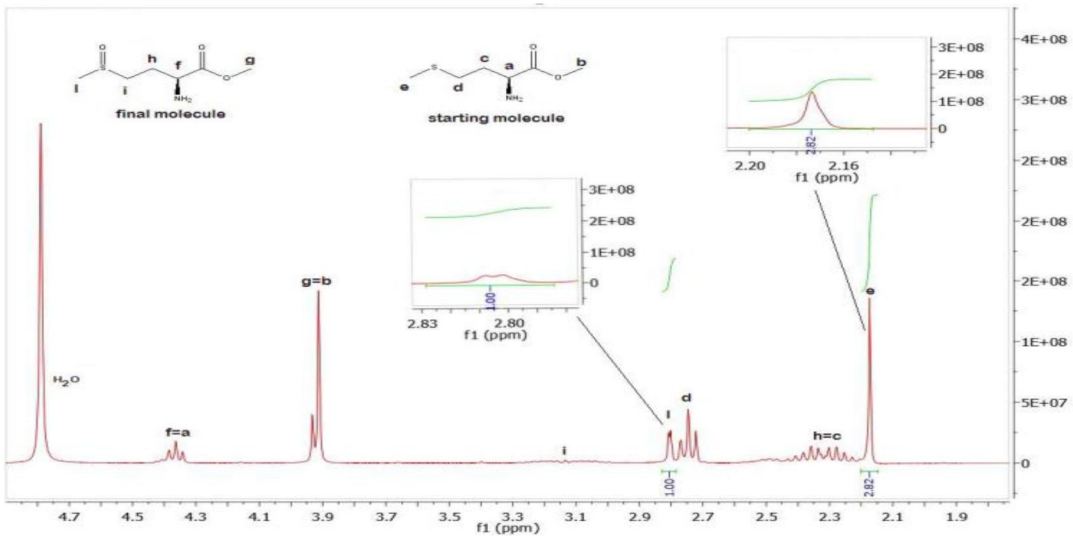

Figure 3.72: ^{1}H-NMR spectrum (D_2O) for photo oxygenation carried out in cuvette 1 (in the presence of TMβCD)

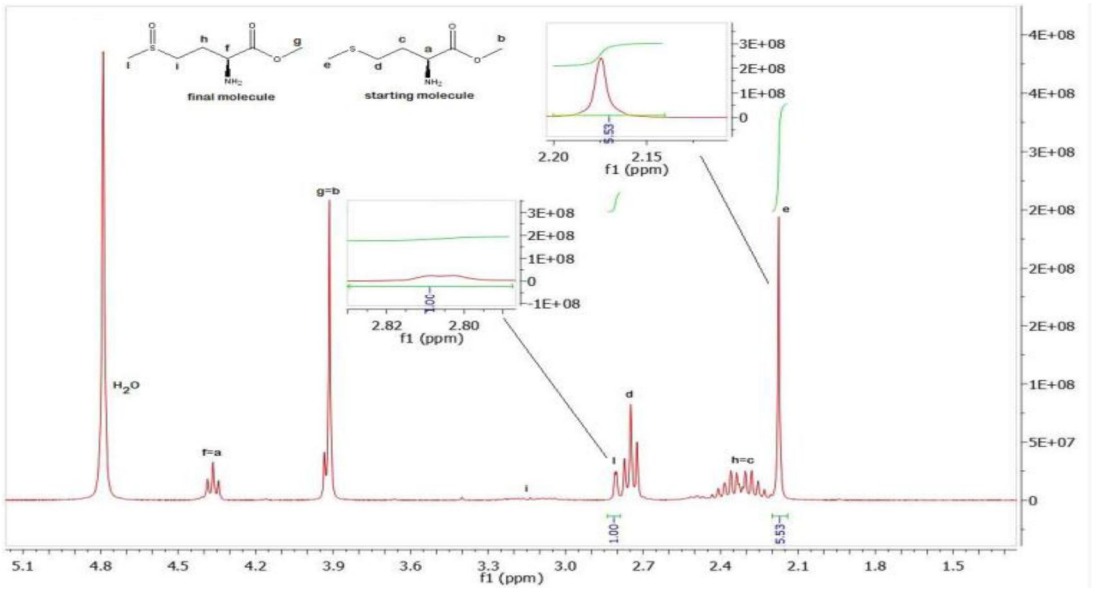

Figure 3.73: ^{1}H-NMR spectrum (D_2O) for photo oxygenation carried out in cuvette 2 (in the absence of TMβCD)

The presence of cyclodextrin does not seem to promote the photo-oxidation, indeed it seems to inhibit it. As a result the ^{1}H NMR signal of the oxidized product after 75 min. of illumination was less intense compared to the corresponding in the absence of cyclodextrin. On the other hand, the photo stability measurement of the adduct made by illuminating a suspension of NCC- TPPS, showed that the cyclodextrin inhibits the photo bleaching porphyrin.

In the absence of cyclodextrin, the corresponding sulphoxide was formed in 36% amount corresponding to 25139 turnovers, with a turnover frequency of 335 TO per min. While, in the presence of cyclodextrin gave a lower conversion (18%, 12818 Turnovers, 171 TO per min).

6.4.2 Photo oxidation of 9,10-Anthracenediyl-bis(methylene)dimalonic acid (ABDA)

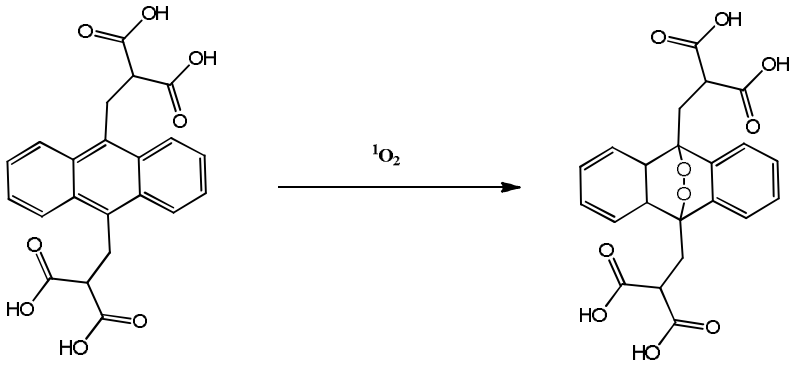

Scheme 3.50: Photo oxidation of 9,10-Anthracenediyl-bis(methylene)dimalonic acid (ABDA)

9,10-Anthracenediyl-bis(methylene)dimalonic acid, ABDA, can be used as a singlet oxygen probe due to the formation of the corresponding endoperoxide.

It was based on the principle that the singlet oxygen reacts with the ABDA forming the corresponding endoperoxide, with a corresponding decrease in absorbance at 380 nm in the UV-Vis spectrum. The experiment was conducted in two stages: during the first phase it has been verified the stability to photo-bleaching of ABDA while in the second phase photo-oxidation took place in the presence of NCC-TPPS (Zn).

To this purpose a 0.13 mM aqueous solution (in D_2O) of ABDA was mixed with phosphate buffer (0.01M, pH=7). It was saturated with oxygen then it was illuminated with a system of white LEDs (1.5 W) for interval of 2 minutes until total illumination time of 12 minutes was reached. Under these conditions the UV-Vis spectrum of ABDA was not affected (Figure 3.74).

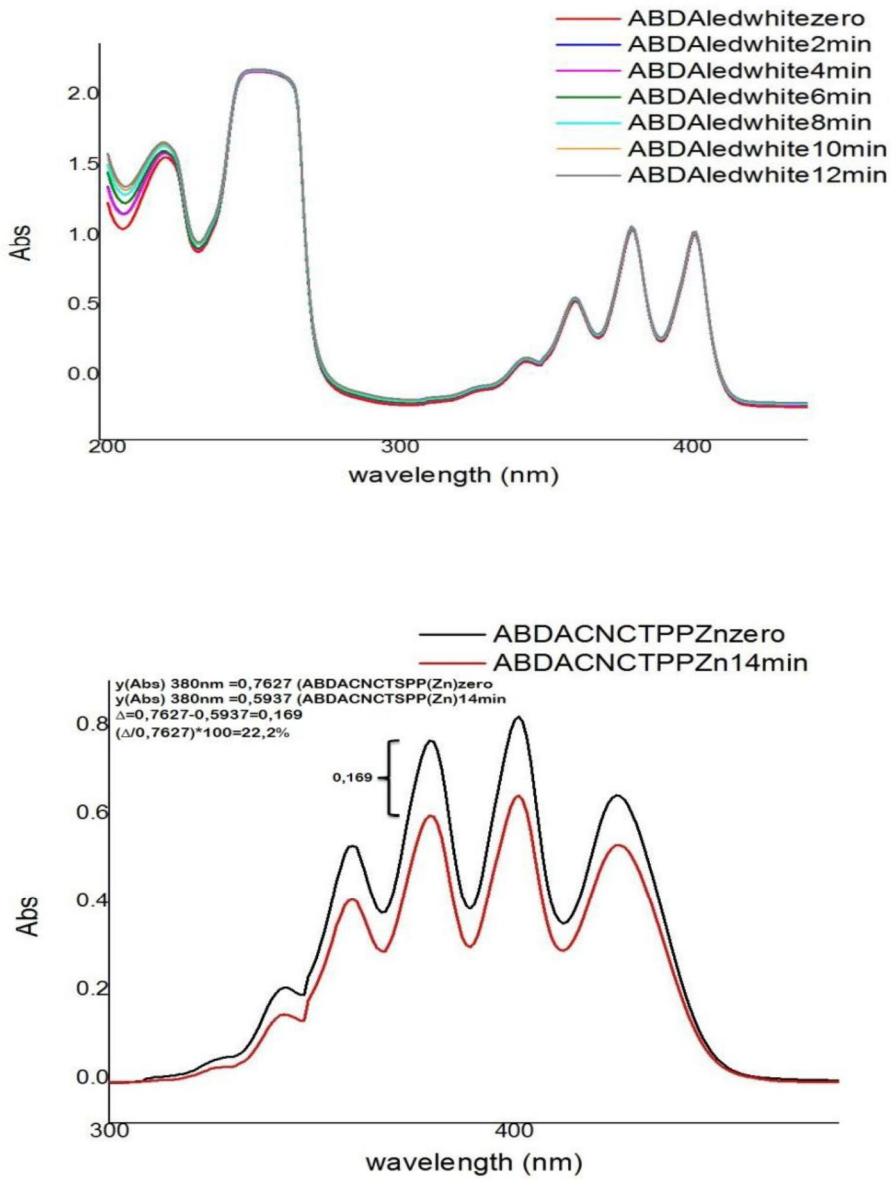

Figure 3.74: UV-visible spectra for photo oxidation of 9,10-Anthracenediyl-bis(methylene)dimalonic acid (ABDA)

On the other hand, the same experiment was carried out in the presence of NCC-TPPS (Zn) (0.5 mg) led to a 22% decrease of the ABDA spectrum thus confirming the production of singlet oxygen under illumination conditions.

Hence, the water soluble amino tri sulphonated porphyrin was covalently bind on the surface of nanocellulose *via* amidic linkage using the carbodiimide chemistry. The supramolecular interaction of porphyrin-nanocellulose with TMβCD was also studied using fluorescence spectrometry. From the application point of view this material was also demonstrated for generation of singlet oxygen in situ.

Due to the success with the synthesis of NCC-porphyrin hybrid and its application for generation of singlet oxygen, we decided to further synthesize NCC-nitrobenzene amine derivative and study its applications of NO radical release. The following will be discussed in the following section.

7. Nanocrystalline cellulose-Nitrobenzene Hybrid

In this section it will be illustrated the functionalization strategy adopted to introduce a group nitroderivative[53], on the surface of the nanocrystals of NCC-COOH. The nitroderivative, N-(3-aminopropyl)-3-(trifluoromethyl)-4-nitrobenzenamine, is a species that, under appropriate conditions of light irradiation, is capable of releasing NO radical, which can be exploited for Photo dyanamic therapy (PDT) and other therapeutic applications.[51] The synthetic methodology used to form a covalent bond between the nitro-derivative and the NCC-COOH was based again on carbodiimide chemistry with the use of EDC / NHS.

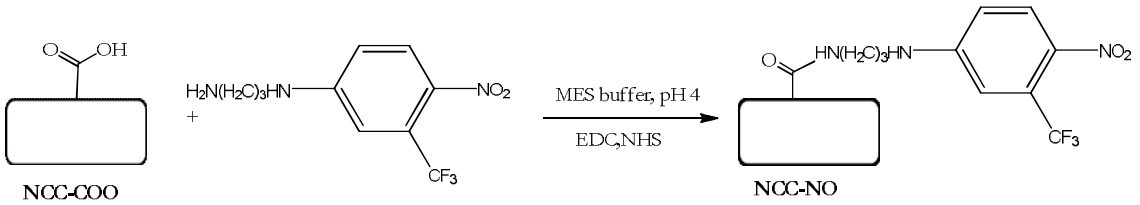

Scheme 3.51: Synthesis of NCC-Nitro adduct

Firstly, the carboxylated nanocellulose was suspended in an aqueous of solution of 2-(N-morpholino)-ethanesulfonic acid (MES, 50 mM, pH = 4) in the presence of N-(3-dimethylaminopropyl)-N'-ethylcarbodiimide hydrochloride (EDC.HCl) and N-hydroxy succinimide (NHS). To this, N-(3-aminopropyl)-3-(trifluoromethyl)-4-nitrobenzenamine was added. After four days under stirring at room temperature, the reaction mixture was washed by ultracentrifugation with MeOH and water. The solid was isolated by centrifugation at 7500 rpm for 5 minutes, resuspended in water and centrifuged again. The suspension/centrifugation step were repeated several times and finally lyophilized. After lyophilization a yellow solid was obtained and this was disperses readily in water by a brief sonication (Figure 3.75). The product so obtained was characterized as follows.

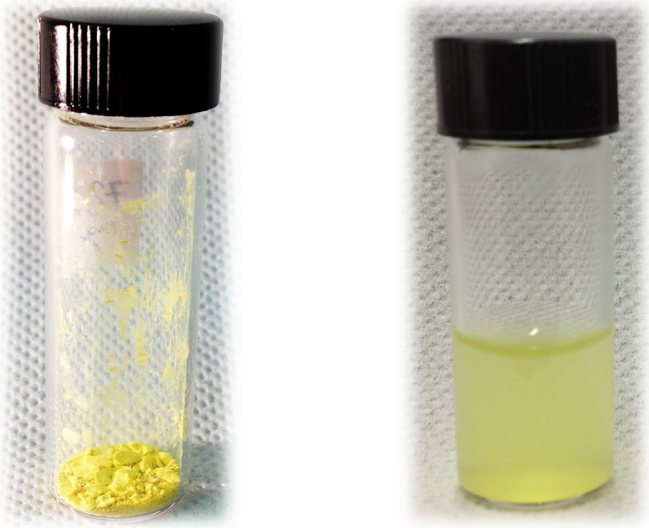

Figure 3.75: NCC-NO adduct solid and suspension

As expected, in the elemental analysis of NCC-NO the presence of nitrogen confirmed the successful chemical functionalization.

Table 3.5: Elemental analysis of NCC and NCC-NO

NCC-NO	Composition %
C	37.91
H	6.07
N	1.12
S	0.39

The product was further analysed by Infra-red spectroscopy. Unfortunately, the IR spectrum (Figure 3.76) was dominated by that of the NCC, so the diagnostic absorptions of the nitro group at 1550 cm^{-1} and 1250 cm^{-1} were virtually invisible.

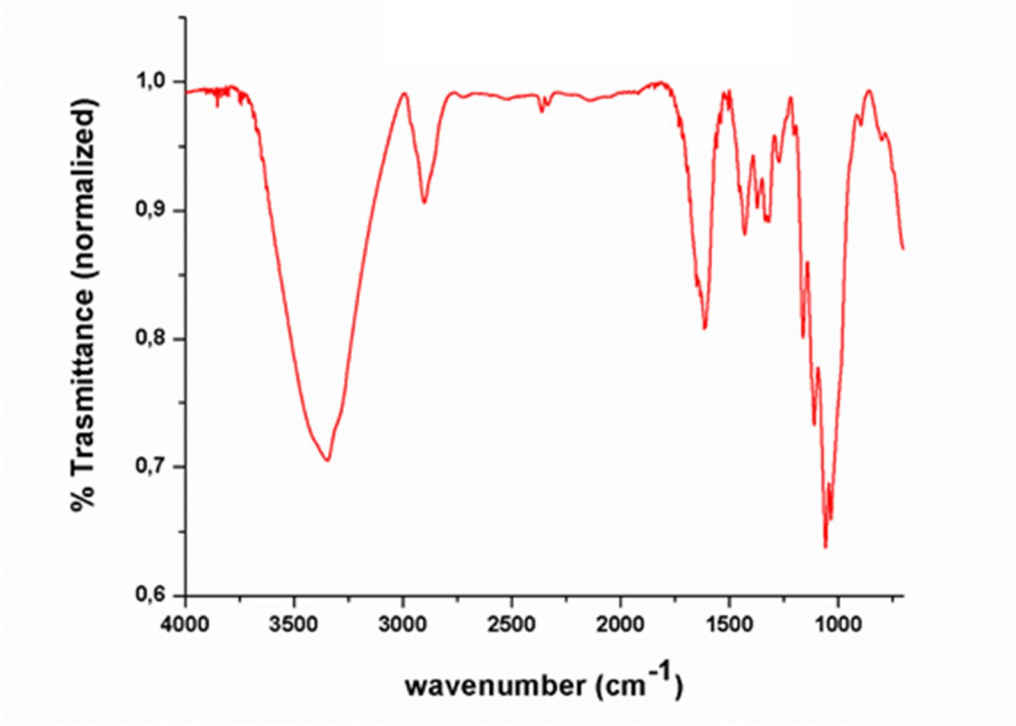

Figure 3.76: Infra-red spectrum of NCC-NO

The thermogravimetric analysis (Figure 3.77) does not show significant difference as compared to the pristine material.

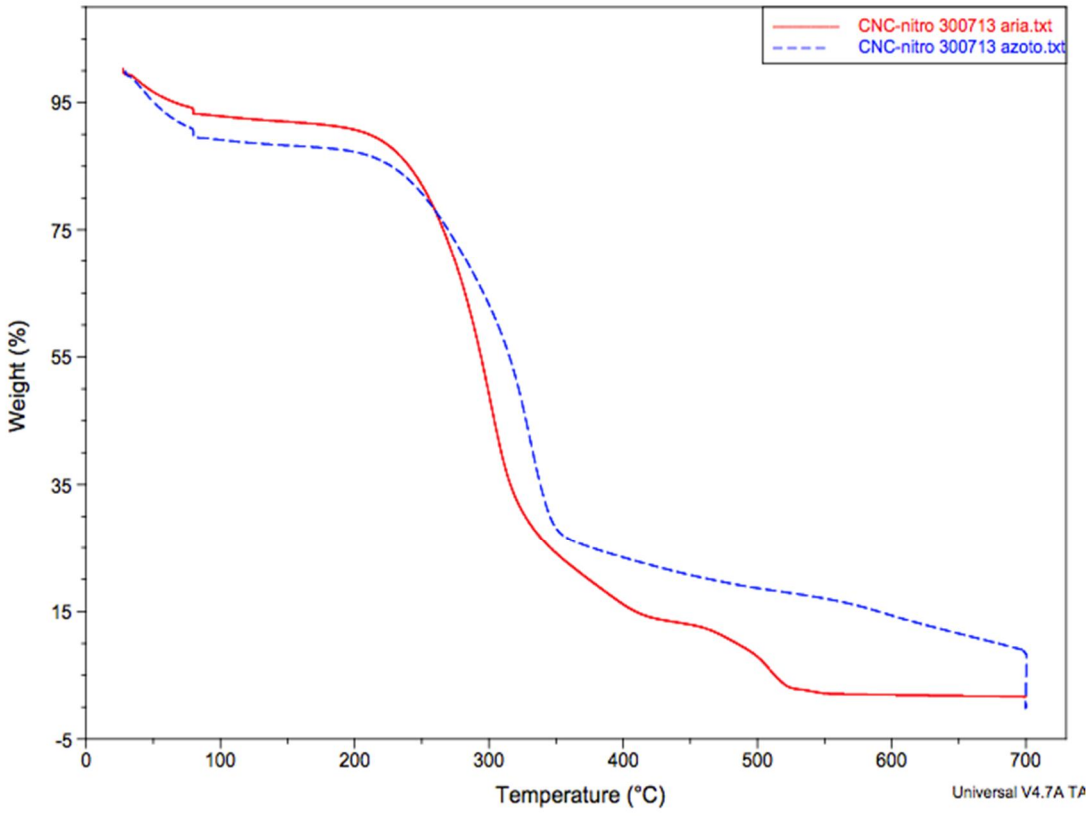

Figure 3.77: TGA of NCC-NO

The DLS studies of NCC-NO material provided an average dimension value of 211±19 nm. The z-potential studies provided a value of -25.2±0.7 mV. This value was lower than that of obtained for NCC-COOH and it can be interpreted as some of carboxylic group has been neutralized by functionalization.

This sample was analysed by Atomic force microscopy (AFM) and following images were obtained as shown in Figure 3.78.

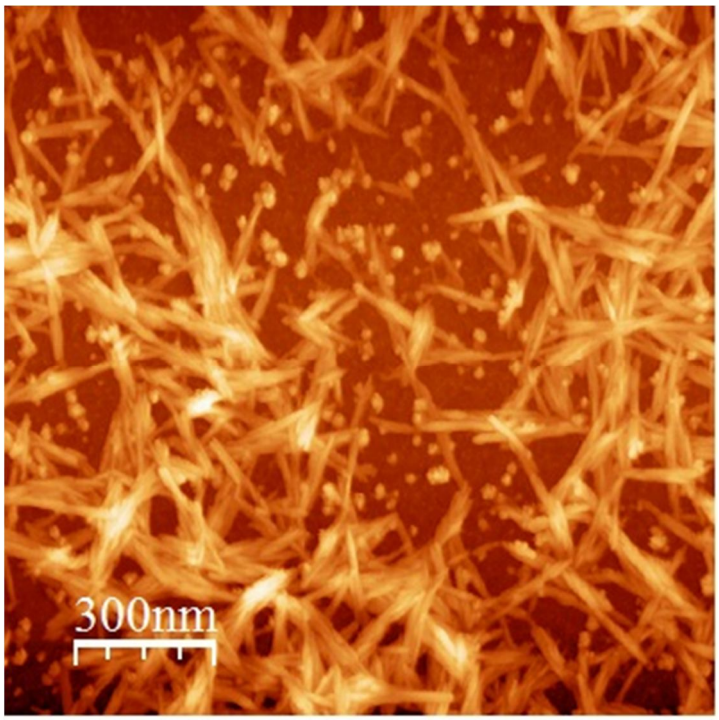

Figure 3.78: AFM image of NCC-NO

The AFM images of NCC-NO shows that nanofibrils tends to increase their diameter by joining each, which does not happen for NCC-COOH. From these images random 70 length measurements were taken into account and its corresponding histogram provided an arithmetic mean of 219±61 nm.

UV-vis spectroscopic analysis of the compound was able to confirm the presence of the nitroderivative group bound on the surface of the NCC-COOH, as it presents a characteristic band at 398 nm.

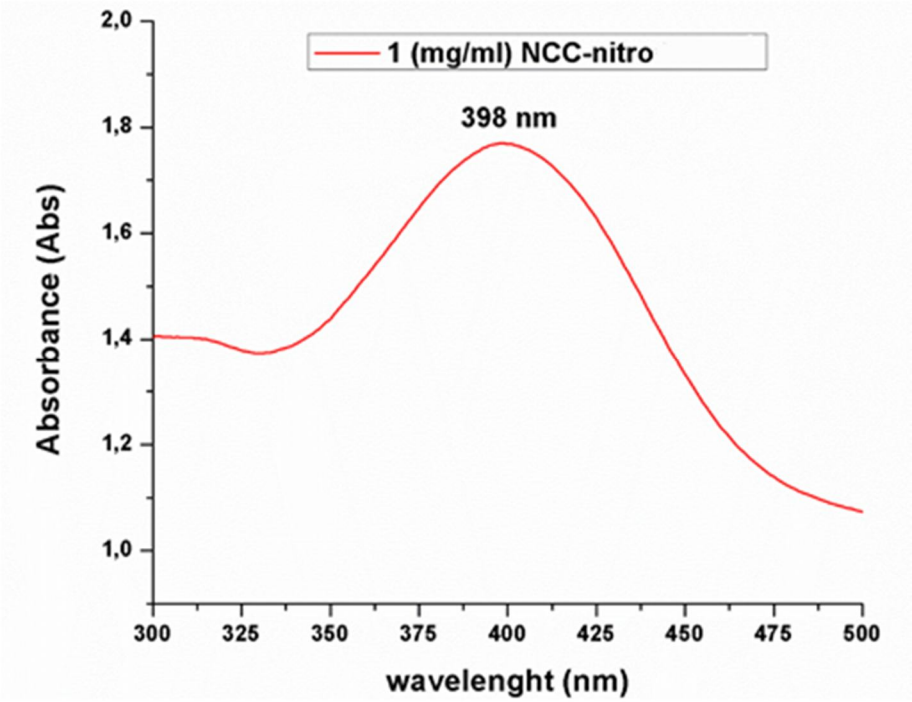

Figure 3.79: UV-visible spectrum of NCC-NO

To check if the NCC-NO derivative is able to release the NO radical species under the same conditions of illumination that were previously used for the generation of singlet oxygen in NCC-porphyrin hybrid, the following experiment was performed.

In reduced volume quartz cuvette it was placed an aqueous suspension of NCC-NO derivative. The cuvette containing the suspension was irradiated, behind a high pass filter to cut off the ultraviolet component of the radiation, at regular intervals up to a maximum of 3.5 hours, between each interval UV-visible spectrum was recorded.

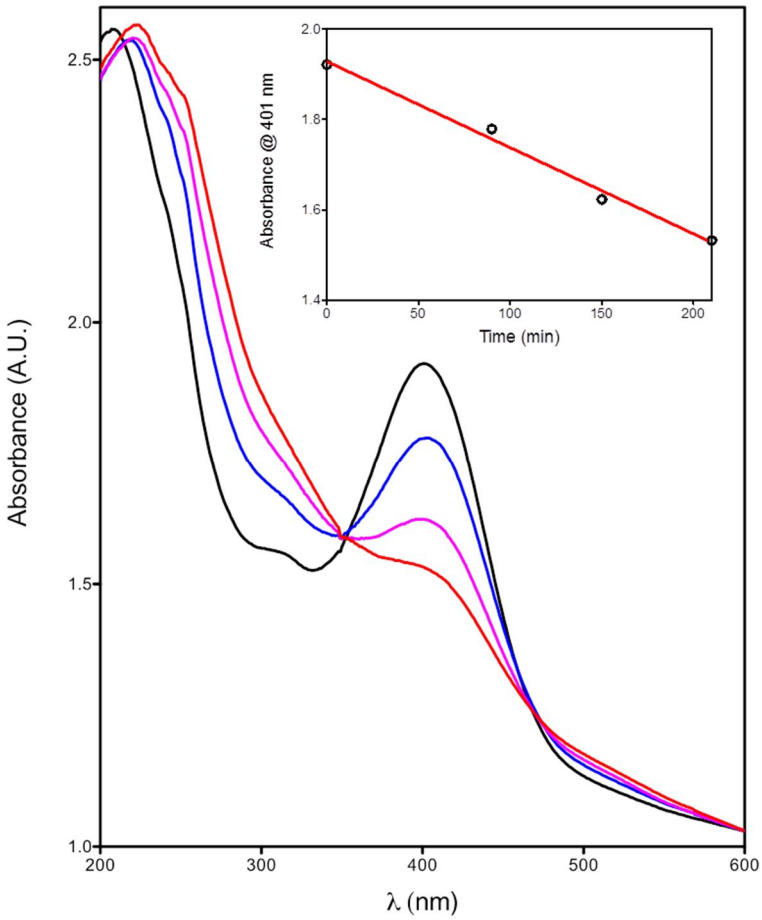

Figure 3.80: UV-visible spectra of NCC-NO at different time of illumination

As seen in Figure 3.80, the absorption band of the NCC-NO hybrid material undergoes a gradual decrease with an increasing time of illumination. In particular, after 3.5 hours it shows a 94% decrease with respect to the initial absorbance.

So, in this test, it was demonstrated that the system NCC-NO hybrid is able to release the NO radical species under illumination. This may be further used exploited for therapeutic applications as reported in the literature.[53]

REFRENCES

1. J. Rochford, D.Chu, A. Hagfeldt and E. Galoppini, *J. Am. Chem. Soc.,* **2007**, *129*, 4655-4665.
2. H. Imahori, S. Hayashi, T. Umeyama, S. Eu, A. Oguro, S. Kang, Y. Matano, T. Shishido, S. Ngamsinlapasathian and S Yoshikawa, *Langmuir*, **2006**, *22*, 11405-11411.
3. Q. Wang, W. M. Campbell, E. E. Bonfantani, K. W. Jolley, D. L. Officer, P. J. Walsh, K. Gordon, R. Humphry-Baker, M. K. Nazeeruddin and M. Gratzel, *J. Phys. Chem. B*, **2005**, *109*, 15397-15409.
4. A.D. Adler, F. R. Longo, J. D. Finarelli, J. Goldmacher, J. Assour and L. Korsakoff, *J. Org. Chem.*, **1967**, *32*, 476-477.
5. L. Barloy, D. Dolphin, D. Dupre and T. P. Wijesekerai, *J. Org. Chem.*, **1994**, *59*, 7976-7985.
6. A. Hosseini, S. Taylor, G. Accorsi, N. Armaroli, C. A. Reed and P. D. W. Boyd, *J. Am. Chem. Soc.*, **2006**, *128*, 15903.
7. S. Yagi, M. Ezoe, I. Yonekura, T. Takagishi and H. Nakazumi, *J. Am. Chem. Soc.*, **2003**, *125*, 4068.
8. Y. Kuroda, A. Kawashima, Y. Hayashi and H. Ogoshi, *J. Am. Chem. Soc.*, **1997**, *119*, 4929.
9. K. Phillips-McNaughton and J. T. Groves, *Org. Lett.*, **2003**, *5*, 1829.
10. Y. Kuramochi, A. Satake and Y. Kobuke, *J. Am. Chem. Soc.*, **2004**, *126*, 8668.
11. E. Lubian, F. Baldini, A. Giannetti, C. Trono and T. Carofiglio, *Chem. Commun.*, **2010**, *46*, 3678-3680.
12. P. Gamez and P. de Hoog, *Tetrahedron Letters*, **2002**, *43*, 6783.
13. T. Carofiglio, A. Varotto and U. Tonellato, *J. Org. Chem.*, **2004**, *69*, 8121.
14. X. Huang, B. H. Rickman, B. Borhan, N. Berova and K. Nakanishi, *J. Am. Chem. Soc.*, **1998**, *120*, 6185.
15. X. Huang, B. Borhan, B. H. Rickman, K. Nakanishi and N. Berova, *Chem. Eur. J.*, **2000**, *6*, 216.
16. T. Kurtan, N. Nesnas, Y. Q. Li, X. F. Huang, K. Nakanishi and N. Berova, *J. Am. Chem. Soc.*, **2001**, *123*, 5962.
17. G. Proni, G. Pescitelli, X. F. Huang, K. Nakanishi and N. Berova, *J. Am. Chem. Soc.*, **2003**, *125*, 12914.
18. M. Tanasova, C. Vasileiou, O. Olumolade and B. Borhan, *Chirality*, **2009**, *21*, 374.
19. V. V. Borovkov, G. A. Hembury and Y. Inoue, *Acc. Chem. Res.*, **2004**, *37*, 449.

20. A. G. Petrovic, G. Vantomme, L. Yashira, Negrón-Abril, E. Lubian, G. Saielli, I. Menegazzo, R. Cordero, G. Proni, K. Nakanishi, T. Carofiglio and N. Berova, *Chirality*, **2011**, *23*, 808-19.
21. M. A. Fazio, O. P. Lee and D. I. Schuster, *Org. Lett.*, **2008**, *21*, 4979-4982.
22. Y. Peng, H. Liu, M. Tang, L. Cai and V. Pike, *Ch. J. Chem.*, **2009**, *27*, 1339-1344.
23. H. C. Kolb, M. G. Finn and K. B. Sharpless, *Angew. Chem. Int. Ed.,* **2001**, *40*, 2004.
24. S. Punidha, J. Sinha, A. Kumar and M. Ravikanth, *J. Org. Chem.*, **2008**, *73*, 323-326.
25. M. Severac, L. Pleux, A. Scarpaci, E. Blart and F. Odobel, *Tet. Lett.*, **2007**, *48*, 6518-6522.
26. B. J. Littler, M. A. Miller, C. H. Hung, R. W. Wagner, D. F. O'Shea, P. D. Boyle and J. S. Lindsey, *J. Org. Chem.*, **1999**, *64*, 1391-1396.
27. M. J. Plater, S. Aiken and G. Bourhill, *Tetrahedron*, **2002**, *58*, 2405-2413.
28. S. L. Elmer, S. Man and S. C. Zimmerman, *Eur. J. Org. Chem.,* **2008**, 3845-3851.
29. K. Flavin, M. N. Chaur, L. Echegoyen and S. Giordani, *Org. Lett.*, **2010**, *12*, 840.
30. M. Severac, L. Pleux, A. Scarpaci, E. Blart and F. Odobel, *Tet. Lett.*, **2007**, *48*, 6518-6522.
31. G. Zhang, Y. Wang, X. Wen, C. Ding and Y. Li, *Chem. Commun.*, **2012**, *48*, 2979-2981.
32. J. X. Zhang, K. Wong, W. Wong, N. Mak, D. W. J. Kwong and H. Tam, *Org. Biomol. Chem.*, **2011**, *9*, 6004.
33. J. T. Fletcher, B. J. Bumgarner, N. D. Engels and D. A. Skoglund, *Organometallics*, **2008**, *27*, 5430–5433.
34. C. Danumah and Hicham Fenniri, *Mater. Res. Soc. Symp. Proc.*, **2001**, *1312*, 467-472.
35. R. Rusli and S. J. Eichhorn, *Appl. Phys. Lett.*, **2008**, *93*, 033111.
36. G. Siqueira, J. Bras and A. Dufresne, *Polymers*, **2010**, *2*, 728-765.
37. T. Carofiglio, C. Fregonese, G. J. Mohr, F. Rastrelli and U. Tonellato, *Tetrahedron*, **2006**, *62*, 1502-1507.
38. M. Hasani, E. D. Cranston, G. Westmana and D. G. Gray, *Soft Matter*, **2008**, *4*, 2238-2244.
39. S. Dong and M. Roman, *J. Am. Chem. Soc.*, **2007**, *129*, 13810-13811.
40. E. Kaiser, R. L. Colescott, C. D. Bossinger and P.I. Cook, *Anal. Biochem.*, **1970**, *34*, 595-598
41. M. D. Bowman, R. C. Jeske and H. E. Blackwell, *Org. Lett.*, **2004**, *6*, 2019-2022.
42. Q. Yang and X. Pan, J. Appl. Polym. Sci, **2010**, *117*, 3639-3644.

43. D. P. Kamdem, B. Riedel, A. Adnot and S. Kaliaguine, *J. Appl. Polym. Sci.*, **1991**, *43*, 1901-1912.
44. A. C. W. Leung, S. Hrapovic, E. Lam, Y. Liu, K. B. Male, K. A. Mahmoud and J. H. T. Luong, *Small*, **2011**, *7*, 302-305 .
45. N. Lin, C. Bruzzese and A. Dufresne, *ACS Appl. Mater. Interfaces*, **2012**, *4*, 4948-4959.
46. E. Feese, H. Sadeghifar, H. S. Gracz, D. S. Argyropoulos and R. A. Ghiladi, *Biomacromolecules*, **2011**, *12*, 3528-3539.
47. B. L. Carpenter, E. Feese, H. Sadeghifar, D. S. Argyropoulos and R. A. Ghiladi, *Photochem Photobiol.*, **2012**, *88*, 527-36.
48. J. S. Lindsey, P. A. Brown and D. A. Siesel, *Tetrahedron*, **1989**, *45*, 4845-4846.
49. E. Sansiaume, R. Ricoux, D. Gori and J. P. Mahy, *Tetrahedron: Asymmetry*, **2010**, *21*, 1593-1600.
50. I. Filipponen and D. S. Argyropoulos, *Biomacromolecules*, **2010**, *11*, 1060-1066.
51. T. Carofiglio, R. Fornasier, G. Gennari, V. Lucchini, L. Simonato and U. Tonellato, *Tetrahedron Lett.*, **1997**, *38*, 7919.
52. T. Carofiglio, R. Fornasier, V. Lucchini, L. Simonato and U. Tonellato, *J. Org. Chem.*, **2000**, *65*, 9013.
53. F. L. Callari and S. Sortino, *Chem. Commun.*, **2008**, 1971.

Chapter-4

CONCLUSION

Here are summarized the results achieved during this thesis in the two main projects I have been involved.

PORPHYRIN

- Several porphyrin based chromophores have been synthesized that served as references materials for an ongoing project on solar energy conversion. That has allowed to me to acquire the necessary skills for the synthesis, purification and characterization of porphyrin derivatives.
- Three different porphyrin-porphyrin dimers were prepared, based on the use of trichlorotriazine chemistry, in collaboration with Professor Nina Berova at Columbia University that is studying their use for the determination of the absolute configuration of chiral molecules by circular dichroism.
- Two porphyrin derivatives were prepared involving "click reaction" which is a 1,3-dipolar addition of an azide to a terminal alkyne. In particular, a novel triazole linked porphyrin was prepared between an azido-porphyrin and ethynylpyridine. The product was well characterized by different spectroscopic techniques and its structure was determined by x-rays analysis. Then, coordination of triazole linked porphyrin with palladium acetate and with ruthenium derivatives was studied. However, poor solubility of these metal complexes proved to be detrimental for the purification so it was decided to develop another research line based on nano crystalline cellulose.

NANO CRYSTALLINE CELLULOSE

- The successful production of nanocellulose from microcrystalline cellulose was realized through the sulphuric acid hydrolysis on microcrystalline cellulose. The NCC characterization was carried out by multiple techniques such as microscopy (TEM, SEM, AFM), elemental analysis, thermogravimetry, infrared spectroscopy, dynamic light scattering and z-potential.
- The nanocellulose is chemically modifiable exploiting the OH groups on the surface. That allowed the covalent attachment of a pH sensitive dye via vinysulfone chemistry. The NCC-dye showed marked colour variations depending upon the pH of the solution, which was also confirmed by UV visible spectroscopy. From

application point of view, this material can be used as optical sensor for check the quality of food products.

- Several strategies were employed to functionalize NCC with more versatile groups than hydroxyls. Among the various methods explored, the oxidation of the NCC to NCC-COOH through the use of TEMPO proved to be a robust and reproducible functionalization procedure, with relatively high yields and good efficacy of functionalization.
- A novel nanocellulose-porphyrin (NCC-TPPS) hybrid adduct was obtained by coupling reaction between carboxylated nanocellulose with the water soluble amino porphyrin involving carbodiimide chemistry. The adduct, both in its free form and in that metallated form, produces singlet oxygen when irradiated with a light source in the visible range.
- A nitro derivative, i.e. N-(3-aminopropyl)-3-(trifluoromethyl)-4-nitrobenzenamine was grafted on the surface of carboxylated-NCC using carbodiimide chemistry. This derivative has ability to release NO radical under illumination with a light source of visible range. By UV-visible spectroscopy, it was proved that NCC hybrid release NO radical which can be potentially used for therapeutic applications.

Chapter-5

EXPERIMENTAL

1. Materials and Reagents

Tetraphenyl porphyrin (TPP) was purchased from EGA-CHEMIE, Germany. Microcrystalline cellulose was purchased from Sigma-Aldrich with a crystallinity degree of 80%. Other reagents and solvents (Sigma-Aldrich, Fluka and Reagenti Carlo Erba) were of the highest grade available and were used without further purification. Solvents employed in the spectroscopic studies are of spectroscopic grade and used as received. Silica gel MN 60 (70-230 Mesh) by Macherey-Nagel and neutral alumina (Brockmann Grade III) were used for column chromatography. Analytical thin layer chromatography (TLC) was performed using a Polygram SilG/UV254 TLC plates with fluorescent indicator.

2. Instruments

IR analysis was carried out in KBr on a Nicolet 5700 FT-IR instrument. UV-vis and fluorescence measurements were performed on a Cary 100 Scan Varian spectrophotometer and Cary Eclipse Varian or Perkin Elmer LS55 fluorimeters, respectively. ^{1}H-NMR spectra were collected on a NMR Bruker Advance at 250, 300 or 400 MHz. Dynamic light scattering and z-potential experiments were conducted on a Malvern Instrument Zetasizer Nanoseries. Thermal analyses were performed on TgaQ5000 TA instrument (Temperature program: 10°C/min until 80 °C, maintained at 80 °C for 2 minutes then increased the temperature to 700 °C at 5 °C/min, maintained at 7 °C for 2 minutes). Centrifugations were carried out with a Thermo scientific SL16 centrifuge. TEM analysis was performed on a Tecnai G^{2} Fei - 100kV microscope and the images where analysed with the help of Image-J package for size measurements and the data were averaged and elaborated graphically with Origin 8.0 software.

3. Synthesis of Compounds

3.1 Synthesis of 5-(4-Methoxycarbonylphenyl)-10,15,20-tris(2,4,6-trimethyl phenyl) porphyrin (TPMM)[1]

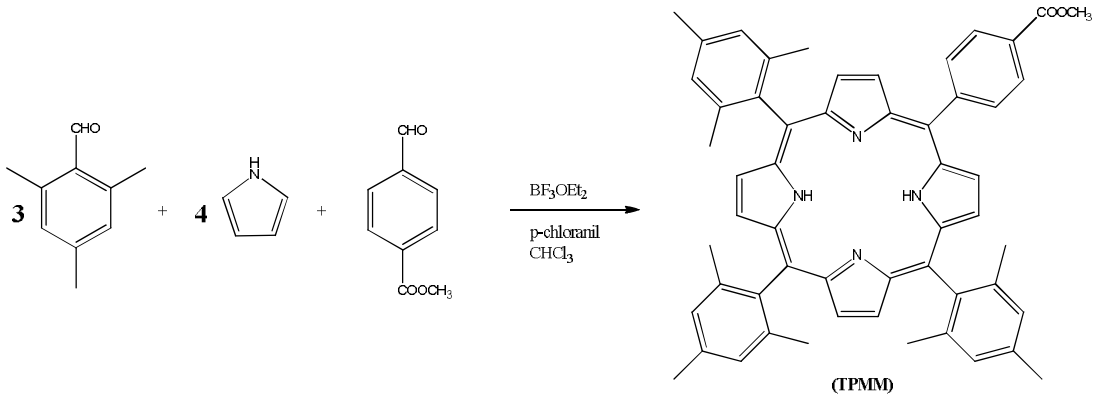

To a solution of 2,4,6-trimethylbenzaldehyde (3.6 g, 24 mmol) in $CHCl_3$ (800 mL) was added methyl 4-formylbenzoate (1.3 g, 8 mmol), pyrrole (2.2 mL, 32 mmol) and BF_3OEt_2 (1.3 mL). The solution was stirred at room temperature for 2 hours. Then, p-chloranil (5.0 g) was added and stirred at room temperature for 1 hour. To this, Et_3N (1.0 mL) was added and the solvent was removed in vacuo. The residue was subjected to column chromatography on silica gel (CH_2Cl_2/hexane, 1:1) afforded the target porphyrin as a purple red solid in 13% yield. ESI-MS: calculated-798, found-799. ^1H NMR (400 Hz, CD_2Cl_2): 8.73-8.43 (br s, 8H), 8.42 (d, J=8.4 Hz, 2H), 8.32 (d, J=8.0 Hz, 2H), 7.30 (s, 6H), 4.08 (s, 3H), 2.61 (s, 9H), 1.86 (s, 6H), 1.84 (s, 12H), -2.74 (s, 2H, pyrrole NH).

3.2 Synthesis of 5-(4-Carboxyphenyl)-10,15,20-tris(2,4,6-trimethylphenyl) porphyrin (TPMC)[1]

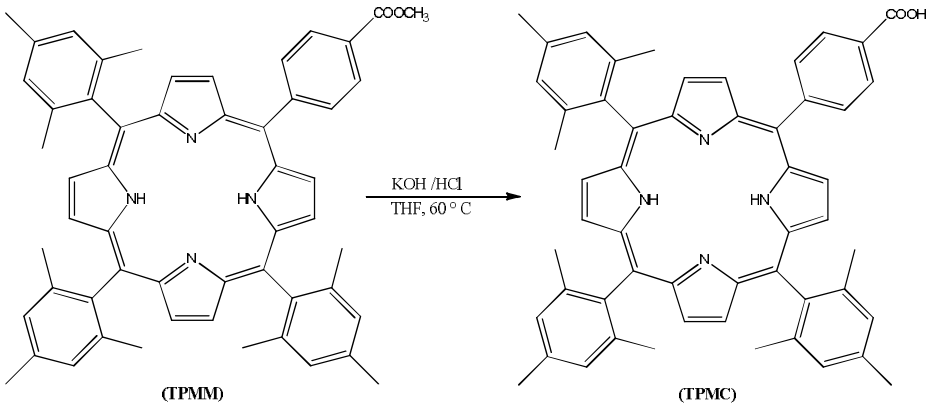

To a solution of TPMM (160 mg, 0.2 mmol) in THF (100 mL) was added a solution of KOH (400 mg) in H_2O (8 mL). The solution was refluxed for 2 hours. After the reaction

mixture was cooled to room temperature, aqueous 1M HCl (2 mL) was added. The solution was washed with saturated aqueous $NaHCO_3$ (50 mL), H_2O (50mL x 3) dried over anhydrous sodium sulfate and the solvent was removed in vacuo. Recrystallization from CH_2Cl_2/MeOH gave TPMC porphyrin as a purple red solid in 0.13 g yield. ESI-MS: calculated-785, found-786 ^{1}H NMR (400 Hz, CD_2Cl_2) 8.78 (br s, 2H), 8.63 (br s, 6H), 8.42 (d, J= 8.4 Hz, 2H), 8.28 (d, J= 8.4 Hz, 2H), 7.29 (s, 2H), 7.28 (s, 4H), 2.61 (s, 3H), 2.60 (s, 6H), 1.86 (s, 6H),1.83 (s, 12H), -2.74 (s, 2H, pyrrole NH).

3.3 Synthesis of chromophore (1) [5-(4-Carboxyphenyl)-10,15,20-tris(2,4,6-trimethyl phenyl) porphyrinato zinc (II)](TPMC-Zn)[1]

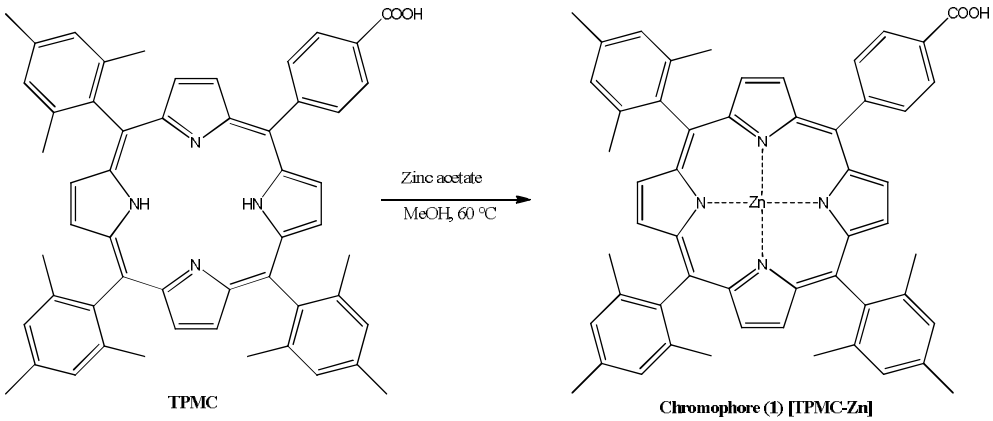

To a solution of TPMC (40 mg, 0.05 mmol) in CH_3Cl (8 mL) was added a solution of $Zn(OAc)_2$ (0.1 g, 0.45 mmol) in MeOH (3 mL). The solution was refluxed for 2 hours. The reaction mixture was washed with H_2O (30mL x3) and dried over anhydrous sodium sulfate, and then the solvent was removed in vacuo. Recrystallization from CH_2Cl_2/MeOH gave desired porphyrin as a purple red solid in 90% yield. ESI-MS: calculated-848, found-849. ^{1}H NMR (400 Hz, CD_2Cl_2) 8.78 (br s, 2H), 8.63 (br s, 6H), 8.42 (d, J= 8.4 Hz, 2H), 8.28 (d, J= 8.4 Hz, 2H), 7.29 (s, 2H), 7.28 (s, 4H), 2.61 (s, 3H), 2.60 (s, 6H), 1.86 (s, 6H),1.83 (s, 12H).

3.4 Synthesis of Copper (II) tetra phenyl porphyrin (Cu-TPP)[2]

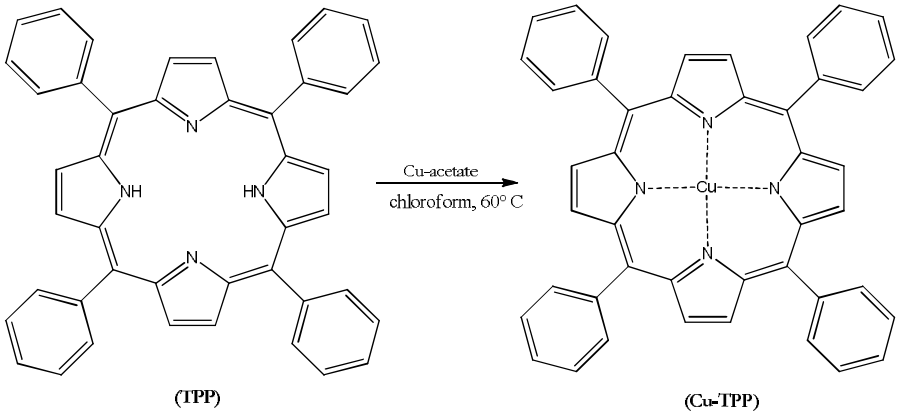

TPP (200 mg, 0.32 mmol) was dissolved in 150 mL of chloroform. To this a solution of copper acetate (1 g, 5.52 mmol) dissolved in 75 mL methanol was added. The reaction mixture was refluxed for 1.5 hours at 60° C. The progress of the reaction was monitored by TLC using diethyl ether /chloroform (6:4) as eluent. The formation of new spot R_f=0.7 was observed on TLC. After the complete disappearance of tetra phenyl porphyrin, the desired product was recovered by column chromatography using same eluent as used in TLC analysis. The solvent was evaporated on rota vapour Cu-TPP was recovered in 91% yield. ESI-MS: calculated-675, found- 676.

3.5 Synthesis of 2-Formyl-5,10,15,20-tetraphenylporphyrin (CHO-TPP)[3]

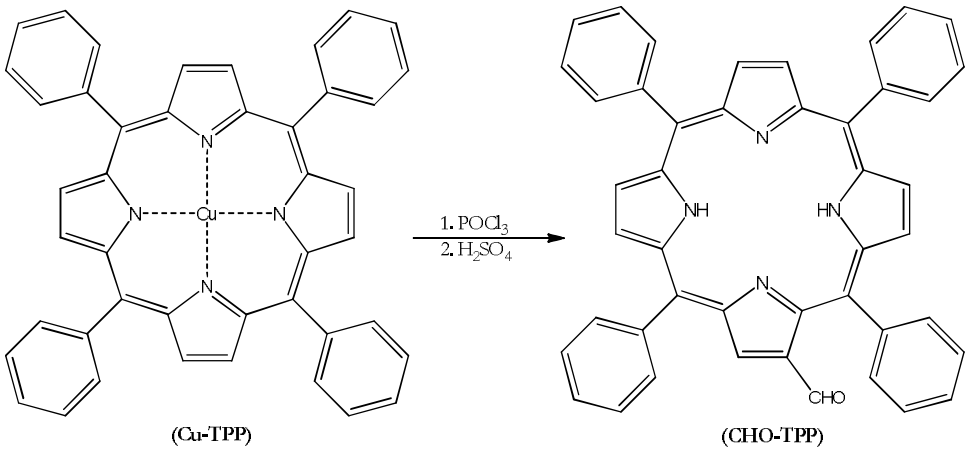

In a sealed round bottom flask containing dry DMF (6 mL), $POCl_3$ (8 mL) was added and cooled to 0 °C. A cold solution of Cu-TPP (100 mg, 0.14 mmol) was made in dry dichloromethane (70 mL) which was added to $POCl_3$ solution. The reaction mixture was stirred for 15 minutes at room temperature and then refluxed for 5 hours.

Removal of copper (II) was carried out by adding 2 mL of concentrated sulphuric acid. After stirring for 10 minutes, the reaction mixture was poured over an ice cold aqueous solution of NaOH (5 g in 200ml water), chloroform (25 mL) was added and solution basicity was monitored. The organic layer which contains the target porphyrin was separated using a separating funnel and washed again with $NaHCO_3$ solution. The organic layer was dried over anhydrous Na_2SO_4 and solvent was removed in vacuo. The desired product was obtained by column chromatography using CH_2Cl_2/Toluene 2:1 as eluent. The solvent was evaporated, thus obtaining the desired CHO-TPP porphyrin in 45 % yield. ESI-MS: calculated-641, found-642.

3.6 Synthesis of 2-formyl-5,10,15,20-tetra phenyl porphyrinato zinc (II) (CHO-Zn-TPP)[4]

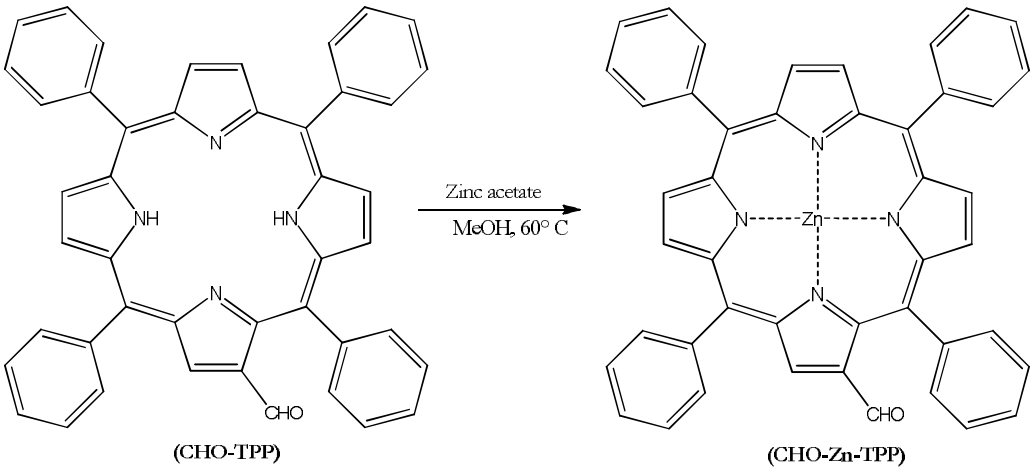

(CHO-TPP) (CHO-Zn-TPP)

In a round bottom flask, a solution of zinc acetate (41 mg, 0.186 mmol) dissolved in methanol was added to a solution of CHO-TPP (100 mg, 0.155 mmol) in chloroform. The reaction mixture was refluxed for 1 hour at 60° C. The progress of reaction was monitored by TLC using CH_2Cl_2/Toluene (2:1) as eluent. After complete disappearance of the starting material, the reaction mixture was poured in water. The organic layer was recovered using the separating funnel and dried over Na_2SO_4. The solvent was evaporated giving a purple solid as desired porphyrin CHO-Zn-TPP in 90% yield. ESI-MS: calculated-703 found-704. ^{1}H NMR (300 MHz, $CDCl_3$) 7.71-7.83 (m, 12H, H m,p-Ph), 8.15-8.23 (m, 8H, H o-Ph), 8.88-8.94 (m, 6H, H(β-pyrrolic), 9.22 (s, 1H, H(β-pyrrolic)), 9.51(s, CHO).

3.7 Synthesis of chromophore (2) [2-Cyano-3-(2'-(5',10',15',20'-tetraphenyl porphyrinato zinc-(II))yl)acrylic Acid][4]

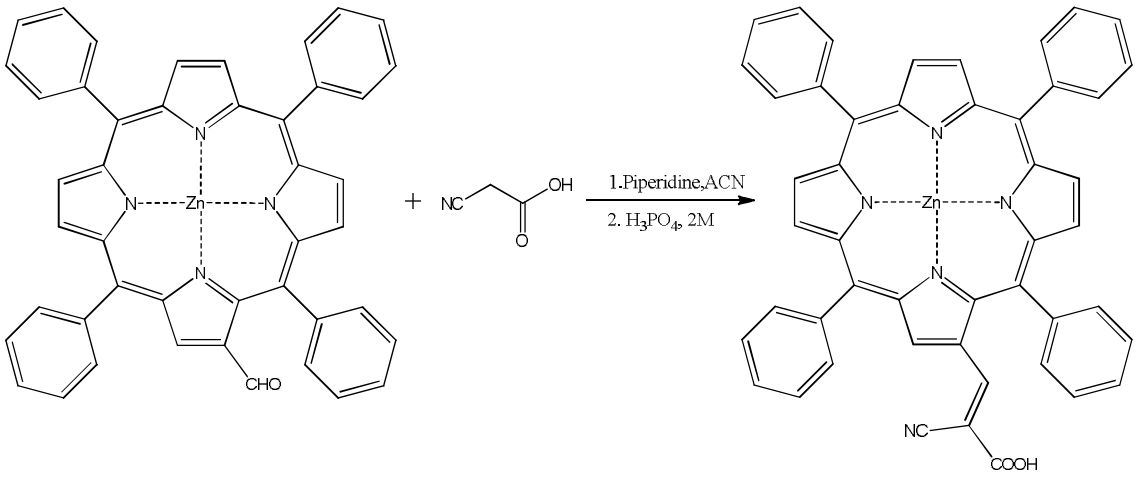

(CHO-Zn-TPP) Chromphore (2)

In a round bottom flask, a solution of CHO-Zn-TPP porphyrin (110 mg, 0.156 mmol), cyanoacetic acid (39.86 mg, 0.468) and piperidine (292.2 mg, 3.43 mol) was made in 22 mL of acetonitrile. The reaction mixture was refluxed for 1 hour at 80 °C. After being cooled to room temperature, the resulting green precipitate of porphyrin as piperidine salt was collected by using a glass filter and then rinsed with acetonitrile.

The solid was dissolved DMSO, to this water (3 mL) and chloroform (10 mL) were added. To this, 2M H_3PO_4 solution was added and stirred vigorously (pH≈2). The solution was transferred to separating funnel. The organic layer was washed with water (3 times) and later dried over anhydrous Na_2SO_4. The solvent was removed, yielding the target porphyrin in 58% yield. ESI-MS: calculated-770, found-771.

3.8 Synthesis of bis-phenyl porphyrin adduct (PTP)[5]

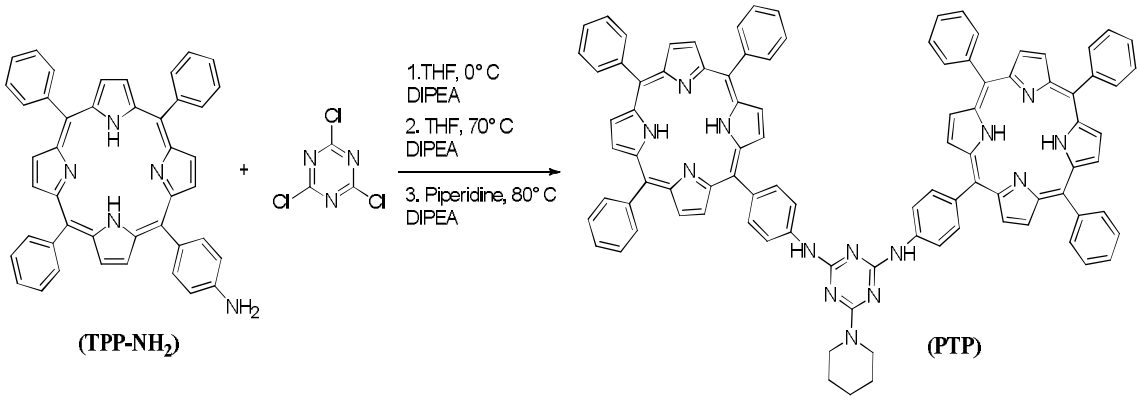

(TPP-NH_2) (PTP)

To a solution of amino porphyrin (10 mg, 16 μmol) in THF (1.0 mL) cooled at 0 °C were added to a THF solution of cyanuric chloride (2.9 mg, 16 μmol) and DIPEA (2.5 mg, 19 μmol). After 10 minutes under stirring the solution was left to reach room temperature. The reaction was complete as witnessed by TLC analysis (silica gel, petroleum ether/ethylacetate 3:2 v/v) showing the disappearance of amino porphyrin (R_f = 0.33). Another equivalent of amino porphyrin (10 mg, 16 μmol) was then added and stirred at room temperature together with 1.2 equivalents of DIPEA. After stirring for 24 hours, an excess of piperidine (4.1 mg, 48 μmol) was added together with 1.2 equivalents of DIPEA and the mixture was stirred at 80 °C. After 3 hours, the solvent was evaporated and the solid was subjected to flash column chromatography on silica-gel (eluent: petroleum ether/ethyl acetate 3:2 v/v) to give desired porphyrin dimer as a purple solid in 71% yield. ESI-MS $C_{96}H_{70}N_{14}$ (CH_3CN + 1% HCOOH as eluent) m/z: observed 1420.5 $[MH]^+$ (calcd 1420.68). ^{1}H-NMR ($CDCl_3$, 250 MHz): 8.98 (m, 4H, ß-pyrrole), 8.96 (m, 12H, β-pyrrole), 8.23-7.68 (m, 38H, porphyrin phenyl aromatic protons), 7.07 (s, broad, 2H, NH), 3.99 (s, 4H, ortho piperidine), 1.75 (s, 6H, meta\para piperidine), -2.75 (s, 4H, pyrrole NH).

3.9 Synthesis of bis-phenyl porphyrin zinc (II) dimer (3)[5]

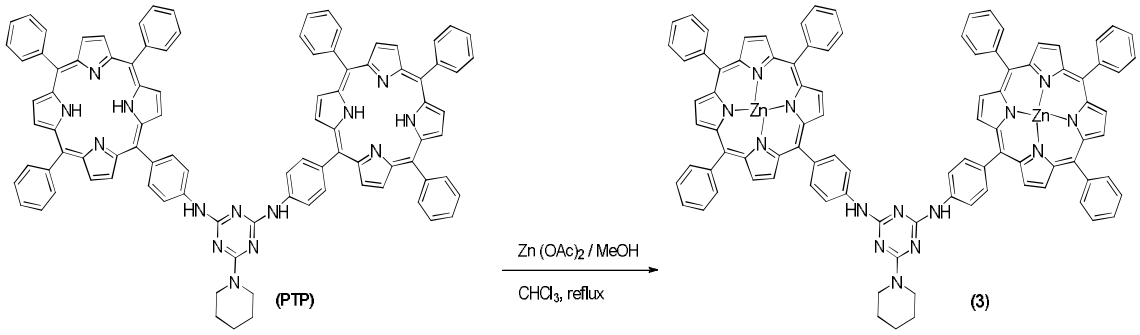

To a solution of bis-phenyl dimer porphyrin (10 mg, 7 μmol) in $CHCl_3$ (5 mL) was added a saturated solution of zinc acetate (0.5 mL) in CH_3OH and refluxed for 1 hour. The solvent was evaporated. The residue was dissolved with CH_2Cl_2 and washed with water in order to remove zinc acetate in excess. The organic phases were combined, dried over Na_2SO_4, filtered and concentrated under reduced pressure to give a purple solid as zinc complex in 97% yield. ESI-MS $C_{96}H_{66}N_{14}Zn_2$ (CH_3CN + 1% HCOOH as eluent) m/z: observed 1546.4 $[MH]^+$ (calcd 1546.8).^{1}H-NMR ($CDCl_3$, 250 MHz): 9.08 (d, 2H, β-pyrrole), 8.94 (m, 6H, β-pyrrole), 8.24-7.74 (m, 19H, porphyrin phenyl aromatic protons), 7.07 (s, broad, 1H, NH), 3.84 (s, 4H, ortho piperidine), 1.67 (s, 6H, m-H and p-H piperidine).

3.10 Synthesis of 5-(4-acetamidophenyl)-10,15,20-tri-(3,5-di-tert-butylphenyl) porphyrin (t-butyl-Ac-TPP)[6]

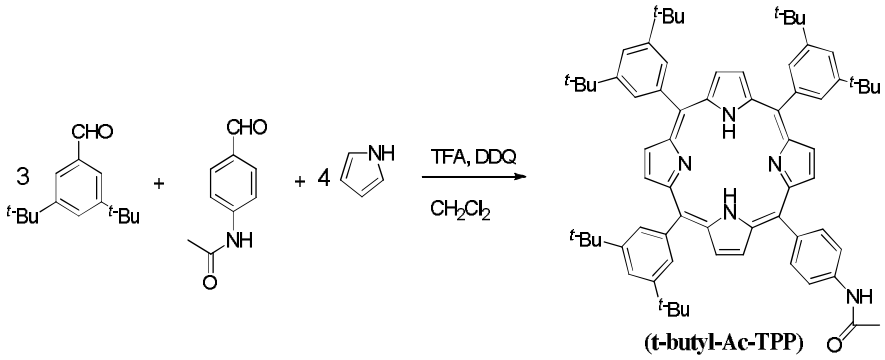

In a 2 L three neck flask, 3,5-di-tert-butylbenzaldehyde (1.637 g, 7.5 mmol) and p-acetamidobenzaldehyde (0.410 g, 2.5 mmol) were dissolved in 1 L of CH_2Cl_2. The flask was covered with aluminium foil and purged with N_2 for 10 minutes before freshly-distilled pyrrole (700 μL, 10 mmol) was injected. The solution was stirred for another 10 minutes, and the reaction was initiated by the injection of TFA (1.4 mL, 20 mmol). The reaction was stirred at room temperature for 1.5 hours, DDQ (1.70 g, 7.5 mmol) was added and stirred for 1 hour at room temperature. The solution was neutralized with triethylamine (2.8 mL, 20 mmol) and the solvent was evaporated. The crude residue was purified by flash chromatography. Elution with CH_2Cl_2 was able to remove all tetraryl porphyrin and the desired A_3B porphyrin was then eluted with 20% EtOAc in CH_2Cl_2. Solvent was removed under vacuum, affording a purple solid as desired porphyrin in ~18 % yield. MALDI-TOF calculated for $C_{70}H_{80}N_5O$ = 1006.64 [M^+] found 1007.43 [M^+]. ^1H NMR (400 MHz, $CDCl_3$): δ = 8.8 ppm (s, 4H, βH), 8.8 ppm (d, 2H, βH), 8.7 ppm (d, 2H, βH), 8.0 ppm (m, 6H, Ar-meta-H), 7.9 ppm (d, 2H, ArH), 7.7 ppm (m, 3H, Ar-para-H), 7.4 ppm (d, 2H, ArH), 7.1 ppm (s, 1H, NH), 2.0 ppm (s, 3H, CH_3), 1.4 ppm (s, 54H, tert-butyl H), -2.8 ppm (s, 2H, pyrrole H).

3.11 Synthesis of 5-(4-aminophenyl)-10,15,20-tri-(3,5-di-tert-butylphenyl) porphyrin (t-butyl-TPP-NH_2)[6]

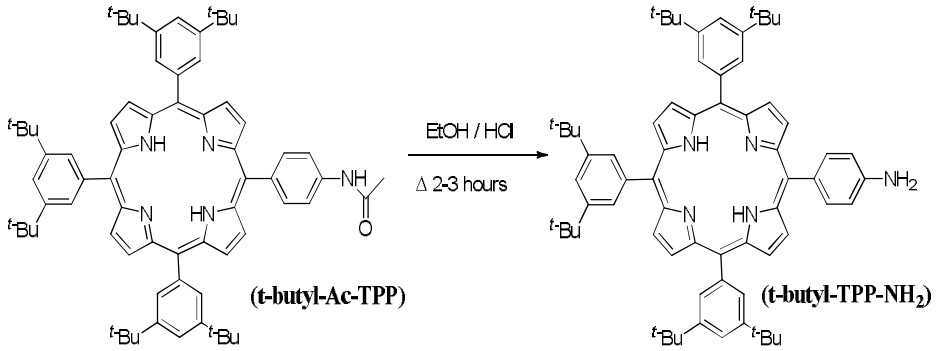

5-(4-acetamidophenyl)-10,15,20-tri-(3,5-di-tert-butylphenyl) porphyrin (0.2067 g, 0.2 mmol) was dissolved in 60 mL EtOH in a 250 mL flask. Concentrated HCl (40 mL) was added to the reaction mixture, which was heated at reflux for 17 hours. The crude mixture was diluted with water and extracted with CH_2Cl_2 for five times. The pooled organic layer was washed with water for three times and with saturated $NaHCO_3$ solution twice. The organic layer was dried over Na_2SO_4 and filtered. The solvent was removed under vacuum and flash chromatography with silica gel and CH_2Cl_2 eluent afforded the desired amino porphyrin in nearly quantitative yield. MALDI-TOF calculated for $C_{68}H_{79}N_5$- calculated-965.63 found 966.64. ^{1}H NMR (300 MHz, $CDCl_3$): $\delta = 8.8$ ppm (d, 2H, βH), 8.8 ppm (m, 6H, βH), 8.0 ppm (m, 6H, Ar-meta-H), 7.9 ppm (d, 2H, ArH), 7.7 ppm (m, 3H, Ar-para-H), 6.9 ppm (d, 2H, ArH), 3.9 ppm (s, 2H, NH_2), 1.4 ppm (d, 54H, tert-butyl H), -2.7 ppm (s, 2H, pyrrole H).

3.12 Synthesis of bis-(3,5-di-tert-butylphenyl-porphyrin) adduct (BTB)[7]

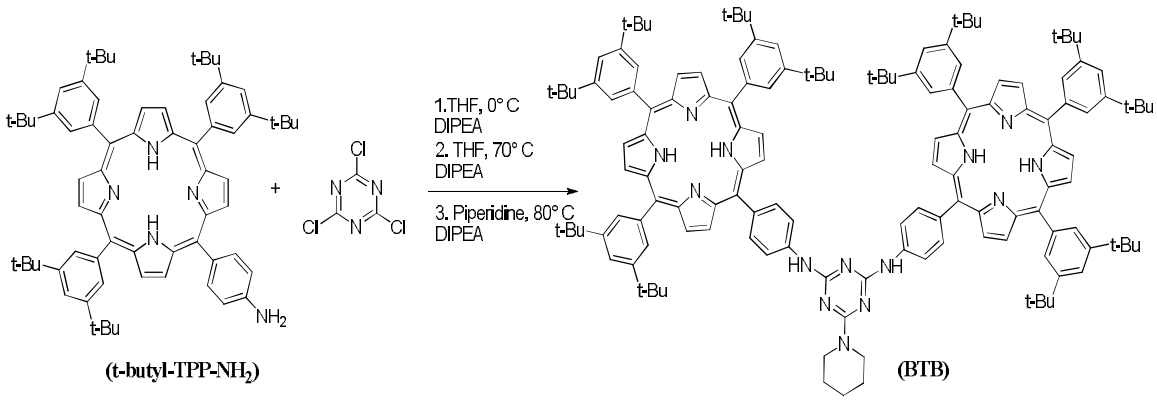

To a solution of 5-(4-aminophenyl)-10,15,20-tri-(3,5-di-tert-butylphenyl) porphyrin (19.1 mg, 20 μmol) in THF (1.0 mL) cooled at 0 °C, a THF solution of cyanuric chloride (3.7 mg, 20 μmol) and DIPEA (3 mg, 24 μmol) were added. After stirring for 10 minutes at 0 °C, the solution was left to reach room temperature. The reaction was complete, as evident from TLC analysis (silica gel, petroleum ether/ethyl acetate 3:2 v/v) showing the disappearance of amino porphyrin (R_f = 0.31) and the formation of a new spot at R_f = 0.63 corresponding to the cyanuric chloride mono-adduct. At this point, a second equivalent of amino porphyrin (19.1 mg, 20 μmol) was added together with 1.2 equivalent of DIPEA and the reaction was stirred at 70 °C for 24 hours. After observing the almost complete formation of the bis-adduct (R_f = 0.73), an excess of piperidine (5.0 mg, 60 μmol) was added together with 1.2 equivalents of DIPEA and the mixture was stirred at 80 °C for 3 hours. After removal of the solvent, the residue was purified by flash chromatography (silica gel, eluent: petroleum ether/ethyl acetate 3:2 v/v) affording 70 mg (82%) of

porphyrin dimer (R_f = 0.78). ESI-MS $C_{144}H_{166}N_{14}$ (CH_3CN + 1% HCOOH as eluent) m/z: observed 2093.4 $[MH]^+$ (calculated 2093.95). ^{1}H-NMR ($CDCl_3$, 250 MHz) : 9.09 (d, 4H, β-pyrrole), 9.02 (m, broad 12H, β-pyrrole), 8.04 (d, 4H, phenyl aromatic protons near triazine ring), 8.10-7.78 (m, 14H, phenyl aromatic protons) 7.19 (br s, 2H, NH), 3.99 (br s, 4H, piperidine), 1.74-1.68 (br s, 6H, piperidine), -2.46 (s, 4H, pyrrole NH).

3.13 Synthesis of bis-(3,5-di-tert-butylphenyl-porphyrin) zinc (II) dimer (4)[7]

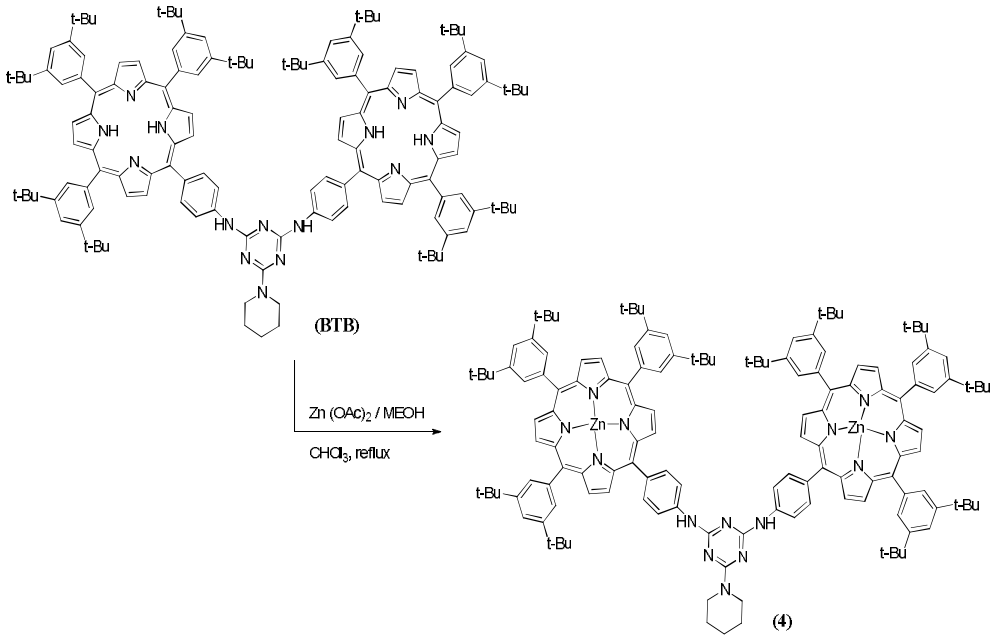

To a solution of bis(3,5-di-tert-butylphenyl) porphyrin dimer (40 mg, 19 μmol) in $CHCl_3$ (5 mL), a saturated solution of zinc acetate (0.5 mL) in CH_3OH was added and refluxed for 1 hour. The solvent was evaporated. The residue was dissolved with CH_2Cl_2 and washed with water in order to remove zinc acetate in excess. The organic phases were combined, dried over anhydrous Na_2SO_4, filtered and concentrated under reduced pressure to give a purple solid as zinc complex in 90 % yield. ESI-MS $C_{144}H_{162}N_{14}Zn_2$ (CH_3CN + 1% HCOOH as eluent) m/z: observed 2221.4 $[MH]^+$ (calcd 2219.68).^{1}H-NMR ($CDCl_3$, 250 MHz): 9.09 (d, 4H, β-pyrrole), 9.02 (m, broad 12H, β-pyrrole), 8.04 (d, 4H, phenyl aromatic protons near triazine ring), 8.10- 7.78 (m, 14H, phenyl aromatic protons), 7.19 (br s, 2H, NH), 3.99 (br s, 4H, piperidine), 1.74-1.68 (br s, 6H, piperidine) 1.53 (s, 108H, tert-butyl protons).

3.14 Synthesis of N-methyl p-acetamido benzaldehyde (6)[8]

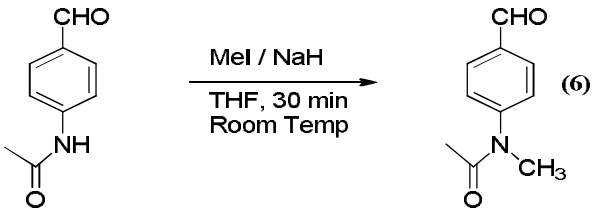

Sodium hydride (177mg, 7.3 mmol) was added to the magnetically stirred acetamido benzaldehyde (1g, 6.1 mmol) in anhydrous THF. Iodomethane (459 µL, 7.3 mmol) was added drop wise to the mixture, which was maintained below 5 °C for 0.5 hour then stirred at room temperature. The reaction was monitored by TLC. After the reaction was judged complete, the reaction mixture was partitioned between saturated aqueous NH_4Cl and ethyl acetate. The organic layer was separated and the aqueous layer was extracted with ethyl acetate. The combined organic layers were washed with water, dried over Na_2SO_4, and concentrated. The residue was purified by flash chromatography with petroleum ether/ethyl acetate to give the N-methyl p-acetamido benzaldehyde in 60% yield. ESI-MS $C_{10}H_{11}NO_2$ (CH_3CN as eluent) m/z: observed 178 $[MH]^+$ (calculated 178).

3.15 Synthesis of 5-(N-methyl-4-acetamidophenyl)-10,15,20-tri-(3,5-di-tert-butylphenyl) porphyrin (N-met-t-butyl-Ac-TPP)[6]

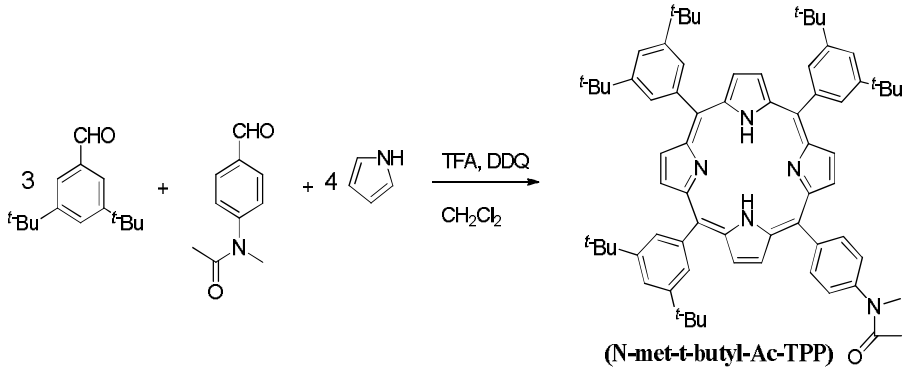

3,5-di-tert-butylbenzaldehyde (1.637 g, 7.5 mmol) and N-methyl p-acetamidobenzaldehyde (0.443 g, 2.5 mmol) were dissolved in 1 L of CH_2Cl_2 contained in a 2 L three-neck flask. The flask was covered with aluminium foil and purged with N_2 for 10 minutes before freshly-distilled pyrrole (700 µL, 10 mmol) was injected. The mixture was stirred for another 10 minutes, before to initiate the reaction, by the injection of TFA (1.4 mL, 20 mmol). After 1.5 hours DDQ (1.70 g, 7.5 mmol) was added, the reaction was stirred for 1 hour at room temperature. Then it was neutralized with triethylamine (2.8 mL, 20 mmol) and the solvent was evaporated. The residue was purified with silica gel flash

chromatography. Elution with CH_2Cl_2 was able to remove all tetraryl porphyrin and the desired A_3B porphyrin was then eluted with 20% EtOAc in CH_2Cl_2. Solvent was removed under vacuum, affording a purple solid as desired porphyrin in ~16 % yield. ESI-MS (CH_3CN as eluent) m/z: calculated for $C_{71}H_{83}N_5O$ = calculated-1021.6 found-1022.4. ^1H NMR (300 MHz, $CDCl_3$): $\delta = 8.9$ ppm (s, 4H, βH), 8.8 ppm (d, 2H, βH), 8.7 ppm (d, 2H, βH), 8.0 ppm (m, 6H, Ar-meta-H), 7.9 ppm (d, 2H, ArH), 7.7 ppm (m, 3H, Ar-para-H), 7.4 ppm (d, 2H, ArH), 3.5 ppm (s, 3H, N-CH_3), 2.2 ppm (s, 3H, CH_3), 1.4 ppm (s, 54H, tert-butyl H), -2.8 ppm (s, 2H, pyrrole H).

3.16 Synthesis of 5-(N-methyl-4-aminophenyl)-10,15,20-tri-(3,5-di-tert-butylphenyl) porphyrin (N-met-t-butyl-TPP-NH_2)[6]

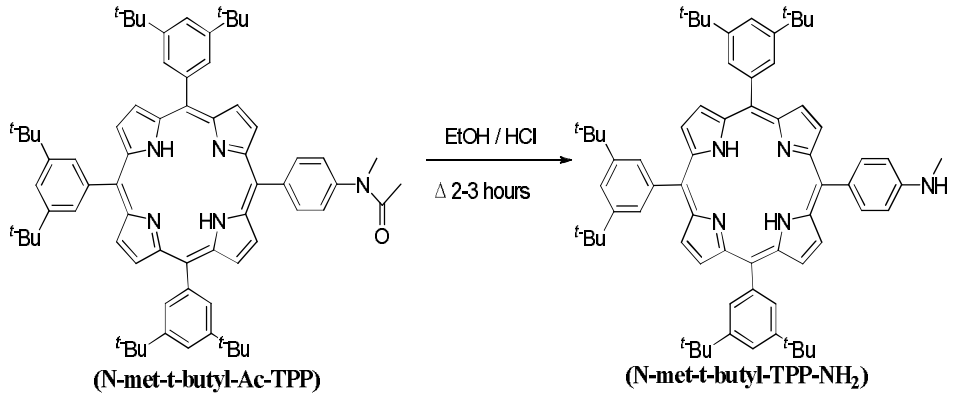

5-(N-methyl-4-acetamidophenyl)-10,15,20-tri-(3,5-di-tert-butylphenyl) porphyrin (0.21 g, 0.2 mmol) was dissolved in 60 mL EtOH in a 250 mL flask. Concentrated HCl (40 mL) was added to the reaction mixture, which was heated at reflux for 17 hours. The crude mixture was diluted with water and extracted with CH_2Cl_2 for five times. The organic layer was washed with water (three times) and with saturated $NaHCO_3$ solution (twice). The pooled organic layer was dried over Na_2SO_4 and filtered. The solvent was removed under vacuum and flash chromatography with silica gel and CH_2Cl_2 afforded the desired amino porphyrin in nearly quantitative yield. ESI-MS (CH_3CN as eluent) m/z: calculated for $C_{69}H_{81}N_5$ = calculated-979.6 found-980.9. ^1H NMR (300 MHz, $CDCl_3$): $\delta = 8.8$ ppm (d, 2H, βH), 8.8 ppm (m, 6H, βH), 8.0 ppm (m, 6H, Ar-meta-H), 7.9 ppm (d, 2H, ArH), 7.7 ppm (m, 3H, Ar-para-H), 6.9 ppm (d, 2H, ArH), 4.5 ppm (s, 1H, NH), 3.0 ppm (s, 3H, N-CH_3), 1.4 ppm (d, 54H, tert-butyl H), -2.7 ppm (s, 2H, pyrrole H).

3.17 Synthesis of N-methyl bis-(3,5-di-tert-butylphenyl-porphyrin) adduct (N-BTB)

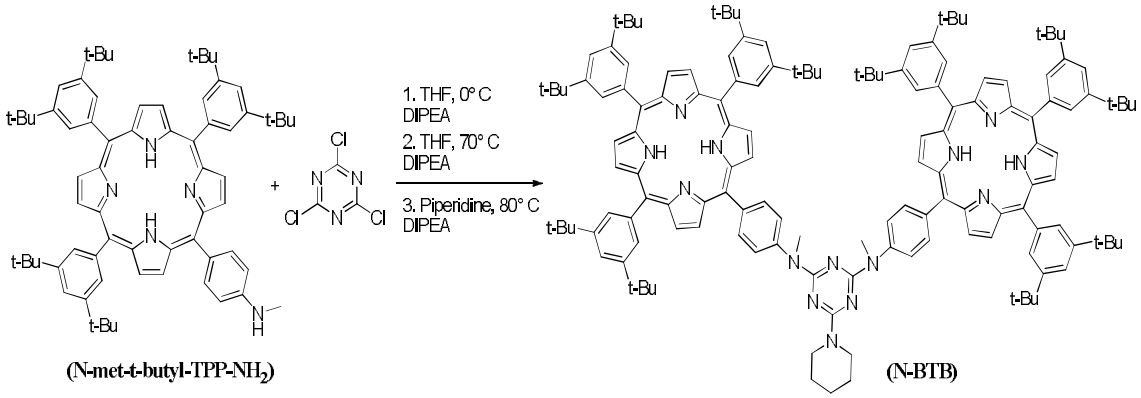

To a solution of 5-(N-methyl-4-aminophenyl)-10,15,20-tri-(3,5-di-tert-butylphenyl) porphyrin (19.7 mg, 20 μmol) in THF (1.0 mL) cooled at 0 °C, a THF solution of cyanuric chloride (3.7 mg, 20 μmol) and DIPEA (3 mg, 24 μmol) was added. After stirring for 10 minutes at 0 °C, the solution was left to reach room temperature. The formation of the mono adduct from cyanuric chloride was complete, as evident from TLC analysis (silica gel, petroleum ether/ethyl acetate 3:2 v/v) showing the disappearance of amino porphyrin (R_f = 0.40) and the formation of a new spot at R_f = 0.65. At this point, a second equivalent of amino porphyrin (19.7 mg, 20 μmol) was then added together with 1.2 equivalents of DIPEA and the reaction was stirred at 70 °C for 24 hours. After observing the almost complete formation of the bis-adduct (R_f = 0.80), an excess of piperidine (5.0 mg, 60 μmol) was added together with 1.2 equivalents of DIPEA and the mixture was stirred at 80 °C for 3 hours. After removal of the solvent, the residue was purified by flash chromatography (silica gel, eluent: petroleum ether/ethyl acetate 3:2 v/v) affording 75 mg (78%) of porphyrin dimer (R_f = 0.85). ESI-MS $C_{146}H_{170}N_{14}$ (CH_3CN + 1% HCOOH as eluent) m/z: observed 2121.6 $[MH]^+$ (calculated 2121). ^{1}H-NMR ($CDCl_3$, 250 MHz) : 9.09 (d, 4H, β-pyrrole), 9.02 (m, broad 12H, β-pyrrole), 8.04 (d, 4H, phenyl aromatic protons near triazine ring), 8.10-7.78 (m, 14H, phenyl aromatic protons), 3.99 (br s, 10H, piperidine + CH_3), 1.74-1.68 (br s, 6H, piperidine), -2.46 (s, 4H, pyrrole NH).

3.18 Synthesis of N-methyl bis-(3,5-di-tert-butylphenyl-porphyrin) zinc (II) dimer (5)[7]

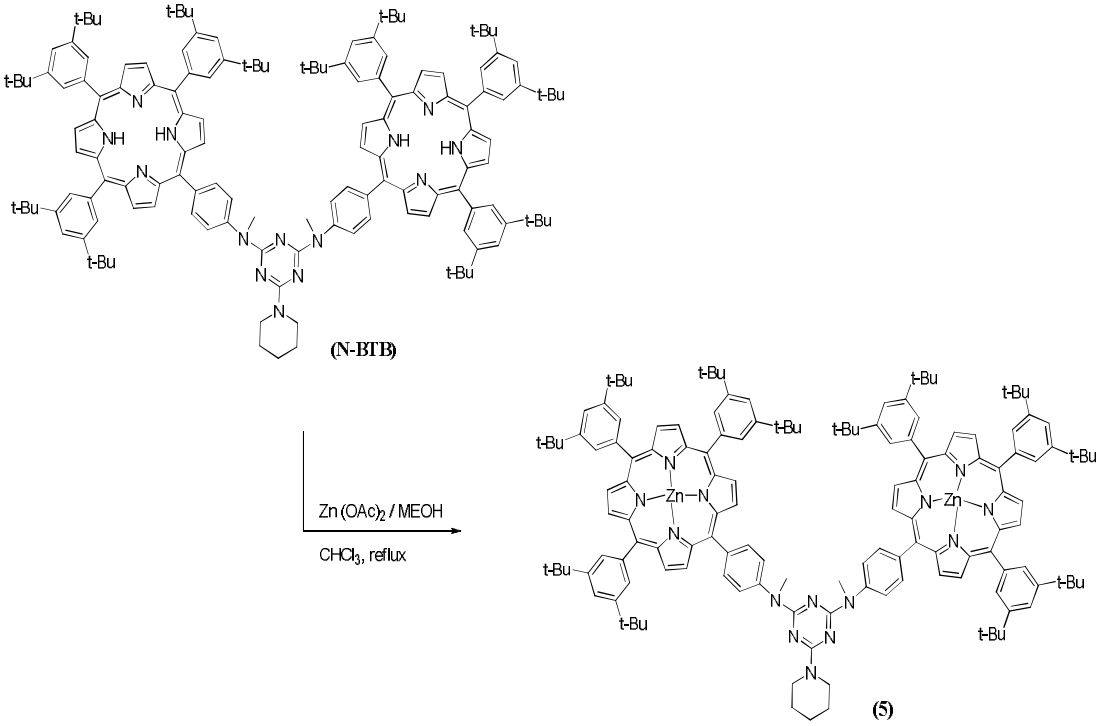

To a solution of N-methyl bis(3,5-di-tert-butylphenyl) porphyrin dimer (38 mg, 19 μmol) in $CHCl_3$ (5 mL), a saturated solution of zinc acetate (0.5 mL) in CH_3OH was added and refluxed for 1 hour. The solvent was evaporated. The residue was dissolved with CH_2Cl_2 and washed with water in order to remove zinc acetate in excess. The organic phases were combined, dried over Na_2SO_4, filtered and concentrated under reduced pressure to give a purple solid as zinc complex in 90 % yield. ESI-MS $C_{146}H_{166}N_{14}Zn_2$ (CH_3CN + 1% HCOOH as eluent) m/z: observed 2243.5 $[MH]^+$ (calculated 2243).^{1}H-NMR ($CDCl_3$, 250 MHz): 9.09 (d, 4H, β-pyrrole), 9.02 (m, broad 12H, β-pyrrole), 8.04 (d, 4H, phenyl aromatic protons near triazine ring), 8.10- 7.78 (m, 14H, phenyl aromatic protons), 3.99 (br s, 10H, piperidine + CH_3), 1.74-1.68 (br s, 6H, piperidine) 1.53 (s, 108H, tert-butyl protons).

3.19 Synthesis of Dipyrromethane (8)[9]

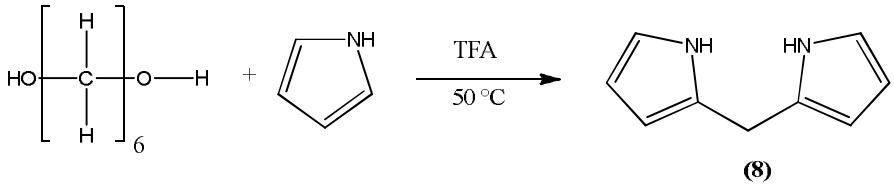

A suspension of paraformaldehyde (0.865 g, 28.85 mmol) in pyrrole (50 mL, 0.72 mol) was placed in a 250-mL two-necked round-bottomed flask equipped with an internal thermometer and a water condenser. The solution was heated to 50 °C, and then the heat

source was removed and TFA (222 µL, 2.88 mmol) was added immediately. A sharp increase in the temperature of the solution was observed (to ca. 70 °C), and the solution rapidly became clear and dark. After 5 minutes the reaction was quenched with 0.1 NaOH. To this, ethyl acetate was added and the organic phase was washed extensively with water. After this, organic phase was dried over sodium sulfate and solvent was removed in vacuum to afford on orange oil. The oil was subjected to bulb-to-bulb distillation to get white crystals of dipyrromethane in 1.57g yield. ESI-MS- 146. ^{1}H NMR (300 MHz, $CDCl_3$) 3.96 (s, 2H), 6.03 (m, 2H), 6.15 (q, J= 2.9 Hz, 2H), 6.64 (m, 2H), 7.81 (br s, 2H).

3.20 Synthesis of 5,15-Bis-(3,5-bis-tert-butylphenyl)porphyrin (9)[10]

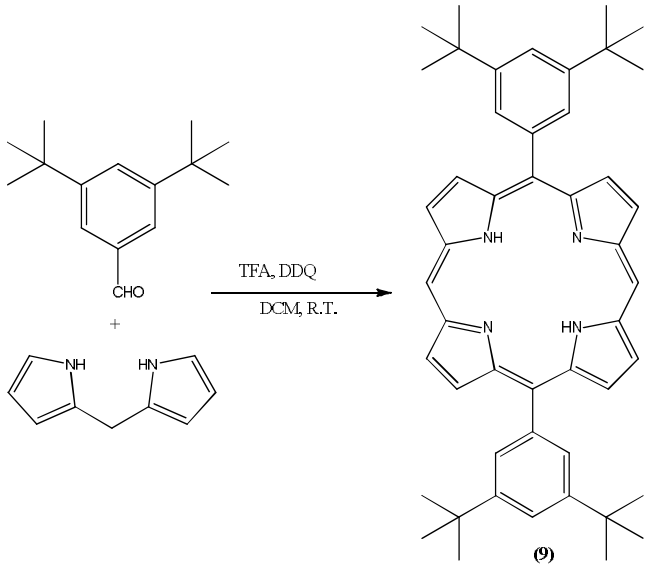

(9)

A solution of dipyrromethane (1.5 g, 10.2 mmol) and 3,5-di-tert -butylbenzaldehyde (2.28 g, 10.2 mmol) in dichloromethane (1.38 L) was stirred for 2 hours, under nitrogen, in the presence of trifluoroacetic acid (0.7 mL, 10.2 mmol). The reaction was quenched by the addition of DDQ (3.5 g, 15.4 mmol) and stirring was continued for another 0.5 hour. The mixture was basified with Et_3N (3.46 mL) and filtered through plug of silica using dichloromethane as eluent. The solvent was removed under reduced pressure to give the desired product as purple solid (40% yield). ESI-MS: 687. ^{1}H NMR (250 MHz, $CDCl_3$): 10.33 (s, 2H, meso), 9.42 (d, J=4.8 Hz, 4H), 9.17 (d, J=4.8 Hz, 4H), 8.16 (d, J=1.8 Hz, 4H, o-Ph), 7.83 (t, J=1.8 Hz, 2H, p-Ph), 1.57 (s, 36H), -3.02 (s, 2H, NH)

3.21 Synthesis of 5,15-Bis-(3,5-bis-tert-butylphenyl)porphinato zinc (II) (10)[10]

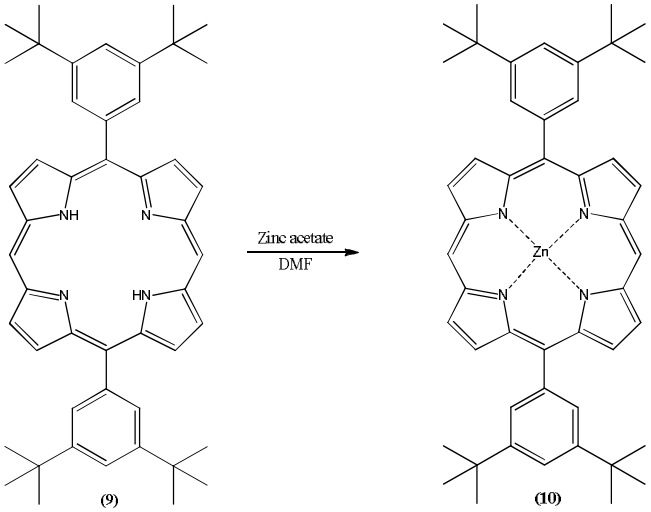

(9) (10)

A suspension of 5,15-Bis-(3,5-bis-tert-butylphenyl)porphyrin (1.14 g, 16.5 mmol) and zinc acetate (3.6 g, 16.5 mmol) in DMF (68 mL) was refluxed for 3 hours. To this water (75 mL) was added and precipitate was collected by filtration. The solid was washed consequently with water, methanol and acetone. The residue was dissolved in chloroform and filtered. MeOH was added and volume reduced to precipitate the product. The filtration gave the desired porphyrin as purple solid in 92 % yield. ESI-MS: calculated-748 found-749. ^{1}H NMR (250 MHz, $CDCl_3$): 10.33 (s, 2H, meso), 9.42 (d, J=4.8 Hz, 4H), 9.17 (d, J=4.8 Hz, 4H), 8.16 (d, J=1.8 Hz, 4H, o-Ph), 7.83 (t, J=1.8 Hz, 2H, p-Ph), 1.57 (s, 36H)

3.22 Synthesis of 5,15-bis-bromo-10,20-bis(3,5-bis-tert-butylphenyl)porphinato zinc (II) (11)[10]

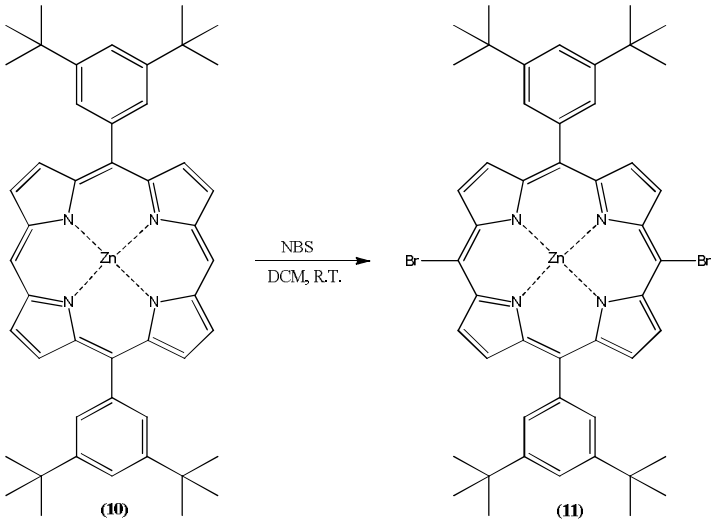

(10) (11)

NBS (0.48 g, 2.72 mmol) was added to stirred solution of porphyrin (1.02 g, 1.36 mmol) in dichloromethane (50 mL). After 5 minutes the reaction was quenched with acetone (10

mL). To this methanol was added and solvent was reduced to a small volume by evaporation. The solution was then filtered and the residue was washed with methanol to give desired porphyrin as a purple solid in 80% yield. ESI-MS: calculated: 927, found: 927/929/931.

3.23 Synthesis of 5,15-bis(3,5-bis-tert-butylphenyl)-10,20-bis-tri-methylsilylethynyl porphinato zinc (II) (12)[10]

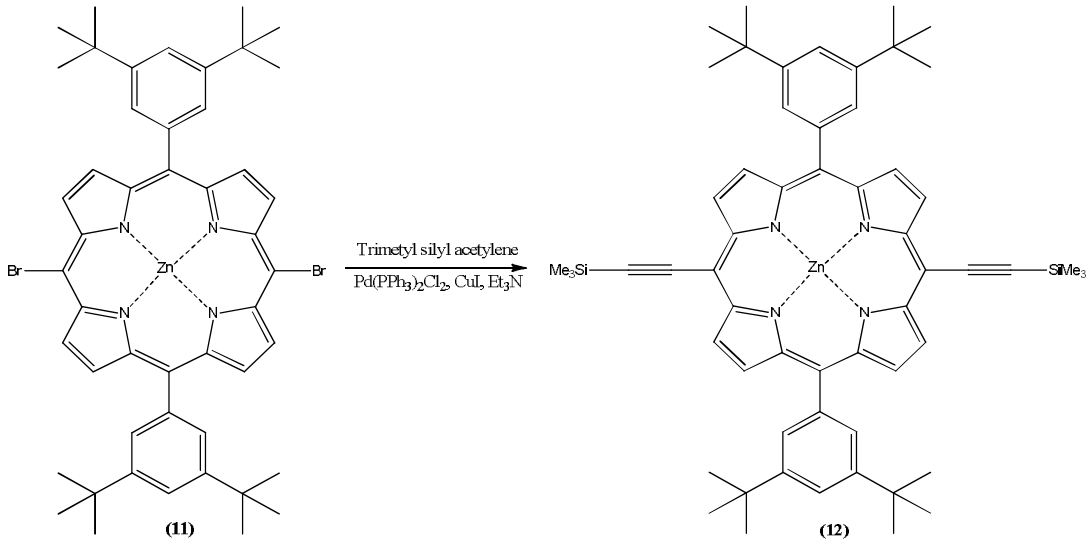

(11) (12)

Triethyl amine (1.25 mL), distilled from CaH_2 under nitrogen, was added to a stirred solution of dibromo porphyrin (500 mg, 0.54 mmol), in the presence of trimethylsilylacetylene (58.4 mg, 0.54 mmol), $Pd(PPh_3)_2Cl_2$ (20 mg, 0.028 mmol) and CuI (5 mg, 0.026 mmol) in THF (25 mL). The resulting solution was stirred for 16 hours at room temperature. The solvent was removed under reduced pressure. The residue was dissolved in PET/CH_2Cl_2 (1:1) and the solution was filtered through a plug of silica. The solvent was removed under pressure and the butadiynyl compound formed was removed by sublimation. The residue was recrystallized from CH_2Cl_2/ACN to yield target porphyrin as deep blue solid in 70 % yield. ESI-MS: calculated-940 found-941. ^{1}H NMR (250 MHz, $CDCl_3$): 9.71 (d, 4H), 8.97 (d, 4H), 8.04 (d, 4H, o-Ph), 7.82 (t, 2H, p-Ph), 1.55 (s, 36H, t-butyl), 0.60 (s, 18H, Si-Me).

3.24 Synthesis of 10,20-bis(3,5-bis-tert-butylphenyl)-5,15-bis-ethynylporphinato zinc (II) (13)[10]

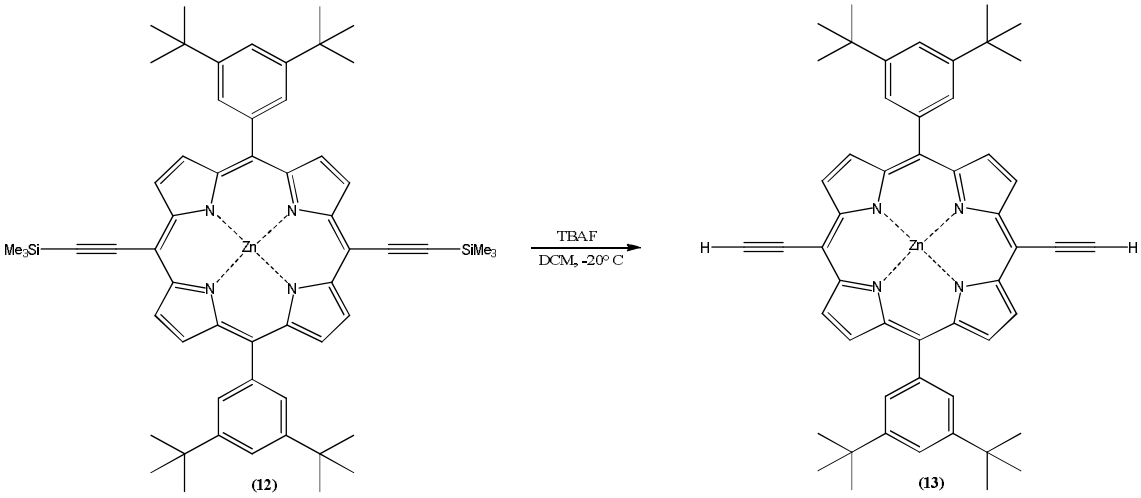

Tetrabutylammonium fluoride (1 mL, 1M in THF) was added to a stirred solution of porphyrin (440 mg, 0.46 mmol) in dichloromethane (15 mL). After 5 minutes, acetic acid (1 mL) and methanol (20 mL) were added and solution was cooled to -20 °C. After 1 hour, the precipitate formed was filtered and washed with methanol to give desired porphyrin in quantitative yield. ESI-MS: calculated-797 found-798. ^{1}H NMR (250 MHz, $CDCl_3$): 9.68 (d, 4H), 8.90 (d, 4H), 8.10 (d, 4H, o-Ph), 7.92 (t, 2H, p-Ph), 4.63 (s, 2H, C-CH), 1.59 (s, 36H, t-butyl).

3.24 Synthesis of Porphyrin chromophore (7) [Meso Triazole clicked Porphyrin][11]

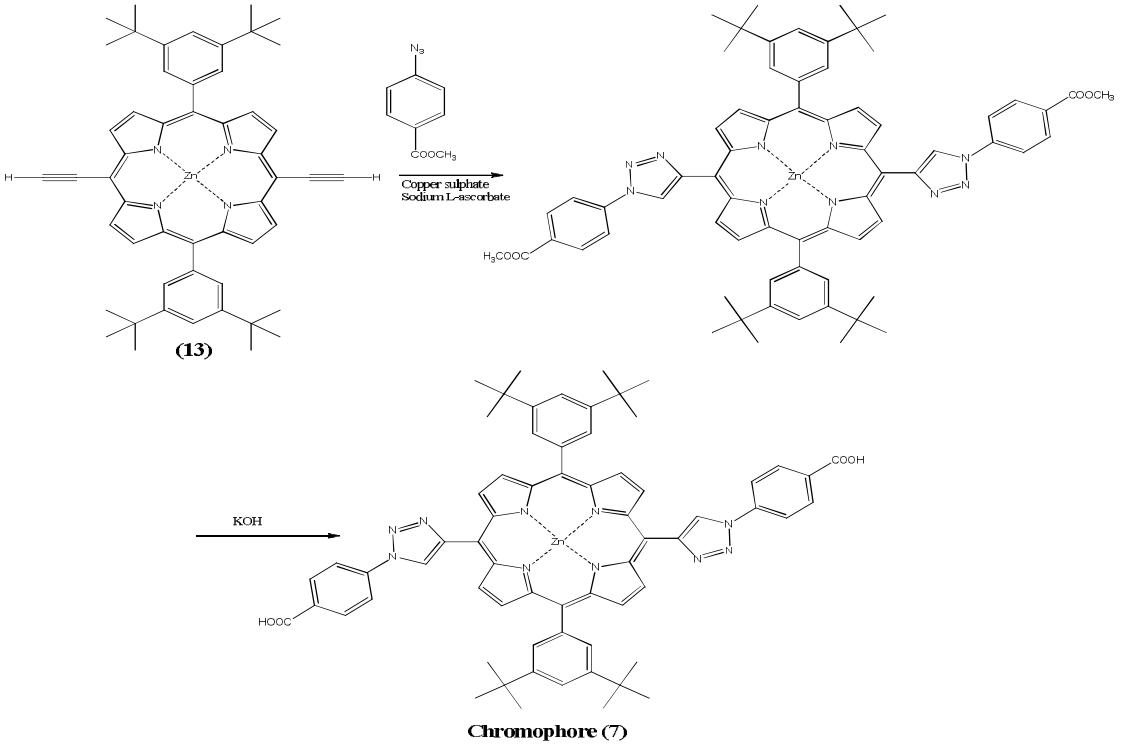

To a stirred solution of porphyrin (100 mg, 0.12 mmol) in dichloromethane (25 mL), methyl 4-azidobenzoate (54.67 mg, 0.31 mmol) was added. After stirring for 10 minutes at room temperature, an aqueous solution of copper sulfate (39.69 mg, 0.15 mmol) and sodium L-ascorbate (49.72 mg, 0.25 mmol) in 5 mL water was added to the reaction mixture. After stirring for 3 days, the mixture was diluted with water and extracted with dichloromethane. The organic phase was separated using separating funnel and dried over sodium sulfate. The solvent was removed by evaporation getting a purple solid that was directly subjected to hydrolysis without any purification.

To this purpose, the solid was treated with KOH. To a solution of methyl ester porphyrin (80 mg, 0.07 mmol) in THF, was added an aqueous solution of KOH (266 mg, 4.76 mmol). The solution was refluxed for 2 hours at 65 °C. The progress of the reaction was monitored by TLC using dichloromethane/ethyl acetate (8:2) as eluent. After the reaction mixture was cooled to room temperature and neutralized with 1M HCl solution. Then dichloromethane was added and the organic layer was washed extensively with water and dried over anhydrous sodium sulfate. The solvent was removed over rota vapour giving the desired porphyrin in 30 mg yield.

3.25 Synthesis of azido zinc(II) porphyrin (14)[12]

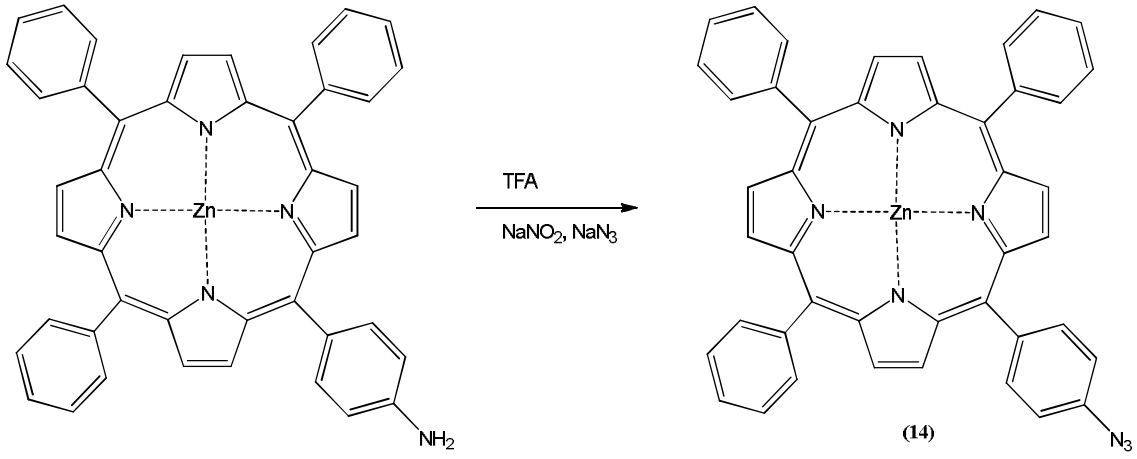

(14)

To a stirred solution of zinc triphenyl-4-aminophenyl porphyrin (100 mg, 0.144 mmol) in TFA (1 mL) at 0 °C was added a solution of $NaNO_2$ (30 mg, 0.434 mmol) in deionized water (0.5 mL). The mixture was stirred for 10 minutes at 0 °C. A solution of NaN_3 (50 mg, 0.767 mmol) in deionized water (0.5 mL) was added dropwise and the reaction stirred for 45 minutes. The solution was diluted with deionized water (5 mL) and extracted with CH_2Cl_2 (3 x 5mL). The organic layer was washed with saturated $NaHCO_3$ (5 mL). The

organic layer was collected and the solvent removed under vacuum to yield a purple solid (88 mg, 93% yield) as azido phenyl porphyrin.

Metallation of Azidophenyl Porphyrin:

To a stirred solution of triphenyl-4-azidophenyl porphyrin (85 mg, 0.130 mmol) in chloroform (30 mL) was added a solution of $Zn(OAc)_2$ (184 mg, 1.009 mmol) in methanol (1 mL). The solution was stirred for 1 hour and then solvent was removed under vacuum. Dichloromethane (30 mL) was added to the residue and the mixture was filtered through a small plug of silica. The solvent was removed under vacuum to yield a deep purple solid (55 mg, 59 % yield). ESI-MS $C_{44}H_{27}N_7Zn$ (CH_3CN + 1% HCOOH as eluent) m/z: 717 $[MH]^+$ observed (calculated 716.4). ^1H NMR ($CDCl_3$) δ 8.8 (8H, □ - pyrrolic), 8.2 (8H, Ar H), 7.7 (9H, Ar H), 7.4 (d, 2H, J=8.2 Hz).

3.26 Synthesis of triazole porphyrin derivative (15)[13]

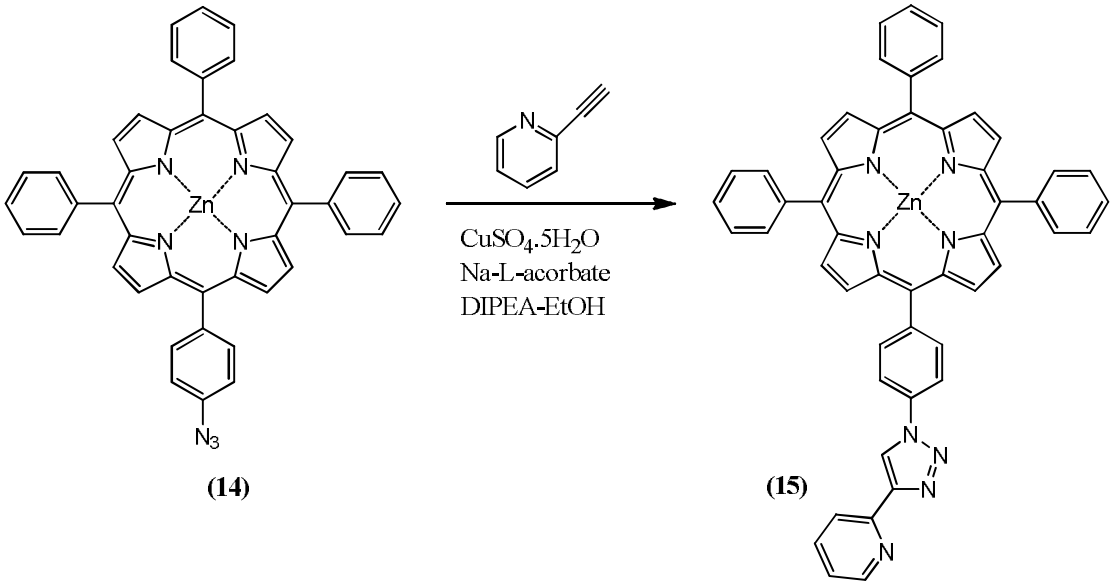

(14) **(15)**

In anhydrous THF (10 mL), zinc-azido porphyrin (30 mg, 0.04 mmol) and 2-ethynyl pyridine (8.6 mg, 0.08 mmol) was added to a 50 mL round bottom flask. The mixture was degassed with nitrogen. After 10 minutes, a saturated solution of copper sulfate (26 mg, 0.10 mmol) and sodium-L-ascorbate (33mg, 0.16 mmol) was added to the solution using syringe. Further, a solution of (1:1 DIPEA/EtOH) 1mL was added to reaction mixture. After stirring for 3 days, the mixture was diluted with H_2O (50 mL) and extracted with CH_2Cl_2 (3 x 50 mL). The organic layer was dried over anhydrous sodium sulfate, filtered, and concentrated under vacuum. The crude product was purified by column chromatography (silica gel, 8:2 CH_2Cl_2/EtOAc). The solvent was removed under vacuum

to yield a deep purple solid (28 mg, 82 % yield). **X-ray-quality crystals were obtained** by crystallization from CH_2Cl_2/MeOH solution. ESI-MS: calculated-820, found-821 ^{1}H NMR (300 MHz, $CDCl_3$) δ 9.03-8.98 (8H, □ pyrollic H), δ 8.91 (1H, triazole ring), δ 8.78-8.68 (2H, pyridine H), δ 8.64-8.43 (2H, phenyl H), δ 8.38-3.6 (1H, pyridine H), δ 8.26-8.23 (8H, phenyl H), δ 7.93-7.88 (1H, pyridine H), δ 7.79-7.77 (9H, phenyl H), δ 7.37-7.33 (1H, pyridine H).

3.27 Synthesis of palladium complexed porphyrin derivative (16)[14]

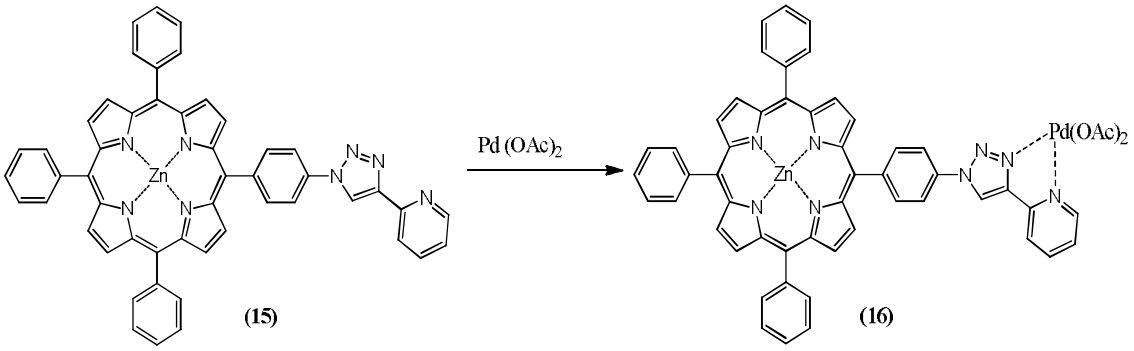

Porphyrin (15) (10 mg, 0.012 mmol) was added in toluene (25 mL), to this palladium acetate (2.73 mg, 0.012 mmol) added and stirred for 1 hour at room temperature. The progress of the reaction was monitored by TLC (DCM), after complete disappearance of starting porphyrin, the solvent was evaporated and subjected to column chromatography. However, even with the use of highly polar solvent, the product did not elute.

3.28 Synthesis of ruthenium complexed porphyrin derivative (17)[15]

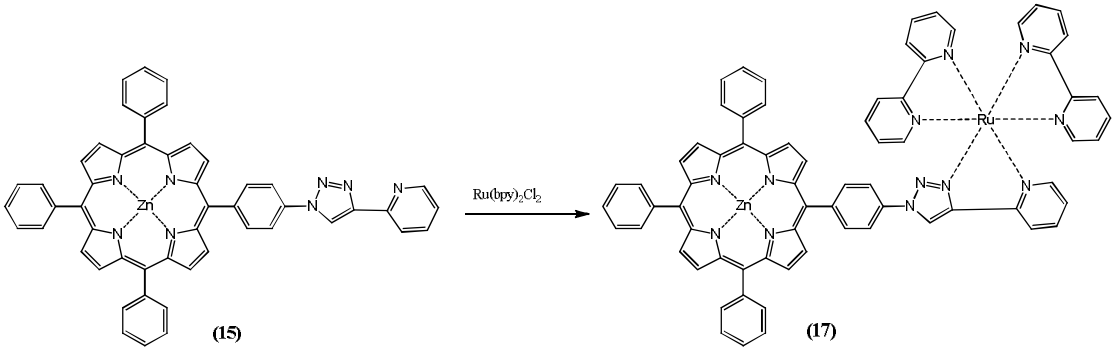

The porphyrin derivative (15) (20 mg, 0.024 mmol) was dissolved in ethanol (10 mL) and cis-$Ru(bpy)_2Cl_2$ (47 mg, 0.097 mmol) was added to it. The reaction mixture was stirred for 3 hours at 78 °C. The solvent was evaporated and the solid thus obtained was subjected to column chromatography over alumina using dichloromethane/methanol (9:1) as eluent. ESI-MS: 617 $[MH_2]^{2+}$ (found).

3.29 Synthesis of ruthenium complexed porphyrin derivative (18)[16]

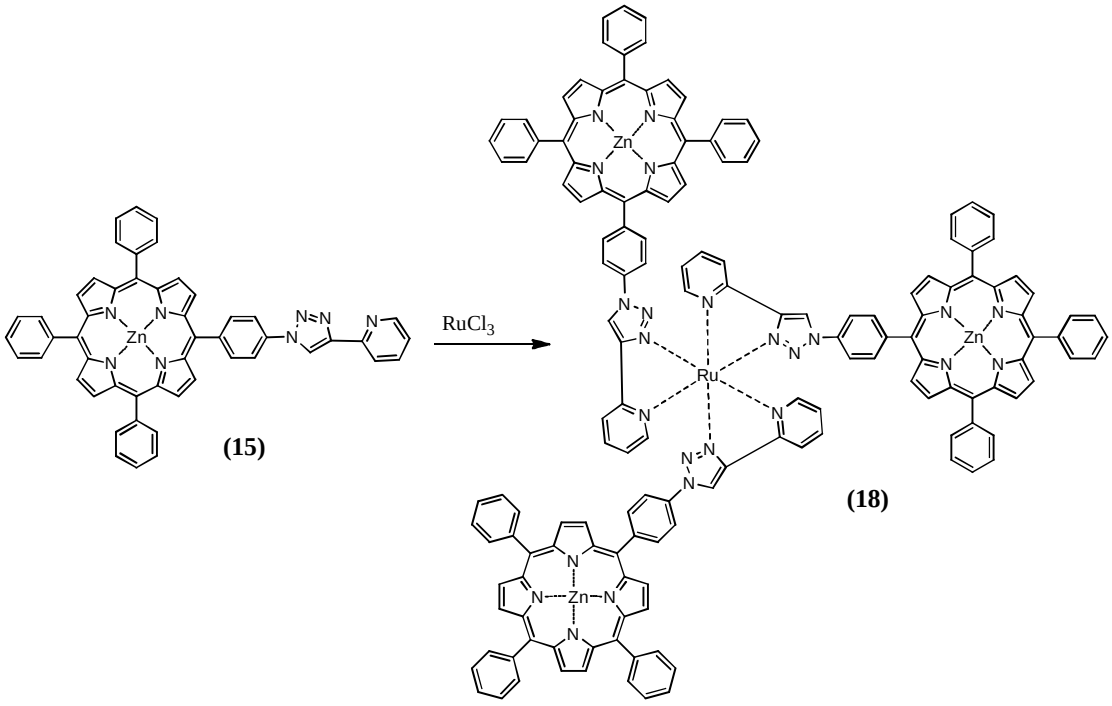

The porphyrin derivative (15) (20 mg, 0.024 mmol) was dissolved in ethanol (10 mL) and ruthenium chloride ($RuCl_3$) (1.68 mg, 0.008 mmol) was added to it. The reaction mixture was stirred for 4 hours at 78 °C. The solvent was evaporated and the solid thus obtained was subject to column chromatography over alumina using chloroform/methanol (9:1) as eluent. ESI-MS: 853 $[MH_3]^{3+}$

3.30 Synthesis of Nanocrystalline cellulose (NCC)[17]

Microcrystalline cellulose (5.0 g) was added to a pre-heated solution (temperature- 45 °C) of sulphuric acid (63% w/w; made by mixing 95-98% H_2SO_4 (21.5 mL) with water (22.5 mL)). The suspension was stirred for 2 hours. The hydrolysis was stopped by dilution with water (900 mL). Most of the supernatant was decanted, then the remaining suspension was centrifuged at 4000 rpm for 5 minutes in order to remove most of the acidic supernatant solution. The solids were collected together, washed once by suspension in water and recovered by centrifugation at 8000 rpm for 5 minutes. The suspension was then transferred in dialysis tubes (12 kD cut-off), and dialyzed first against tap water (6 days) and then milliQ-water (2 days). The final product was recovered by lyophilization. The yield of NCC obtained was 2.94 g (58%).

3.31 Synthesis of pH sensitive Azo dye (19)[18]

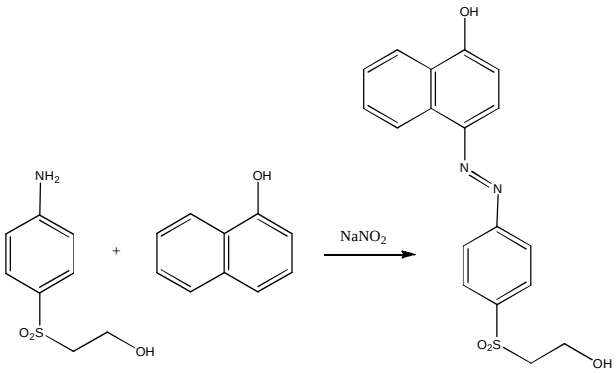

In a beaker, a solution of 4-(2-hydroxyethylsulphonyl) aniline (1 g, 4.96 mol) in HCl (6M) (1.5 mL) was cooled to 0°C. A solution of sodium nitrite ($NaNO_2$) (0.27 g, 3.98 mol) in water (5 mL) was added drop wise. After 5 minutes, a solution of α-Napthol (0.57 g, 3.98 mol) in acetic acid (6 mL) was added to the reaction mixture. After stirring at room temperature for 4 hours, the red solid was filtered and washed with water. The solid dye was obtained in 77 % yield. ESI-MS: calculated-356, found-357.

3.32 Synthesis of NCC-Dye[18]

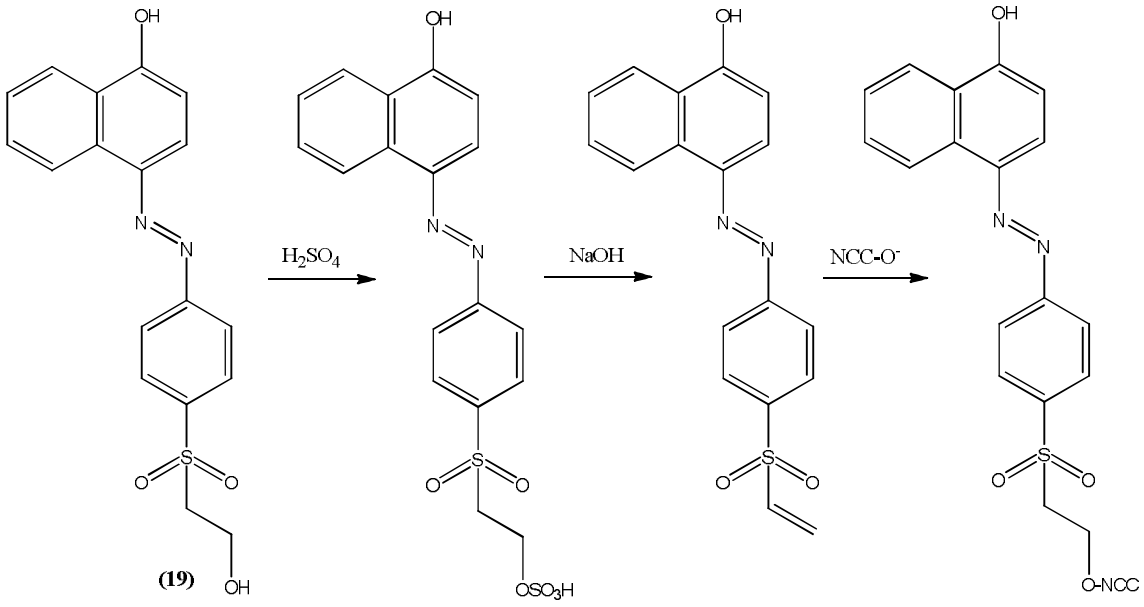

Firstly, dye (19) (50 mg) was dissolved in conc. H_2SO_4 (150 mg). After 30 minutes, solution was diluted with water (10 mL) and neutralized with NaOH (1M). After 5 minutes, Na_2CO_3 (70 mg) was added. Then a suspension of NCC (100mg) in NaOH (1M) (4mL) was added to the dye solution. The suspension was stirred overnight at room temperature. The solid was isolated by centrifugation (7,500 rpm, 15 min), re-suspended in water and centrifuged

down. This suspension/centrifugation step was repeated five times with sonication between each step. The solid NCC-Dye obtained after centrifugation step was subjected to dialysis against distilled water for 3 days at room temperature until a constant neutral pH was reached inside the dialysis tubes. The final product was recovered by lyophilization in 80% yield.

3.33 Synthesis of cationic nanocellulose (NCC-CAT)[19]

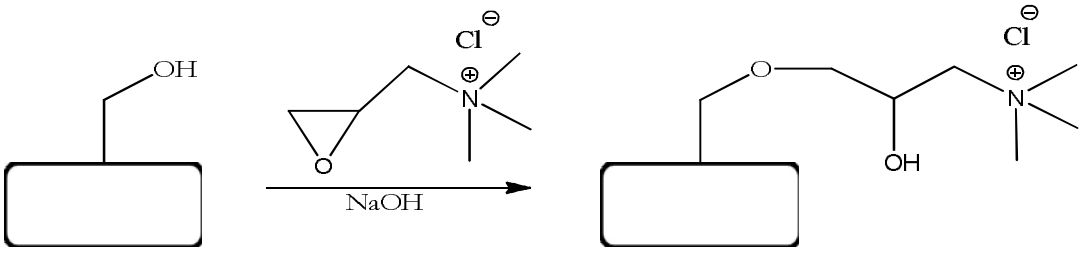

Sodium hydroxide (NaOH) (0.78 g, 0.19 mol) was dissolved in 11 mL of MilliQ-water. NCC (100 mg) were added to the solution and sonicated for 15 minutes After 30 minutes stirring at room temperature, EPTMAC (2.7 g, 0.018 mol) was added and the mixture was stirred for 5 hours at 65°C temperature. After 5 hours, the reaction mixture was diluted 5-fold with water and dialyzed (dialysis membranes, molecular weight cut-off of 12000–14000Da) against purified water for 7 days. The final product was recovered by lyophilization in 60 % yield. The degree of substitution was found to be 0.084 mmol per g of NCC by conductometric titration.

3.34 Synthesis of Amino Nanocrystalline cellulose (NCC-NH_2)[20]

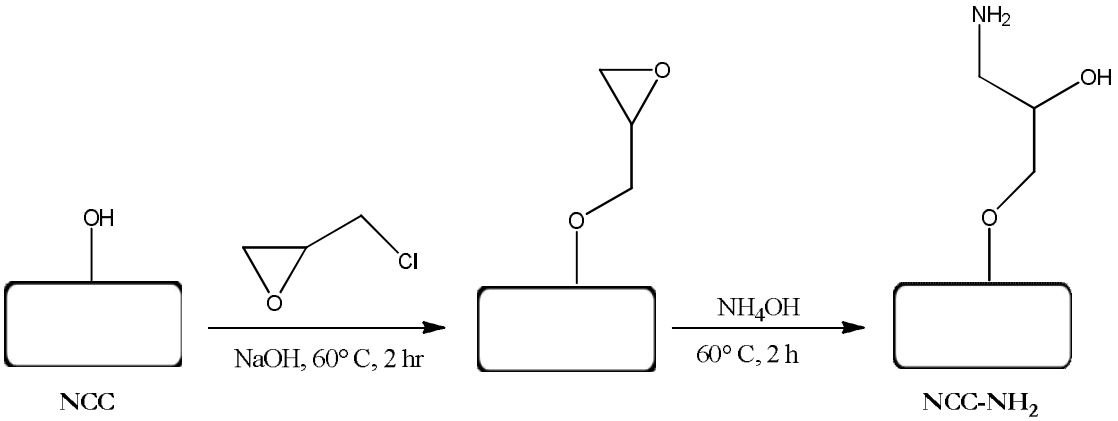

NCC (100 mg) were dispersed in 8 mL NaOH (1M) by sonication (15 minutes). The epichlorohydrin (46.25 µL, 0.6 mmol) was added to suspension and stirred for 2 hours at

60 °C. Then the reaction mixture was transferred in dialysis tube and dialyzed (Spectra/Por 4 dialysis tubing) against deionized water until the pH was below 12. Next, the epoxy ring was opened with ammonium hydroxide to introduce primary amino groups. After adjusting the pH to 12 with 50% (w/v) sodium hydroxide, ammonium hydroxide (0.5 mL) was added and the reaction mixture was heated to 60 °C for 2 hours. The reaction mixture was transferred in dialysis tube until the pH was 7. The solid product was recovered by lyophilization. The yield was 50 mg and the degree of amination was found to be 0.04 mmol per gram of nanocellulose by Kaiser test.

3.35 Synthesis of Amino Nanocrystalline cellulose by tosylation (NCC-Ts-NH_2)[21]

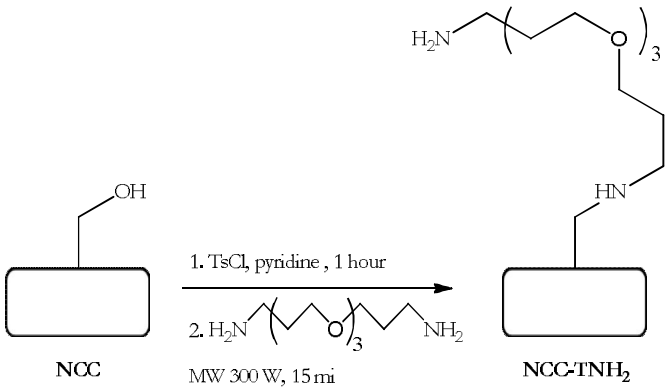

NCC (100 mg) was added to a 2M solution of tosyl chloride (TsCl) 0.38 g/mL in 1.2 ml of pyridine. After stirring for 1 hour at room temperature, the cellulose was washed with ethanol 3 times using the centrifugation and re-suspension method. After washing, the cellulose tosylate was placed in a microwave tube and 4,7,10-trioxa-1,13-tridecanediamine (5 mL) was added. The reaction mixture was subjected to microwave irradiation at 20 W power for 15 minutes at 120 °C temperature. After cooling down at room temperature, it was washed with following solvents DMF (x2), EtOH (x2), NaOH (x2) and finally with distilled water until neutral pH was observed. After drying under flow of nitrogen, the yield was found to be 0.3 g of NCC-Ts-NH_2. Yellow colour was observed in the Kaiser test i.e. no free amino groups.

3.36 Synthesis of Silane Amino Nanocrystalline cellulose (NCC-Si-NH_2)[22]

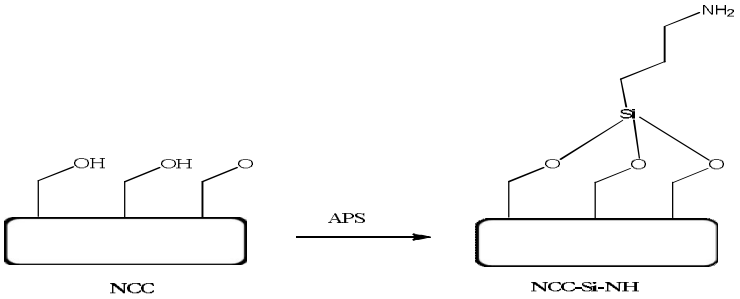

NCC (100 mg) was dissolved in 10 mL of anhydrous DMF and sonicated for 10 minutes. 3-aminopropyltrimethoxysilane (APS), (0.25 mL, 2.86mmol) was added to the suspension. The reaction mixture was stirred for 2 hours at room temperature. After, the cellulose was washed by centrifugation first with DMF and with acetone to remove excess APS. Cellulose was dried with a flow of nitrogen and yield of 90 mg of NCC-Si-NH_2 were obtained. The degree of amination by Kaiser test was found to be 0.2 mmol NH_2 per g NCC.

3.37 Synthesis of Carboxylated Nanocrystalline cellulose by ammonium persulfate (NCC-APS-COOH)[23]

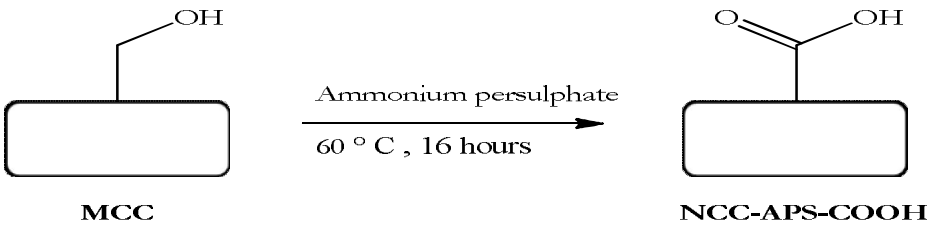

2.5 g of microcrystalline cellulose were added to 250 mL of 1M ammonium persulfate (APS). The suspension was heated at 60 °C temperature for 16 hours to give a white suspension, which was centrifuged at 12,000 rpm for 10 minutes. The solution was removed and ~200 mL of water was added to the cellulose pellet, followed by 5 minutes of vigorous mixing and repeated centrifugation. This centrifugation/washing cycles were repeated 4 times until the solution pH was around 4. The product was lyophilized to yield a white powder in 1.6 g of NCC-APS-COOH. The degree of oxidation by conductomeric titration was found to be 0.09 mmol per gm NCC.

3.38 Synthesis of Carboxylated Nanocrystalline cellulose (NCC-COOH)[24]

NCC NCC-COOH

0.5 g of NCC were suspended in 50 mL water and subjected to sonication in order to obtain a stable suspension. An aqueous solution (50 mL) of 2,2,6,6-tetramethylpiperidin-1-yl)oxidanyl (TEMPO) (14.83 mg, 0.095 mmol) and sodium bromide (NaBr) (162.9 mg, 1.58 mmol) was added together with a solution of sodium hypochlorite (NaOCl) 2.73 M (1.78 mL). The pH was adjusted to 10 with 1M NaOH solution. The mixture was stirred at room temperature for 3 hours. The reaction was stopped by addition of ethanol (1 mL) and then pH was adjusted to neutral pH by adding 0.5 M HCl solution. The supernatant was removed by centrifugation at 13000 rpm for 10 minutes and the residue was washed 3 times by suspension in water by centrifugation. The final product was recovered by lyophilization, yielding to 0.250 g (50%) of NCC-COOH. The degree of oxidation by conductomeric titration was found to be 0.82 mmol per gram of NCC.

3.39 Synthesis of 5-(4-acetamidophenyl)-10,15,20-triphenyl porphyrin (Ac-NH-TPP)[25]

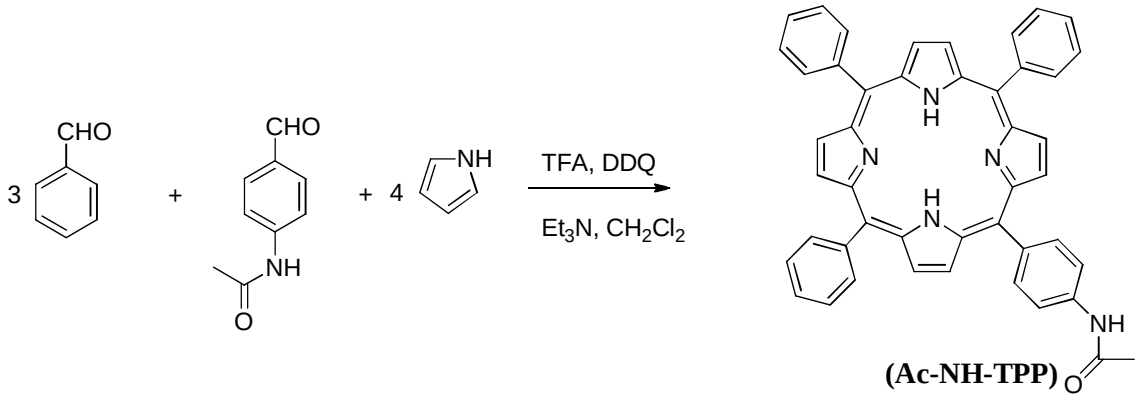

(Ac-NH-TPP)

Benzaldehyde (760 µL, 7.5mmol) and p-acetamido benzaldehyde (410 mg, 2.5 mmol) were dissolved in 1 L of dichloromethane contained in a 2 L three-neck flask. The flask was covered with aluminium foil and purged with Nitrogen for 10 minutes before freshly-distilled pyrrole (700 µL, 10 mmol) was injected. The reaction mixture was stirred for another 10 minutes and then the reaction was initiated by the injection of TFA (1.4 mL, 20 mmol). After stirring at room temperature for 1.5 hours, DDQ (1.85 g, 7.5 mmol) was

added. The solution was stirred for another 1 hour and then it was neutralized with triethylamine (2.8 mL, 20 mmol). The crude mixture was purified with silica gel flash chromatography. Elution with CH_2Cl_2 was able to remove all tetrarylporphyrin, and the desired A_3B porphyrin was then eluted with 20% EtOAc in CH_2Cl_2. The solvent was removed under vacuum, affording a purple solid as p-acetamido tetraphenyl porphyrin in ~16 % yield. MALDI-TOF calculated for $C_{46}H_{33}N_5O$: 671.2 found 672.4. ^{1}H-NMR ($CDCl_3$, 250 MHz): 8.84 (m, 8H, β-pyrrole), 7.5-8.22 (m, 19H, Ar), 1.5 (s, 3H, CH_3), -2.79 (s, 2H, pyrrole NH).

3.40 Synthesis of 5-(4-aminophenyl)-10,15,20-triphenyl porphyrin (TPP-NH_2)[25]

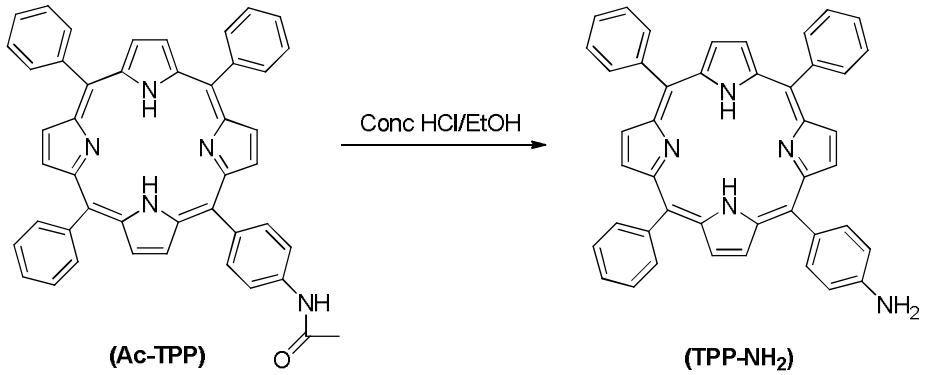

p-Acetamidophenyltriarylporphyrin (200 mg, 0.3 mmol) was dissolved in 60 mL EtOH in a 250 mL flask. Concentrated HCl (40 mL) was added to the reaction mixture, which was heated at reflux temperature for 17 hours. The crude mixture was diluted with water and extracted with CH_2Cl_2 for five times. The organic phase was washed with H_2O three times and with the saturated $NaHCO_3$ solution twice. The pooled organic layer was dried over Na_2SO_4 and filtered. The solvent was removed under vacuum and flash chromatography with silica gel and CH_2Cl_2 afforded the desired amino tetraphenyl porphyrin in quantitative yield. MALDI-TOF calculated for $C_{46}H_{31}N_5O$-629.4 found 630. ^{1}H-NMR ($CDCl_3$, 250 MHz): 8.91 (d, J=4.8 Hz, 2H), 8.78(m, 6H), 8.28 (m, 6H), 8.4 (d, J=8.3 Hz, 2H), 7.79 (m, 9H), 8.61 (d, J=8.3 Hz, 2H), -2.79 (s, 2H, pyrrole NH).

3.41 Synthesis of 5-(4-Aminophenyl)-10,15,20-tris(4-sulfonatophenyl)porphyrin, trisodium salt (TPPS-NH_2)[26]

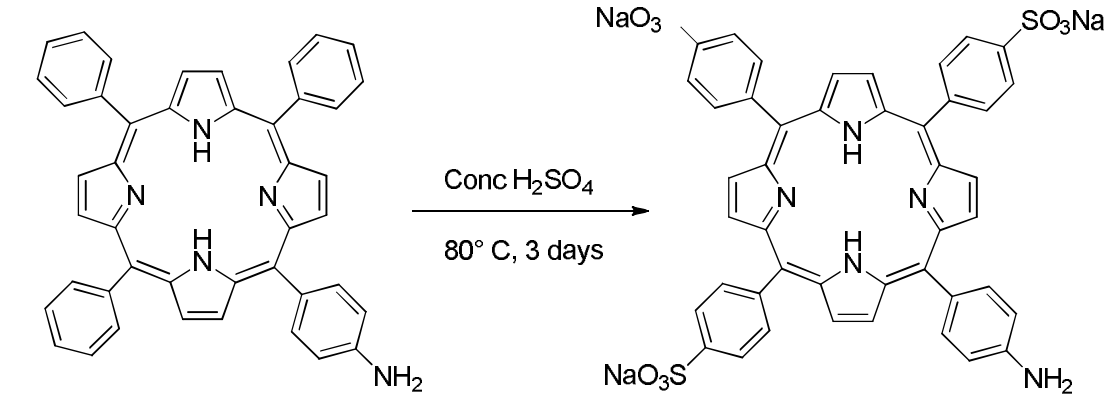

94 mg (0.15 mmol) of amino tetraphenyl porphyrin was dissolved in 10 mL of concentrated H_2SO_4 and subjected to heating at 80°C under dry atmosphere for 48 hours. After cooling down to room temperature, the mixture was poured into an ice/water (50 mL) giving a suspension that was washed by centrifugation for 10 minutes at 6000 rpm. The supernatant was repeatedly removed and replaced with neutral water until pH 3-4 was observed in supernatant. The residual solid was then dissolved in 30% ammonium hydroxide (20 mL) and the solvent was removed in vacuo. The solid was dissolved in a minimum amount of water and applied to a Na^+-activated cation exchange column (AG-50W-X8). The solvent was removed in vacuo and solid product was obtained by lyophilization. MALDI-TOF calculated for $C_{44}H_{31}N_5O_9S_3$- 869.2 [M] found 870 [M^+]. ^1H NMR (CD_3OD, 250MHz: 8.8 (m, 16H), 7.9 (d, 6H, J=8.5 Hz), 7.1 (d, 6H, J=8.5 Hz), -2.79 (s, 2H, pyrrole NH).

3.37 Synthesis of NCC-TPPS[27]

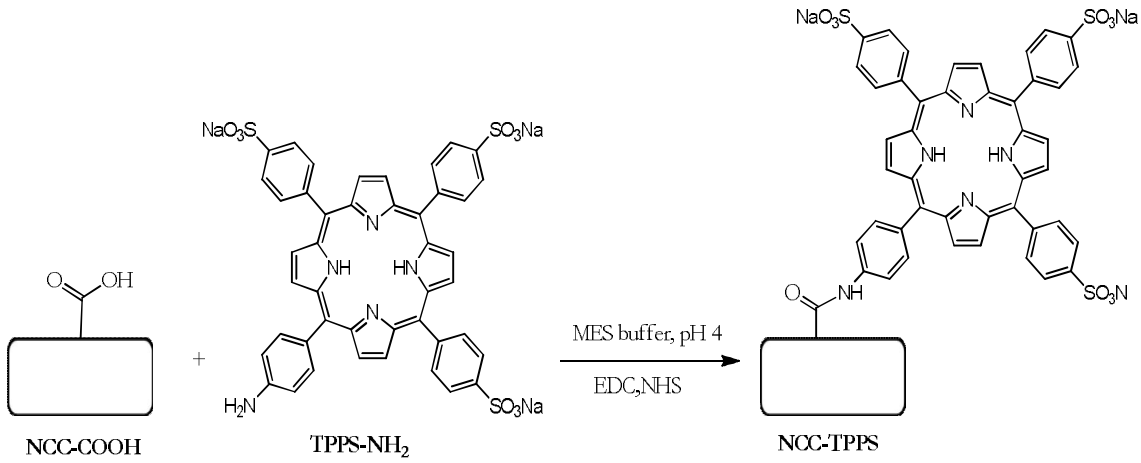

NCC-COOH (0.153 g, 0.126 mmol of COOH groups) was suspended in a solution of 50 mM 2-(N-morpholino)-ethanesulfonic acid (MES) buffer (18 mL) at pH = 4. The suspension was sonicated for 5 minutes. Then, N-(3-dimethylaminopropyl)-N'-ethyl-carbodiimide hydrochloride (EDC·HCl) (0.242 g, 1.26 mmol) and N-hydroxy succinimide (NHS) (0.149 g, 1.29 mmol) was added to the suspension. After 5 minutes, the TPPS-NH_2 (0.072 g, 0.0827 mmol) was added and suspension was stirred for 4 days at room temperature. The solid was recovered by centrifugation at 13000 rpm for 10 minutes and re-suspended in water and centrifuged again, until the supernatant was colourless. The suspension was transferred in a dialysis tube and dialyzed against brine for one day then against milliQ-water for 6 days. The product was recovered by lyophilization obtaining 68.7 mg of NCC-TSPP as a green solid (Yield: 44.8%).

3.38 Synthesis of NCC-TPPS (Zn)

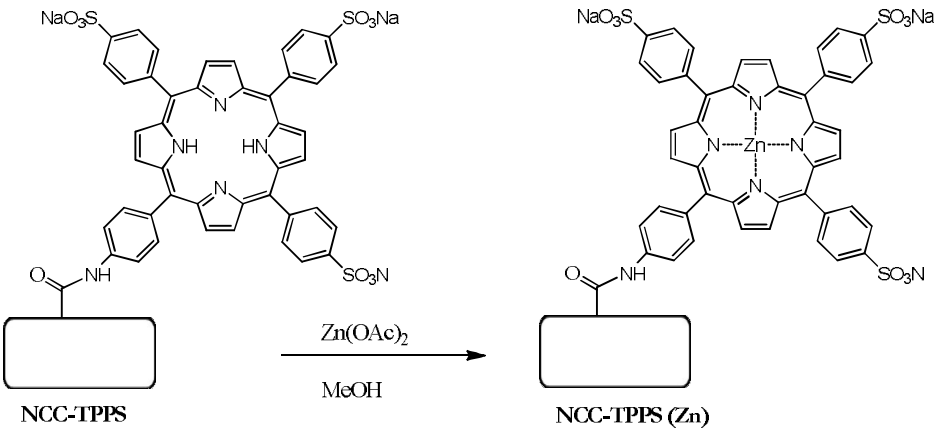

NCC-TPPS (25.3 mg) was suspended in methanol (3 mL). To this a solution of $Zn(OAc)_2$ (11.4 mg in 2 mL of methanol) was added and stirred at 30°C temperature for 3 hours. The solid was recovered by centrifugation at 12000 rpm for 5 minutes and then washed first with methanol (3 times), with water (2 times) by re-dispersion followed by centrifugation at 12000 rpm for 5 minutes. The product was recovered by lyophilization obtaining 21.7 mg of a green solid (yield: 85.8 %).

3.39 Synthesis of N-(3-aminopropyl)-3-(trifluoromethyl)-4-nitrobenzenamine (20)[28]

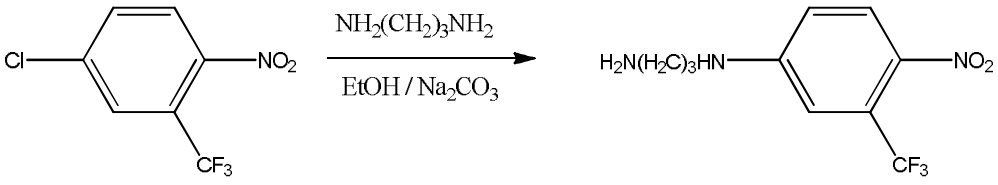

1,3-propyldiamine (1.7 ml, 20 mmol) and Na_2CO_3 (2.12 g, 20 mmol) was refluxed in 50 ml of ethanol for 15 minutes. To this 4-chloro-2-(trifluoromethyl)-1-nitrobenzene (600 μL, 4 mmol) was then added and the mixture was kept under continuous stirring for 3 days. After cooling down to ambient temperature the resulting suspension was filtered. The organic solution was concentrated under reduced pressure and purified by column chromatography (methanol 100%) to give product (yield 30 %) as a yellow powder. ESI-MS: calculated-263, found- 264.

3.40 Synthesis of NCC-NO[27]

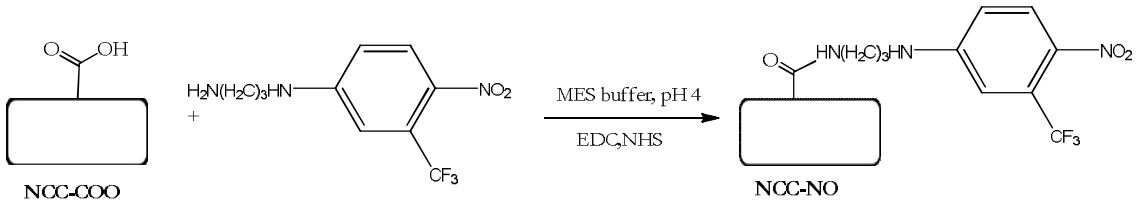

150mg of NCC-COOH (DO- 0.2mmol of COOH group) was suspended in a 5 mL solution of 50 mM MES buffer (18 mL) at pH = 4. The suspension was sonicated for 5 minutes then EDC.HCl (500mg, 2.6 mmol) and NHS (350mg, 3.04 mmol) were added. After 5 minutes, nitro derivative (20) (150mg, 0.57 mmol) was added. The mixture was stirred for 4 days at room temperature. The product was washed extensively with MeOH for 7 times and then with water for 3 times by centrifugation for 10 min at 13000 rpm until the supernatant was colourless. The suspension was transferred in a dialysis tube and dialyzed against milliQ-water for 4 days. The suspension was subjected to lyophilization yielding to yellow solid in 50% yield.

REFERENCES

1. H. Imahori, S. Hayashi, T. Umeyama, S. Eu, A. Oguro, S. Kang, Y. Matano, T. Shishido, S. Ngamsinlapasathian and S Yoshikawa, *Langmuir*, **2006**, *22*, 11405-11411.
2. A.D. Adler, F. R. Longo, J. D. Finarelli, J. Goldmacher, J. Assour and L. Korsakoff, *J. Org. Chem.*, **1967**, *32*, 476-477.
3. L. Barloy, D. Dolphin, D. Dupre and T. P. Wijesekerai, *J. Org. Chem.*, **1994**, *59*, 7976-7985.
4. Q. Wang, W. M. Campbell, E. E. Bonfantani, K. W. Jolley, D. L. Officer, P. J. Walsh, K. Gordon, R. Humphry-Baker, M. K. Nazeeruddin and M. Gratzel, *J. Phys. Chem. B*, **2005**, *109*, 15397-15409.
5. E. Lubian, F. Baldini, A. Giannetti, C. Trono and T. Carofiglio, *Chem. Commun.*, **2010**, *46*, 3678-3680.
6. M. A. Fazio, O. P. Lee and D. I. Schuster, *Org. Lett.*, **2008**, *21*, 4979-4982.
7. A. G. Petrovic, G. Vantomme, L. Yashira, Negrón-Abril, E. Lubian, G. Saielli, I. Menegazzo, R. Cordero, G. Proni, K. Nakanishi, T. Carofiglio and N. Berova, Chirality, **2011**, *23*, 808-19.
8. Y. Peng, H. Liu, M. Tang, L. Cai and V. Pike, *Ch. J. Chem.*, **2009**, *27*, 1339-1344.
9. B. J. Littler, M. A. Miller, C. H. Hung, R. W. Wagner, D. F. O'Shea, P. D. Boyle and J. S. Lindsey, J. Org. Chem., **1999**, *64*, 1391-1396.
10. M. J. Plater, S. Aiken and G. Bourhill, *Tetrahedron*, **2002**, *58*, 2405-2413.
11. S. L. Elmer, S. Man and S. C. Zimmerman, *Eur. J. Org. Chem.*, **2008**, 3845-3851.
12. K. Flavin, M. N. Chaur, L. Echegoyen and S. Giordani, *Org. Lett.*, **2010**, *12*, 840.
13. M. Severac, L. Pleux, A. Scarpaci, E. Blart and F. Odobel, *Tet. Lett.*, **2007**, *48*, 6518-6522.
14. G. Zhang, Y. Wang, X. Wen, C. Ding and Y. Li, *Chem. Commun.*, **2012**, *48*, 2979-2981.
15. J. X. Zhang, K. Wong, W. Wong, N. Mak, D. W. J. Kwong and H. Tam, *Org. Biomol. Chem.*, **2011**, *9*, 6004.
16. J. T. Fletcher, B. J. Bumgarner, N. D. Engels and D. A. Skoglund, *Organometallics*, **2008**, *27*, 5430-5433.
17. C. Danumah and Hicham Fenniri, *Mater. Res. Soc. Symp. Proc.*, **2001**, *1312*, 467-472.
18. T. Carofiglio, C. Fregonese, G. J. Mohr, F. Rastrelli and U. Tonellato, *Tetrahedron*, **2006**, *62*, 1502–1507.

19. M. Hasani, E. D. Cranston, G. Westmana and D. G. Gray, *Soft Matter*, **2008**, *4*, 2238-2244.
20. S. Dong and M. Roman, *J. Am. Chem. Soc.*, **2007**, *129*, 13810-13811.
21. M. D. Bowman, R. C. Jeske and H. E. Blackwell, *Org. Lett.*, **2004**, *6*, 2019-2022.
22. Q. Yang and X. Pan, *J. App. Pol. Sci.*, **2010**, *117*, 3639-3644.
23. A. C. W. Leung, S. Hrapovic, E. Lam, Y. Liu, K. B. Male, K. A. Mahmoud and J. H. T. Luong, *Small*, **2011**, *7*, 302-305 .
24. N. Lin, C. Bruzzese and A. Dufresne, *ACS Appl. Mater. Interfaces*, **2012**, *4*, 4948-4959.
25. J. S. Lindsey, P. A. Brown and D. A. Siesel, *Tetrahedron*, **1989**, *45*, 4845-4846.
26. E. Sansiaume, R. Ricoux, D. Gori and J. P. Mahy, *Tetrahedron: Asymmetry*, **2010**, *21*, 1593-1600.
27. I. Filipponen and D. S. Argyropoulos, *Biomacromolecules*, **2010**, *11*, 1060-1066.
28. F. L. Callari and S. Sortino, *Chem. Commun.*, **2008**, 1971.